



**Chemical Absorption and Degradation Kinetics of  
Iron(III)chelate in H<sub>2</sub>S Removal Process**

**Rattana Saelee**


**A Thesis Submitted in Partial Fulfillment of the Requirements  
for the Degree of Doctor of Engineering  
Prince of Songkla University  
2010**

**Copyright of Prince of Songkla University**


**Thesis Title**            Chemical Absorption and Degradation Kinetics of  
Iron(III)chelate in H<sub>2</sub>S Removal Process  
**Author**                    Miss Rattana Saelee  
**Major Program**        Chemical Engineering


---

**Advisor :**


  
.....Chairman  
(Assoc. Prof. Dr.Charun Bunyakan)


**Co-advisors :**


  
.....  
(Asst. Prof. Dr.Jantima Chungsiriporn)

  
.....  
(Professor Dr. John O'Haver)

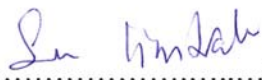
**Examining Committee :**

  
.....Chairman  
(Asst.Prof. Dr.Lupong Kaewsichan)

  
.....Committee  
(Assoc. Prof. Dr.Charun Bunyakan)

  
.....Committee  
(Asst. Prof. Dr.Jantima Chungsiriporn)

  
.....Committee  
(Assoc. Prof. Dr.Proespichaya Kanatharana)

  
.....Committee  
(Assoc.Prof. Dr.Sunun Limtrakul)

The Graduate School, Prince of Songkla University, has approved this thesis as partial fulfillment of the requirements for the Doctor of Engineering Degree in Chemical Engineering

.....  
(Assoc. Prof. Dr.Krerckchai Thongnoo)  
Dean of Graduate School

ชื่อวิทยานิพนธ์	การดูดซับทางเคมีและจลนพลศาสตร์ของการเสื่อมสภาพของไอออนคีเลท ในกระบวนการกำจัดไฮโดรเจนซัลไฟด์
ผู้เขียน	นางสาวรัตนา แซ่หลี่
สาขาวิชา	วิศวกรรมเคมี
ปีการศึกษา	2552

### บทคัดย่อ

การกำจัดไฮโดรเจนซัลไฟด์โดยใช้การดูดซับทางเคมีของสารละลายไอออนคีเลทชนิด Fe(III)EDTA เป็นเทคนิคที่คุ้มค่าทางเศรษฐศาสตร์ เพราะสารละลาย Fe(III)EDTA ที่ใช้แล้วสามารถฟื้นฟูสภาพได้ง่ายด้วยการป้อนอากาศให้กับสารละลายดูดซับ ในการศึกษาครั้งนี้จึงเลือกใช้ Fe(III)EDTA ในการบำบัดแก๊สชีวภาพที่ผลิตจากน้ำเสียของโรงงานอุตสาหกรรมน้ำยางข้นซึ่งมีความเข้มข้นของไฮโดรเจนซัลไฟด์สูง ดำเนินการทดลองโดยใช้คอลัมน์บรรจุขนาดต้นแบบ บรรจุตัวกลางสูง 0.8 เมตร มีเส้นผ่านศูนย์กลาง 0.5 เมตร แก๊สชีวภาพที่เข้าระบบมีอัตราการไหลในช่วง  $5.16 \times 10^{-3}$ - $5.61 \times 10^{-3}$  ลูกบาศก์เมตร/วินาที และมีความเข้มข้นของไฮโดรเจนซัลไฟด์อยู่ในช่วง 0.35-0.77 โมล/ลูกบาศก์เมตร จากผลการทดลองพบว่าการใช้สารละลาย Fe(III)EDTA สามารถกำจัดไฮโดรเจนซัลไฟด์ได้ดี เมื่อใช้ความเข้มข้นของ Fe(III)EDTA อัตราการไหลของสารละลาย Fe(III)EDTA และอัตราการไหลของอากาศที่เหมาะสม จะให้ประสิทธิภาพการกำจัดสูงสุดถึง 97 เปอร์เซ็นต์ นอกจากนี้ยังพบว่า Fe(III)EDTA ไม่ทำปฏิกิริยากับมีเทนซึ่งเป็นองค์ประกอบที่ต้องการ แบบจำลองทางคณิตศาสตร์ที่พิจารณาทั้งการเกิดปฏิกิริยาและการถ่ายโอนมวลได้ถูกเสนอขึ้นสำหรับอธิบายกระบวนการดูดซับและปฏิกิริยาเคมีระหว่างไฮโดรเจนซัลไฟด์และ Fe(III)EDTA ในคอลัมน์บรรจุและตรวจสอบความถูกต้องของแบบจำลองโดยเปรียบเทียบกับข้อมูลผลการทดลอง แบบจำลองที่เสนอนี้สามารถใช้เป็นข้อมูลเบื้องต้นสำหรับการออกแบบคอลัมน์บรรจุสำหรับกำจัดไฮโดรเจนซัลไฟด์จากแก๊สชีวภาพโดยใช้การดูดซับร่วมกับการออกซิเดชันด้วย Fe(III)EDTA ได้เป็นอย่างดี

การศึกษาความสัมพันธ์ระหว่างตัวแปรดำเนินการที่มีผลต่อการกำจัดไฮโดรเจนซัลไฟด์ด้วย Fe(III)EDTA โดยละเอียด ได้ดำเนินการเพิ่มเติมในระดับห้องปฏิบัติการ โดยใช้คอลัมน์บรรจุแบบไหลสวนทางขนาดห้องปฏิบัติการ เพื่อศึกษาผลของตัวแปรดำเนินการที่มีผลต่ออัตราการดูดซับและอัตราการเกิดปฏิกิริยา ซึ่งได้แก่ อัตราการไหลของสารดูดซับ (0.167-0.833 มิลลิลิตร/วินาที), ความเข้มข้นเริ่มต้นของสารดูดซับ (10-310 โมล/ลูกบาศก์เมตร) อัตราการ

นอกจากสภาวะการดำเนินการที่ศึกษาแล้ว การเสื่อมสภาพของสารละลาย Fe-EDTA ในระหว่างกระบวนการกำจัดไฮโดรเจนซัลไฟด์สามารถทำให้ประสิทธิภาพการกำจัดไฮโดรเจนซัลไฟด์ด้วย Fe(III)EDTA ลดลงได้ งานวิจัยนี้จึงศึกษาผลของอัตราการไหลเชิงโมลของไฮโดรเจนซัลไฟด์ ความเข้มข้นเริ่มต้นของ Fe(III)EDTA และความเข้มข้นของ sodium citrate ต่ออัตราการเสื่อมสภาพของ Fe-EDTA ในเครื่องปฏิกรณ์ชนิด เซมิแบทช์ ซึ่งมีแก๊สชีวภาพไหลเข้าระบบอย่างต่อเนื่อง โดยดำเนินการทดลองที่ pH เริ่มต้นเท่ากับ 7.0 อัตราการไหลเชิงโมลของไฮโดรเจนซัลไฟด์  $1.08 \times 10^{-3}$  -  $3.40 \times 10^{-3}$  โมล/ชั่วโมง ความเข้มข้นเริ่มต้นของ Fe(III)EDTA 2.17-8.16 โมล/ลูกบาศก์เมตร และความเข้มข้นของ sodium citrate 0-300 โมล/ลูกบาศก์เมตร จากผลการทดลองพบว่า sodium citrate สามารถทำหน้าที่เป็นสารช่วยเพิ่มความเสถียรที่สามารถลดอัตราการเสื่อมสภาพของ Fe-EDTA ได้เป็นอย่างดี จากการศึกษาพบว่าจลนพลศาสตร์ของการเสื่อมสภาพของ Fe-EDTA เป็นปฏิกิริยาอันดับหนึ่งเทียมและสามารถใช้เพื่อทำนายอัตราการเสื่อมสภาพของ Fe-EDTA ที่สภาวะการดำเนินการต่าง ๆ ได้ โดยการสร้างแบบจำลองที่แสดงความสัมพันธ์ระหว่างค่าคงที่การเสื่อมสภาพของ Fe-EDTA กับตัวแปรต่าง ๆ คือ อัตราการไหลเชิงโมลของไฮโดรเจนซัลไฟด์ ความเข้มข้นเริ่มต้นของ Fe(III)EDTA และความเข้มข้นของ sodium citrate นอกจากนี้จากการศึกษาวิเคราะห์องค์ประกอบของตะกอนของแข็งที่เกิดขึ้นระหว่างการเกิดปฏิกิริยา หรือที่เรียกกันว่าซัลเฟอร์เค้ก พบปริมาณธาตุซัลเฟอร์มากกว่า 98 เปอร์เซ็นต์ ส่วนองค์ประกอบที่เหลือเกือบทั้งหมดเป็นธาตุเหล็ก และไม่พบว่ามี การเสื่อมสภาพหรือการตกตะกอนของ EDTA ปรากฏอยู่ในซัลเฟอร์เค้กอย่างมีนัยสำคัญ

ส่วนสุดท้ายของการวิจัยได้ทำการประเมินค่าใช้จ่ายในการกำจัดไฮโดรเจนซัลไฟด์จากแก๊สชีวภาพเมื่อใช้คอลัมน์บรรจุ ที่มีอัตราการไหลของแก๊สชีวภาพเท่ากับ 2 ลิตร/นาที่ และมีความเข้มข้นของไฮโดรเจนซัลไฟด์ 1,300 มิลลิกรัม/ลูกบาศก์เมตร พบว่าต้องใช้งบลงทุน 10,000 - 15,000 บาท และมีค่าใช้จ่ายในการดำเนินการ 0.81 บาท/ลูกบาศก์เมตรของแก๊สชีวภาพ ซึ่งเมื่อเปรียบเทียบกับการใช้สารเคมีตัวอื่นพบว่าการใช้ Fe(III)EDTA เป็นสารเคมีดูดซึม มีค่าใช้จ่ายในการดำเนินการต่ำกว่าระบบที่ใช้  $\text{KMnO}_4$  เล็กน้อย แต่จะต่ำกว่าระบบที่ใช้ NaOCl ถึงประมาณ 2 เท่า

**Thesis Title**            Chemical Absorption and Degradation Kinetics of  
Iron(III)chelate in H<sub>2</sub>S Removal Process

**Author**                 Miss Rattana Saelee

**Major Program**        Chemical Engineering

**Academic Year**        2009

## **ABSTRACT**

Hydrogen sulfide (H<sub>2</sub>S) removal using chemical absorption by iron chelate solution catalyzed by Fe(III)EDTA is an economically promising technique. Fe(III)EDTA can be easily regenerated by bubbling air into the absorbing liquid. In this study a chemical oxidation using Fe(III)EDTA was selected for the treatment of high H<sub>2</sub>S concentration in biogas which produced from wastewater of concentrated latex rubber industry (CLRI). Experiments were performed using a pilot packed column with diameter and packed height of 0.5 and 0.8 m, respectively. The biogas flow rate and H<sub>2</sub>S concentration were in the range of  $5.16 \times 10^{-3}$ - $5.61 \times 10^{-3}$  m<sup>3</sup>/s and 0.35-0.77 mol/m<sup>3</sup>, respectively. Experimental results indicated that Fe(III)EDTA solution was effective at removing H<sub>2</sub>S from biogas with a maximum removal efficiency of about 97%. Suitable operating conditions, including Fe(III)EDTA concentration, flow of Fe(III)EDTA and air flow rate were determined. In addition, no side-reaction of Fe(III)EDTA with valuable methane was found. A mathematical model of the absorption and the reaction between H<sub>2</sub>S and Fe(III)EDTA in a packed column was proposed and verified against the experimental data. The results confirmed the potential use of the model to design packed column for H<sub>2</sub>S removal from biogas using absorption coupled with oxidation by Fe(III)EDTA.

A counter-current laboratory packed column was used to study the process variables which were known to influence the absorption and reaction rate such as scrubbing liquid flow rate (0.167-0.833 mL/s), initial Fe(III)EDTA concentration (10-30 mol/m<sup>3</sup>), gas flow rate (0.033-0.167 L/s), inlet H<sub>2</sub>S concentration (0.025-0.167 mol/m<sup>3</sup>), and height of packed bed (0.15-0.45 m). The effects of these variables on absorption and reaction performance were analyzed via evaluating the absolute removal efficiency. A central composite design was used in

the design of experiments. The H<sub>2</sub>S removal efficiency was modeled statistically and optimized using linear Regression method. A quadratic model was suggested and validated experimentally with the coefficient of determination equal to 0.872. All significant variables were presented in the model and the interaction effects between variables were found. Results showed that the developed regression model provides a better understanding of the interactions involved in the studied H<sub>2</sub>S removal process.

Moreover, the effect of H<sub>2</sub>S molar flow rate, the initial concentration of Fe(III)EDTA and the presence of sodium citrate in Fe(III)EDTA solution on the degradation of Fe-EDTA were investigated. The semibatch reactor with continuous flow of H<sub>2</sub>S containing biogas was used under a wide range of experimental conditions; initial pH = 7.0, H<sub>2</sub>S molar flow rate ( $1.08 \times 10^{-3}$ - $3.40 \times 10^{-3}$  mol/h), the initial concentration of Fe(III)EDTA (2.17-8.16 mol/m<sup>3</sup>) and the concentration of sodium citrate (0-310 mol/m<sup>3</sup>). The result showed that sodium citrate acted as stabilizer with a good ability to reduce the degradation rate. The degradation rate of Fe-EDTA was found to follow pseudo first order kinetics. The correlation model between degradation rate constant and H<sub>2</sub>S molar flow rate, the initial concentration of Fe(III)EDTA and the concentration of sodium citrate was developed and can be used to predict the degradation rate of Fe-EDTA for H<sub>2</sub>S removal from biogas. The precipitated solid, called sulfur cake precipitated during the reaction was also recovered and analyzed for its compositions. The result revealed that the sulfur cake contained more than 98% sulfur element almost balances with iron and no significant EDTA was degraded into the solid form.

Finally, the cost of H<sub>2</sub>S removal from biogas using the packed column were analyzed. The investment cost for removing 1,300 mg/m<sup>3</sup> of H<sub>2</sub>S from biogas at 2 L/min was about 10,000-15,000 Baht while the operating cost was 0.81 Baht/m<sup>3</sup> biogas. The cost comparison of using Fe(III)EDTA with other oxidant, KMnO<sub>4</sub> and NaOCl was investigated and it revealed that the operating cost for Fe(III)EDTA system was slightly lower than KMnO<sub>4</sub> system but about two times lower than that of NaOCl.

# CONTENTS

	<b>Page</b>
CONTENTS	ix
LIST OF TABLES	xiii
LIST OF FIGURES	xvii
LIST OF ABBREVIATIONS	xxi
LIST OF SYMBOLS	xxii
CHAPTER 1 Introduction	1
1.1 Background and Rationale	1
1.2 Literature Review	5
1.2.1 Biogas composition and quality requirements for biogas utilization	5
1.2.2 H <sub>2</sub> S gas phase removal methods	7
1.2.2.1 Dry H <sub>2</sub> S removal processes	7
1.2.2.2 Physical solvents process	8
1.2.2.3 Membrane processes	9
1.2.2.4 Biological removal processes	9
1.2.2.5 Liquid phase oxidation processes	10
1.2.3 Iron chelate based hydrogen sulfide removal processes	12
1.2.3.1 Background	12
1.2.3.2 Hydrogen sulfide absorbers	16
1.2.3.3 Regenerators	16
1.2.3.4 Liquid formation	17
1.2.3.5 Production of sulfur	18
1.2.3.6 Using stabilizer eliminate iron chelated application degradation	20
1.2.4. Gas absorption in packed column	29
1.2.4.1 Mass transfer in packed column	30
1.2.4.2 Variables effect on absorption and reaction in packed column	33



## CONTENTS (Continued)

	<b>Page</b>
1.2.5 Theories of model formation and fitting (Multiple regression and Experimental design)	35
1.2.5.1 Choice of experimental design	36
1.2.5.2 Statistical analysis of the data	37
1.2.5.3 Experimental Design	43
1.2.5.4 Model formation and fitting in this work	45
1.3 Research Objectives	45
CHAPTER 2 Removal of H <sub>2</sub> S in Biogas from Concentrated Latex Industry with Iron(III)chelate in Packed Column	46
2.1 Abstract	46
2.2 Introduction	47
2.3 Materials and Method	49
2.3.1 Chemical	49
2.3.2 Preparation of Fe(III)EDTA	49
2.3.3 Apparatus	49
2.3.4 Analysis	52
2.4. Results and Discussion	53
2.4.1 Iron analysis	53
2.4.2 H <sub>2</sub> S Removal efficiency	54
2.4.3 The composition of inlet and outlet biogas	57
2.4.4 Absorption and reaction model for H <sub>2</sub> S removal by oxidation with Fe(III)EDTA in packed column	58
2.4.5 Comparison with other literatures in term of the overall height of a gas film transfer unit, $H_{OG}$ and the overall number gas film transfer unit, $N_{OG}$	65
2.5. Conclusions	66

## CONTENTS (Continued)

	<b>Page</b>
CHAPTER 3 Statistical Optimization of Packed Column Operating Conditions by Response Surface Methodology on Iron(III)chelate Absorption Process for the Removal of Hydrogen Sulfide	68
3.1 Abstract	68
3.2. Introduction	68
3.3 Materials and Method	70
3.3.1 Chemical	70
3.3.2 Apparatus	70
3.3.3 Design of experiments	72
3.3.4 Statistical analysis	74
3.4. Results and discussion	74
3.4.1 Response analysis and interpretation	74
3.4.2 Effects of variables on H <sub>2</sub> S removal efficiency ( <i>RE</i> )	79
3.4.3 Discussion of interaction between the variables	84
3.5. Conclusion	87
CHAPTER 4 The degradation of Fe(III)EDTA in hydrogen sulfide removal	88
4.1 Abstract	88
4.2 Introduction	88
4.3 Materials and Method	91
4.3.1 Chemical	91
4.3.2 Experimental procedure	91
4.4 Results and discussion	93
4.4.1 Degradation of Fe-EDTA kinetics studies	93
4.4.2 Analysis of sulfur cake	100
4.4.3 The effect of chemicals additive into Fe-EDTA solution	101

## CONTENTS (Continued)

	<b>Page</b>
4.4.4 The effect of sodium citrate concentration in Fe-EDTA degradation	102
4.5 Conclusion	106
CHAPTER 5 Economic comparison of using various chemical scrubbing liquid to remove H <sub>2</sub> S from biogas in packed column	107
CHAPTER 6 Summary and Future Works	111
6.1 Summary	111
6.2 Future Works	113
REFERENCES	114
APPENDICES	123
A Experimental Results	124
B Analytical Methods	148
C Essential Experimental Design and Essential Regression	165
VITAE	172

## LIST OF TABLES

Table		Page
1.1	Physical, chemical and safety characteristics of hydrogen sulfide	6
1.2	Biogas utilization technologies and gas processing requirements	8
1.3	Stability Constants ( $\log K_{ML}$ ) of Fe(II)chelates and Fe(III)chelates with Polyamino polycarboxylic acids	13
1.4	The effectiveness of the stabilizers of in comparison to the non-stabilized Fe-NTA (nitrilotriacetic acid) solution	21
1.5	The effectiveness of the stabilizers of in comparison to the non-stabilized Fe-HEDTA (hydroxyethylethylenediaminetriacetic) solution	22
1.6	Stability constants ( $\log K_i$ ) of various iron chelates	28
1.7	ANOVA table for a model with $i$ regressor variables and $n$ observations	39
2.1	Packed bed operating conditions	52
2.2	Mass percent of $CH_4$ and $CO_2$ in the biogas at the inlet and outlet	58
2.3	The actual and the predicted packed height and other related parameters	63
2.4	Parameter values for absorption and reaction modeling	64
2.5	Comparison of $H_{OG}$ and $N_{OG}$ values to other literatures	66
3.1	Experimental range and levels of the independent variables designed by Essential Experimental Design	74
3.2	Circumscribed central composite design matrix of five variables in uncoded variables with observed and predicted $H_2S$ removal efficiency	76
3.3	Analysis of variance (ANOVA) for the regression model	77
3.4	The least square fit and model coefficients (significant of regression coefficients)	77

## LIST OF TABLES (Continued)

<b>Table</b>	<b>Page</b>
<b>4.1</b> Fe-EDTA degradation rate ( $R_d$ ) at various $H_2S$ molar flow rate ( $Q_{H_2S}$ ) and initial Fe(III)EDTA concentration ( $C_{Fe,0}$ )	95
<b>4.2</b> The composition of sulfur cake for each sample	101
<b>4.3</b> Fe-EDTA degradation rate ( $R_d$ ) with and without additive	102
<b>5.1</b> Economic comparison of using Fe(III)EDTA, $KMnO_4$ and $NaOCl$ as a chemical scrubbing liquid in $H_2S$ removal from biogas	108
<b>A-1.1</b> $H_2S$ removal efficiency (%) with time in the oxidation reaction with Fe(III)EDTA (Run No. 1)	124
<b>A-1.2</b> $H_2S$ removal efficiency (%) with time in the oxidation reaction with Fe(III)EDTA (Run No. 2)	125
<b>A-1.3</b> $H_2S$ removal efficiency (%) with time in the oxidation reaction with Fe(III)EDTA (Run No. 3)	126
<b>A-1.4</b> $H_2S$ removal efficiency (%) with time in the oxidation reaction with Fe(III)EDTA (Run No. 4)	127
<b>A-1.5</b> Change of Fe(III)EDTA concentration ( $mol/m^3$ ) as function of reaction time of Run No. 2	128
<b>A-1.6</b> Change of Fe(III)EDTA concentration ( $mol/m^3$ ) as function of reaction time of Run No. 4	128
<b>A-1.7</b> Temperature profile of the scrubbing liquid of Run No. 1	129
<b>A-1.8</b> Temperature profile of the scrubbing liquid of Run No. 2	129
<b>A-1.9</b> Temperature profile of the scrubbing liquid of Run No. 3	130
<b>A-1.10</b> Temperature profile of the scrubbing liquid of Run No. 4	130
<b>A-2.1</b> $H_2S$ removal efficiency ( $RE$ ) at reaction time 10, 15, 20 and 25 min at various conditions	131
<b>A-3.1</b> Experimental conditions for Fe-EDTA kinetics degradation study	133
<b>A-3.2</b> Fe(III) concentration ( $mol/m^3$ )-time data of Run no.1-8	134
<b>A-3.3</b> Fe(III) concentration ( $mol/m^3$ )-time data of Run no.9-16	134

## LIST OF TABLES (Continued)

<b>Table</b>	<b>Page</b>
<b>A-3.4</b> Fe(III) concentration (mol/m <sup>3</sup> )-time data of Run no.17-26	135
<b>A-3.5</b> $-\ln(C_{Fe,t}/C_{Fe,0})$ -time data of Run no.1-8	135
<b>A-3.6</b> $-\ln(C_{Fe,t}/C_{Fe,0})$ -time data of Run no.9-16	136
<b>A-3.7</b> $-\ln(C_{Fe,t}/C_{Fe,0})$ -time data of Run no.17-24	136
<b>A-3.8</b> Soluble Fe(II) concentration (mol/m <sup>3</sup> ) in the solution-time data of Run no.1-8	137
<b>A-3.9</b> Soluble Fe(II) concentration (mol/m <sup>3</sup> ) in the solution-time data of Run no.9-16	137
<b>A-3.10</b> Soluble Fe(II) concentration (mol/m <sup>3</sup> ) in the solution-time data of Run no.17-24	138
<b>A-3.11</b> pH-time data of Run no. 1-8	138
<b>A-3.12</b> pH-time data of Run no. 9-16	139
<b>A-3.13</b> pH-time data of Run no. 17-24	139
<b>A-3.14</b> $k_d$ values of each experimental run	143
<b>A-3.15</b> $R_d$ values of each experimental run	144
<b>A-3.16</b> Analysis of variance (ANOVA) for the regression model Equation (4.4)	145
<b>A-3.17</b> The least square fit and model coefficients (significant of regression coefficients) for the regression model Equation (4.4)	145
<b>A-3.18</b> Analysis of variance (ANOVA) for the regression model Equation (4.5)	145
<b>A-3.19</b> The least square fit and model coefficients (significant of regression coefficients) for the regression model Equation (4.5)	146
<b>A-3.20</b> Analysis of variance (ANOVA) for the regression model Equation (4.6)	146
<b>A-3.21</b> The least square fit and model coefficients (significant of regression coefficients) for the regression model Equation (4.5)	146

## LIST OF TABLES (Continued)

<b>Table</b>		<b>Page</b>
<b>A-3.22</b>	The comparison of Fe found in sulfur cake and degraded from solution after 30 h of reaction	147
<b>B-2.1</b>	Results for performing calibration curve in phenanthroline method	158
<b>B-2.2</b>	Results for Fe calibration curve using atomic absorption spectrometry	161
<b>B-2.3</b>	Iron concentration in samples as determined by phenanthroline method and atomic absorption spectrophotometric method	163

## LIST OF FIGURES

<b>Figure</b>	<b>Page</b>
1.1 Schematic of Fe-EDTA complex	24
1.2 The EDTA degradation during H <sub>2</sub> S oxidation with Fe-EDTA	25
1.3 Thiosulfate ion associated with the dimer form of the NTA-iron complex	25
1.4 The effect of ligands and mixed ligands in % iron solubilization	28
2.1 Schematic diagram of the gas scrubbing packed column for H <sub>2</sub> S removal from biogas	50
2.2 The Pilot packed column used in H <sub>2</sub> S removal from biogas process	51
2.3 UV-VIS bands of (a) Fe(III)EDTA, (b) Na <sub>2</sub> S and (c) Fe(II) phenanthroline	53
2.4 Standard curve for Fe determination by photometric method at 510 nm	54
2.5 H <sub>2</sub> S removal efficiency (%) with time in the oxidation reaction with Fe(III)EDTA at various conditions	56
2.6 Change of Fe(III)EDTA concentration (mol/m <sup>3</sup> ) as function of reaction time for Run No. 2 and Run No. 4	57
2.7 Temperature profile of the scrubbing liquid during the reaction period	58
3.1 A schematic of the laboratory packed column system	71
3.2 Laboratory packed column used for H <sub>2</sub> S removal from gas stream	72
3.3 Normal probability plot	78
3.4 Predicted and experimental H <sub>2</sub> S removal efficiency	79
3.5 Effect of height of packed bed ( <i>h</i> ) on removal efficiency ( <i>RE</i> ) ( <i>L</i> = 0.5 mL/s, <i>C</i> <sub>Fe,0</sub> = 160 mol/m <sup>3</sup> , <i>G</i> = 0.1 L/s, <i>C</i> <sub>H<sub>2</sub>S(g),in</sub> = 0.07 mol/m <sup>3</sup> )	81
3.6 Effect of liquid flow rate ( <i>L</i> ) on removal efficiency ( <i>RE</i> ). ( <i>h</i> = 0.30 m, <i>C</i> <sub>Fe,0</sub> = 160 mol/m <sup>3</sup> , <i>G</i> = 0.1 L/s, <i>C</i> <sub>H<sub>2</sub>S(g),in</sub> = 0.08 mol/m <sup>3</sup> )	81



## LIST OF FIGURES (Continued)

Figure		Page
3.7	Effect of initial Fe(III)EDTA concentration ( $C_{Fe,0}$ ) on removal efficiency ( $RE$ ). ( $h = 0.30$ m, $L = 0.5$ mL/s, $G = 0.1$ L/s, $C_{H_2S}(g)_{in} = 0.08$ mol/m <sup>3</sup> )	82
3.8	Effect of liquid to gas ratio ( $L/G$ ) on removal efficiency ( $RE$ ) for low $L/G$ . ( $h = 0.30$ m, $L = 0.17$ – $0.83$ mL/s, $C_{Fe,0} = 160$ mol/m <sup>3</sup> , $G = 0.1$ L/s, $C_{H_2S}(g)_{in} = 0.08$ mol/m <sup>3</sup> )	82
3.9	Effect of liquid to gas ratio ( $L/G$ ) on removal efficiency ( $RE$ ) for large $L/G$ . ( $h = 0.30$ m, $L = 0.5$ mL/s, $C_{Fe,0} = 16$ mol/m <sup>3</sup> , $G = 0.03$ – $0.17$ L/s, $C_{H_2S}(g)_{in} = 0.09$ mol/m <sup>3</sup> )	83
3.10	Effect of gas flow rate ( $G$ ) on removal efficiency ( $RE$ ). ( $h = 0.30$ m, $L = 0.5$ mL/s, $C_{Fe,0} = 160$ mol/m <sup>3</sup> , $C_{H_2S}(g)_{in} = 0.09$ mol/m <sup>3</sup> )	83
3.11	Effect of inlet H <sub>2</sub> S concentration ( $C_{H_2S}(g)_{in}$ ) on removal efficiency. ( $h = 0.30$ m, $L = 0.5$ mL/s, $C_{Fe,0} = 160$ mol/m <sup>3</sup> , $G = 0.1$ L/s)	84
3.12	Interaction between initial Fe(III)EDTA concentration ( $C_{Fe,0}$ ) and height of packed bed ( $h$ ) ( $L = 0.5$ mL/s, $G = 0.1$ L/s, $C_{H_2S}(g)_{in} = 0.08$ mol/m <sup>3</sup> )	85
3.13	Interaction between inlet H <sub>2</sub> S concentration ( $C_{H_2S}(g)_{in}$ ) and packing bed height ( $h$ ). ( $L = 0.5$ mL/s, $C_{Fe,0} = 160$ mol/m <sup>3</sup> , $G = 0.1$ L/s)	86
3.14	Interaction between initial Fe(III)EDTA concentration ( $C_{Fe,0}$ ) and liquid flow rate ( $L$ ). ( $h = 0.30$ m, $G = 0.1$ L/s, $C_{H_2S}(g)_{in} = 0.08$ mol/m <sup>3</sup> )	86
4.1	The semi-batch system	92
4.2	Soluble Fe concentration ( $C_{Fe}$ )-time of various H <sub>2</sub> S molar flow rate ( $Q_{H_2S}$ ) at initial Fe(III)EDTA concentration ( $C_{Fe,0}$ ) of 5.78 mol/m <sup>3</sup>	94

## LIST OF FIGURES (Continued)

Figure		Page
4.3	Soluble Fe concentration ( $C_{Fe}$ )-time of various initial Fe(III)EDTA concentration ( $C_{Fe,0}$ ) at the H <sub>2</sub> S molar flow rate ( $Q_{H_2S}$ ) of $2.0 \times 10^{-3}$ mol/h	94
4.4	Effect of H <sub>2</sub> S molar flow rate on the degradation ( $Q_{H_2S}$ ) of Fe(III)EDTA. First order plots for Fe(III)EDTA degradation at the initial Fe(III)EDTA concentration of $5.78 \text{ mol/m}^3$	97
4.5	Effect of initial Fe(III)EDTA concentration ( $C_{Fe,0}$ ) on the degradation of Fe(III)EDTA. First order plots for Fe(III)EDTA degradation at the H <sub>2</sub> S molar flow rate of $2.0 \times 10^{-3}$ mol/h	97
4.6	Effect of H <sub>2</sub> S molar flow rate ( $Q_{H_2S}$ ) on observed degradation rate constant ( $k_d$ ) at the initial Fe(III)EDTA concentration of $5.78 \text{ mol/m}^3$	98
4.7	Effect of initial Fe(III)EDTA concentration ( $C_{Fe,0}$ ) on observed degradation rate constant ( $k_d$ ) at the average H <sub>2</sub> S molar flow rate of $2.0 \times 10^{-3}$ mol/h	98
4.8	Plot of experimental and predicted $k_d$ (from Equation (4.4))	99
4.9	Plot of <i>measured</i> $R_d$ and predicted $R_d$ calculated using $k_d(Q_{H_2S}, C_{Fe,0})$ model	100
4.10	Effect of sodium citrate concentration ( $C_{CI}$ ) on the degradation of Fe(III)EDTA. First order plots for Fe(III)EDTA degradation at the H <sub>2</sub> S molar flow rate of $1.84 \times 10^{-3}$ mol/h and initial Fe(III)EDTA concentration of $5.80 \text{ mol/m}^3$	103
4.11	Effect of sodium citrate concentration ( $C_{CI}$ ) on observed degradation rate constant ( $k_d$ ) at the average H <sub>2</sub> S molar flow rate of $1.84 \times 10^{-3}$ mol/h and initial Fe(III)EDTA concentration of $5.80 \text{ mol/m}^3$	104
4.12	Plot of <i>measured</i> $R_d$ and predicted $R_d$ calculated using $k_d(Q_{H_2S}, C_{Fe,0}, C_{CI})$ model	105

## LIST OF FIGURES (Continued)

<b>Figure</b>		<b>Page</b>
<b>A-3.1</b>	Soluble Fe concentration-time of Run no.1-8: linear equations with $R^2$ values	140
<b>A-3.2</b>	Soluble Fe concentration-time of Run no.9-16: linear equations with $R^2$ values	140
<b>A-3.3</b>	Soluble Fe concentration-time of Run no.17-24: linear equations with $R^2$ values	141
<b>A-3.4</b>	$-\ln(C_{Fe,t}/C_{Fe,0})$ -time of Run no.1-8: linear equations with $R^2$ values	141
<b>A-3.5</b>	$-\ln(C_{Fe,t}/C_{Fe,0})$ -time of Run no.9-16: linear equations with $R^2$ values	142
<b>A-3.6</b>	$-\ln(C_{Fe,t}/C_{Fe,0})$ -time of Run no.17-24: linear equations with $R^2$ values	142
<b>B-2.1</b>	Calibration curve for Fe determination by phenanthroline method at 510 nm	159
<b>B-2.2</b>	Calibration curve for iron determination by using atomic absorption spectrometry	161
<b>B-2.3</b>	Comparison Fe standard calibration curve and standard addition curve method of Fe-EDTA sample before and after reaction	162
<b>B-2.4</b>	Comparison Fe standard calibration curve and standard addition curve method of Fe-EDTA+sodium citrate sample before and after reaction	162
<b>B-2.5</b>	Comparison Fe standard calibration curve and standard addition curve method of Fe-EDTA+sodium thiosulfate sample before and after reaction	163

## LIST OF ABBREVIATIONS

CRLI	Concentrated rubber latex industry
EDTA	Ethylenediaminetetraacetic acid
HEDTA	Hydroxyethyl)-ethylenediaminetriacetic acid
NTA	Nitrilotriacetic acid
CDTA	Cyclohexane-1,2-diaminetetraacetic acid
CCD	Central composite design
RSM	Response Surface Methodology
DTA	Racemic-propylenediaminetetraacetic acid
DMEDTA	Racemic-1,2-dimethylethylenediaminetetraacetic acid
TMDTA	Trimethylenediaminetetraacetic acid
EEDTA	Oxybis(ethylenitrilo)tetraacetic acid
EGTA	Ethylenebis(oxyethylenitrilo)tetraacetic acid
TTHA	Triethylenetetraminehexaacetic acid
EIDA	Ethyl imino diacetic acid
IDA	Imino diacetic acid
ANOVA	Analysis of variance
SSR	Regression Sum of Squares
SSE	Sum of Squared Errors or Error Sum of Squares
PRESS	Prediction Error Sum of Square
CV	Coefficient of variance
R	Correlation coefficient
R <sup>2</sup>	Coefficient of determination

## LIST OF SYMBOLS

### Chapter 2

$C_{Fe(III)EDTA,in}$	Initial concentration of Fe(III)EDTA (mol/m <sup>3</sup> )
$C_{Fe(III)EDTA}$	Fe(III)EDTA concentration at any time (mol/m <sup>3</sup> )
$C_{Fe-EDTA}$	Total iron concentration (mol/m <sup>3</sup> )
$C_{Fe(II)EDTA}$	The Fe(II)EDTA concentration (mol/m <sup>3</sup> )
$C_{H_2S}(g)_{in}$	H <sub>2</sub> S concentration in biogas at inlet (mol/m <sup>3</sup> )
$C_{H_2S}(g)_{out}$	H <sub>2</sub> S concentrations in biogas at outlet (mol/m <sup>3</sup> )
$C_{H_2Si}(g)$	Concentration of H <sub>2</sub> S at the gas-liquid interface (mol/m <sup>3</sup> )
$C_{H_2S}$	Concentration of H <sub>2</sub> S in bulk liquid phase (mol/m <sup>3</sup> )
$C_{H_2S}(g)$	Concentration of H <sub>2</sub> S in bulk gas phase (mol/m <sup>3</sup> )
$G$	Biogas flow rate (m <sup>3</sup> /s)
$-r_{H_2S}$	H <sub>2</sub> S mass transfer rate (mol/m <sup>3</sup> ·s)
$a_i$	Gas-liquid interfacial area per volume of bed (m <sup>2</sup> /m <sup>3</sup> )
$k_G$	Gas film mass transfer coefficient (m/s)
$k_L$	Liquid film mass transfer coefficient (m/s)
$Re_G$	Reynolds number in the gas phase
$Sc_G$	Schmidt number in the gas phase
$W_G$	Superficial mass gas velocity (kg/m <sup>2</sup> ·s)
$d_P$	Nominal packing diameter (m)
$\mu_G$	Gas viscosity (Pa·s)
$\rho_G$	Gas density (kg/m <sup>3</sup> )
$D_{H_2S,G}$	Diffusivity of H <sub>2</sub> S in the gas phase (m <sup>2</sup> /s)
$D_{H_2S,L}$	Diffusivity of H <sub>2</sub> S in liquid (m <sup>2</sup> /s)
$D_{Fe(III)EDTA,L}$	Diffusivity of Fe(III)EDTA (m <sup>2</sup> /s)
$P$	Pressure (atm)

## LIST OF SYMBOLS (Continued)

$P_{H_2S_i}$	Inlet partial pressure of H <sub>2</sub> S (atm)
$P_{C,H_2S}$	Critical pressure of H <sub>2</sub> S (atm)
$P_{C,CH_4}$	Critical pressure of CH <sub>4</sub> (atm)
$T_{C,H_2S}$	Critical temperature of H <sub>2</sub> S (K)
$T_{C,CH_4}$	Critical temperature of CH <sub>4</sub> , (K)
$M_{H_2S}$	Molecular weights of H <sub>2</sub> S (g/mol)
$M_{CH_4}$	Molecular weights of CH <sub>4</sub> (g/mol)
$He$	is defined as $H_{H_2S} / RT$
$H_{H_2S}$	Henry's law constant of H <sub>2</sub> S (Pa m <sup>3</sup> /mol)
$R$	Gas constant (m <sup>3</sup> Pa /mol K)
$T$	Reaction temperature (K)
$E_{H_2S}$	Liquid film enhancement factor
$M_H$	The Hatta modulus
$v_L$	Gas mass flux (kg/m <sup>2</sup> ·s)
$a_T$	Specific surface area (m <sup>2</sup> /m <sup>3</sup> )
$\mu_L$	Liquid viscosity (Pa·s)
$\rho_L$	Liquid density (kg/m <sup>3</sup> )
$g$	Gravitational acceleration (m/s <sup>2</sup> )
$k_r$	Reaction rate constant (m <sup>3</sup> /mol·s)
$f_l$	Ratio of volume of liquid to the reactor volume
$h$	The height of the absorption tower (m)
$b$	Stoichiometric coefficient for Fe(III)EDTA
$A$	Cross-sectional area of the tower (m <sup>2</sup> )
$H_{OG}$	The overall height of the gas film transfer unit (m)
$N_{OG}$	The overall number gas film transfer unit
$W_{H_2S}$	Superficial H <sub>2</sub> S mass velocity (kg /m <sup>2</sup> ·s)

## LIST OF SYMBOLS (Continued)

### Chapter 3

$G$	Gas flow rate (L/s)
$C_{H_2S(g),in}$	Inlet H <sub>2</sub> S concentration (mol/m <sup>3</sup> )
$C_{Fe,0}$	Initial Fe(III)EDTA concentration (mol/m <sup>3</sup> )
$h$	Height of packed bed (m)
$L$	Scrubbing liquid flow rate (mL/s)
$RE$	Average H <sub>2</sub> S removal efficiency (%)
$L/G$	Liquid to gas ratio (mL/L)

### Chapter 4

$R_d$	Fe-EDTA degradation rate (mol m <sup>-3</sup> h <sup>-1</sup> )
$k_d$	Pseudo first order degradation rate constant (h <sup>-1</sup> )
$C_{Fe,0}$	Concentration of Fe(III)EDTA at initial (mol/m <sup>3</sup> )
$C_{Fe,t}$	Concentration of Fe(III)EDTA at any reaction time (mol/m <sup>3</sup> )
$t$	Reaction time (h)
$Q_{H_2S}$	H <sub>2</sub> S molar flow rate (mol/h)
$C_{Cl}$	Sodium citrate concentration (mol/m <sup>3</sup> )

# CHAPTER 1

## Introduction

### 1.1 Background and Rationale

Anaerobic wastewater treatment is generally advantageous for removing organic matter from wastewater without consuming a large amount of electrical energy. A by-product of the anaerobic treatment is biogas which can be used as a renewable energy. Due to the energy crisis, industries are seeking various kinds of the alternative energies, including biogas. Biogas can be produced from the wastewater of many industries including the beverage, animal farm, starch, palm oil and rubber industries. The concentrated rubber latex industry (CRLI) is the main industry in the southern part of Thailand. The wastewater from CRLI is being used to produce biogas which is currently used as an indirect heat source for rubber block drying. A problem arises since CRLI wastewater contains high sulfate content, up to 1000 mg/L (Rerngnarong, 2007), due to the use of sulfuric acid,  $H_2SO_4$ , in skim rubber production. Consequently, the biogas produced from the wastewater of CRLI is high  $H_2S$  concentration of 0.35-0.77 mol/m<sup>3</sup>, which prevents its direct use as a fuel.

Biogas production is still increasing in Thailand, especially in the pig farms that can be found in all parts of the country. Owners use pig excrement to produce biogas and then use the biogas to generate electricity. This electricity can be used for building ventilators, heating baby pig nurseries and pumping for the farm. Although the amount of  $H_2S$  in biogas produced from pig farm is much lower than that produced through CRLI (around 1200-1600 mg/m<sup>3</sup> or 0.035-0.047 mol/m<sup>3</sup>) it is still greater than the minimum  $H_2S$  concentration of generator use (100-200 mg/m<sup>3</sup>). Thus, corrosion in the generation equipment occurs. In order to use biogas more effectively and safely for an engine, the removal of  $H_2S$  from the biogas is necessary and an effective  $H_2S$  removal system is required.

Numerous processes for  $H_2S$  removal from biogas have been developed, including amine absorption, alkaline absorption, dry-based processes,



caustic absorption, membrane, biological processes and chemical oxidation. Iron is an excellent oxidizing agent for the conversion of  $\text{H}_2\text{S}$  to elemental sulfur. Iron, in its ferric state, can be held in a solution by a chelating agent (i.e. ethylenediaminetetraacetic acid (EDTA), (hydroxyethyl)ethylenediaminetriacetic acid (HEDTA), or nitrilotriacetic acid (NTA)). The intent of the process is to oxidize hydrosulfide ( $\text{HS}^-$ ) ions to elemental sulfur by the reduction of the ferric (Fe(III)) iron to ferrous (Fe(II)) iron, and subsequently, the ferrous ions are then oxidized back to ferric ions by oxygen in the air. In recent years, the gas desulfurization processes based on iron chelate chemistry has received increasing attention from both industrial and academic research groups. Demmink and Beenackers (1998), using a new penetration model for mass transfer parallel to chemical reaction, describes the oxidative absorption of  $\text{H}_2\text{S}$  by using ferric chelates of EDTA and HEDTA. Iliuta and Larachi (2003) presented a modeling framework for the design of a scrubbing packed bed column for a bifunctional redox process for treating  $\text{H}_2\text{S}$  containing effluents arising from the kraft mill processes. The framework consisted of an exhaustive absorption reaction transport model in which are integrated both the oxidation of  $\text{H}_2\text{S}$  in reactive ferric chelate solutions of EDTA and the regeneration of ferrous chelates resulting from oxidation of  $\text{H}_2\text{S}$ . The kinetic effect of electrolytes and impact of pH on the oxidation of  $\text{H}_2\text{S}$  with Fe(III)CDTA in anoxic conditions were determined by Piché and Larachi (2006a) and Piché and Larachi (2006b). They proposed the reaction mechanism of  $\text{H}_2\text{S}$  oxidation on both effects. Demmink *et al.* (1998) reported that the freshly precipitated sulfur particles acted as the catalyst for  $\text{H}_2\text{S}$  absorption into aqueous solution of Fe-NTA and Demmink *et al.* (2002) described this phenomenon by developing a model based on Higbie's penetration theory. Horikawa *et al.* (2004) used Fe(III)EDTA to remove  $\text{H}_2\text{S}$  from synthetic biogas using a lab scale randomly packed column. The chelated iron process is now used to remove  $\text{H}_2\text{S}$  from gas streams in several industries, such as: natural gas processing, geothermal plants, refinery fuel gas, municipal odor control, landfill gas and municipal waste gasification.

Although much effort has been put into the development of  $\text{H}_2\text{S}$  removal process using wet scrubbing with iron chelate oxidation as mentioned above, the previous works, however, have been focused on  $\text{H}_2\text{S}$  removal from the atmospheric emissions of the sulfur or sulfate related industries such as the natural gas

and the oil refining industry and the pulp and paper industry. Only a few works dealt with H<sub>2</sub>S removal from biogas and these investigated using a synthetic biogas or mixture of H<sub>2</sub>S with N<sub>2</sub>, CO<sub>2</sub> and air. It is noteworthy that the iron chelate route has never been explored with real biogas produced from the wastewater of the concentrated rubber latex industry where the H<sub>2</sub>S concentration is very high compared to the H<sub>2</sub>S content in atmospheric emissions of the industries or in the biogas produced from others sectors such as the animal farm and the palm oil industries. The concentration of H<sub>2</sub>S in the gas stream is known to play an important role on H<sub>2</sub>S removal efficiencies (Piché *et al.*, 2005). The study of H<sub>2</sub>S removal from the biogas of the concentrated rubber latex industry will provide the useful information to operate and design the wet scrubber with iron chelate process under high H<sub>2</sub>S concentration. The aim of this work was removing H<sub>2</sub>S from CRLI-produce biogas using an industrially sized packed column which can handle H<sub>2</sub>S concentrations that up to 0.77 mol/m<sup>3</sup>. The suitable operating conditions (i.e., Fe(III)EDTA concentration, flow of Fe(III)EDTA and air) for this case are determined for the highest removal efficiency. A mathematical model describing the absorption and the reaction between H<sub>2</sub>S and Fe(III)EDTA in a packed column under high H<sub>2</sub>S concentrations is also proposed.

The operating variables, such as the scrubbing liquid flow rate, the gas mass flow rate, the liquid to gas ratio ( $L/G$ ), the initial scrubbing concentration and height of packed bed are known to influence packed bed performance. Because the concentrations of H<sub>2</sub>S from actual biogas vary from day to day, repeated tests at the same input H<sub>2</sub>S concentration are not possible. A laboratory scale packed column was used to study the affect of the various operating conditions on H<sub>2</sub>S removal.

Chen *et al.* (2001) studied the feasibility of H<sub>2</sub>S removal from air streams utilizing aqueous solutions in a pilot scale packed bed scrubber. They found the gas mass flow rate played a significant role in the process while the liquid flow rate demonstrated a minimal effect on absorption efficiency. Godini and Mowla (2008) reported about the effect of amine concentration to H<sub>2</sub>S and CO<sub>2</sub> absorption. The results showed that increasing amine concentration increases the driving force for absorption of both H<sub>2</sub>S and CO<sub>2</sub> and thus their absolute removal efficiency. However, H<sub>2</sub>S absorption is influenced by more than one factor and thus can be poorly

understood when examined by changing one separate factor at a time. Response Surface Method (RSM) design was used to identify the detailed dependence of different factors. As far we know, no study has been done on H<sub>2</sub>S removal from gas stream by oxidation with Fe(III)EDTA by using RSM. Therefore in this section of research, the experiments were performed according to Central composite design (CCD) and RSM to understand the relationship between the operating variables and the average H<sub>2</sub>S removal efficiency (*RE*). An empirical model correlating the *RE* to the five variables, the scrubbing liquid flow rate (*L*), the gas flow rate (*G*), the inlet H<sub>2</sub>S concentration ( $C_{H_2S}(g)_{in}$ ), the initial Fe(III)EDTA concentration ( $C_{Fe,0}$ ) and the height of packed bed (*h*) was then developed. This model will provide a better understanding of the interactions involved in the H<sub>2</sub>S removal process at the industrial scale and allow faster development of more efficient systems.

The polyamino polycarboxylate chelated iron process is extremely effective and allows total conversion of H<sub>2</sub>S to be obtained. It is also a very flexible process and has been widely utilized throughout the world. This process, however, has various drawbacks. Above all, when operating in an alkaline solution, there is the radical oxidation of the iron ligand with the degradation of the ligand itself and the precipitation of iron as sulfide. This has two strong consequences on the process: the ligand, which is expensive, must be continuously reintegrated, the sulfur produced has iron sulfide as an impurity which makes it unsuitable for commercialization. For these reason the ability to reduce the degradation of iron chelate is necessary. The prediction of the extent and rate of Fe-EDTA degradation is vital in the estimation of the exact Fe(III)EDTA make up rate needed to maintain the H<sub>2</sub>S absorption capacity of the removal process. The goal of this part of research is to determine the potential for Fe(III)EDTA degradation as a function of degradation parameters such as the H<sub>2</sub>S molar flow rate, the initial Fe(III)EDTA concentration, and the concentration of the stabilizer based on the initial Fe-EDTA degradation rate.

## 1.2 Literature Review

### 1.2.1 Biogas composition and quality requirements for biogas utilization

In the world that is increasingly accepting the imperative nature of sustainable development, the junction of energy and environment has become a field of intense activity, with both R&D and technology implementation given top priority. Biogas, naturally occurring from the decomposition of all living matter, has yielded important industrial products or by-products. Its commercial value has risen for two reasons because its release into the atmosphere contributes largely to greenhouse gas concentration with consequent and significant remediation costs, and because its energetic content is high. Systematic biogas sources linked to anthropogenic activities include non-exclusive units of: landfill, commercial composting, wastewater sludge anaerobic fermentation, animal farm manure anaerobic fermentation, and agro food industry sludge anaerobic fermentation. The biogas produced by all these activities is rich in CH<sub>4</sub> (typically ranging between 35 and 75%vol), and its higher heating value is between 15 and 30 MJ/Nm<sup>3</sup> (Abatzoglou and Boivin, 2009).

Biogas composition depends heavily on the feedstock, but mainly consists of methane and carbon dioxide, with smaller amounts (ppm) of H<sub>2</sub>S and ammonia. Trace amounts of organic sulfur compounds, halogenated hydrocarbons, hydrogen, nitrogen, carbon monoxide, and oxygen are also occasionally present. Usually, the mixed gas is saturated with water vapor and may contain dust particles and siloxanes. The most common contaminant is H<sub>2</sub>S and other malodorous sulfur containing compounds (i.e., mercaptans, such as CH<sub>3</sub>SH) coming from the anaerobic fermentation of sulfur bearing organic molecules (i.e., proteins or another sulfur containing chemical). Depending on the composition of the organic material fermented, the H<sub>2</sub>S content of biogas can vary from some 10 to about 10,000 ppmv (0.0001–1%vol). This contaminant, besides its bad smell, is highly non desirable in energy recovery processes because it converts to highly corrosive, unhealthy and environmentally hazardous sulfur dioxide (SO<sub>2</sub>) and sulfuric acid H<sub>2</sub>SO<sub>4</sub>. Its removal is a must for any eventual utilization of biogas.

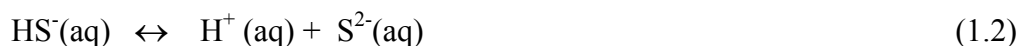
H<sub>2</sub>S is poisonous, odorous, and highly corrosive. Some characteristics of H<sub>2</sub>S are described in Table 1.1. Because of these characteristics, H<sub>2</sub>S removal is usually performed directly at the gas production site.

**Table 1.1** Physical, chemical and safety characteristics of hydrogen sulfide

Characteristics	Value
Molecular Weight	34.08
Specific Gravity (relative to air)	1.192
Auto Ignition Temperature	250° C
Explosive Range in Air	4.5 to 45.5 %
Odor Threshold	0.47 ppb
8-hour time weighted average (TWA) (OSHA)	10 ppm
15-minute short term exposure limit (STEL) (OSHA)	15 ppm
Immediately Dangerous to Life of Health (IDLH) (OSHA)	300 ppm
Henry's constant (atm / mole fraction) at 20 °C	0.483 x 10 <sup>-5</sup>
Henry's constant (atm / mole fraction) at 30 °C	0.609 x 10 <sup>-5</sup>

Source: OSHA (2002), Occupational Safety and Health Administration, [www.OSHA.gov](http://www.OSHA.gov)

H<sub>2</sub>S is a very weak acid dissociating in two steps (Kolthoff *et al.*, 1963).



At an ionic strength of 1.0 M (KCl) and 20 °C the ionization constants of H<sub>2</sub>S are

$$\frac{[\text{H}^+][\text{HS}^-]}{[\text{H}_2\text{S}]} = K_1 = 1.32 \times 10^{-7} \quad \text{p}K_1 = 6.88 \quad (1.3)$$

$$\frac{[\text{H}^+][\text{S}^{2-}]}{[\text{HS}^-]} = K_2 = 7.1 \times 10^{-15} \quad \text{p}K_2 = 14.15 \quad (1.4)$$

$$\frac{[H^+]^2[S^{2-}]}{[H_2S]} = K_1K_2 = 9.4 \times 10^{-22} \quad (1.5)$$

Since biogas is similar in composition to raw natural gas, purification techniques developed and used in the natural gas industry can be evaluated for their suitability with biogas systems. The ultimate process chosen is dependent on the gas use, composition, physical characteristics, energy and resources available, byproducts generated, and the volume of gas to be treated.

Biogas can be used for all applications designed for natural gas, assuming sufficient purification. On site, stationary biogas applications generally have fewer gas processing requirements. A summary of potential biogas utilization technologies and their gas processing requirements are given in Table 1.2.

Technologies such as boilers and stirling engines have the least stringent gas processing requirements because of their external combustion configurations. Internal combustion engines and micro turbines are the next most tolerant to contaminants. Fuel cells are generally less tolerant to contaminants due to the potential for catalytic poisoning. Upgrading to natural gas quality usually requires expensive and complex processing and must be done when injection into a natural gas pipeline or production of vehicle fuel is desired.

## **1.2.2 H<sub>2</sub>S gas phase removal methods**

H<sub>2</sub>S removal processes will be divided into dry-based, liquid-based, physical-solvent, membrane, alternative, and biological processes for this summary.

### **1.2.2.1 Dry H<sub>2</sub>S removal processes**

All of the dry sorption processes are configured with the dry media in box or tower type vessels where gas can flow upwards or downwards through the media. Several dry media have been used for H<sub>2</sub>S removal process such as iron oxides, zinc oxides, alkaline solids and adsorbents. Molecular Sieves and Activated Carbon are widely used as an effectiveness adsorbent. Since all of the dry sorption

media to be discussed eventually becomes saturated with contaminant and inactive, it is common to have two vessels operated in parallel so one vessel can remain in service while the other is offline for media replacement.

**Table 1.2** Biogas utilization technologies and gas processing requirements

<b>Technology</b>	<b>Recommended Gas Processing Requirements</b>
Heating (Boilers)	H <sub>2</sub> S < 1000 ppm, 0.8-2.5 kPa pressure, remove condensate (kitchen stoves: H <sub>2</sub> S < 10 ppm)
Internal Combustion Engines	H <sub>2</sub> S < 100 ppm, 0.8-2.5 kPa pressure, remove condensate, remove siloxanes (Otto cycle engines more susceptible to H <sub>2</sub> S than diesel engines)
Microturbines	H <sub>2</sub> S tolerant to 70,000 ppm, > 350 BTU/scf, 520 kPa pressure, remove condensate, remove siloxanes
Fuel Cells	PEM: CO < 10 ppm, remove H <sub>2</sub> S PAFC: H <sub>2</sub> S < 20 ppm, CO < 10 ppm, Halogens < 4 ppm MCFC: H <sub>2</sub> S < 10 ppm in fuel (H <sub>2</sub> S < 0.5 ppm to stack), Halogens < 1 ppm SOFC: H <sub>2</sub> S < 1 ppm, Halogens < 1 ppm
Stirling Engines	Similar to boilers for H <sub>2</sub> S, 1-14 kPa pressure
Natural Gas Upgrade	H <sub>2</sub> S < 4 ppm, CH <sub>4</sub> > 95%, CO <sub>2</sub> < 2 % volume, H <sub>2</sub> O < (1x10 <sup>-4</sup> ) kg/MMscf, remove siloxanes and particulates, > 3000 kPa pressure

Source: Zicari, M., 2003

### 1.2.2.2 Physical solvents process

Physical solvents, where the acid gases are simply dissolved in a liquid and flashed off elsewhere by reducing the pressure, have been employed with limited

success. Since these processes depend on partial pressure, driving forces, some product will invariably be lost, especially at higher pressures.

Liquids with increased solubility for CO<sub>2</sub> and H<sub>2</sub>S are typically chosen over water, but the principal advantages of water as an absorbent are its availability and low cost. Solvents such as methanol, propylene carbonate, and ethers of polyethylene glycol, among others, are offered as improved physical solvents. Criteria for solvent selection include high absorption capacity, low reactivity with equipment and gas constituents, and low viscosity. Additionally, loss of product can be higher with these solvents.

### **1.2.2.3 Membrane processes**

H<sub>2</sub>S has a better sorption and diffusion behavior than CH<sub>4</sub> so that polymer membrane separation to purify biogas can be performed (Busca and Pistarino, 2003). Membranes are generally not used for selective removal of H<sub>2</sub>S from biogas but are becoming more attractive for upgrading of biogas to natural gas standards because of attributes such as reduced capital investment, ease of operation, low environmental impact, gas dehydration capability, and high reliability. Membrane separation techniques do not seem to have more extensive application for sulfide compound recovery up to now (Busca and Pistarino, 2003). This process is still in a developmental stage but may prove to be desirable in the future.

### **1.2.2.4 Biological removal processes**

Biological processes are widely employed for H<sub>2</sub>S removal, especially in biogas applications. They are usually cited and considered as economical and environmentally friendly, notably because chemical use is limited. Biologically active agents have since been used in a variety of process arrangements, such as biofilters, fixed film bioscrubbers, and suspended growth bioscrubbers (Dawson, 1993). These processes may also be effective at removing multiple contaminants from a gas stream, increasing their functionality. Different bacteria can be responsible for the oxidation of sulfur to sulfate ions. Mixed micro organism cultures naturally grow on appropriate

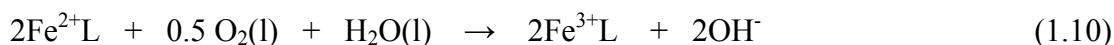


natural biofilter beds and abatement of all volatile compounds can be obtained simultaneously. This technique is becoming widely accepted due to the high processing efficiency at low sulfur concentration, the moderate capital cost and the very low maintenance cost (Busca and Pistarino, 2003).

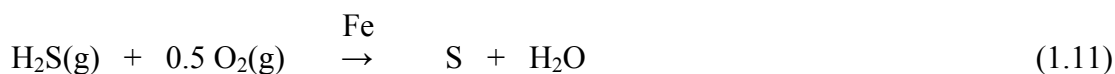
#### 1.2.2.5 Liquid phase oxidation processes

Oxidation is a process involving a loss of electrons while reduction involves a gain. The substance that gains electrons in an oxidation reduction reaction is an oxidant. The substance that loses electron is a reductant. The common chemical in liquid phase H<sub>2</sub>S removal involved several oxidants. The general oxidants are sodium hypochlorite (NaOCl), potassium permanganate (KMnO<sub>4</sub>), hydrogen peroxide (H<sub>2</sub>O<sub>2</sub>), sodium hydroxide (NaOH), amine Solutions, metal salts and iron chelate. Among the various chemicals for removal H<sub>2</sub>S, iron chelate are the most common and widely used.

In this process, iron, in its ferric state (+3), is held in solution by chelating agents (L). The intent of the process is to oxidize hydrosulfide (HS<sup>-</sup>) ions to elemental sulfur by the reduction of the ferric (Fe(III)) iron to ferrous (Fe(II)) iron, and the subsequent reoxidation of the ferrous ions to ferric ions by contact with air. The chemistry of all chelated iron processes is summarized as follows with (l) and (g) representing the liquid and vapor states, respectively;



### Overall Reaction



Equations (1.6) and (1.7) represent the absorption of H<sub>2</sub>S into the aqueous, chelated iron solution and its subsequent ionization, while equation (1.8) represents the oxidation of hydrosulfide ions to elemental sulfur and the accompanying reduction of the ferric iron to the ferrous state. Equations (1.9) and (1.10) represent the absorption of oxygen into the aqueous solution followed by oxidation of the ferrous iron back to the ferric state. Equations (1.8) and (1.10) are very rapid. Consequently, iron-based systems generally produce relatively small amounts of by product thiosulfate ions, and in properly designed units, air streams can actually be processed. However, equations (1.6) and (1.9) are relatively slow and are the rate controlling steps in all chelated iron processes.

It is interesting to note that the chelating agents do not appear in the process chemistry, and in the overall chemical reaction (Equation (1.11)), the iron cancels out. So why is chelated iron required at all, if it doesn't take part in the overall reaction? The iron serves two purposes in the process chemistry. First, it serves as an electron donor and acceptor, or in other words, a reagent. Secondly, it serves as a catalyst in accelerating the overall reaction. Because of this dual purpose, the iron is often called a "catalytic reagent". The chelating agent(s) do not take part at all in the process chemistry. The sole purpose of the chelating agents is to solubilize iron in water, thus making it possible to have a solution of iron (Heguy *et al.*, 2003).

Iron-based, liquid oxidation has developed into a very versatile processing scheme for treating gas streams containing moderate amounts of H<sub>2</sub>S. Advantages of these systems include the ability to treat both aerobic and non-aerobic gas streams, removal efficiencies in excess of 99.9%, essentially 100% turndown on H<sub>2</sub>S concentration and quantity, and the production of innocuous products and by-products.

Because of the advantage and applicable, iron chelated with EDTA was chosen for removing H<sub>2</sub>S from biogas in this study. The following will describe more details and literature review.

### 1.2.3 Iron chelate based hydrogen sulfide removal processes

#### 1.2.3.1 Background

Iron is an excellent oxidizing agent for the conversion of  $H_2S$  to element sulfur. However, due to the very low solubility of iron in aqueous solutions, the iron had to be present in the dry state (iron sponge) or in suspension (the Ferrox process) or compounded with toxic materials such as cyanides. In the 1960's development work has begun in England to increase the solubility of elemental iron in aqueous solution. This work led to the introduction of the chelated iron process. (Heguy *et al.*, 2003). It was found that solutions of the iron, when complexed with certain chelants, were reduced to the ferric form by aeration. Polyamino polycarboxylic acids appeared to be favored as complexing agent such as ethylenediaminetetraacetic acid (EDTA), cyclohexane-1,2-diaminetetraacetic acid (CDTA), diethylenetriaminepentacetic acid (DTPA) and (hydroxyethyl)ethylene diaminetriacetic acid (HEDTA), nitrilotriacetic acid (NTA) including aromatic polyamino polycarboxylic acids as benzene-xy-1,2-di-aminete-traacetic acid, with x to be chosen from the positions 3 to 6 and y being at least one chlorine or methyl group. The most important chelates applied in hydrodesulfurisation are the iron chelates of NTA, HEDTA and EDTA base on their cost. Stability constants of various iron chelates are shown in Table 1.3.

It was realized that the scrubbing liquids had an optimum pH range related to the stability of the iron chelates as well as to the reaction rate of these chelates with  $H_2S$  (Meuly, 1975). The chelates showed only reactivity toward  $H_2S$  above a minimum pH value, the hydroxyl-point of the chelates, which depends on the type of chelate. The minimum pH value was about 6.5, 8, 8.5 and 2.5 for the ferric chelate of EDTA, CDTA, DPTA and HEDTA, respectively. Increase of the pH beyond 10 finally results in the weakening of the chelant-iron bond and in the precipitation of ferric hydroxide.

Wubs and Beenackers (1994) studied the kinetics of the reaction of  $H_2S$  with ferric chelates of ethylenediaminetetraacetic acid at 22 °C and with ferric chelates of (hydroxyethyl)ethylenediaminetriacetic acid from 21 °C to 60 °C in a

stirred cell reactor under industrial conditions. The concentration of ferric chelate varied from 40 to 150 mol/m<sup>3</sup>, and the pH ranged from 4 to 10. Under the conditions applied, the reaction of H<sub>2</sub>S with ferric chelates of EDTA and HEDTA appeared to be first order in both H<sub>2</sub>S and ferric chelate. Demmink *et al.* (1994) studied the oxidative absorption of H<sub>2</sub>S by ferric NTA solutions at 13 °C in a co-current down flow column packed with stainless steel Sulzer SMV-4 static mixers under approximate industrial conditions. The concentration of ferric chelate varied from 30 to 200 mol/m<sup>3</sup> and the pH ranged from 6.7 to 8.3. The reaction kinetics of hydrogen H<sub>2</sub>S sulfide with ferric chelate of NTA was found to be first order in both ferric NTA and H<sub>2</sub>S.

**Table 1.3** Stability Constants (log K<sub>ML</sub>) of Fe(II)chelates and Fe(III)chelates with Polyamino polycarboxylic acids

Ligand to Iron	Stability Constants (log K <sub>ML</sub> )	
	Iron(II)	Iron(III)
NTA	8.05	15.9
HEDTA	12.20	19.80
EDTA	14.30	25.10
PDTA	15.50	26.0
DMEDTA	17.80	28.05
CDTA	18.90	30.00
TMDTA	13.46	21.61
EEDTA	14.20	24.70
EGTA	11.20	20.50
DTPA	16.40	28.00
TTHA	17.00	26.80

Source: Martell *et al.*, 1996

Where DTA = racemic-propylenediaminetetraacetic acid  
 DMEDTA = racemic-1,2-dimethylethylenediaminetetraacetic acid  
 TMDTA = trimethylenediaminetetraacetic acid  
 EEDTA = oxybis(ethylenitrilo)tetraacetic acid

EGTA	= ethylenebis(oxyethylenenitrilo)tetraacetic acid
TTHA	= triethylenetetraminehexaacetic acid

Several factors are known to influence packed bed performance. Whether their impacts are substantial or insignificant remain to be seen. Piché *et al.* (2005) studied the oxidative absorption of H<sub>2</sub>S (H<sub>2</sub>S) into a solution of ferric chelate of *trans*-1,2-diaminocyclohexanetetraacetate (CDTA) in a counter current laboratory column randomly packed with 15 mm plastic Ralu rings. The present investigation examines a Kraft pulping situation where dilute H<sub>2</sub>S concentrations are present in large volume gas effluents. A fractional two level factorial approach was instigated to determine the significance of six operating variables: the solution's alkalinity (pH; 8.5-10.5), the liquid mass flow rate (1.73-5.19 kgm<sup>-2</sup> s<sup>-1</sup>), the solution's ionic strength (0.01–0.1 mol dm<sup>-3</sup>), the gas mass flow rate (0.19-0.57 kgm<sup>-2</sup> s<sup>-1</sup>), the inlet H<sub>2</sub>S concentration (70-430 ppm) and the initial ferric CDTA concentration (100-400 μmol/L). Through factorial analysis, pH was determined as the governing factor along with less significant variables like gas and liquid flow rates and inlet H<sub>2</sub>S concentration. The maximum observed H<sub>2</sub>S conversion in the scrubber approached 91%. Further examination about the influence of ferric CDTA on H<sub>2</sub>S absorption rate was set up over a broader concentration range (0-2000 μmol/L) at pH of 9.5 and 10.5. It showed good potential at 2000 μmol/L as H<sub>2</sub>S conversion increased by 25% for both pH values in comparison to pure alkaline solutions containing no ferric CDTA.

In 2006, Piché and Larachi studied the effect of pH on kinetics of H<sub>2</sub>S oxidation process using iron CDTA. The experimental was performed in a Plexiglass stirred cell in the pH range of 9-11 at room temperature. Controlling the pH between 9 and 11 ensure that HS<sup>-</sup> remains the major sulfide species compared to dianionic polysulfide. The nonhydroxylated iron(III) complex component (Fe<sup>3+</sup> CDTA<sup>4-</sup>) being in larger proportion at lower alkaline pH is more reactive than the hydroxylated Fe<sup>3+</sup>OH<sup>-</sup>CDTA<sup>4-</sup> towards HS<sup>-</sup> and dianionic polysulfides. Improvement in the HS<sup>-</sup> conversion rate for pH going from 10 to 9 does not look significant although the proportion of Fe<sup>3+</sup>CDTA<sup>4-</sup> species increases a great deal. Conversely, higher pH (i.e., pH>10) greatly reduces the efficiency of Fe(III)CDTA (Piché and Larachi, 2006a).

These results come in complete opposition with previous works (Wubs and Beenackers, 1994; Demmink and Beenackers, 1998) asserting that  $\text{Fe}^{3+}\text{OH}^-\text{EDTA}^{4-}$  and  $\text{Fe}^{3+}(\text{OH}^-)_2\text{HEDTA}^{3-}$  are much more reactive towards  $\text{H}_2\text{S}$  when compared to their non-hydroxylated counterparts. A maximum in the observed enhancement factor occurs at  $\text{pH} \approx 7$ . This maximum does not follow from the equilibrium concentrations of ferric species. At  $\text{pH} < 6$ , most Fe(III)EDTA is present in its hydrated form,  $\text{Fe(III)EDTA}^{4-}$ , which appears to have a relatively low reactivity to  $\text{H}_2\text{S}$ . At  $\text{pH} > 6$ , most ferric EDTA is present as reactive hydroxylated species. They acknowledge that trend variations may occur when using different chelating agents, therefore some additional tests were carried out with the Fe(III)-EDTA chelate to clarify that matter. The results provide comparable trends as a function of pH as observed in using CDTA.

DeBerry (1997) argued that maximum  $\text{H}_2\text{S}$  conversion rates with Fe(III)-EDTA were reached when pH was maintained just above 7. Higher pH leading to larger  $\text{Fe}^{3+}\text{OH}^-\text{EDTA}^{4-}$  proportions obviously reduces the effectiveness of the process while lower reactivity in slightly acidic conditions can be accounted by the increasing presence of  $\text{H}_2\text{S}$  instead of  $\text{HS}^-$ .

Piche and Larachi (b) (2006) also studied the kinetic electrolyte effect of dissolved NaCl, LiCl and  $\text{Na}_2\text{SO}_4$  on the oligomerization of the hydrosulfide ion ( $\text{HS}^-$ ) into polysulfides then in colloidal sulfur assisted by Fe(III)-CDTA complexes in anoxic alkaline solutions. The  $\text{HS}^-$  and corresponding Fe(III)-CDTA conversions clearly improved when electrolytes were added. For example,  $\text{HS}^-$  overall conversion improved from 10% in demineralized water ( $\text{pH}=10.5$ ) to 40% for the corresponding 0.01 mol/L NaCl solution after 10 min of reaction. This value amplified to 85% for a 0.1 mol/L NaCl solution. It was shown as well that cations are the sub species from electrolytes interacting with the reaction species.

The sulfur content of the cake can range from 30% to 90% depending on the type of sulfur filter incorporated (Heguy *et al.*, 2003). This sulfur particle also plays another role. Demmink *et al.*, (1996, 2002) expressed that gas absorption rates in a stirred cell reactor, for the absorption of  $\text{H}_2\text{S}$  into aqueous Fe(III)NTA solutions of low pH ( $\text{pH} = 4.5$ ), can be enhanced by the precipitated sulfur particles which adhere to the gas liquid interface. This auto catalytic effect increases with increasing

ferric chelate concentrations. A model based on Higbie's penetration theory, which incorporates particle to interface adhesion, as well as a growing particle coverage during a liquid element's contact time at the interface, is used to analyze the experimental data. This model gives a reasonable description of the local auto catalytic effects on the gas absorption rate.

Horikawa *et al.* (2004) presented an experimental study of purification of the H<sub>2</sub>S containing synthetic biogas. The H<sub>2</sub>S was removed by mean of chemical absorption in iron EDTA solution using continuous countercurrent contactor. The absorber unit dimensions were 5.4 cm diameter with 36 cm height. The Fe-EDTA solution was prepared by mixing FeBr<sub>2</sub> as iron source and EDTA solution to be 0.2 mol/L of concentration. The solution flow rate used in the experiments was 68-84 mL/min while the gas flow rate was 1 L/min. The H<sub>2</sub>S removal efficiency can reach 100% within 1 hour.

### **1.2.3.2 Hydrogen sulfide absorbers**

H<sub>2</sub>S can be removed in almost any type of contactor. Contactors that have been examined include spray columns, venturi scrubbers, packed columns operated counter currently or co currently, upstream or downstream, and packed with dumped or structured packings. Bubble columns are usually not applied because of an unfavorable pressure drop, where as the presence of a large amount of bulk liquid is not required. The selection of a particular type of contactor may be based on mass transfer efficiency, fouling characteristics by sulfur and pressure drop. Further, investment and operation cost play a role. Often the bulk of the H<sub>2</sub>S is removed in a venture scrubber where after final clean up of the gas is realized in a packed column or a spray chamber.

### **1.2.3.3 Regenerators**

The variety in regenerators is less extensive when examining H<sub>2</sub>S contactors. Usually the regenerators are bubble columns or to a minor extent packed columns. Shell developed regenerators that operate in either co current up flow or

down flow to ensure a controlled partial oxidation of ferrous iron to ferric iron. A method of Dow Chemical to electrolytically regenerate the liquid was probably not successful because later effort focused on finding chelant stabilizing methods (Chang and Bedell, 1987). In 2008, Nagl *et al.*, claimed the improved oxidizer contains a bundle of hollow fiber membranes having extremely small pore sizes that allows air or other oxygen containing gas to diffuse through the pores in the membrane wall. The bundle of fibers is adjustably supported within the oxidizer housing. Pressurized air is introduced to the interior of the tubular membrane and a spent liquid redox catalyst is allowed to contact the exterior of the membrane. The air diffuses through the small pores in the membrane and into the catalyst solution as extremely small bubbles having high surface areas, thus yielding high mass transfer rates, thus significantly increasing the mass transfer rates and minimizing the amount of excess air needed to regenerate the redox spent catalyst solution. The preferred membrane is a hollow fiber membrane that can be fabricated from polymers, metals, ceramics, glasses, carbon and other like materials that allows air to diffuse from inside the membrane to the outside (Nagl *et al.*, 2008).

#### **1.2.3.4 Liquid formation**

The most important chelates applied in hydrodesulfurisation are the iron chelates of NTA, HEDTA and EDTA. The concentration of iron chelate in solution usually is in the range of 10 to 1000 mol/m<sup>3</sup>, though concentrations up to saturation can be applied. The chelant/iron ratio varies from 1.1 to 1.6 for EDTA and HEDTA to about two for NTA because two molecules of NTA can complex one Fe. The pH of the solutions usually is in the range of 6 to 9, the actual value depending on type of chelant and the presence of other stabilizers.

Co chelants are usually chemicals that complexate with iron under conditions where EDTA, NTA or HEDTA are no longer complexing iron. This way iron remains dissolved. Example are sorbitol, manitol and TEA, which complex ferric iron at high pH values (Thompson, 1980) or ammonia or amines, which complex ferrous iron at low pH values (Lynn and Dubs, 1981). Glycolic acid and diglycolic



acid also may act as co chelating agent (Roberts *et al.*, 1971 and 1972) but their functionality is as yet unclear.

Chelant degradation is the major contributor to chemical cost. The most important cause is a degradation reaction which occurs during regeneration. Variables affecting the oxidative degradation rate include: pH, chelant concentration, total iron concentration, ferrous iron concentration, chelant to iron ratio and the degradation product family formed (Buenger *et al.*, 1987; 1988). Chen *et al.* (1992) studied the degradation of NTA, the initial ratio of NTA to iron being two, in a continuously operated desulfurization apparatus. It was found that iminodiacetic acid, glycine and oxalate were the major degradation products. More information will be given in the next section. Biocide had to be added to prevent the forming of biological colonies that consumed the chelants (Primack *et al.*, 1984).

#### **1.2.3.5 Production of sulfur**

It is true that typical iron redox sulfur has entrained water and residual catalyst in sulfur cake form. The sulfur content of the cake can range from 30% to 90% depending on the type of sulfur filter incorporated. Though sulfur in this unmelted cake form is typically undesirable as a chemical feedstock; it actually has superior properties as a sulfur fertilizer when compared to typical pure sulfur produced by more traditional processes.

One California chemical manufacturer typically handles 20,000 tons of iron-redox sulfur per year, and would like more. The fact that iron redox sulfur was formed in the liquid phase at low temperature means that the sulfur particle is amorphous (softer) than solidified molten sulfur, and has a smaller particle size, for faster reaction in the soil. In addition, the other catalyst elements in the iron redox solution, and present in the sulfur cake (iron, chelates), are micronutrients in their own right and sold as such by several suppliers of agricultural products (Heguy, 2003). It is now clear that sulfur plays three roles in agriculture, soil amendment for pH adjustment, plant nutrient and fungicide. Sulfur application lowers the pH of alkaline soil and increases the uptake and efficiency of all of the other plant nutrients. The pH adjustment takes place through the bacterial conversion (primarily by the *Thiobacillus*

species) of sulfur to sulfuric acid. In the world where NPK are the three macronutrients, sulfur is becoming the fourth macronutrient. Sulfur is a component in three amino acids, and therefore essential for protein synthesis. Because sulfur is an acid producing element, it has a devastating effect on molds, fungus, and mildew. The sulfur produced from iron chelate process can be removed on an intermittent or continuous basis by any known technique such as filtration or centrifugation. Alternatively, the solution can be heated to melt the sulfur and the molten sulfur can then be separated by known techniques. A number of patents describe the method to separate the sulfur particle from the iron chelate solution.

Baker *et al.* (1986) disclosed that passage of the suspension through the multi passage filtering includes randomly oriented fibrous filter material and sintered metal filters initiates coalescence of the finely dispersed sulfur suspension into larger droplets so that the sulfur can be more easily separated out from the aqueous suspension by appropriate means such as gravity settling. In 1989, Kliem *et al.* separated sulfur from the alkaline suspension solution by heating the solution at temperature above the melting temperature of the sulfur (about 119 °C), and preferably about 130 °C to 135 °C. Thereafter the liquid sulfur/alkaline solution mixture is separated in the separating tank, preferably by decantation. The lighter fraction (alkaline solution) gathers in the upper part, the heavier fraction (liquid sulfur) gathers in the bottom of the separating tank. From the separating tank, settled liquid sulfur and alkaline solution is continuously withdrawn (Kliem *et al.*, 1989). In this method, the slurry is heated sufficiently to melt the sulfur and two different separation zones, in an extremely complicated apparatus, separate and transport the sulfur and the aqueous liquid. This process is expensive with regard to energy and for smaller installations is uneconomical because of high capital cost. To improve the separation of dispersedly precipitated sulfur from a washing solution used in the oxidative washing of H<sub>2</sub>S containing waste gases, the suspension is heated before filtration to about 45 °C. to 70 °C. Such heating causes the sulfur contained in the solution to coagulate into large flocks and form a mass of high purity sulfur which is largely non thixotropic. This mass, often called a filter cake, can be washed and utilized in a large number of ways as a source of sulfur (70.1% wt) (Hartmann, A., 1999).

### 1.2.3.6 Using stabilizer eliminate iron chelated degradation

The polyamino polycarboxylate chelated iron process is extremely effective and allows total conversions of H<sub>2</sub>S to be obtained. It is also a very flexible process and has in fact been widely used throughout the world. This process, however, has various drawbacks. Above all, when operating in an alkaline solution, there is the radical oxidation of the iron ligand with the degradation of the ligand itself and the precipitation of iron as sulfide. This has two strong consequences on the process: the ligand, which is expensive, must be continuously reintegrated, furthermore the sulfur produced is impure of iron sulfide and this makes it absolutely unsuitable for commercialization. In practice, the loss of the chelating agents turns out to be the most significant factor affecting the economic feasibility of large scale operation.

A few of the prior art workers have acknowledged that chelated iron solutions are unstable and that undesirable precipitation of iron compounds may occur. Nichol and Sapiro (1965a and 1965b) recommended careful control of the regeneration of the catalyst solution to avoid over oxidation of the iron chelate. Thompson (1980) indicates that restricting the molar ratio of chelating agent to iron is an important consideration in avoiding breakdown of the chelate molecule. Lynn and Dubs (1981) suggested the addition of selected amine salt stabilizers to achieve chelate stability at low pH levels. The Diaz (1983a; 1983b and 1983c) and Blytas (1983) propose the addition of various sulfur containing and nitrogen containing compounds as stabilizers to reduce the rate of chelate degradation, but the reported data show only a relatively modest improvement in the chelate loss as shown in Table 1.4.

These prior art studies have not provided an effective, environmentally acceptable, and inexpensive solution to the problem of chelate degradation. Moreover, there has been no adequate explanation of the mechanism of chelate instability in a H<sub>2</sub>S removal process.

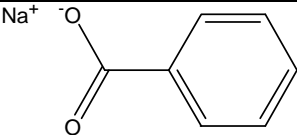
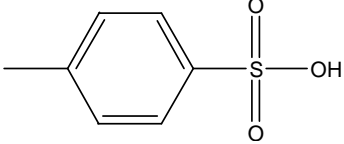
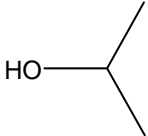
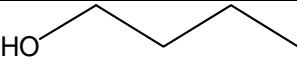
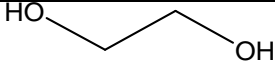
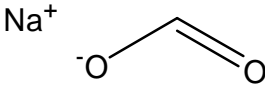
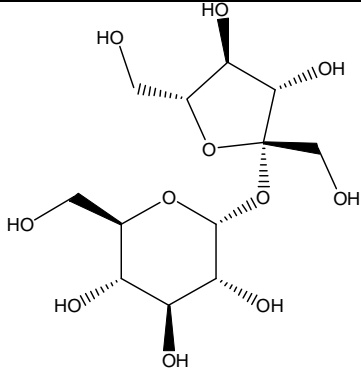
Bedell 1990 disclosed that soluble chemical compounds having a high affinity for hydroxyl radicals are effective stabilizers for chelating agents used in the

H<sub>2</sub>S removal process. Table 1.5 demonstrates the effectiveness of the stabilizers (0.75 mol/L) of in comparison to the non-stabilized ferric chelate solution.

**Table 1.4** The effectiveness of the stabilizers of in comparison to the non-stabilized Fe-NTA (nitrilotriacetic acid) solution. (Diaz, U.S. Patents Nos. 4,382,918, 4,388,293, and 4,400,368 and Blytas, U.S. Patent No. 4,421,733)

Stabilizers		NTA degraded per sulfur produced (g/g)
Name	Structure	
None		0.14
2,2-thiodiethanol (0.1M)		0.07
zinc isopropylxanthate (0.008M)		0.11
zinc isopropylxanthate (0.03M)		0.05
sodium thiocyanate (0.1M)		0.06
sodium dithionite (0.1M)		0.06
Sodium bisulfite (0.1M)		0.07

**Table 1.5** The effectiveness of the stabilizers of in comparison to the non-stabilized Fe-HEDTA (hydroxyethylethylenediaminetriacetic) solution.  
(Bedell, U.S. Patent No. 4891205)

Stabilizers		HEDTA degraded per sulfur produced (g/g)
Name	Structure	
None		1.83
Sodium Benzoate		0.39
Paratoluene Sulfonic Acid		0.33
KI		0.51
KBr		0.43
KCl		1.72
2-Propanol		0.74
1-Butanol		0.51
Ethylene Glycol		0.89
Sodium Formate		0.65
Sucrose		0.94

The present stabilizers have a high affinity for hydroxyl radicals as previously mentioned and many have been shown effective by the examples below. The stabilizers are sacrificed during the H<sub>2</sub>S removal process in favor of a longer useful life for the metal chelates. However, the soluble aromatic compounds have an additional benefit when used as stabilizers because the addition of hydroxyl radicals to the aromatic compounds can form chelating agents capable of complexing with metal ions released by degraded chelating agents. Thus, such aromatic compounds can further retard the degradation of the original metal chelate solution by reducing the amount of free hydroxyl radicals in the solution and by later complexing with metal ions released by degraded chelating agents before the aromatic compounds are degraded by additional hydroxyl radicals. Preferred compounds can be selected based upon solubility, costs and relative effectiveness.

McManus and Kin (1993) studied effective and stable oxidation solutions for H<sub>2</sub>S removal. A small anaerobic pilot plant system having separate vessels for H<sub>2</sub>S absorption and catalyst regeneration was used to evaluate the effectiveness of sodium thiosulfate as a stabilizing additive in an aqueous NTA-iron chelate solution when used in a cyclic H<sub>2</sub>S removal catalyst regeneration process. The operating solution having an iron content of about 1000 ppm and a 2:1 mole ratio of NTA to iron. During the pilot plant runs, only one minimal addition of ammonium hydroxide was required in the test run to maintain the pH in the desired range of about 7.0. The sodium thiosulfate was dissolved in water and added to the catalyst solution to obtain a thiosulfate concentration of about 50 g/L.

The result showed the NTA concentration changed from 10.09 g/L to 8.73 g/L (a decrease of 13.5%) in 92.5 hours, whereas in the control run the NTA was totally degraded shortly after 47 hours with no thiosulfate degradation or loss. The soluble Fe changed from 990 to 900 g/L (10%) in the presence of sodium thiosulfate whereas in the control run the soluble Fe concentration decreased about 30% within 92.5 hours. For the other stabilizers they found, t-butanol was as effective as sodium thiosulfate in eliminating degradation of NTA. Highly effective results were also obtained in the run using ethylene glycol as the additive, as shown by the fact that degradation of the NTA was limited to about 10%.

The effect of thiosulfate addition on degradation of EDTA in a chelated iron solution was also investigated at a mole ratio of EDTA to iron of about 1.1:1. It was seen from the half-life values that the runs with added thiosulfate showed a six-fold to ten-fold increase in EDTA stability compared to the control run.

Figure 1.1 is a schematic representation of the complexes formed by tetrasodium EDTA and iron in an aqueous solution. In Figure 1.1, six complexing ligands or "hooks" are attached to the iron in its ferric form and satisfy all of its ordinary coordination requirements. Four of the hooks are associated with acetic acid ligands and two are satisfied by bonds between the iron and the two nitrogens in each EDTA molecule. As is well known, when an aqueous solution of the iron EDTA complex is utilized to absorb  $H_2S$  from a gas stream, the  $H_2S$  is oxidized to elemental sulfur and at the same time the iron is reduced from its higher valence ferric state to its lower valence ferrous state so that the coordination number of the iron is changed from six to four. Figure 1.1 also illustrates this form of the complex in which the iron is in its ferrous or lower valence state. Since the coordination number of the iron was changed from six to four, two of the iron bonds must be freed, i.e., either iron-carbon or iron-nitrogen bonds. As reflected in Figure 1.1, however, it is believed that the release of iron-nitrogen bonds is the cause of the degradation of the aminopolycarboxylic acid molecule.

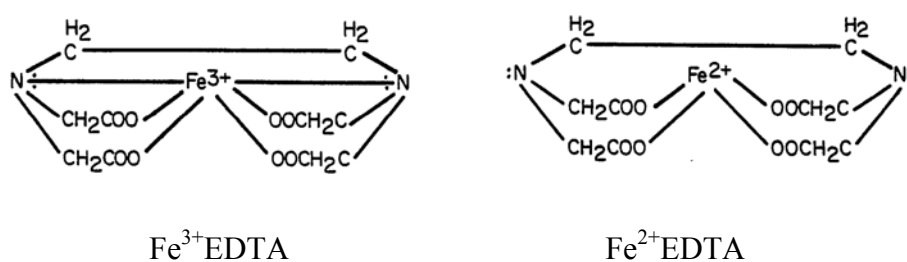


**Figure 1.1** Schematic of Fe-EDTA complex

They have determined that the primary degradation products of EDTA are ethyl imino diacetic acid (EIDA) and imino diacetic acid (IDA), these two materials accounting for substantially all of the EDTA which disappears from the catalyst solution during oxidative regeneration. The primary degradation products are

EIDA and IDA, but we have also found that the IDA ultimately undergoes further degradation, probably to N-methyl-glycine and glycine or glycine-related compounds, with the ultimate degradation product being acetic acid as show in Figure1.2.

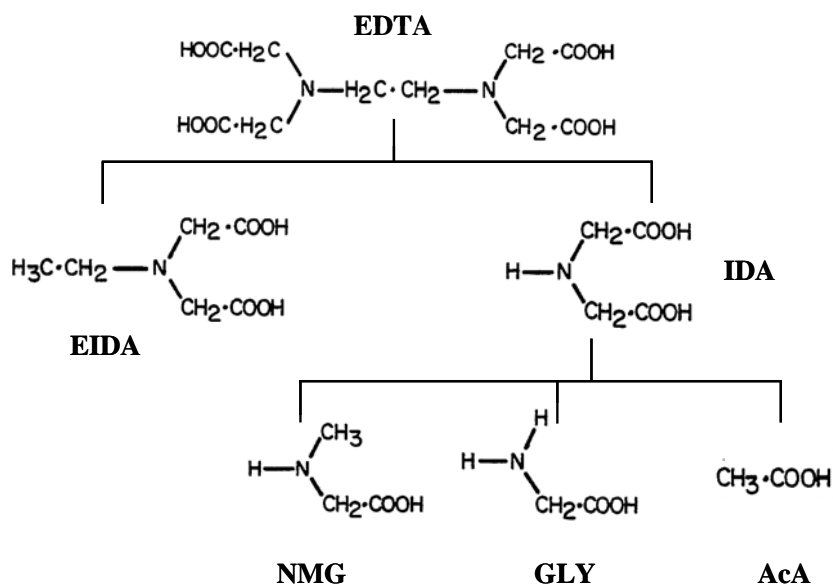


**Figure 1.2** The EDTA degradation during H<sub>2</sub>S oxidation with Fe-EDTA

In accordance with the mechanism previously described, the degradation of the aminopolycarboxylic acid chelating agent occurs as a result of the loss of an unpaired electron from the nitrogen during oxidative regeneration of the catalyst solution, and it is believed that the alkaline thiosulfate stabilizing agent retards or prevents such degradation by complexing or associating with the chelating agent and sharing the unpaired electron freed by the nitrogen atom during reduction of the iron from its ferric to its ferrous state. Figure 1.3 is a schematic representation of the manner in which the thiosulfate ion is believed to be associated with the dimer form of the NTA-iron complex so as to stabilize the nitrogen atoms against bond rupture during oxidation of the reduced iron complex.

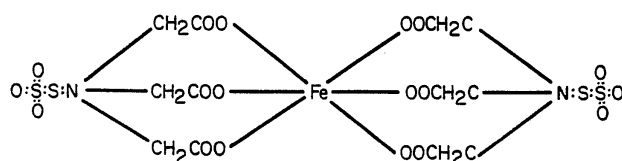


**Figure 1.3** Thiosulfate ion associated with the dimer form of the NTA-iron complex



Effects of temperature, pH, and light on equilibrium dissociation constants for Fe–EDTA chelates were determined by Sunda and Huntsman (2003). They found that increases in pH (7.7-9) increased equilibrium dissociation constants for Fe–EDTA chelates, apparently due to the formation of mixed EDTA-hydroxy chelates. Light also increased the dissociation constant due to photo reductive dissociation of ferric–EDTA chelates. A decrease in temperature from 20 and 10 °C had little effect on dissociation constants in the dark, indicating that rate constants for Fe–EDTA association and dissociation were about equally affected by temperature. Many iron chelates, such as Fe–EDTA, undergo photochemical ligand to metal charge transfer reactions in which the iron is reduced to Fe(II) and the ligand is oxidatively degraded. The resulting chelated ferrous iron dissociates to dissolved inorganic Fe(II), which is subsequently oxidized by O<sub>2</sub> or H<sub>2</sub>O<sub>2</sub> and then rechelated by the ligand. This increase in dissociation kinetics at higher pH may result from the progressive formation of mixed EDTA hydroxy complexes. FeEDTA(OH)<sup>2-</sup>, which predominates at pH 7.7 to 9.0, and FeEDTA(OH)<sub>2</sub><sup>3-</sup>, the dominant complex at higher pH based on equilibrium calculations. The addition of hydroxide ligands into the ferric iron coordination sphere occupies bonding positions that would otherwise be free to coordinate with the functional groups of EDTA. This decreases the denticity of the Fe–EDTA chelates from six-coordinates for FeEDTA<sup>-</sup> to four or five-coordinates for FeEDTA(OH)<sub>2</sub><sup>3-</sup>, which should increase dissociation kinetics. In addition, the binding of hydroxide ligands imparts additional negative charge, which should weaken the remaining Fe-EDTA chelate bonds, and thereby further increase dissociation kinetics. These pH effects are not specific to Fe-EDTA and should also occur in other hydrolyzable ferric chelates.

More recently, De Angelis *et al.* (2007) studied the oxidation of H<sub>2</sub>S to sulfur by mean of treatment with an aqueous acid solution containing trivalent iron and a hetero polyacid having formula H<sub>n</sub>XV<sub>y</sub>M<sub>(12-y)</sub>O<sub>40</sub> or a sole hetero polyacid having formula H<sub>n</sub>MeM<sub>12</sub>O<sub>40</sub> wherein the symbol X is an element selected from P, Si, As, B, Ge and M consists of Mo or W. The oxidation cycle of H<sub>2</sub>S to sulfur (10 hours), filtration of the sulfur and re-oxidation of the solution with air (4 hours) are repeated four times, on the same solution, without there being any decrease in the catalyst performance. However, the preparation of the oxidation solution is very

complex. Ascorbic acid and Citric acid are weak acids, commonly used as food additives, usually as a preservative, but sometimes as a flavor component. They also act as an antioxidant by being available for energetically favourable oxidation. Many oxidants such as the hydroxyl radical, contain an unpaired electron, and, thus, are highly reactive and damaging to humans and plants at the molecular level. This is due to their interaction with nucleic acid, proteins, and lipids. Reactive oxygen species oxidize (take electrons from) ascorbate first to monodehydroascorbate and then dehydroascorbate. The reactive oxygen species are reduced to water, while the oxidized forms of ascorbate are relatively stable and unreactive, and do not cause cellular damage. The buffering properties of citrates are used to control pH in household cleaners and pharmaceuticals. Citric acid's ability to chelate metals makes it useful in soaps and laundry detergents. By chelating the metals in hard water, it lets these cleaners produce foam and work better without need for water softening. In a similar manner, citric acid is used to regenerate the ion exchange materials used in water softeners by stripping off the accumulated metal ions as citrate complexes.

Kojima *et al.* presented that the combination of ascorbic acid+EDTA and ascorbic acid+citric acid led to the solubilization of about 70% of the Fe from cooked pinto beans as shown in Figure 1.4. Thus, ascorbic acid, citric acid and their salts have a feasibility to retard the degradation of the chelating agent (i.e. EDTA) because their properties in an antioxidant as mentioned above and the ability to chelate metal as shown in Table 1.6.

Thus, the properties of ascorbate and citrate mentioned above may have potential to reduce the degradation rate of Fe-EDTA with 2 functions. One it may acts as ligand instead of the degraded EDTA or it can retard the degradation rate of Fe-EDTA by play an important role free radical scavenger. However ascorbate is more expensive than citrate, so citrate would be used for the reduction of iron chelate degradation study.

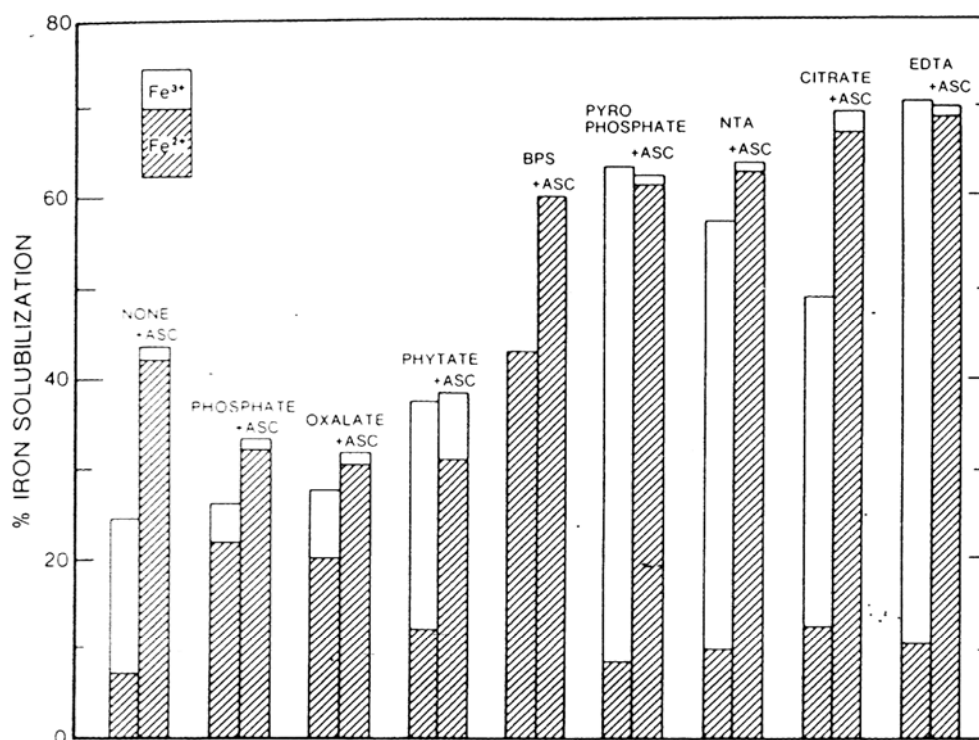


FIGURE 5. The effect of ascorbic acid, chelating agents, and combinations of ascorbic acid and chelating agents on the solubilization of Fe from bean suspension. The bean suspension was first incubated at pH 2 with (+ ASC) or without ascorbic acid. The pH was then adjusted to 6 with NaOH and the chelating agents added to give a concentration of 10 mM. A second incubation was carried out at pH 6. The bar on the left of each pair indicates the results obtained for that chelating agent in the absence of ascorbic acid and the bar on the right (+ ASC) with 10 mM ascorbic acid. (From Kojima, N. et al., *Am. J. Clin. Nutr.*, 34, 1392, 1981. With permission.)

From: Kratzer, F.H. and Vohra, P. 1986. Chelate in nutrition.

**Figure 1.4** The effect of ligands and mixed ligands in % iron solubilization

**Table 1.6** Stability constants ( $\log K_1$ ) of various iron chelates

Ligand to Iron	Stability Constants ( $\log K_1$ )	
	Iron(II)	Iron(III)
Citric acid	3.2	11.85
EDTA	14.3	25.7
NTA	8.84	15.87
Oxalic acid	>4.7	9.4
Salicylic acid	6.55	16.35
b-Phenylalanine	3.26	8.9

From: Furia (1972).

#### 1.2.4 Gas absorption in packed column

Gas–liquid counter-current packed columns are among the most ubiquitous contacting devices in separation processes. Nowadays, they are widely used in such diverse fields as distillation, scrubbing, and stripping. Due to lower power consumption and liquid inventory, they are also increasingly evoked as cheaper replacement alternatives to existing tray column operations but also as potent candidates in catalytic distillation and petroleum refining operations. Furthermore, since packed column operation is cheap and high removal efficiency it is of great interest for pollution abatement (Iliuta *et al*, 2003). The economic comparison revealed that the actual unit cost for the biofilter was higher than for the wet packed scrubber. (Gao *et al*, 2003).

Usually packed column are cylindrical columns up to several meters in diameter and over 10 meters height. The packing is placed on a support whose free cross section should be at least equal to the packing porosity. Liquid is fed in at the top of the column and distributed over the packing through which it flows downwards. To guarantee a uniform liquid distribution over the cross-section of the column, a liquid distributor is employed. Gas flows upwards countercurrent to the falling liquid, which absorbs soluble species from the gas. The gas which is not absorbed flow away from the top of the column usually through a mist eliminator. The mist eliminator separates liquid drops entrained by the gas from packing. The separator may be a layer of the packing, mesh or it may be specially designed (Zarzycki and Chacuk, 1993).

Packed column media for gas liquid contact in chemical scrubbing have been made in myriad shapes and forms in all type of materials including wood, rock, ceramic, metal, plastic, and woven filaments. Packed column media may be divided into three categories: random packing, structured packing, and mesh packing. Usually packed columns are filled with random packing media, consisting of individual pieces of packing that are randomly dumped in the column (Rafson and Harold, 1998).

Dumped packings consist of units 6 to 75 mm in major dimension. Packings, which are smaller than 25 mm are used mainly in laboratory or pilot plant columns. In stack packing the unit are 50 to 200 mm in size (McCabe *et al.*, 2001)

However, structured packing represents an alternative choice to random packing. Structural packing are manufactured for a given column diameter and column height. Usually the same packing cannot be used in column of different diameter. Random packings may be relocated to various columns. Random packed-media comparisons are typically based on four characteristics of the packing: size, packing factor, height of a transfer unit, and surface area. The size number of random packing media is typically the minor dimension of the individual packing piece. Common packings and their physical characteristic can be found in many books or from manufacturers. All packing media suppliers developed the shape and form of their packing with the goal to fill the basic requirements for an ideal packing media: (Rafson and Harold, 1998).

1. Low weight per unit volume
2. Low cost per unit volume
3. Large active surface area per unit volume
4. Large free volume (void space)
5. Low liquid hold-up (or high liquid hold up)
6. High strength, durability, and temperature stability
7. High chemical resistance
8. High mixing properties of the gas and the liquid
9. Low pressure drop (low gas flow resistance) with high flooding velocity
10. High mass transfer coefficient
11. Minimum side thrust on column walls
12. Good liquid redistribution properties
13. Ease of cleaning

#### **1.2.4.1 Mass transfer in packed column**

When one or more components of gas transfer to a liquid, because of physical solubility, absorption occurs. The transfer phenomenon from the gas to the

liquid is known as mass transfer. Chemical reaction that may occur in the liquid phase may affect the overall mass transfer of the component from the gas. Physical absorption phenomena can be understood by using models to describe the mass transfer that occurs from the gas phase to the liquid phase. The two models that provide simple conceptual understanding of the absorption are the two-film model and the surface renewal model (Rafson and Harold, 1998).

The two-film model defines an interface between the gas phase and the liquid phase. At the interface, two boundary layers exist. These boundary layers, called film, represent the zones of mass transfer from the bulk gas phase, through the interface, to the bulk liquid phase. The two-film model presumes that one of the films, the gas film or the liquid film control the rate of mass transfer from the gas to the liquid. An absorption process can be either gas-film controlling (gas-film limiting) or liquid-film controlling (liquid-film limiting). In packed bed reactor where the absorption and the reaction are taking place in series. A number of mass transfer and reaction steps were involved.

The mass-transfer coefficient is considered as the chief design parameter in the sizing and/or the rating of packed towers' mass transfer capacity. Often, the success of design and the selection of safety factors for scale up depend primarily on the accuracy with which the mass-transfer coefficient is evaluated. Yet, since a long time ago, the procurement of separate correlations for  $a_i$  (gas liquid interfacial area) and  $k$  (mass transfer coefficient) was felt to be useful for extracting the areal effect from the interphase transfer effect in the volumetric investigators attempted the split by proposing correlations for the interfacial area ( $a_i$ ) and local mass transfer coefficients ( $k_L$  and  $k_G$ ) apart, resulting thus in three structurally different correlations. Eventually, estimates of overall mass-transfer coefficients ( $Ka_i$ ) can be constructed using these three correlations and the two film theory. Among the existing correlative methods, the Onda *et al.* correlations are considered as the first potent, still widely used procedure for packed tower design with regard to mass-transfer coefficient prediction (Iliuta and Larachi 2003, Sieres and Seara, 2007, Piché *et al.*, 2002 and Piché *et al.*, 2003). However, the other correlations were presented in the literatures (Godini and Mowla, 2008; Christie, 1993).

The second model that provides a simple conceptual understanding of the absorption phenomenon is the surface renewal model. The surface renewal model, developed by Danckwerts in 1951, assumes that the bulk liquid phase consists of small packets of liquid that are brought into contact with the bulk gas phase. The surface renewal model calculates an average exposure time for gas and liquid contact. The average exposure time of the surface renewal model translates to a minimum contact time requirement for scrubbing a gas with a liquid in a packed column (Zarzycki and Chacuk, 1993).

Mass transfer coefficient, experimentally determined, provide the most direct method for predicting packed-column performance and for designing packed column scrubbers. An overall coefficient incorporates gas and liquid film mass transfer coefficient. Overall mass transfer coefficients are system specific. The specific system includes the temperature, gas component, liquid composition, liquid flow rates, and packed column type. The mass transfer coefficient provides a method to calculate the required total volume of the packed column scrubber, especially when accompanied by correction factors. (i.e., temperature, liquid rates, and liquid composition concentration).

Estimating mass transfer coefficients for systems with limited or no experimental data leads to predictions with uncertainty in the packed column design. The designer aware of the estimating uncertainties, must recognize that the predictions may be an order of magnitude only with errors up to 50 percents. Therefore, the careful use of overall mass transfer coefficients must be preceded with an extensive search and verification for the most applicable experimental data.

The efficiency of gas absorption process usually present as the ratio of the amount of removed gas to the amount of inlet gas. The measure of the efficiency of the absorption process can be also expressed in terms of the overall height of the gas film transfer unit,  $H_{OG}$  (m). The smaller  $H_{OG}$  is, the more efficient the absorption process will be.  $H_{OG}$  is a function of the overall number gas film transfer unit,  $N_{OG}$ . This quantity represents the degree of difficulty of the absorption process. A high  $N_{OG}$  value corresponds to a difficult separation.

#### 1.2.4.2 Variables effect on absorption and reaction in packed column

The performance factor that might predominate packed column media selection is pressure drop and the related issue of flooding. The resistance to gas flow through a packed column is influenced by both the gas flow rate and the liquid flow rate. The gas phase flowing through a packed column is generally turbulent. The liquid phase flowing through the packing column covers the surface of the packing media and flows from one surface to the next. Increases in gas flow rate or liquid flow rate would increase in gas flow resistance, i.e., pressure drop. The condition of maximum practical gas and liquid flow is called flooding conditions, the pressure drop rise rapidly as the liquid flow through the packed column prohibit uniform gas flow. Packed media suppliers and research organization have developed pressure drop data and methods for estimating pressure drop through packed columns. The majority of these methods provide excellent predictions of operating pressure drop and flooding conditions.

The gas velocity in an operating packed column must obviously be lower than the flooding velocity. However, as flooding is approached, most of or all the packing surface is wetted, maximizing the contact area between gas and liquid. The designer must choose a velocity far enough from the flooding velocity to ensure safe operation but not so low as to require a much larger column.

The flooding velocity depends strongly on the type and size of packing and the liquid mass velocity. Flooding was assumed to occur at a pressure drop of 2.0 in. H<sub>2</sub>O/ft (16.67 cm H<sub>2</sub>O/m) of packing. Several generalized correlations have been proposed for the pressure drop and flooding velocity in packed column, for example the Stoneware's generalized pressure drop correlation.

The operating conditions such as, the scrubbing liquid flow rate, the gas flow rate, the concentration of gas and liquid, the liquid to gas ratio ( $L/G$  ratio), the packing bed height, pH or temperature, to the packed column efficiency were study by many research. (Piché *et al*, 2005, Chen *et al*, 2001, Couvert *et al*, 2006, Setameteekul *et al*, 2008 and Godini and Mowla, 2008). These parameters play a vital role in mass transfer rate that influent to the conversion of the impurities.



Gas contaminant conversion significantly increases with liquid flow rate because the increasing of driving force but decrease with growing contaminant load up. Addition of the scrubbing solution content will gradually increase the contaminant absorption rate until the system efficiency dim to a maximum. Adjustment of other parameters like liquid flow rate, bed height and others is necessary (Piché *et al.*, 2005).

In a chemical scrubber, contaminant is continuously removed by its reaction with scrubbing chemical solution. Therefore, no contaminant accumulates in the scrubbing solution. As long as a scrubbing solution is provided to cover a reasonable portion of the interfacial area of the packing in the scrubber, liquid flow rate demonstrates a minimal effect on absorption efficiency. However, because contaminant removal is accomplished by chemical reactions, residence time is an important consideration. Thus, gas flow rate is expected to play a significant role in this process (Chen *et al.*, 2001). Therefore contactors must have a very high, gas-liquid contact surface and long residence times, thus necessitating large volumes and, consequently, high capital investment.

The  $L/G$  ratio is the most important parameter for the design of an absorption column. Thus for given gas flow rate, a reduction in liquid flow decreases the slope of the operating line. Increasing of  $L/G$  (increase  $L$  while  $G$  is constant) has a positive effect on removal efficiency. However, it should be noted that the range of variation of  $L/G$  is within permissible hydrodynamic range, namely between dryness and flooding regions (Godini and Mowla, 2008).

Using smaller packing size causes higher available mass transfer area per bed volume. In this manner the amount of absorption per bed volume is increased. The effect of packing size on the process performance and strongly depends on the states of other conditions. Therefore, this parameter was studied in a variety of operating conditions. (Godini and Mowla, 2008).

The liquid physical properties also play a major role in defining the interfacial area. Compared to water, for example, low viscosity and low surface tension liquids (i.e., organic liquids) produce better gas liquid), while high viscosity liquids develop poor  $a_i$ . Gas density displays the significant influence of on  $a_i$ . As it increases, an improved gas-liquid contacting takes place plausibly because of

intensified gas-liquid interfacial shear and instabilities. The gas-liquid interfacial area is also affected by the packing properties as well as the column diameter, small packings (respectively large bed-specific surface area) entrain higher gas-liquid interfacial areas. The vessel walls in smaller columns appear to generate, via an increased bed hydraulic surface area, better  $a_i$ . The wall effect progressively vanishes as the column diameter increases.

The effect of gas superficial velocity, entrains virtually no change on  $k_L$ , in accordance with the Onda *et al.* and the Billet and Schultes correlations. On the other hand, the liquid velocity and diffusion coefficient represent the main factors positively influencing the liquid-film coefficient ( $k_L$ ). The influence of liquid density, surface tension, gas density, and bed dimensions is not discussed in this section considering that they affect marginally the local liquid film mass transfer coefficient. Similarly to the liquid film coefficient, the gas superficial velocity and diffusion coefficient are the main factors characterizing  $k_G$ .  $k_G$  increases as the gas density decreases.

Contrary to the case for  $k_L$ , the liquid flow rate does affect the gas film coefficient. For gas resistive systems, it appears that high liquid hold up, via high liquid velocity, is not desirable. The high surface area packings contribute to the decrease of gas film resistance. However, a point is reached when lower surface area packing only slightly influences  $k_G$ . Because the gas phase usually moves much faster than the liquid in the porous medium,  $k_G$  is much more controlled by the packing structure than  $k_L$ . Being irrelevant to the gas film mass transfer coefficient, the effects of liquid density, viscosity, surface tension, and bed dimension factors are not examined. (Piché *et al.*, 2002).

### **1.2.5 Theories of model formation and fitting (Multiple regression and Experimental design)**

Complex physical or chemical systems are often required to analyze and develop mathematical models, which simulate the behavior of such system. Process analysis is the application of scientific methods to the recognition and definition of problems and to the development of procedures for their solution. In the

hearth of successful process analysis is the step of mathematical modeling. The objective of modeling is to construct, from the theoretical and empirical knowledge of a process, a mathematical expression that can be used to predict the behavior of the process. A mathematical model relates the output, i.e., dependent variables(s), to independent variable(s). Each equation in the model usually includes one or more coefficients or parameters that are presumed constant. The best model presumably exhibits the least error between experimental data and the predicted response. The least square is a method that minimizes the values of the squares of the errors, which can be used to estimate the coefficients in a model from experimental data. For regression analysis, mathematical models are classified as linear or nonlinear with respect to the unknown parameters.

To use the statistical approach in designing and analyzing an experiment, it is necessary for everyone involved in the experiment to have a clear idea in advance exactly what is to be studied, how the data are to be collected, and at least a qualitative understanding of how these data are to be analyzed. The outline of the recommended procedure is shown in the following.

Guideline for designing an experiment:

1. Recognition of and statement of the problem.
2. Choices of the factors, levels and ranges.
3. Selection of the response variable.
4. Choice of experimental design.
5. Performing the experiment.
6. Statistical analysis of the data.
7. Conclusions and recommendations.

The detail of step 4 and 6 are reviewed below.

#### **1.2.5.1 Choice of experimental design**

Choice of the experimental design involved the consideration of sample size, the selection of a suitable run order for the experimental trials, and the determination of whether or not blocking or other randomization restrictions are involved. There are also several interactive statistical software packages that support

this phase of experimental design. The experimenter can enter information about the number of factors, levels, and range, and these programs will either present a selection of designs for consideration or recommend a particular design. These programs will usually also provide a worksheet for use conducting the experiment. In selecting the design, it is important to keep the experimental objectives in mind. In many engineering experiments, we already know at the outset that some of the factor levels will result in different values for the response. Consequently, we are interested in identifying which factors cause this difference and in estimating the magnitude of the response change. In other situations, we may be more interested in verifying uniformity.

#### **1.2.5.2 Statistical analysis of the data (Steppan *et al.*, 1998)**

Statistical methods should be used to analyze the data so that results and conclusions are objective rather than judgmental in nature. If the experiment has been designed correctly and if it has been performed according to the design, the statistical methods required are not elaborate. There are many excellent software packages designed to assist in data analysis, and many of these programs used in step 4 to select the design provide a seamless, direct interface to the statistical analysis and interpretation. Because many of the questions that the experimenter wants to answer can be cast into the hypothesis-testing framework, hypothesis testing and confidence interval estimation procedures are very useful in analyzing data from a designed experiment. It is also usually very helpful to present the results of many experiments in terms of an empirical model, that is, an equation derived from the data that expresses the relationship between the response and the important design factors. Residual analysis and model adequacy checking are also important analysis techniques. Remember that statistical methods cannot prove that a factor has a particular effect. They only provide guidelines as to reliability and validity of results. Properly applied, statistical methods do not allow anything to be proved experimentally, but they do allow us to measure the likely error in a conclusion or to attach a level of confidence to a statement. The primary advantage of statistical methods is that they add objectivity to the decision making process. Statistical

technique coupled with good engineering or process knowledge and common sense will usually lead to sound conclusions.

The general approach to fitting empirical models is called regression analysis. When regression is performed, one approximates an observed, empirical variable (output, response) by an estimated one, based on a functional relationship between the estimated variable ( $y_{est}$ ) and one or more regressor or input variables  $x_1, x_2, \dots, x_i$ . The regression analysis is often used to describe data sets, when parameters in known scientific equations have to be estimated, to develop new models describing and even predicting a specific response, or to control and optimize processes.

Developing this functional relationship to obtain expected empirical data to be explained without any residual doubt is impossible. Possible sources for error are random or measurement error, and the “lack-of-fit” error caused by the inaccuracies of our estimation function. Our ultimate goal in regression is to minimize this lack-of-fit error.

The method used to find the coefficients ( $b_j$ ) of general model equation is called least squares estimation. This means that the error term used in the model equations is defined as the difference between observed response variable  $y$  and estimated  $y_{est}$  for a given setting of the  $x_j$  at each data point. The desired optimum regression model then has to give us a minimum for this sum of squared errors, hence “least squares estimation method”.

The test for significant of the regression model and the individual regression coefficient will be used for test the statistical significance of the model and model coefficient. In order to test the significance of the model, the assumption “The null hypothesis is true if there is no linear relationship between any of the independent variables” is performed. This is equivalent to the equations:

$$H_0: b_1 = b_2 = \dots b_i = 0 \quad (1.12)$$

$$H_1: b_j \neq 0 \text{ for at least one } j \quad (1.13)$$

with  $H_0$  denoting the null hypothesis,  $H_1$  being the rejection of the null hypothesis, and  $b_1$ - $b_i$  representing the intercept and the regression coefficients of the  $i$  independent.

If  $H_0$  is rejected, there is at least one independent variable significantly contributing to the linear model, and it can be concluded that there exists a functional relationship between the response and at least one of the variables. Similarly, the hypotheses for the individual coefficients  $b_j$  can be defined:

$$H_0: b_j = 0 \quad (1.14)$$

$$H_1: b_j \neq 0 \quad (1.15)$$

If  $H_0$  is rejected, the respective coefficient significantly contributes to the model. If  $H_0$  cannot be rejected, the corresponding variable can be eliminated from the model equation.

An **analysis-of-variance-** or ANOVA-table such as Table 1.7 is commonly used to summarize the test for significance of the model. There are variations in the layout of this table.

**Table 1.7** ANOVA table for a model with  $i$  regressor variables and  $n$  observations.

<i>Source of Variation</i>	<i>Sum of Squares</i>	<i>Degree of Freedom</i>	<i>Mean Square</i>	$F_0$	<i>Significance or Error Probability P</i>
Regression Model	SSR	$i$	$MSR = SSR/i$	$MSR/MSE$	$= P(H_0: F_0 \leq F_{crit})$
Residual (Error)	SSE	$n-1-i$	$MSE = SSE/(n-1-i)$		
Total	$S_{yy}$	$n-1$			

The null hypothesis for the regression model (Equation (1.12)) is simply tested by comparing the effect or variability caused by the regression model to the overall error. This comparison is based on the so-called Total Sum of Squares ( $S_{yy}$ ), the Regression Sum of Squares (SSR), and the Sum of Squared Errors or Error Sum of Squares (SSE).

The test for the significance of the regression model is performed as an analysis-of variance procedure by calculating the ratio between the Regression Sum of Squares (SSR) and the Error Sum of Squares (SSE) and comparing the result to the F-statistic with the appropriate degrees of freedom at a given significance level.

$$F_0 = \frac{SSR/i}{SSE/(n-1-i)} = \frac{MSR}{MSE} \quad (1.16)$$

The null hypothesis  $H_0$  is rejected if  $F_0$  is greater than the corresponding critical value  $F_{crit}$  of the F-distribution for a given significance level with  $i$  and  $(n-1-i)$  degrees of freedom. In other words, for a significance level  $\alpha$ , the hypothesis that the regression model is not significant can be rejected at the  $\alpha$ -level if  $F_0 > F_{crit} = F_{\alpha, i, n-1-i}$ . Note that the significance level  $\alpha$  stands for the probability that the null hypothesis is true, i.e., the model is not significant. Usually, significance levels  $\alpha$  of 0.10, 0.05, and 0.01 are used to determine critical values  $F_{crit}$ , where decreasing significance levels indicate a higher confidence for the model. The values  $F_{crit}$  for the F distribution increase with decreasing significance level  $\alpha$  and increasing degrees of freedom  $f_{SSR}$  for the regression model, and they decrease with increasing degrees of freedom  $f_{SSE}$  for the error contribution. For a given model, the larger the value of  $MSR/MSE$ , the lower the significance level  $\alpha$  leading to critical values for  $F_{crit}$  which are smaller than  $F_0$ , and the higher the confidence level for the significance of the model, i.e. a rejection of  $H_0$ . On the other hand, increasing the number of model terms for a given data set, i.e., increasing  $f_{SSR}$  and decreasing  $f_{SSE}$ , can lead to a decrease of  $MSR$  and an increase of  $MSE$  up to a point where the  $F_0$  becomes smaller than  $F_{crit}$  and the model is no longer significant. If this occurs at significance levels  $\alpha$  of higher than 0.1, the model is considered to be no longer significant. In computer programs, usually the significance level  $\alpha$  is calculated and given in addition to the corresponding value of  $F_0 = MSR/MSE$ , so we do not have to look up the values for  $F_{crit}$  in a table anymore.

If replicate measurements are present, i.e., responses based on the same settings for the independent variables, a test can be performed which gives the significance of the replicate error in comparison to the model dependent error. In

other words, the test splits the Residual or Error Sum of Squares, SSE, into a contribution from the *pure error*, which is based on the replicate measurements, and a fraction which is due to the *lack of fit* based on the model performance. Similar to the F-test for significance of the model, it also used for the test statistic of lack of fit. If  $F_0$  is larger than the critical value  $F_{crit}$  for a given significance level  $\alpha$  with  $m-2$  and  $n-m$  degrees of freedom, the lack of fit error is significant, i.e., there might be contributions in the regressor-response relationship not accounted for by the model. When performed on a linear (first order) model, this test indicates curvature if  $F_0$  is significant.

The significance test on the regression model tells us if at least one of the regression coefficients is different from zero. It is necessary to test the significance of the individual coefficients. This test forms the basis for model optimization by adding or deleting coefficients (*Backward Elimination*, *Forward Selection*, and *Autofitting*). A model with many coefficients is not necessarily the best, and a model with only a few coefficients might improve dramatically by adding another, but we have to know which coefficient actually plays a significant role in the model. The underlying null hypothesis was described above. A t-test statistic is used to test this hypothesis. Similar to the F-test used for checking the model significance, we compare the calculated  $t_0$  to the critical t-value  $t_{crit}$  for a given significance level  $\alpha$  and the error degrees of freedom,  $n-1-i$ . If the calculated value for  $t_0$  is larger than  $t_{crit}$ , we reject the null hypothesis at the given significance level. For instance, with  $\alpha=0.05$ , we would say that there is only a 5% error probability that the corresponding coefficient is not significant. Note that this significance is based on the presence of all the other regressor variables in the model. It might change dramatically with a different set of regressor variables.

There are parameters called R (correlation coefficient) or  $R^2$  which somehow describe the quality of the fit. Most people consider these parameters as most important in assessing the quality of a regression model. In addition to the basic analysis of variance, the program displays some additional useful information.  $R^2$ , the coefficient of determination in Simple Linear Regression is called the coefficient of multiple determination in Multiple Linear Regression. It is defined by the ratio of the Regression Sum of Squares (SSR) over the Total Sum of Squares ( $S_{yy}$ ) Clearly, we



must have  $0 \leq R^2 \leq 1$  with larger values being more desirable. There are also some other  $R^2$  like statistics displayed in the output. The adjusted  $R^2$  is a variation of the ordinary  $R^2$  statistic that reflects the number of factors in the model. It can be a useful statistic for more complex experiments with several design factors when we wish to evaluate the impact of increasing or decreasing the number of model term. Standard deviation is the square root of the error mean square and the coefficient of variance (CV). The CV measures the unexplained or residual variability in the data as a percentage of the mean of the response variable. PRESS stand for Prediction Error Sum of Square and it is a measure of how well the model for the experiment is likely to predict the response in a new experiment. Small values of PRESS are desirable. Alternatively one can calculate an  $R^2$  for Prediction based on PRESS.

So,  $R^2$ , adjusted  $R^2$ , and  $R^2$  for Prediction together are very convenient to get a quick impression of the overall fit of the model and the predictive power based on one data point removed. In a good model, these three parameters should not be too different from each other. However, for small data sets, it is very likely that every data point is influential. In these cases, a high value for  $R^2$  for prediction cannot be expected.

After calculating a model, a thorough analysis of the residuals is very important to evaluate the adequacy of the regression. The most commonly used methods in residual analysis are:

1. Normal Probability Plots of the Residuals.
2. Plots of the Residuals vs. the Predicted Responses.
3. Outlier Analysis using threshold or cut off values.

Outlier analysis uses threshold or cut off values. In a computer program such as ER, the ranked residuals are plotted against the expected normal value or *rankit*, which is equal to the inverse of the normal cumulative distribution for a given cumulative probability. In such a plot, the points should form a straight line if the residuals are perfectly normally distributed. In reality, the plot is usually slightly s-shaped, which can be tolerated if the deviation from linearity is not too bad. A pronounced s-shape, however, indicates a distribution with heavy “tails”, i.e. the residuals should be inspected for outliers.

In addition to inspecting the normal probability plots of residuals, it is helpful to plot the residuals versus the predicted responses. If the residuals are not correlated with the value of the predicted response, then this plot should look like a horizontal band on both sides of the expected average for the residuals, zero. If the pattern looks dramatically different, it indicates that the error variance is not constant and depends on the response. Usually, transformations in the regressors or the response are employed to correct this model inadequacy. The shape of the residual vs. predicted response plot can indicate which transformation of the response  $y$  could improve the model.

### 1.2.5.3 Experimental Design

The whole area of experimental design is a very large field which has enjoyed a renewed industrial interest in the past two decades. A good experimental design methodology allow properly distribute experiments within factor space so that can minimize the number of experiments required to develop a statistically sound relationship between factors and a response. We will start by covering designs used for screening. These designs are used to determine if a factor is important or not. They are normally done to gain insight into which factors are important in a particular process. This is followed up by response surface modeling (RSM) where more details regression models are used to determine response behavior. In this case full quadratic model is the response regression model. In all the RSM designs we will present there is no aliasing between the terms of the full quadratic response model. Aliasing with higher order terms may well be present. In order for one to properly access a quadratic term, a minimum of three levels of each factor is required. The full quadratic model define as the following,

$$Y = b_0 + \sum_{n=1}^5 b_n X_n + \sum_{n=1}^5 b_{nn} X_n^2 + \sum_{n < m}^5 b_{nm} X_n X_m + \varepsilon \quad (1.17)$$

where,  $b_0$  is intercept term,  $b_n$ ,  $b_{nn}$  and  $b_{nm}$  are linear, squared and interaction coefficients, respectively,  $\varepsilon$  represents the noise or error observed in the response.

There are many class of design in response surface modeling. The central composite design or CCD for fitting a second-order-model is the most popular class of design used for fitting these models. Generally, the CCD consists of  $2^n$  run.

Many studies have used response surface methodology to optimize processes. Gurusamy *et al.* (2007) used a four level Box Behnken factorial design combining with response surface methodology to optimize the medium composition for the degradation of phenol by *pseudomonas putida*. Second order polynomial regression model was used for analysis of the experiment. Cubic and quadratic terms were incorporated into the regression model to variable selection procedures. The experimental values are in good agreement with predicted values and the correlation coefficient was found to be 0.9980.

Sayan and Edecan (2008) applied the central composite designed to estimate the main effects and second order effects as well as interaction effects for decolorization of RB19 from aqueous solutions using ultrasound and activated carbon. Furthermore, three central replicates were also employed to calculate pure experimental error. As usual, the selected experiments were performed in random order to minimize the effect of systematic error. Matlab computer software was used to evaluate the experimental results.

Yuan *et al.* (2008) designed the experiments for the production of biodiesel by an alkaline catalyzed transesterification process by using  $2^4$  full factorial central composite designed. The RSM was used to optimize the conditions for the maximum conversion to biodiesel and understand the significance and interaction of the factors affecting the biodiesel production. The examples discussed show that CCD and RSM were used to design and analyze many different types of studies. Regression was also used for providing the empirical equation detailed the relationship between dependent and independent variables. Researchers have used this method to design the experimental runs and models in order to describe the effect of operating conditions, the scrubbing liquid flow rate, the gas flow rate, the concentration of gas

and liquid, the packing bed height, pH or temperature to the removal efficiency Piché *et al.* (2005) and Setameteekul (2008).

#### **1.2.5.4 Model formation and fitting in this work**

A regression model was used in this work to represent the result of experiments which were set by using central composite design. Typical quadratic model was employed to express the relationship between dependent and independent variables. Selection of significant variables for inclusion in this empirical model is carried out by Microsoft Excel essential regression, statistical package. The multiple regression starts with all possible quadratic terms. The value of the coefficients are then determined. Elimination of the non significant term is performed having the level of significance ( $P$  value  $\leq 0.05$ ) as criteria. A low  $P$  value of the particular independent variable indicates its significant role in improving the curve fitting of the model. The regression models were validated statistically by the analysis of variance (ANOVA).

### **1.3 Research Objectives**

- 1.3.1 To remove  $H_2S$  in biogas produced from concentrated latex industry by oxidation reaction with iron chelate of ethylenediamine tetraacetic acid (Fe(III)EDTA) in packed column.
- 1.3.2 To study the effect of the operating conditions on the efficiency of  $H_2S$  removal from gas stream by Fe(III)EDTA in laboratory scale packed column, and to develop a mathematic model.
- 1.3.3 To study the degradation of Fe-EDTA in biogas treatment.
- 1.3.4 To estimate the cost of  $H_2S$  removal from biogas using Fe(III)EDTA in packed column system.

## CHAPTER 2

### Removal of H<sub>2</sub>S in Biogas from Concentrated Latex Industry with Iron(III)chelate in Packed Column

#### 2.1 Abstract

This work concerns hydrogen sulfide (H<sub>2</sub>S) removal from biogas produced from wastewater of concentrated latex rubber industry (CLRI). H<sub>2</sub>S content in the biogas of CLRI is significantly high (i.e., up to 0.77 mol/m<sup>3</sup> or about 26,000 ppm) due to the use of H<sub>2</sub>SO<sub>4</sub> during rubber coagulation process. Attempts to treat biogas with high H<sub>2</sub>S have not been found in literature reviews. In this work, a chemical oxidation using an iron-chelated solution catalyzed by Fe(III)EDTA is selected for the treatment of such high H<sub>2</sub>S concentrations. Experiments were performed using a pilot packed column with diameter and packed height of 0.5 and 0.8 m, respectively. The biogas flow rate and H<sub>2</sub>S concentration were in the range of 5.16 x10<sup>-3</sup>-5.61x10<sup>-3</sup> m<sup>3</sup>/s and 0.35-0.77 mol/m<sup>3</sup>, respectively. Experimental results indicated that Fe(III)EDTA solution was effective at removing H<sub>2</sub>S from biogas with a maximum removal efficiency of about 97%. Suitable operating conditions, including Fe(III)EDTA concentration, flow of Fe(III)EDTA and air flow rate were determined. In addition, no side-reaction of Fe(III)EDTA with methane was found. Thus, chemical oxidation using an iron-chelated solution catalyzed by Fe(III)EDTA is a promising technology for H<sub>2</sub>S removal from biogas produced from CLRI or other industries. Finally, a mathematical model of the absorption and the reaction between H<sub>2</sub>S and Fe(III)EDTA in a packed column is proposed and verified against the experimental data. The results confirm the potential use of the model to design packed column for H<sub>2</sub>S removal from biogas using absorption coupled with oxidation by Fe(III)EDTA.

\* Chapters is the manuscript which has been published in Songklanakarin Journal of Science and Technology, volume 31, issue 2, year 2009, page 195-203.

## 2.2 Introduction

Anaerobic wastewater treatment is generally advantageous for removing organic matter from wastewater without consuming a large amount of electrical energy. A by-product of the anaerobic treatment is biogas which can be used as a renewable energy. Due to the energy crisis, industries are seeking various kinds of alternative energies, including biogas. Biogas can be produced from wastewater of many industries such as beverage, animal farm, starch, palm oil and rubber industries. Concentrated rubber latex industry (CRLI) is a major industry in the southern part of Thailand. Wastewater from CRLI is being used to produce biogas which is currently used as an indirect heat source for rubber block drying. Problem arises since wastewater of CRLI contains high sulfate content, up to 1000 mg/L (Rerngnarong, 2007), due to the use of sulfuric acid,  $\text{H}_2\text{SO}_4$ , in skim rubber production. Consequently, biogas produced from wastewater of CRLI is high in hydrogen sulfide ( $\text{H}_2\text{S}$ ) ( $0.35 - 0.77 \text{ mol/m}^3$ ), thus, it could not be used as a fuel directly. In order to use biogas more effectively and safely, removal of  $\text{H}_2\text{S}$  from the biogas is necessary and an effective  $\text{H}_2\text{S}$  removal system is required.

Numerous processes for  $\text{H}_2\text{S}$  removal from biogas have been developed. Among these processes are amine absorption, alkaline absorption, caustic absorption, and chemical oxidation. Iron is an excellent oxidizing agent for the conversion of  $\text{H}_2\text{S}$  to elemental sulfur. Iron, in its ferric state, is held in a solution by a chelating agent (i.e. ethylenediaminetetraacetic acid (EDTA), (hydroxyethyl)ethylenediaminetriacetic acid (HEDTA), or nitrilotriacetic acid (NTA)). The intent of the process is to oxidize hydrosulfide ( $\text{HS}^-$ ) ions to elemental sulfur by reduction of ferric (Fe(III)) iron to ferrous (Fe(II)) iron, and subsequently, the ferrous ions are then oxidized back to ferric ions by oxygen in the air. In recent years, gas desulfurization processes based on iron chelate chemistry have received increasing attention from both industrial and academic research groups. Demmink and Beenackers (1998), using a new penetration model for mass transfer parallel to chemical reaction, described the oxidative absorption of  $\text{H}_2\text{S}$  by using ferric chelates of EDTA and HEDTA. Iliuta and Larachi (2003) presented a modeling framework for the design of a scrubbing packed bed column for a bifunctional redox process for treating  $\text{H}_2\text{S}$

containing effluents arising from the kraft mill processes. The framework consisted of an exhaustive absorption-reaction-transport model which integrated both the oxidation of H<sub>2</sub>S in reactive ferric chelate solutions of EDTA and the regeneration of ferrous chelates resulting from oxidation of H<sub>2</sub>S. The kinetic effect of electrolytes and dynamic of pH on the oxidation of H<sub>2</sub>S with Fe(III)CDTA in anoxic condition were determined by Piché and Larachi (2006a) and Piché and Larachi (2006b). They proposed a reaction mechanism of H<sub>2</sub>S oxidation on both effects. Demmink *et al.* (1998) reported that freshly precipitated sulfur particles acted as catalyst for H<sub>2</sub>S absorption into aqueous solution of Fe-NTA and Demmink *et al.* (2002) described this phenomenon by developing a model based on Higbie's penetration theory. Horikawa *et al.* (2004) used Fe(III)EDTA to remove H<sub>2</sub>S from synthetic biogas using a lab scale randomly packed column. The chelated iron process is applied to remove H<sub>2</sub>S from gas streams in various industries, such as: natural gas processing, geothermal plants, refinery fuel gas, municipal odor control, landfill gas and municipal waste gasification.

Although much effort has been put into the development of H<sub>2</sub>S removal process using wet-scrubber with iron-chelate oxidation as mention above, previous works, however, have been focused on H<sub>2</sub>S removal from atmospheric emissions of sulfur or sulfate related industries such as natural gas and oil refining industry and pulp and paper industry. Only a few works were deal with H<sub>2</sub>S removal from biogas and they were investigated using synthetic biogas or mixture of H<sub>2</sub>S and balance gas such as N<sub>2</sub>, CO<sub>2</sub> and air. It is noteworthy that iron-chelated route has never been explored with real biogas produced from wastewater of concentrated rubber latex industry where H<sub>2</sub>S concentration is very high compared to H<sub>2</sub>S content in atmospheric emissions of industries, or in biogas produced from others sectors such as animal farms and the palm oil industries.

Since concentration of H<sub>2</sub>S in gas stream is known to play an important role on H<sub>2</sub>S removal efficiencies (Piché *et al.*, 2005), study of H<sub>2</sub>S removal from biogas of concentrated rubber latex industry will provide useful information to operate and design wet-scrubbers employing iron-chelate process under high H<sub>2</sub>S concentration.

The aim of this work was to remove H<sub>2</sub>S from biogas of CRLI using industry-size packed column which can handle H<sub>2</sub>S concentration up to 0.77 mol/m<sup>3</sup>. Suitable operating conditions (i.e., Fe(III)EDTA concentration, flow of Fe(III)EDTA and air) for this case are determined to seek highest removal efficiency. A mathematical model describing absorptions and reactions between H<sub>2</sub>S and Fe(III)EDTA in packed column under high H<sub>2</sub>S concentration are also proposed.

## **2.3 Materials and Method**

### **2.3.1 Chemicals**

40% w/w Ferric chloride solution (FeCl<sub>3</sub>) and EDTA·4Na powder of commercial grade were purchased from L.B. Science Ltd. Biogas was obtained from UASB (Up-flow Anaerobic Sludge Biodigester) of CRLI located in Songkhla province, Thailand.

### **2.3.2 Preparation of Fe(III)EDTA**

A Fe(III)EDTA solution was prepared using the following recipe: 75 kg of EDTANa<sub>4</sub>·4H<sub>2</sub>O powder was dissolved into 0.20 m<sup>3</sup> of water. 0.04 m<sup>3</sup> of 40% FeCl<sub>3</sub> solution was diluted to 0.20 m<sup>3</sup> with water (700 mol Fe/m<sup>3</sup>). The EDTA solution was then gently rinsed into the diluted FeCl<sub>3</sub> with continuous stirring. 0.40 m<sup>3</sup> of Fe(III)EDTA solution was obtained with a concentration of 350 mol/m<sup>3</sup>. The mole ratio of iron and EDTA in the solution was 1:1.2.

### **2.3.3 Apparatus**

Figure 2.1 is a schematic diagram of the H<sub>2</sub>S removal system which comprises of a packed column, a sedimentation tank, and a regeneration tank. The packed column is 2.2 m high, 0.5 m in diameter with 0.8 m packed section thickness. The packing material is composed of 5.0 cm Bio-Balls with a 190 m<sup>2</sup>/m<sup>3</sup> surface area per volume. The top of column holds a demister head packed with 5.0 cm Bio-Balls for removing entrained droplets from the gas stream. The entire packed column sits on



top of a vessel which serves as the sedimentation tank. The packed column used in this the experiments is illustrated in Figure 2.2

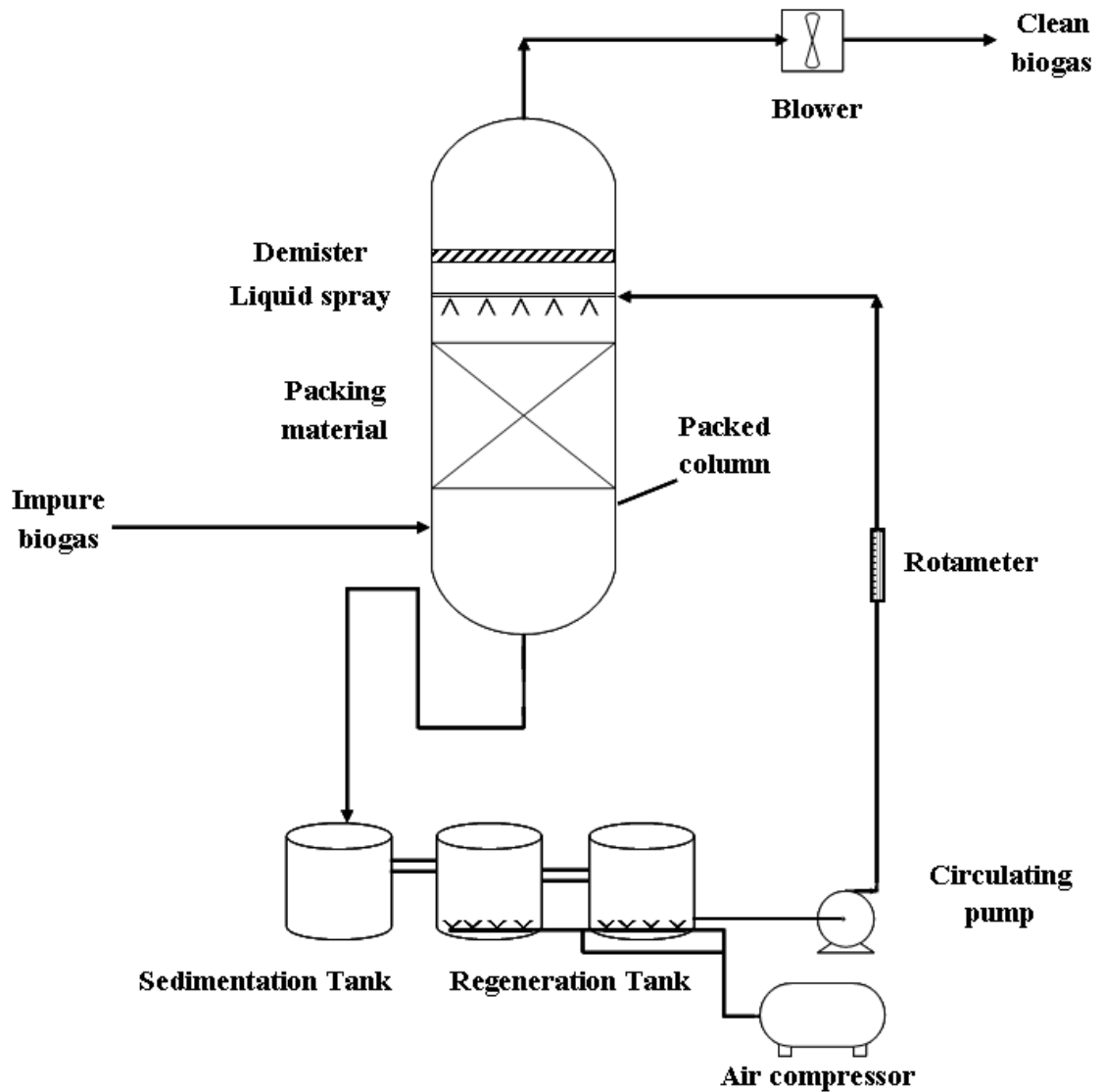


**Figure 2.1** Schematic diagram of the gas scrubbing packed column for  $H_2S$  removal from biogas

The scrubbing solution (Fe(III)EDTA solution) was pumped at a flow rate of  $6.67 \times 10^{-4} \text{ m}^3/\text{s}$  from the regeneration tank and fed into the packed column at the top, countercurrent to the biogas which was drawn from the UASB and fed to the packed column at the bottom with a flow rate of  $5.16 \times 10^{-3} - 5.61 \times 10^{-3} \text{ m}^3/\text{s}$ .  $H_2S$  in the biogas stream was absorbed into Fe(III)EDTA solution and transformed into a

sulfur compound. The spent Fe(III)EDTA solution flowed out of the bottom of the packed column into the sedimentation tank where sulfur got settled and separated. The overflow of Fe(II)EDTA solution from the sedimentation tank was regenerated into Fe(III)EDTA using air bubbling in the regeneration tank and recycled back to the packed column.



**Figure 2.2** The Pilot packed column used in H<sub>2</sub>S removal from biogas process

The concentration of H<sub>2</sub>S in biogas produced by UASB from the CRLI varied from day to day depending on wastewater characteristics but remaining constant throughout each day. Thus, for each experiment, the inlet H<sub>2</sub>S concentration was considered constant throughout the experimental time of 6 h. The initial H<sub>2</sub>S concentration in biogas ( $C_{H_2S}(g)_{in}$ ), biogas flow rate ( $G$ ), initial concentration of

Fe(III)EDTA ( $C_{Fe(III)EDTA,in}$ ), Volume of Fe-EDTA and air flow rate for each run are listed in Table 2.1.

**Table 2.1** Packed bed operating conditions

Run No.	$G \times 10^3$ ( $m^3/s$ )	$C_{H_2S}(g)_{in}$ mol/ $m^3$	$C_{Fe(III)EDTA,in}$ (mol/ $m^3$ )	Fe-EDTA Volume ( $m^3$ )	Air flow rate ( $m^3/min$ )
1	5.61	0.57	59.1	0.35	0.07
2	5.44	0.71	268.6	0.35	0.07
3	5.52	0.36	268.6	0.50	0.30
4	5.16	0.77	268.6	0.50	0.30

#### 2.3.4 Analysis

Samples of biogas at the inlet and the outlet of the packed column were taken during each experimental run using a gas sampling set which consists of an air sampling pump and a series of impingers containing a solution of Cadmium sulfate ( $CdSO_4$ ). The biogas sample was drawn into the  $CdSO_4$  solution which turned into Cadmium sulfide ( $CdS$ ) upon contacting with  $H_2S$ . The concentration of  $H_2S$  was then measured from the amount of  $CdS$  formed by the iodometric method. The iodometric method procedure is described in Appendix B-1.  $CH_4$  and  $CO_2$  concentrations in the biogas were determined by gas chromatography using the ShinCarbon ST 100/120 micropacked column, expressed as a mass percentage. The Fe(II)EDTA concentration ( $C_{Fe(II)EDTA}$ ) in the inlet scrubbing liquid, as mol Fe(II)/ $m^3$ , was determined by Phenanthroline method. The procedure of iron determination using phenanthroline method is described in Appendix B-2.1.

The amount of iron was determined from the absorbance at wavelength of 510 nm using HP 8453 UV-VIS Spectrophotometer. Fe(III) in the solution is reduced to Fe(II) state by boiling with acid and hydroxylamine, and treated with 1,10-phenanthroline at pH 3.2 to 3.3, (APHA, 1985). The total iron concentration ( $C_{Fe-EDTA}$ ) is obtained and Fe(III)EDTA concentration ( $C_{Fe(III)EDTA}$ ) can be determined by the following Equation:

$$C_{Fe(III)EDTA} = C_{Fe-EDTA} - C_{Fe(II)EDTA} \quad (2.1)$$

## 2.4 Results and Discussion

### 2.4.1 Iron analysis

Scrubbing liquid contains a number of species which can absorb UV light such as  $HS^-$ ,  $S^{2-}$ ,  $Fe(III)EDTA$  and  $Fe(II)EDTA$ . To analyze the iron concentration remaining in the scrubbing liquid by photometric measurement, the suitable wavelength must be determined.

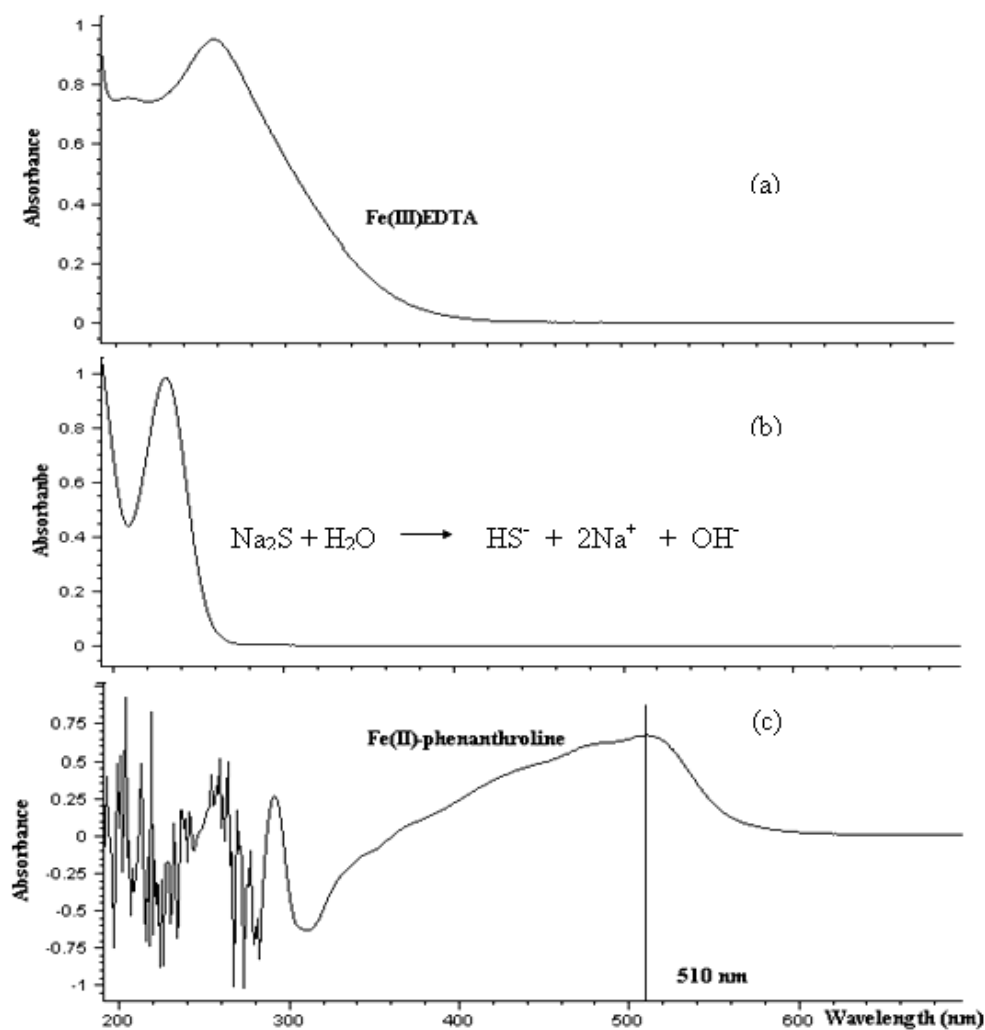


**Figure 2.3** UV-VIS bands of (a)  $Fe(III)EDTA$ , (b)  $Na_2S$  and (c)  $Fe(II)$ -phenanthroline

Figure 2.3 shows the UV band of  $\text{Na}_2\text{S}$  (represent  $\text{HS}^-$ ,  $\text{S}^{2-}$  species),  $\text{Fe(III)EDTA}$  and  $\text{Fe(II)-phenanthroline}$ . It is clearly shown from Figure 2.3 that all species absorb UV light at difference wavelengths. The UV bands of  $\text{Na}_2\text{S}$  (represent  $\text{HS}^-$ ,  $\text{S}^{2-}$  species) and  $\text{Fe(III)EDTA}$  were 210-260 nm, 230-400 nm, respectively. These results were consistent with Piché and Larachi (2006a). While the absorption of  $\text{Fe(II)-phenanthroline}$  was found at 370-590 nm. This spectra was similar to other literature (Blanco *et al.*, 1994). Thus,  $C_{\text{Fe(II)EDTA}}$  and  $C_{\text{Fe-EDTA}}$  in scrubbing liquid was determined at the wavelength of 510 nm. The calibration curve for  $C_{\text{Fe(II)EDTA}}$  and  $C_{\text{Fe-EDTA}}$  measurements at 510 nm is shown in Figure 2.5.

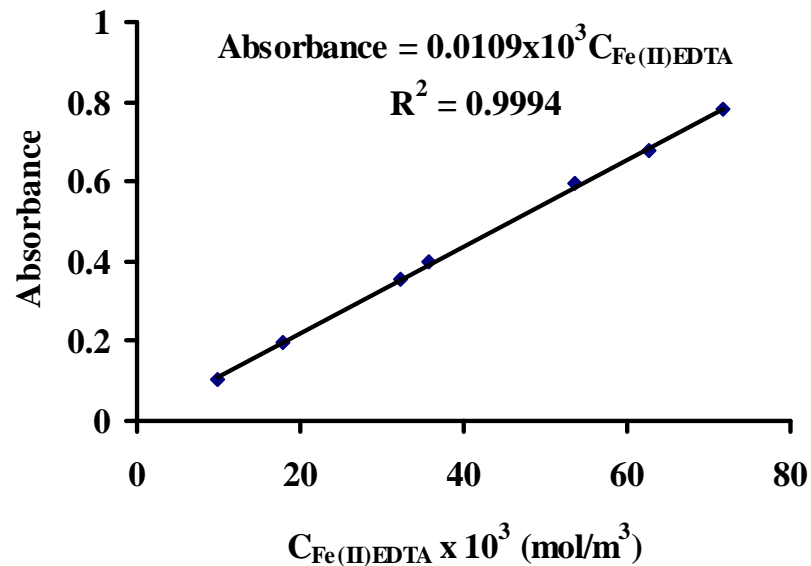


**Figure 2.4** Standard curve for Fe determination by photometric method at 510 nm

#### 2.4.2 $\text{H}_2\text{S}$ Removal efficiency

The removal of  $\text{H}_2\text{S}$  from biogas using a packed column was carried out coinciding with the oxidation reaction using an iron chelate,  $\text{Fe(III)EDTA}$ , as an oxidative reagent. The  $\text{H}_2\text{S}$  removal efficiency (%) was determined from the  $\text{H}_2\text{S}$  inlet concentrations,  $C_{\text{H}_2\text{S}}(g)_{in}$  and  $\text{H}_2\text{S}$  outlet concentrations,  $C_{\text{H}_2\text{S}}(g)_{out}$  as given by Equation (2.2). All results were tabulated in Appendix A-1.

$$H_2S \text{ removal efficiency}(\%) = \frac{C_{H_2S}(g)_{in} - C_{H_2S}(g)_{out}}{C_{H_2S}(g)_{in}} \times 100 \quad (2.2)$$

Figure 2.5 shows the H<sub>2</sub>S removal efficiency (%) of four experiments for various operating conditions. For Run No. 1, the H<sub>2</sub>S removal efficiency for the first 20 minutes was nearly 90%. Efficiency then continuously decreased with time. To improve the removal efficiency, the concentration of Fe(III)EDTA solution was increased to 268.8 mol/m<sup>3</sup> in Run No. 2. However, the H<sub>2</sub>S concentration in the second run, 0.71 mol/m<sup>3</sup> was also higher than that presented in the first run, 0.57 mol/m<sup>3</sup>. The H<sub>2</sub>S removal efficiency of Run No. 2 is also shown in Figure 2.5. As compared to Run No. 1, the removal efficiency of Run No. 2 was slightly improved since it did not steadily decrease. The initial H<sub>2</sub>S removal efficiency was also greater than 90%. As time increased, however, the H<sub>2</sub>S removal efficiency decreased before it remained approximately constant at 75% for 3 h and further declined to 40% within 4 h. The main reason for the decreasing of the removal efficiency was the decreasing of Fe(III)EDTA concentration with time, as depicted in Figure 2.6. The decreasing in Fe(III)EDTA concentration indicated that the Fe(III)EDTA consumption rate was higher than the regeneration rate. Although the high ionic strength or conductivity of the solution caused the H<sub>2</sub>S absorption rate to increase, the dissolved oxygen content also decreased (APHA, 1985). In order to maintain the H<sub>2</sub>S removal efficiency of this system, the air flow rate was increased. The air flow rate of Run No. 3 was increased to 0.30 m<sup>3</sup>/min. As shown in Figure 2.5, H<sub>2</sub>S removal efficiency was significantly improved. The H<sub>2</sub>S removal efficiency can be held constant at approximately 97% throughout the experimental time of 6 h. The same results were obtained in Run No. 4 although the H<sub>2</sub>S inlet concentration was about two times higher than that of Run No. 3. The results from Run No. 3 and No. 4 confirmed that air bubbling at a flow rate of 0.30 m<sup>3</sup>/min is enough for Fe(III)EDTA regeneration, This is supported by the only slight decrease in Fe(III)EDTA concentration with time, as illustrated in Figure 2.6.

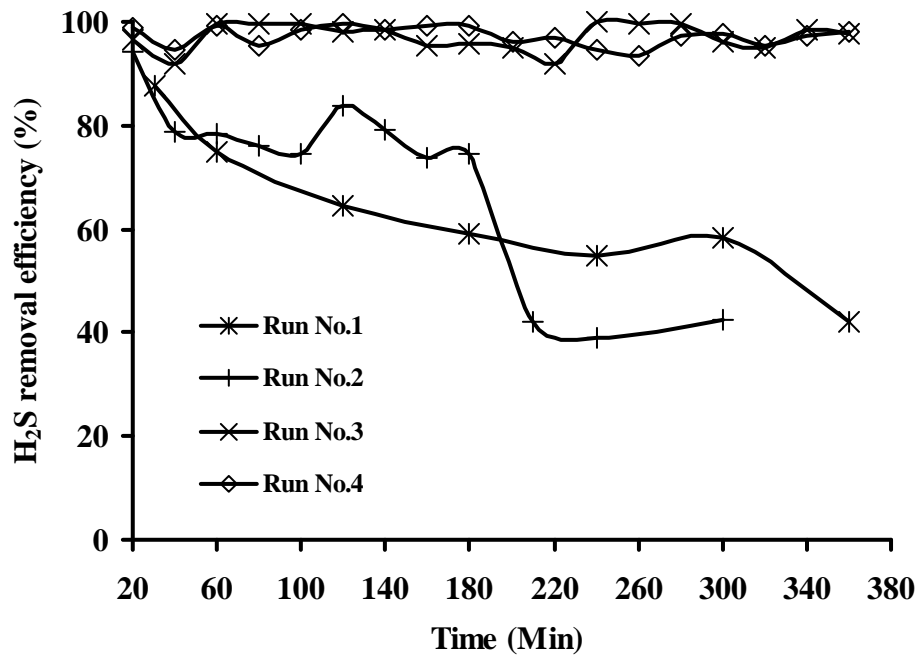


**Figure 2.5** H<sub>2</sub>S removal efficiency (%) with time in the oxidation reaction with Fe(III)EDTA at various conditions

**(Run No. 1:**  $G = 5.61 \times 10^{-3} \text{ m}^3/\text{s}$ ,  $C_{\text{H}_2\text{S}}(\text{g})_{\text{in}} = 0.57 \text{ mol}/\text{m}^3$ ,  $C_{\text{Fe(III)EDTA},\text{in}} = 59.1 \text{ mol}/\text{m}^3$ , Volume of Fe-EDTA =  $0.350 \text{ m}^3$  and Air flow rate =  $0.07 \text{ m}^3/\text{min}$ ;

**Run No. 2:**  $G = 5.44 \times 10^{-3} \text{ m}^3/\text{s}$ ,  $C_{\text{H}_2\text{S}}(\text{g})_{\text{in}} = 0.71 \text{ mol}/\text{m}^3$ ,  $C_{\text{Fe(III)EDTA},\text{in}} = 268.6 \text{ mol}/\text{m}^3$ , Volume of Fe-EDTA =  $0.350 \text{ m}^3$  and Air flow rate =  $0.07 \text{ m}^3/\text{min}$ ;

**Run No. 3:**  $G = 5.52 \times 10^{-3} \text{ m}^3/\text{s}$ ,  $C_{\text{H}_2\text{S}}(\text{g})_{\text{in}} = 0.36 \text{ mol}/\text{m}^3$ ,  $C_{\text{Fe(III)EDTA},\text{in}} = 268.6 \text{ mol}/\text{m}^3$ , Volume of Fe-EDTA =  $0.50 \text{ m}^3$  and Air flow rate =  $0.30 \text{ m}^3/\text{min}$ ;

**Run No. 4:**  $G = 5.16 \times 10^{-3} \text{ m}^3/\text{s}$ ,  $C_{\text{H}_2\text{S}}(\text{g})_{\text{in}} = 0.77 \text{ mol}/\text{m}^3$ ,  $C_{\text{Fe(III)EDTA},\text{in}} = 268.6 \text{ mol}/\text{m}^3$ , Volume of Fe-EDTA =  $0.50 \text{ m}^3$  and Air flow rate =  $0.30 \text{ m}^3/\text{min}$ )

In addition, increasing the liquid temperature during the run, as shown in Figure 2.7, may cause a decrease in H<sub>2</sub>S removal efficiency. The increase in temperature not only decreases the H<sub>2</sub>S absorption rate but also reduces oxygen solubility in Fe(III)EDTA solution, thus decreasing the regeneration rate of Fe(III)EDTA. During the experimental run, pH of the solution decreased from 7 to 6 which is suitable for H<sub>2</sub>S absorption as described by Demmink and Beenackers (1998). A high pH enhances H<sub>2</sub>S absorption rate but a higher OH<sup>-</sup> concentration also

enhances the CO<sub>2</sub> absorption (Couvert *et al.*, 2006). Thus the CO<sub>2</sub> absorption may affect the H<sub>2</sub>S absorption at a pH higher than 7.

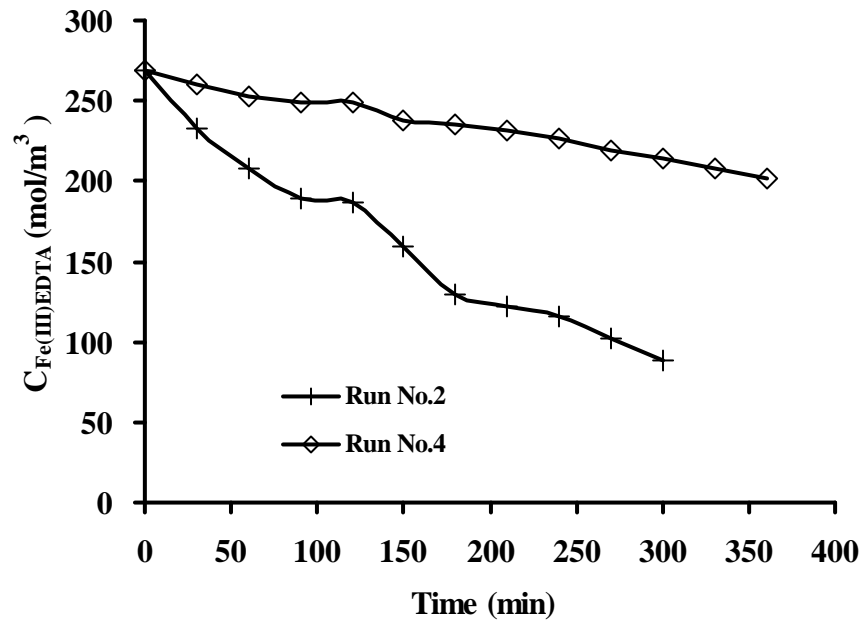


**Figure 2.6** Change of Fe(III)EDTA concentration (mol/m<sup>3</sup>) as function of reaction time for Run No. 2 and Run No. 4

**(Run No. 2:**  $G = 5.44 \times 10^{-3} \text{ m}^3/\text{s}$ ,  $C_{\text{H}_2\text{S}}(\text{g})_{\text{in}} = 0.71 \text{ mol/m}^3$ ,  $C_{\text{Fe(III)EDTA},\text{in}} = 268.6 \text{ mol/m}^3$ , Volume of Fe-EDTA = 0.350 m<sup>3</sup> and Air flow rate = 0.07 m<sup>3</sup>/min;

**Run No.4:**  $G = 5.16 \times 10^{-3} \text{ m}^3/\text{s}$ ,  $C_{\text{H}_2\text{S}}(\text{g})_{\text{in}} = 0.77 \text{ mol/m}^3$ ,  $C_{\text{Fe(III)EDTA},\text{in}} = 268.6 \text{ mol/m}^3$ , Volume of Fe-EDTA = 0.50 m<sup>3</sup> and Air flow rate = 0.30 m<sup>3</sup>/min)

### 2.4.3 Compositions of inlet and outlet biogas

The compositions of biogas at the inlet and the outlet of the system are shown in Table 2.2. It can be concluded that Fe(III)EDTA did not absorb or react with CH<sub>4</sub> or CO<sub>2</sub> as their inlet and outlet concentrations did not change. These results agree well with previous work by Horikawa *et al.* (2004).



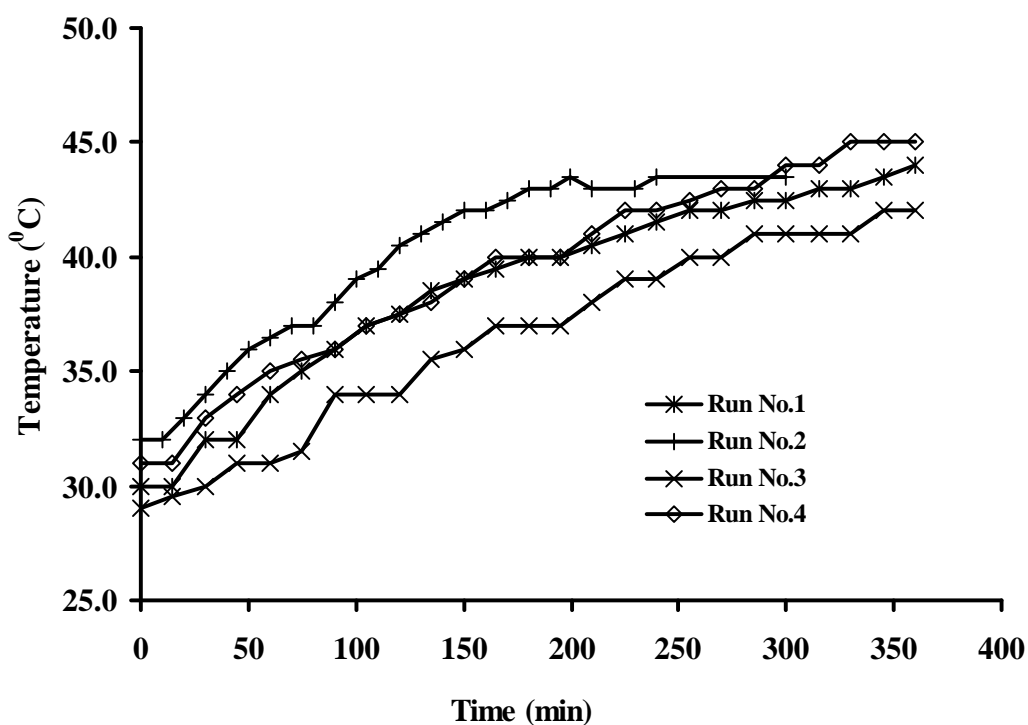


**Figure 2.7** Temperature profile of the scrubbing liquid during the reaction period

**Table 2.2** Mass percent of CH<sub>4</sub> and CO<sub>2</sub> in the biogas at the inlet and outlet

Sample	%CH <sub>4</sub>	%CO <sub>2</sub>
Inlet	77.14	17.69
Outlet	76.66	17.12

#### 2.4.4 Absorption and reaction model for H<sub>2</sub>S removal by oxidation with Fe(III)EDTA in packed column

In order to determine the height of the packed column when dealing with both absorption and reaction of H<sub>2</sub>S with Fe(III)EDTA, the packed column is considered as a packed bed reactor where absorption and reaction are taking place in series. A number of mass transfer and reaction steps were involved. Details of the model development are described step by step as follows.

The rate of H<sub>2</sub>S transfer from the bulk gas to the gas-liquid interface

can be given by Equation (2.3) (Fogler, 1999).

$$-r_{H_2S} = k_G a_i [C_{H_2S}(g) - C_{H_2Si}(g)] \quad (2.3)$$

where,  $-r_{H_2S}$  is a mass transfer rate in mol/m<sup>3</sup>·s,  $a_i$  is a gas-liquid interfacial area per volume of bed in m<sup>2</sup>/m<sup>3</sup>,  $C_{H_2S}(g)$  is the concentration of H<sub>2</sub>S in bulk gas phase (mol/m<sup>3</sup>),  $C_{H_2Si}(g)$  is the concentration of H<sub>2</sub>S at the gas-liquid interface (mol/m<sup>3</sup>), and  $k_G$  is a gas film mass transfer coefficient in m/s.  $k_G$  can be calculated by Equation (2.4) (Geankoplis, 1993).

$$k_G = \frac{0.4548}{\varepsilon} \frac{G}{A} (Re_G)^{-0.4069} (Sc_G)^{-2/3} \quad (2.4)$$

where  $Re_G$  and  $Sc_G$  are the Reynolds number and the Schmidt number in the gas phase, respectively. These are defined in Equations (2.5) and (2.6).

$$Re_G = \frac{W_G d_p}{\mu_G} \quad (2.5)$$

$$Sc_G = \frac{\mu_G}{\rho_G D_{H_2S,G}} \quad (2.6)$$

where,  $W_G$  is the superficial mass gas velocity in kg/m<sup>2</sup>·s,  $d_p$  is the nominal packing diameter (m),  $\mu_G$  is the gas viscosity (Pa·s),  $\rho_G$  is the gas density (kg/m<sup>3</sup>) and  $D_{H_2S,G}$  is the diffusivity of H<sub>2</sub>S in the gas phase (m<sup>2</sup>/s).  $D_{H_2S,G}$  can be estimated from the empirical equation of diffusivity for a binary gas mixture at low temperature as shown in Equation (2.7) (Bird *et al.*, 2002).

$$\frac{PD_{H_2S,G}}{(P_{C,H_2S}P_{C,CH_4})^{1/3} (T_{C,H_2S}T_{C,CH_4})^{5/12} (1/M_{H_2S} + 1/M_{CH_4})^{1/2}} = 2.745 \times 10^{-4} \left( \frac{T}{\sqrt{T_{C,H_2S}T_{C,CH_4}}} \right)^{1.823} \times 10^{-4} \quad (2.7)$$

where  $P$  is pressure (atm),  $p_{C,H_2S}$  is the critical pressure (atm) of  $H_2S$ ,  $p_{C,CH_4}$  is the critical pressure (atm) of  $CH_4$ ,  $T_{C,H_2S}$  is the critical temperature (K) of  $H_2S$ ,  $T_{C,CH_4}$  is the critical temperature (K) of  $CH_4$ , and  $M_{H_2S}$  and  $M_{CH_4}$  are the molecular weights of  $H_2S$  and  $CH_4$ , respectively.

$C_{H_2Si}(g)$  is related to the concentration of  $H_2S$  in the liquid phase at the interface.  $C_{H_2Si}$  is described by Equation (2.8) (Fogler, 1999).

$$C_{H_2Si} = C_{H_2Si}(g)/He \quad (2.8)$$

Here,  $He$  is defined as  $H_{H_2S}/RT$  where  $H_{H_2S}$  is the Henry's law constant in Pa  $m^3/mol$ ,  $R$  is the gas constant ( $m^3 Pa/mol K$ ) and  $T$  is the temperature (K).

The rate of absorption of  $H_2S$  at the liquid film is given by Equation (2.9).

$$-r_{H_2S} = k_L a_i E_{H_2S} [C_{H_2Si} - C_{H_2S}] \quad (2.9)$$

where,  $C_{H_2S}$  is the concentration of  $H_2S$  in bulk liquid phase ( $mol/m^3$ ),  $E_{H_2S}$  is the liquid film enhancement factor which is defined in Equation (2.10) (Levenspiel, 1999).

$$E_{H_2S} = \frac{\text{rate of take up of } H_2S \text{ when reaction occurs}}{\text{rate of take up of } H_2S \text{ for straight mass transfer}} \quad (2.10)$$

$k_L$  is the liquid film mass transfer coefficient (m/s) which can be calculated from the liquid properties and the absorber characteristics as expressed by Equation (2.11) (Onda *et al.*, 1968).

$$k_L = 0.0051 \left( \frac{\rho_L \nu_L}{a_i \mu_L} \right)^{2/3} \left( \frac{\mu_L}{\rho_L D_{AL}} \right)^{-1/2} \left( \frac{\rho_L}{\mu_L g} \right)^{-1/3} (a_T d_p)^{4/10} \quad (2.11)$$

where,  $v_L$  is the gas mass flux in  $\text{kg/m}^2\cdot\text{s}$ ,  $a_T$  is the specific surface area ( $\text{m}^2/\text{m}^3$ ),  $\mu_L$  is the liquid viscosity ( $\text{Pa}\cdot\text{s}$ ),  $\rho_L$  is the liquid density ( $\text{kg/m}^3$ ),  $g$  is the gravitational acceleration ( $\text{m/s}^2$ ) and  $D_{H_2S,L}$  is the diffusivity of  $H_2S$  in liquid.  $D_{H_2S,L}$  can be obtained from Wubs (1994).

The reaction of  $H_2S$  with  $Fe(III)EDTA$  took place in bulk liquid phase and was assumed to be the first order with respect to  $H_2S$  and  $Fe(III)EDTA$  as given by Equation (2.12) (Deberry, 1993).

$$-r_{H_2S} = k_r f_l C_{H_2S} C_{Fe(III)EDTA} \quad (2.12)$$

where,  $k_r$  is the reaction rate constant ( $\text{m}^3/\text{mol}\cdot\text{s}$ ),  $C_{Fe(III)EDTA}$  is the concentration of  $Fe(III)EDTA$  in bulk liquid ( $\text{mol/m}^3$ ) and  $f_l$  is the ratio of volume of liquid to the reactor volume, which is 0.01.

Combining equation (2.3) to (2.12), the reaction rate of  $H_2S$  can be described as,

$$-r_{H_2S} = RC_{H_2S}(g)$$

where  $R$  is defined as (Levenspiel, 1999).

$$R = \left( \frac{1}{k_G a_i} + \frac{He}{k_L a_i E_{H_2S}} + \frac{He}{k_r C_{Fe(III)EDTA} f_l} \right)^{-1} \quad (2.13)$$

The reaction rate is related to the height of the absorption tower,  $h$ , through the material balance of  $H_2S$ , as given by Equation (2.14) (Levenspiel, 1999).

$$h = \frac{G}{AR} \ln \left( \frac{C_{H_2S}(g)_{in}}{C_{H_2S}(g)_{out}} \right) \quad (2.14)$$

where  $G$  is the gas flow rate ( $\text{m}^3/\text{s}$ ),  $A$  is the cross-sectional area of the tower ( $\text{m}^2$ ),  $C_{H_2S}(g)_{,in}$  is the concentration of  $H_2S$  in biogas at the tower inlet ( $\text{mol}/\text{m}^3$ ),  $C_{H_2S}(g)_{,out}$  is the concentration of  $H_2S$  in biogas at the tower outlet ( $\text{mol}/\text{m}^3$ ).

The Hatta modulus,  $M_H$  (Hatta, 1932) is modified for this study and given by Equation (2.15).

$$M_H = \frac{\sqrt{k_r C_{Fe(III)EDTA} D_{H_2S,L}}}{k_L} \quad (2.15)$$

From the experimental data, and other parameters at hand, we can calculate the  $M_H$  for each experimental run. The values of  $M_H$ , and the values of the other parameters required to calculate  $M_H$ , are listed in Table 2.3 and 2.4.

The enhancement factor for an infinitely fast reaction,  $E_i$ , is defined for absorption and reaction by Levenspiel (1999) and is applied to this work with Equation (2.16).

$$E_i = 1 + \frac{D_{Fe(III)EDTA,L} C_{Fe(III)EDTA} H_{H_2S}}{b D_{H_2S,L} p_{H_2Si}} \quad (2.16)$$

where  $D_{Fe(III)EDTA,L}$  is the diffusion coefficient of Fe(III)EDTA in  $\text{m}^2/\text{s}$ ,  $b$  is a stoichiometric coefficient for Fe(III)EDTA, and  $p_{H_2Si}$  is the inlet partial pressure of  $H_2S$ . The  $E_i$  values can be calculated for each experimental run. The obtained  $E_i$  values and values of other parameters for calculating  $E_i$ , are shown in Table 2.3 and 2.4. Once  $E_i$  and  $M_H$  are known  $E_{H_2S}$  for each run is computed from Equation (2.17) (Levenspiel, 1999).

$$E_{H_2S} = M_H \left( 1 - \frac{M_H - 1}{2E_i} \right) \quad (2.17)$$

With the values of  $E_{H_2S}$  at hand, the values of  $R$  can be obtained

according to Equation (2.13). The values of the other parameters including  $k_G a_i$ ,  $k_L a_i$ ,  $k_r$ ,  $f_i$  and other related parameters required for the determination of  $R$ , are listed in Table 2.3 and Table 2.4.

Finally, the height of absorption tower,  $h$  can be calculated from Equation (2.14) where the values of  $G$ ,  $A$ ,  $C_{H_2S}(g)_{in}$  and  $C_{H_2S}(g)_{out}$  were measured experimentally. The calculated  $h$ ,  $h_{cal}$  were then compared with the actual  $h$ ,  $h_{actual}$  used in the experiment, as shown in Table 2.3, and it is shown that the calculated values agree well with the actual values implying that the proposed model explains the absorption and reaction phenomena inside the packed column quite well. Thus, the potential use of the model for designing the packed column for  $H_2S$  removal from biogas using absorption coupled with oxidation by Fe(III)EDTA is confirmed.

**Table 2.3** The actual and the predicted packed height and other related parameters

Run No.	$k_L a_i$ $\times 10^3 (s^{-1})$	$k_g a_i$ $(s^{-1})$	$M_H$	$E_i$ $\times 10^{-3}$	$E_{H_2S}$	$R$	$h_{predicted}$ (m)	$h_{actual}$ (m)
1	3.19	0.265	27.43	1.8	27.22	0.08	1.26	0.8
2	3.28	0.261	56.95	6.5	56.70	0.126	0.78	0.8
3	3.28	0.263	56.95	13.0	56.82	0.126	0.78	0.8
4	3.28	0.253	56.95	5.9	56.68	0.124	0.75	0.8

**Table 2.4** Parameter values for absorption and reaction modeling

Definition	Unit	Symbol	Value	Reference
Gas viscosity	Pa·s	$\mu_G$	$1.75 \times 10^{-5}$	
Gas density	kg/m <sup>3</sup>	$\rho_G$	1.15	
Liquid viscosity	Pa·s	$\mu_L$	0.005	
Liquid density	kg/m <sup>3</sup>	$\rho_L$	1210	
Critical pressures of H <sub>2</sub> S	atm	$p_{C,H_2S}$	88.2	Bird <i>et al.</i> , 2002
Critical pressures of CH <sub>4</sub>	atm	$p_{C,CH_4}$	45.8	Bird <i>et al.</i> , 2002
Critical temperatures of H <sub>2</sub> S	K	$T_{C,H_2S}$	373.0	Bird <i>et al.</i> , 2002
Critical temperatures of CH <sub>4</sub>	K	$T_{C,CH_4}$	191.1	Bird <i>et al.</i> , 2002
Molecular weight of H <sub>2</sub> S	g/gmol	$M_{H_2S}$	34	
Molecular weight of CH <sub>4</sub>	g/gmol	$M_{CH_4}$	16	
Henry's law constant of H <sub>2</sub> S in Fe(III)EDTA	Pa m <sup>3</sup> /mol	$H_{H_2S}$	$1.95 \times 10^3$	Deberry, 1993
Gas constant	m <sup>3</sup> Pa /mol K	$R$	8.314	
Temperature	K	$T$	303	
Nominal packing diameter	m	$d_P$	0.05	
Gas-liquid interfacial area	m <sup>2</sup> /m <sup>3</sup>	$a_i$	100	
Specific surface area	m <sup>2</sup> /m <sup>3</sup>	$a_T$	190	
Void fraction in bed		$\epsilon$	0.85	
Gravitational acceleration	m/s <sup>2</sup>	$g$	9.8	
Diffusivity of H <sub>2</sub> S in liquid	m <sup>2</sup> /s	$D_{H_2S,L}$	$1.44 \times 10^{-9}$	Wubs, 1994
Diffusion coefficient of Fe(III)EDTA	m <sup>2</sup> /s	$D_{Fe(III)EDTA,L}$	$0.54 \times 10^{-9}$	Wubs, 1994
Reaction rate constant	m <sup>3</sup> /mol·s	$k_r$	9	Deberry, 1993
Stoichiometric coefficient of Fe(III)EDTA		$b$	2	Deberry, 1993

#### 2.4.5 Comparison with other literatures in terms of the overall height of a gas film transfer unit, $H_{OG}$ and the overall number gas film transfer unit, $N_{OG}$

This experiment involves the absorption of  $H_2S$  gas from biogas by contacting it with an iron chelated catalyst through a packed column. The biogas used in the trials was approximately 1-3%  $H_2S$ , so it will be treated as a dilute mixture. The measure of the efficiency of the absorption process can be expressed in terms of the overall height of the gas film transfer unit,  $H_{OG}$  (m). The smaller  $H_{OG}$  is, the more efficient the absorption process will be.  $H_{OG}$  is a function of the overall number gas film transfer unit,  $N_{OG}$ . This quantity represents the degree of difficulty of the absorption process. A high  $N_{OG}$  value corresponds to a difficult separation.

The  $N_{OG}$  value can be calculated using a simplified method. The method assumes that the gas components are dilute and that components have ‘unlimited’ solubility in the liquid phase. Chemical reactions in the liquid phase reduce the equilibrium partial pressure of a solute over the solution, which greatly increases the driving force for mass transfer. The limiting case involves the assumption of an instantaneous, irreversible chemical reaction. This case corresponds to the maximum driving force, due to the reduction of the equilibrium partial pressure to zero (the reaction plane coincides with the interface). This is a reasonable assumption when iron chelate is used to oxidize the  $H_2S$ . For dilute systems,  $N_{OG}$  can be calculated using Equation (2.18) (Rafson and Harold, 1998).

$$N_{OG} = \ln \left( \frac{C_{H_2S}(g)_{in}}{C_{H_2S}(g)_{out}} \right) \quad (2.18)$$

Precise values for the  $H_2S$  composition at these points are crucial. Small discrepancies in these values could lead to large errors.  $H_{OG}$  is then calculated from  $N_{OG}$ , as expressed by Equation (2.19).

$$H_{OG} = h / N_{OG} \quad (2.19)$$

The calculated  $H_{OG}$  and  $N_{OG}$  values of our system are compared with other values found from the literature. Packed column system with different size were



used in all literatures, as shown in Table 2.5. The gas mass flow rate in our system is 10-40 times higher than those found in the literature. The gas mass flow rate also plays an important role in the separation process. We account for the superficial H<sub>2</sub>S mass velocity,  $W_{H_2S}$ , by defining the ratio  $H_{OG}/W_{H_2S}$  which includes the effect of mass flow rate on separation efficiency. It can be seen that the  $H_{OG}/W_{H_2S}$  value of our system is lower than those previously reported, indicating that the system provides better efficiency for H<sub>2</sub>S removal even at high H<sub>2</sub>S concentrations.

**Table 2.5** Comparison of  $H_{OG}$  and  $N_{OG}$  values to other literatures

Reference	Moosavi <i>et al.</i> (2005)	Horikawa <i>et al.</i> (2004)	Chen <i>et al.</i> (2001)	This study
System	H <sub>2</sub> S-Air	Synthetic biogas	H <sub>2</sub> S-Air	Biogas
Packing height	0.7	0.36	1.8	0.8
Packing diameter	0.135	0.054	0.45	0.5
Oxidant	NaOCl, H <sub>2</sub> O <sub>2</sub> and KMnO <sub>4</sub>	Fe(III)EDTA	NaOCl/NaOH	Fe(III)EDTA
Superficial H <sub>2</sub> S mass velocity, $W_{H_2S} \times 10^3$ (kg /m <sup>2</sup> ·s)	0.017	0.041	0.088	0.690
$N_{OG}$ , m	5.30	2.30	6.91	3.58
$H_{OG}$ , m	0.13	0.16	0.31	0.22
$H_{OG}/W_{H_2S}$	7.65	3.90	3.52	0.32

## 2.5 Conclusions

Biogas produced from wastewater of concentrated latex industry contains a high level of H<sub>2</sub>S. A low cost H<sub>2</sub>S removal system is needed to treat the biogas before it can be utilized. A chemical oxidation using an iron-chelated solution catalyzed by Fe(III)EDTA in a packed column is proposed for H<sub>2</sub>S removal from the biogas. The experimental results show that combination of absorption and oxidation by iron-

chelated solution catalyzed by Fe(III)EDTA can remove H<sub>2</sub>S from biogas with an efficiency up to 97% and the Fe(III)EDTA can be easily regenerated by bubbling air into the absorbing liquid. We conclude that chemical oxidation using an iron-chelated solution, catalyzed by Fe(III)EDTA is an economically promising technique to remove H<sub>2</sub>S from biogas even at high H<sub>2</sub>S concentrations. Additionally, a mathematical model of the absorption and the reaction between H<sub>2</sub>S and Fe(III)EDTA in a packed column was proposed and verified against the experimental data. The results confirm the potential use of the model for the design of a packed column for H<sub>2</sub>S removal from biogas using absorption coupled with oxidation by Fe(III)EDTA.

## CHAPTER 3

### **Statistical optimization of packed column operating conditions by response surface methodology on iron(III)chelate absorption process for the removal of hydrogen sulfide**

#### **3.1 Abstract**

The removal of hydrogen sulfide ( $H_2S$ ) by combining absorption and oxidation using iron(III)ethylenediaminetetraacetate (Fe(III)EDTA) solution was studied in a counter-current laboratory packed column. Process variables such as scrubbing liquid flow rate, gas flow rate, inlet  $H_2S$  concentration, initial Fe(III)EDTA concentration and height of packed bed are known to influence the absorption and reaction rate. The effects of these variables on absorption and reaction performance were analyzed via evaluating the absolute removal efficiency. A central composite design was used in the design of experiments. The  $H_2S$  removal efficiency was modeled statistically and optimized using Essential Regression Software. A quadratic model was suggested and validated experimentally with the coefficient of determination equal to 0.872. All significant variables were presented in the model and the interaction effects between variables were found. Results showed that the developed regression model provides a better understanding of the interactions involved in the studied  $H_2S$  removal process.

#### **3.2 Introduction**

Hydrogen sulfide ( $H_2S$ ) is typically found in a variety of sources including biogas, natural gas or industrial gases. The two main purposes for removing  $H_2S$  from gas streams are to achieve required air pollution levels and to purify synthetic gas. Because it is toxic and corrosive to most equipment, the removal of  $H_2S$  from biogas is recommended to protect downstream equipment, increase safety, and enable possible utilization of more efficient technologies such as microturbines and

fuel cells. A range of technology is available to treat this problem among which chemical scrubbing in a packed bed column is an established technique which is effective with low contact times. There are a variety of chemical oxidants available, such as chlorine ( $\text{Cl}_2$ ), ozone ( $\text{O}_3$ ), sodium hypochlorite ( $\text{NaOCl}$ ), potassium permanganate ( $\text{KMnO}_4$ ), hydrogen peroxide ( $\text{H}_2\text{O}_2$ ) and ferric salts ( $\text{Fe}^{3+}$ ) (Rafson and Harold, 1998). Many commercial processes are available for the removal of  $\text{H}_2\text{S}$  from gaseous streams. Most of the processes use gas-liquid contactors in which the  $\text{H}_2\text{S}$  is absorbed into a complex reagent to give either another dissolved sulfide containing component or elemental sulfur as a precipitate (Wubs and Beenackers, 1993). A model by Iliuta and Larachi (2003) established the potential of a bifunctional redox process where an iron chelate (i.e.  $\text{Fe(III)EDTA}$ ) is used to throttle  $\text{H}_2\text{S}$  emissions while dissolved oxygen simultaneously regenerates the ferrous chelate product into the active ferric form (Iliuta and Larachi, 2003; Demmink and Beenackers, 1998; McManus and Martell, 1997).

The operating variables, scrubbing liquid flow rate, the gas mass flow rate, the liquid to gas ratio ( $L/G$ ), the initial scrubbing concentration and height of packed bed are known to influence a packed bed performance. Chen *et al.* (2001) studied the feasibility of  $\text{H}_2\text{S}$  removal from air stream utilizing aqueous solutions in a packed bed scrubber pilot plant. They reported that the gas mass flow rate played a significant role in the process while the liquid flow rate demonstrated a minimal effect on absorption efficiency (Chen *et al.*, 2001). Godini and Mowla (2008) reported about the effect of amine concentration on  $\text{H}_2\text{S}$  and  $\text{CO}_2$  absorption. The results showed that increasing amine concentration results in an increased driving force for the absorption of both  $\text{H}_2\text{S}$  and  $\text{CO}_2$  and thus improves their absolute removal efficiency (Godini and Mowla, 2008). However  $\text{H}_2\text{S}$  absorption systems examined by the method of changing one factor at a time may result in data that is difficult to analyze and in which some interactions may be hidden. Response Surface Method (RSM) designs are used to identify the detailed dependence of different factors. To our knowledge, no RSM study has been done on the removal of  $\text{H}_2\text{S}$  from a gas stream by oxidation with  $\text{Fe(III)EDTA}$ . Our experiments were performed according to a central composite design (CCD) and utilized RSM to elucidate the relationships between the operating

variables and the average H<sub>2</sub>S removal efficiency (*RE*). An empirical model correlating the *RE* to the five variables, the scrubbing liquid flow rate (*L*), the gas flow rate (*G*), the inlet H<sub>2</sub>S concentration ( $C_{H_2S}(g)_{in}$ ), the initial Fe(III)EDTA concentration ( $C_{Fe,0}$ ) and the height of packed bed (*h*) was then developed. This information provides a better understanding of the interactions involved in the H<sub>2</sub>S removal process at the industrial scale.

### 3.3 Materials and Method

#### 3.3.1 Chemical

Ferric chloride solution (FeCl<sub>3</sub>, 40% w/w) and EDTANa<sub>4</sub>·4H<sub>2</sub>O powder with commercial grade were purchased from L.B. Science LTD. H<sub>2</sub>S 40% in N<sub>2</sub> was obtained from Thai Industrial Gases Public Company Limited. Fe(III)EDTA solution was prepared using 187 g of EDTA·4 Na powder dissolved into 900 mL of deionized water to which 100 mL of 40% FeCl<sub>3</sub> solution was added. The Fe(III)EDTA solution was obtained with a concentration of 0.35 mol Fe/L. The mole ratio of iron and EDTA in the solution was 1:1.2.

#### 3.3.2 Apparatus

A laboratory scale counter-current packed column system was constructed to study the effects of the system parameters. This system could be used for simultaneous studying the effects of different parameters such as the scrubbing liquid flow rate (*L*), the gas flow rate (*G*), the liquid to gas ratio (*L/G*), the inlet H<sub>2</sub>S concentration ( $C_{H_2S}(g)_{in}$ ), the initial Fe(III)EDTA concentration ( $C_{Fe,0}$ ) and the height of packed bed (*h*). A schematic packed column is shown in Figure 3.1.

The 5 cm diameter column was made of stainless steel with a total height of 65 cm. The column consists of packed bed section randomly packed with 6 mm raschig rings, sampling ports for gas and liquid. A mist eliminator layer of 6 mm

raschig rings which separates liquid drops entrained by the gas stream was located at the top of column.

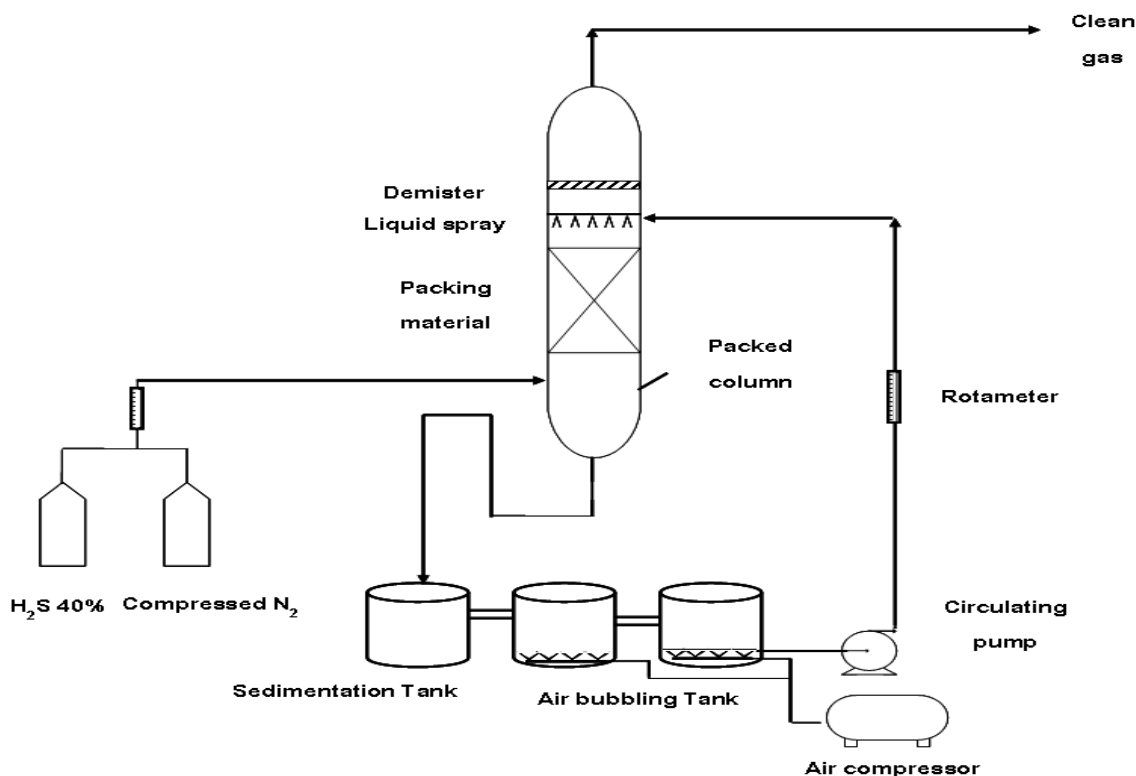


**Figure 3.1** A schematic of the laboratory packed column system

The sedimentation tank with two air bubbling tanks were located below the column. In these air bubbling tanks the Fe(II)EDTA was regenerated by oxygen back to the reactive Fe(III)EDTA and the reactive solution was then circulated to the top of the packed bed. The packed column used in the experiments is shown in Figure 3.2. The 40 % H<sub>2</sub>S/N<sub>2</sub> gas mixture was diluted with compressed N<sub>2</sub> via a mixer to reach the set inlet H<sub>2</sub>S concentration. Each experiment proceeded as follows. Initially, 4.5 L of Fe(III)EDTA solution was filled in the tanks. Once the pump was switched on, the liquid flow rate and the gas flow rate were adjusted to their respective levels with variable area flow meters. During the experiment, the inlet and outlet H<sub>2</sub>S concentration was measured by extracting gas volume from sampling port with air sampling pumps and a series of impingers containing a solution of cadmium sulfate (CdSO<sub>4</sub>). The biogas sample was drawn into CdSO<sub>4</sub> solution which turns to cadmium sulfide (CdS) when contacted with H<sub>2</sub>S. The concentration of H<sub>2</sub>S was then measured

from the amount of CdS formed by iodometric method. The iodometric method procedure is described in Appendix B-1. The Fe(II)EDTA concentration in the inlet scrubbing liquid, as mg Fe(III)/L, was determined by phenanthroline method. The amount of iron was determined from the absorbance at the wavelength of 510 nm by using HP 8453 UV-VIS Spectrophotometer (APHA, AWWA and WPCF, 1985). The procedure of iron determination using phenanthroline method is described in Appendix B-2.1.

At given time intervals, seven samples were taken: two gas samples at the bed inlet, four gas samples at the bed outlet and a sample of the liquid taken from the second air bubbling tank. All experiments were done at room temperature of  $26\pm 1$  °C and constant pH ( $6.8\pm 0.2$ ). Excess O<sub>2</sub> was used in the air bubbling tanks to insure complete regeneration so that the Fe(III)EDTA concentration fed to column was constant.



**Figure 3.2** Laboratory packed column used for H<sub>2</sub>S removal from gas stream

### 3.3.3 Design of experiments

Experimental design is a very large field which has enjoyed a renewed industrial interest in the past two decades. A good experimental design methodology

allows us to properly distribute our experiments within our factor space so that we can minimize the number of experiments required to develop a statistically sound relationship between factors and a response. A Response Surface Modeling (RSM) design was used to identify the detailed dependence of different variables, the scrubbing liquid flow rate ( $L$ ), the gas flow rate ( $G$ ), the inlet  $H_2S$  concentration ( $C_{H_2S}(g)_{in}$ ), the initial Fe(III)EDTA concentration ( $C_{Fe,0}$ ) and the height of packed bed ( $h$ ) on a response, the average  $H_2S$  removal efficiency ( $RE$ ). RSM helps identify the effective variables, study interactions, select optimum operating conditions and quantify the relationship between one or more measured responses and the vital input factors in limited number of experiments (Oskouie *et al.*, 2008). In this case, one is fairly certain that all variables are important and a full quadratic model is the response regression model (Steppan *et al.*, 1998). For five variables ( $x_i$ ) the response regression model for response ( $Y$ ) is

$$Y = b_0 + \sum_{n=1}^5 b_n X_n + \sum_{n=1}^5 b_{nn} X_n^2 + \sum_{n < m}^5 b_{nm} X_n X_m + \varepsilon \quad (3.1)$$

where,  $b_0$  is intercept term,  $b_n$ ,  $b_{nn}$  and  $b_{nm}$  are linear, squared and interaction coefficients, respectively,  $\varepsilon$  represents the noise or error observed in the response. The method used to find the coefficients in Equation (3.1) was the least squares method. This method squares the difference between observed response and predicted response (the error) for each data point and sums these squares. The desired optimum regression model provides a minimum for this sum. Central composite design (CCD) was used to design the set of experiment. This is the most popular class of designs used for fitting second order model (Douglas, 2001). A circumscribed CCD for five independent variables at fives level was employed and the total number of experiments was 29. Twenty six experiments were augmented with three replications at the center points to reduce the prediction variance. Additional ten experiments were conducted for obtain the clearer removal efficiency trend corresponding to the varied operating condition when the others were keep constant. The range and levels of the variables investigated are listed in Table 3.1.



### 3.3.4 Statistical analysis

The statistical analysis was carried out based on the experimental data using a full quadratic model which was fitted to the data to obtain the regression equation using the multiple regression tool in Essential Regression software version 2.210 (Steppan *et al.*, 1998). The procedure for using this software to design the experiments and analyzes data have been described in Appendix C. Stepwise regression was used to evaluate the statistical significance of the regression model whereas the analysis of variance (ANOVA) was used in order to test the significant of the model and model coefficients.

**Table 3.1** Experimental range and levels of the independent variables designed by Essential Experimental Design

Variable	Symbol coded	Range and levels				
		-1	-0.5	0	0.5	1
Gas flow rate (L/s)	$G$	0.033	0.067	0.1	0.133	0.167
Scrubbing liquid(Fe(III)EDTA solution) flow rate (mL/s)	$L$	0.167	0.333	0.500	0.667	0.833
Inlet H <sub>2</sub> S concentration (mol/m <sup>3</sup> )	$C_{H_2S}(g)_{in}$	0.029	0.059	0.088	0.118	0.147
Initial Fe(III)EDTA concentration (mol/m <sup>3</sup> )	$C_{Fe,0}$	10	85	160	235	310
Height of packed bed (m)	$h$	0.150	0.225	0.300	0.375	0.450

## 3.4 Results and discussion

### 3.4.1 Response analysis and interpretation

Response surface methodology (RSM) using central composite design (CCD) was used to develop a correlation between the packed column operating conditions and H<sub>2</sub>S removal efficiency. The completely design matrix together with the response values obtained from the experimental works are given in Table 3.2. The inlet H<sub>2</sub>S concentration in each experiment was slightly different from the design values. The average H<sub>2</sub>S removal efficiency ( $RE$ ) at each condition was calculated at  $t$

= 10, 15, 20 and 25 min. Standard deviation of all measurements remains within 3.4% of the average whereas no specific trend with time was observed. All results data are shown in Appendix A-2. The data were fitted by the multiple regression method. The model which was selected as suggested by the software using stepwise regression was obtained. The best model was chosen as the one which provided the smallest mean error. The final empirical model in terms of operating parameters after excluding the insignificant terms is shown in Equation (3.2).

$$RE = 134.98 - 285.12G - 344.32 C_{H_2S}(g)_{in} - 0.231 C_{Fe,0} - 132.69h + 0.166L C_{Fe,0} + 801.02 C_{H_2S}(g)_{in} h + 0.763 C_{Fe,0} h \quad (3.2)$$

The quality of the model developed was evaluated based on the correlation coefficient value. The R value was 0.934, the relatively high value of R (close to unity) indicating that there was a good agreement between the experimental and the predicted value from model (data is shown in Table 3.2). The R<sup>2</sup> value was 0.872. This indicated that the remaining 12.8% of the variation in removal efficiency is left unexplained. It should be noted that a R<sup>2</sup> value greater than 0.75 indicates the appropriateness of the model (Oskouie *et al.*, 2008). The adjusted R<sup>2</sup> and predicted R<sup>2</sup> value are 0.843 and 0.794, respectively. R<sup>2</sup>, adjusted R<sup>2</sup>, and R<sup>2</sup> for prediction together are very convenient to get a quick impression of the overall fit of the model and the predictive power based on one data point removed. In a good model, these three parameters should not be too different from each other. The large precision index demonstrates the satisfactory ability of the underlying model to predict new values.

The analysis of variance (ANOVA) is a technique frequently used to analyze data from planned or designed experiments. The analysis of variance for model is shown in the Table 3.3. The Fisher F-test ( $F_{model} = 30.19$ ) with a very low probability value indicates a high confidence for the model and it is also noticed that a moderate lack of fit (LOF) with a probability more than 0.05, indicating the applicability of the model.

**Table 3.2** Circumscribed central composite design matrix of five variables in uncoded variables with observed and predicted H<sub>2</sub>S removal efficiency

Run No.	$h$ (m)	$L$ (mL/s)	$C_{Fe,0}$ (mol/m <sup>3</sup> )	$G$ (L/s)	$C_{H_2S(g),in}$ (mol/m <sup>3</sup> )	$RE$	
						<i>Observed</i>	<i>Predicted</i>
1	0.300	0.500	160	0.033	0.061	92.4	92.3
2	0.375	0.333	85	0.067	0.067	75.0	72.7
3	0.225	0.667	85	0.067	0.070	81.4	78.9
4	0.225	0.333	235	0.067	0.055	77.3	76.1
5	0.375	0.667	235	0.067	0.077	99.3	-
6	0.225	0.333	85	0.067	0.149	63.9	61.3
7	0.375	0.667	85	0.067	0.179	76.0	72.4
8	0.375	0.333	235	0.067	0.161	83.4	85.0
9	0.225	0.667	235	0.067	0.141	78.7	74.9
10	0.300	0.500	160	0.100	0.025	72.1	77.0
11	0.300	0.500	10	0.100	0.065	56.5	60.7
12	0.300	0.167	160	0.100	0.084	56.0	62.0
13	0.150	0.500	160	0.100	0.071	70.7	65.2
14	0.300	0.500	160	0.100	0.146	62.8	64.4
15	0.300	0.500	310	0.100	0.071	87.0	84.3
16	0.300	0.833	160	0.100	0.084	75.0	79.7
17	0.450	0.500	160	0.100	0.071	84.3	79.2
18	0.300	0.500	160	0.100	0.084	70.0	70.9
19	0.300	0.500	160	0.100	0.084	69.0	70.9
20	0.300	0.500	160	0.100	0.072	74.2	72.0
21	0.225	0.333	85	0.133	0.071	64.9	55.2
22	0.375	0.667	85	0.133	0.062	62.0	58.6
23	0.375	0.333	235	0.133	0.059	71.7	70.5
24	0.225	0.667	235	0.133	0.053	65.4	70.4
25	0.375	0.333	85	0.133	0.089	52.2	52.7
26	0.225	0.667	85	0.133	0.116	46.5	52.4
27	0.225	0.333	235	0.133	0.106	46.8	48.7
28	0.375	0.667	235	0.133	0.125	81.5	80.6
29	0.300	0.500	160	0.167	0.100	56.2	50.2
30	0.225	0.500	156	0.100	0.072	71.0	68.5
31	0.375	0.500	156	0.100	0.070	78.5	75.1
32	0.300	0.667	156	0.100	0.082	71.8	75.0
33	0.300	0.500	157	0.100	0.060	70.4	73.0
34	0.300	0.500	156	0.100	0.119	57.6	66.9
35	0.300	0.500	157	0.067	0.091	80.1	79.3
36	0.300	0.500	156	0.133	0.100	58.3	59.3
37	0.300	0.333	157	0.100	0.077	58.1	67.0
38	0.300	0.500	81	0.100	0.066	65.4	66.3
39	0.300	0.500	216	0.100	0.068	85.3	77.0

**Table 3.3** Analysis of variance (ANOVA) for the regression model

<i>Source of variation</i>	<i>Sum of quares</i>	<i>% Sum of quares</i>	<i>Mean squares</i>	<i>F-value</i>	<i>F Significant</i>	<i>Degree of freedom</i>
Regression	4857.8	87	693.97	30.19	3.87E-12	7
Residual	712.56	13	22.99			31
LOF Error	712.06	13 (100)	23.74	47.4704	0.114	30
Pure Error	0.500	0 (0)	0.500			1
Total	5570.4	100				38

$R = 0.934$ ,  $R^2 = 0.872$ ,  $R^2$  adjusted = 0.843,  $R^2$  for Prediction = 0.794, Standard Error = 4.794, Coefficient of Variation = 6.802, Precision Index = 165.635

A t-test statistic was used for checking the coefficients significance and the result of least square fit is shown in Table 3.4. A P-value less than 0.05 indicated that the model terms were significant, that is, there is a less than 5% error probability that the corresponding coefficient is not significant. The smaller the P-value in the table, the more significant term. Thus, the *G* term is the most significant term. The model showed coefficient of variation (CV) of 6.80. The relatively low value of the CV indicates a better precision and reliability of the experiments carried out.

**Table 3.4** The least square fit and model coefficients (significant of regression coefficients)

<b>Model Term</b>	<b>Coefficient</b>	<b>P value</b>	<b>Std Error</b>	<b>-95%</b>	<b>95%</b>	<b>t Stat</b>	<b>VIF</b>
Intercept	134.98	1.67E-09	16.04	102.25	167.70	8.413	
<i>G</i>	-285.12	3.18E-11	28.50	-343.25	-227.00	-10.00	1.021
$C_{H_2S(g),in}$	-344.32	0.00715	119.56	-588.16	-100.49	-2.880	25.58
$C_{Fe,0}$	-0.231	0.00181	67.74	-369.40	-93.08	-3.413	28.84
<i>h</i>	-132.69	0.01290	50.28	-235.24	-30.13	-2.639	16.09
$L^* C_{Fe,0}$	0.166	2.11E-05	33.15	98.36	233.59	5.006	2.729
$C_{H_2S(g),in} * h$	801.02	0.04087	375.37	35.44	1566.6	2.134	33.88
$C_{Fe,0} * h$	0.762	0.00122	214.25	325.87	1199.8	3.560	34.45

After calculating the model, a thorough analysis of the residual is very important to evaluate the adequacy of the regression (Steppan *et al.*, 1998). One of the assumptions of linear regression is that the errors or residuals are normally distributed. This is the most commonly used method in residual analysis and can be checked by plotting the individual residuals against the expected normal value or rankit, a normal probability plot. In such a plot, the points should form a straight line if the residual are perfectly normally distributed. A normal probability plot from the H<sub>2</sub>S removal is shown in Figure 3.3. Since the points exhibited linear behavior, we have confirmation of the normal distribution of residuals. From the statistical results obtained, it was shown that the above model was adequate to predict the removal efficiency within the range of variable studied. Figure 3.4 shows the predicted values versus the experimental values of removal efficiency. As can be seen, the predicted values obtained were quite close to the experimental values, indicating that the model developed was successful in capturing the correlation between the packed bed operation variables to removal efficiency.

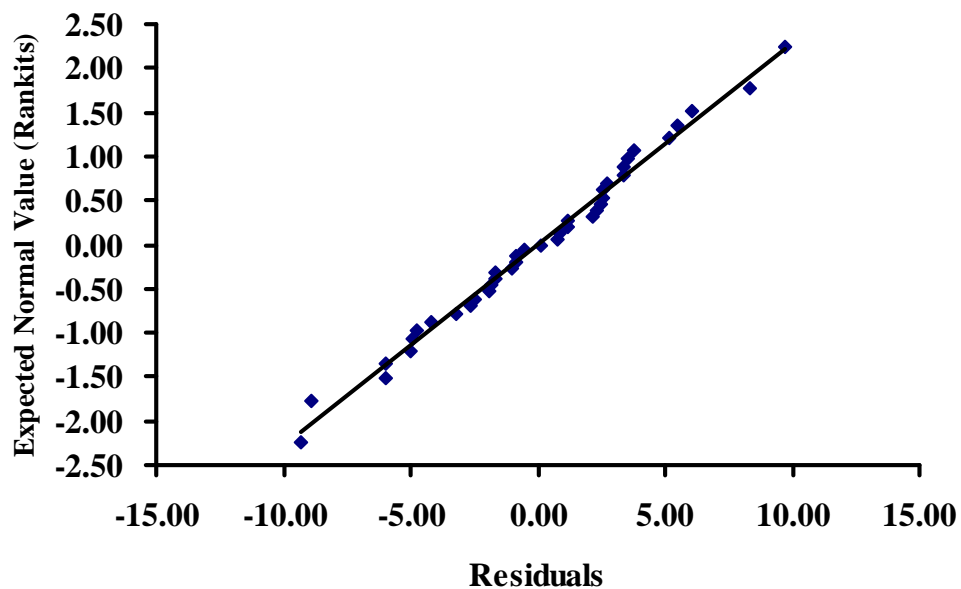


**Figure 3.3** Normal probability plot

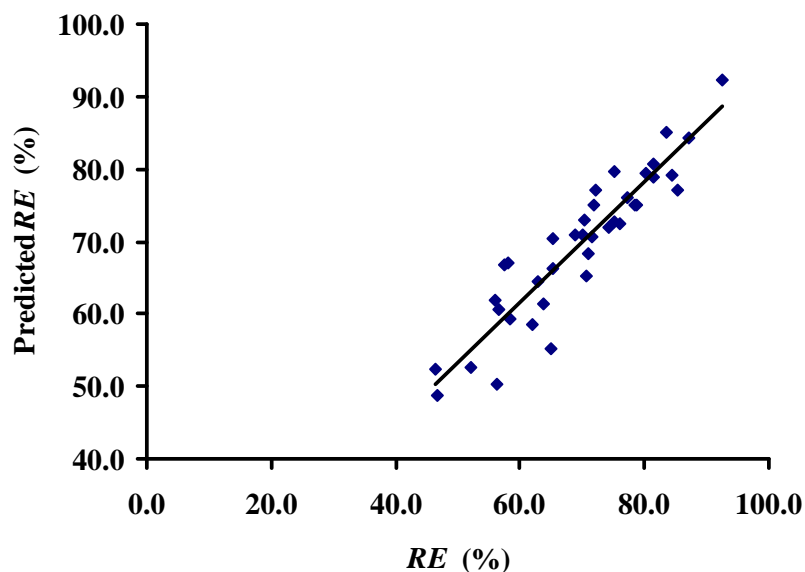


**Figure 3.4** Predicted and experimental H<sub>2</sub>S removal efficiency

### 3.4.2 Effects of variables on H<sub>2</sub>S removal efficiency (*RE*)

Figure 3.5-3.11 illustrate the curvilinear aspect of each effect towards the removal efficiency. The rhombus points were the data from the experiments while the solid line is the data predicted from Equation (3.2). From these figures, it can explain that the predicted removal efficiency from the regression model is in good agreement with the experimentally obtained data.

Figure 3.5 shows the experimental results relating the effect of packed bed height to removal efficiency. As expected, increasing packed bed height increases the removal efficiency. In this manner, greater height of packed bed provide more mass transfer area so the contact time between H<sub>2</sub>S in gas stream and Fe(III)EDTA solution is increased, reducing the outlet concentration of H<sub>2</sub>S. Figure 3.6 shows the dependency of removal efficiency on the flow rate of Fe(III)EDTA solution. Again, as expected, increasing solution flow rate increases removal efficiency. The increase in removal efficiency at liquid flow rate higher than 0.5 mL/s was higher than that liquid flow rate higher lower than 0.5 mL/s. And also the prediction in removal efficiency using regression model in Equation 3.2 at high liquid flow rate was more precision than the lower one. Moreover, it can also be observed that the effect of height of

packed bed on removal efficiency was stronger than the effect of the flow rate of Fe(III)EDTA solution.

Generally speaking, increasing the initial Fe(III)EDTA concentration increases the driving force for absorption and reaction rate of H<sub>2</sub>S, thus increasing its removal efficiency. Dilute Fe(III)EDTA solutions do not provide enough of the reactive ferric species to oxidize much of the H<sub>2</sub>S in the gas stream, resulting in low absorption efficiency and reaction rate. Figure 3.7 illustrates the positive linear effect of initial Fe(III)EDTA concentration on removal efficiency. It can be observed that the increase of removal efficiency trends to be constant at the Fe-EDTA concentration higher than 310 mol/m<sup>3</sup>.

The  $L/G$  ratio is the most important parameter for the design of an absorption column. Thus for given gas flow rate, a reduction in liquid flow decreases the slope of the operating line (Perry and Chilton, 1984). It should be noted that the range of variation of  $L/G$  is within the permissible hydrodynamic range, that is, between dryness and flooding regions.

Removal efficiency is sensitive to the  $L/G$  ratio. Increasing the  $L/G$  ratio has a positive effect on removal efficiency. The  $L/G$  ratio showed a linear relationship which can be divided into two regions, higher and lower  $L/G$  ratios as described in Figure 3.8 and 3.9. The influence of  $L/G$  ratio in the higher  $L/G$  ratio region was greater than that in the lower one. Two empirical equations described the effect of  $L/G$  ratio on removal efficiency for higher and lower  $L/G$  ratios are proposed in Equation (3.3) and (3.4) respectively.

$$RE = 2.349(L/G) + 51.19 \quad (3.3)$$

*at low  $L/G$  ratio and  $G$  is kept constant*

$$RE = 3.015(L/G) + 49.16 \quad (3.4)$$

*at large  $L/G$  ratio and  $L$  is kept constant*

Gas flow rate and inlet H<sub>2</sub>S concentration provide the main negative effects on removal efficiency as show in Figure 3.10 and 3.11 (Chen *et al.*, 2001; Godini and Mowla, 2008; Piché *et al.*, 2005). In a chemical scrubber, H<sub>2</sub>S is continuously removed by its reaction with Fe(III)EDTA. Therefore, no H<sub>2</sub>S

accumulates in the scrubbing solution. As long as a scrubbing solution sufficiently wets the interfacial area of the packing in the scrubber, liquid flow rate demonstrates a minimal effect on absorption efficiency. However, because  $H_2S$  removal is accomplished by chemical reactions, residence time is an important consideration. Thus, gas flow rate is expected to play a significant role in this process (Chen *et al.*, 2001).

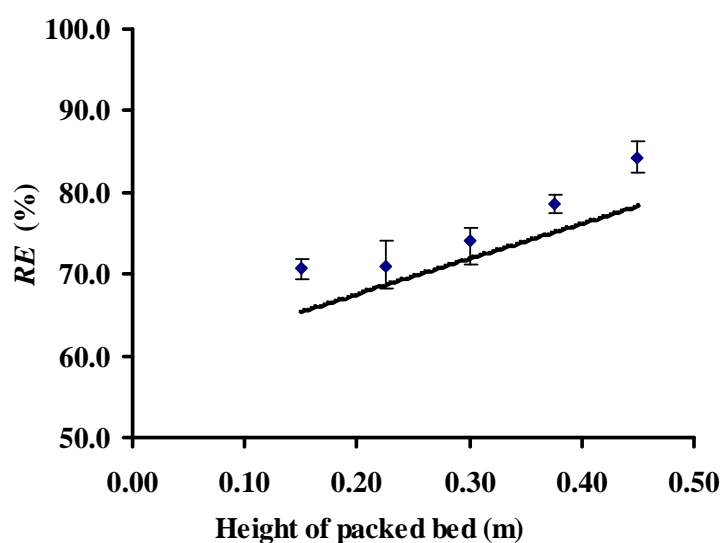


**Figure 3.5** Effect of height of packed bed ( $h$ ) on removal efficiency ( $RE$ ).

$$(L = 0.5 \text{ mL/s}, C_{Fe,0} = 160 \text{ mol/m}^3, G = 0.1 \text{ L/s}, C_{H_2S}(g)_{in} = 0.07 \text{ mol/m}^3)$$

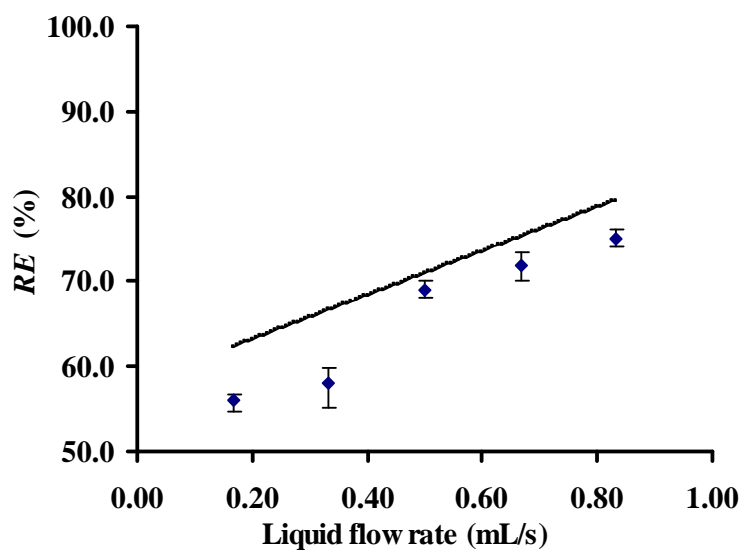


**Figure 3.6** Effect of liquid flow rate ( $L$ ) on removal efficiency ( $RE$ ). ( $h = 0.30 \text{ m}$ ,

$$C_{Fe,0} = 160 \text{ mol/m}^3, G = 0.1 \text{ L/s}, C_{H_2S}(g)_{in} = 0.08 \text{ mol/m}^3)$$



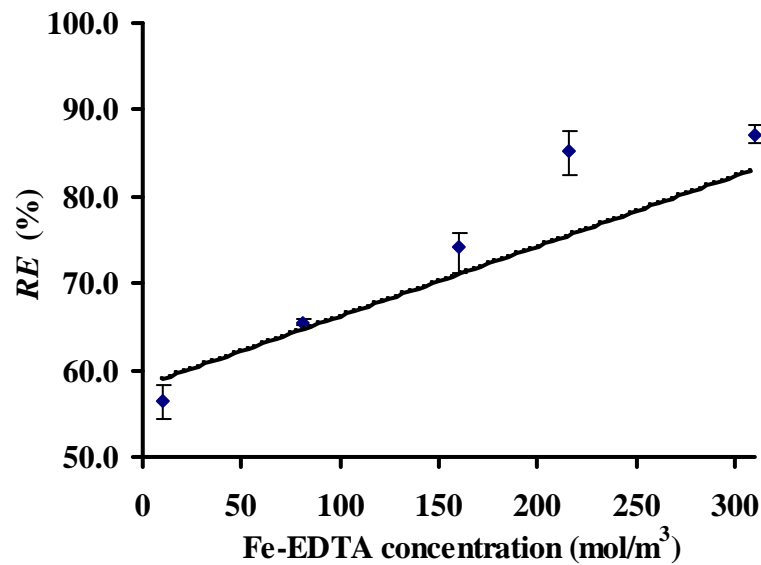


**Figure 3.7** Effect of initial Fe(III)EDTA concentration ( $C_{Fe,0}$ ) on removal efficiency ( $RE$ ). ( $h = 0.30$  m,  $L = 0.5$  mL/s,  $G = 0.1$  L/s,  $C_{H_2S}(g)_{in} = 0.08$  mol/m<sup>3</sup>)

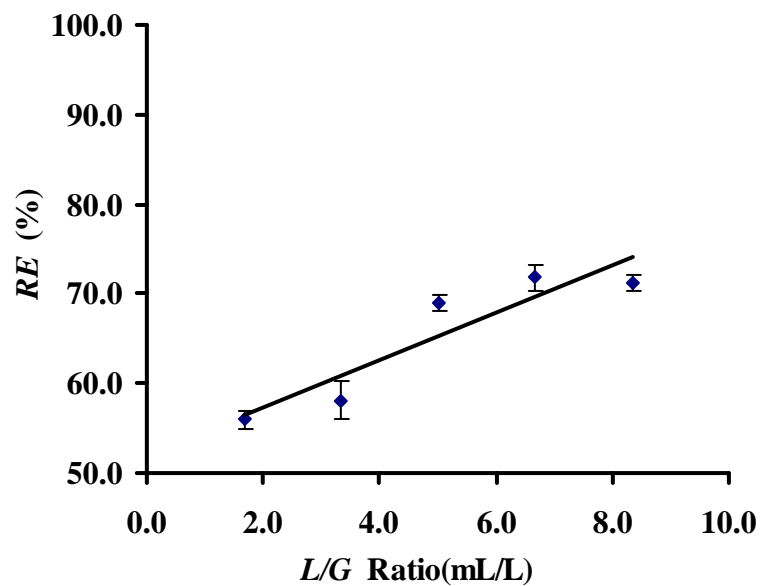


**Figure 3.8** Effect of liquid to gas ratio ( $L/G$ ) on removal efficiency ( $RE$ ) for low  $L/G$ . ( $h = 0.30$  m,  $L = 0.17$ – $0.83$  mL/s,  $C_{Fe,0} = 160$  mol/m<sup>3</sup>,  $G = 0.1$  L/s,  $C_{H_2S}(g)_{in} = 0.08$  mol/m<sup>3</sup>)

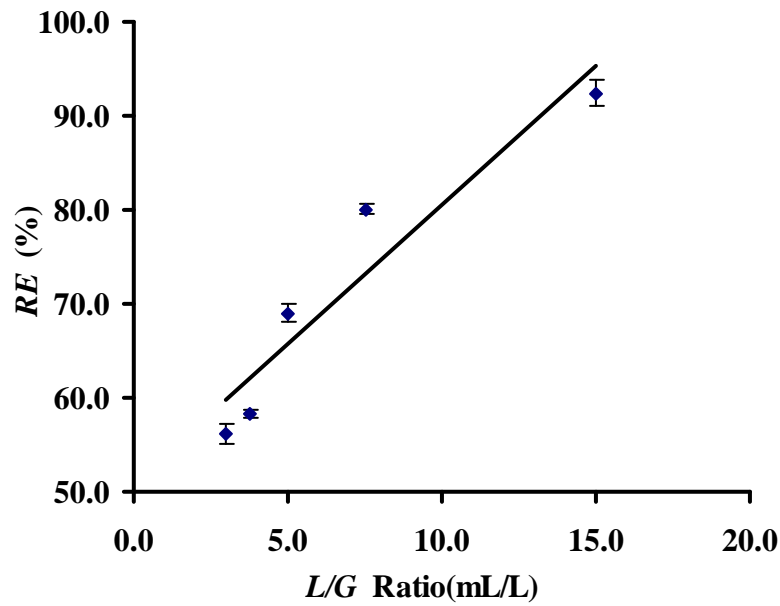


**Figure 3.9** Effect of liquid to gas ratio ( $L/G$ ) on removal efficiency ( $RE$ ) for large  $L/G$ . ( $h = 0.30$  m,  $L = 0.5$  mL/s,  $C_{Fe,0} = 16$  mol/m<sup>3</sup>,  $G = 0.03$ - $0.17$  L/s,  $C_{H_2S}(g)_{in} = 0.09$  mol/m<sup>3</sup>)

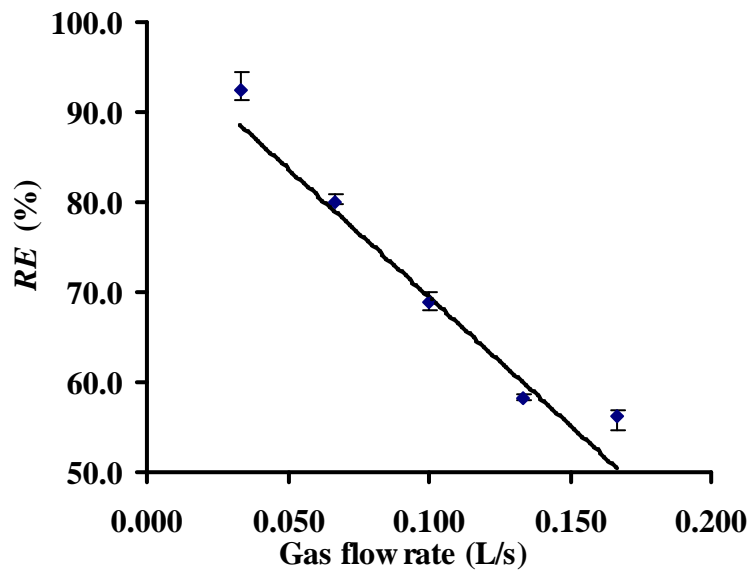


**Figure 3.10** Effect of gas flow rate ( $G$ ) on removal efficiency ( $RE$ ). ( $h = 0.30$  m,  $L = 0.5$  mL/s,  $C_{Fe,0} = 160$  mol/m<sup>3</sup>,  $C_{H_2S}(g)_{in} = 0.09$  mol/m<sup>3</sup>)

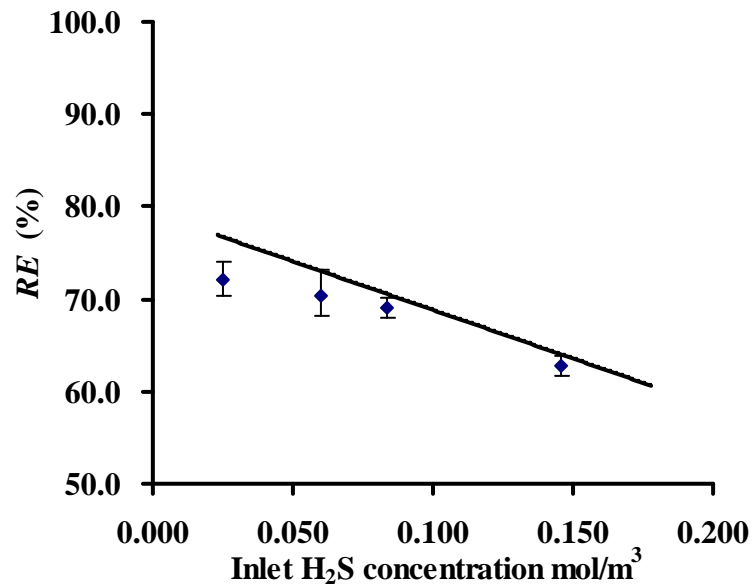


**Figure 3.11** Effect of inlet H<sub>2</sub>S concentration ( $C_{H_2S}(g),in}$ ) on removal efficiency.

$$(h = 0.30 \text{ m}, L = 0.5 \text{ mL/s}, C_{Fe,0} = 160 \text{ mol/m}^3, G = 0.1 \text{ L/s})$$

### 3.4.3 Discussion of interaction between the variables

There are three main interactive effects on removal efficiency in the H<sub>2</sub>S-Fe(III)EDTA system according to Equation (3.2). Figure 3.12 shows the effect of height of packed bed on removal efficiency at three different initial Fe(III)EDTA concentration (i.e. 100, 200 and 300 mol/m<sup>3</sup>). It is apparent that there is an interaction between packed bed height and initial Fe(III)EDTA concentration. At the initial Fe(III)EDTA concentration of 200 and 300 mol/m<sup>3</sup>, an increase in height of packed bed results in increased removal efficiency. As the initial Fe(III)EDTA concentration is decreased to 100 mol/m<sup>3</sup>, the removal efficiency remains virtually unchanged regardless of the packed bed height. This is due to the variation in the concentration of ferric species through the packed bed. As previously mentioned, too diluted Fe(III)EDTA will not retain enough reactive ferric species to efficiently oxidize the H<sub>2</sub>S in the column.

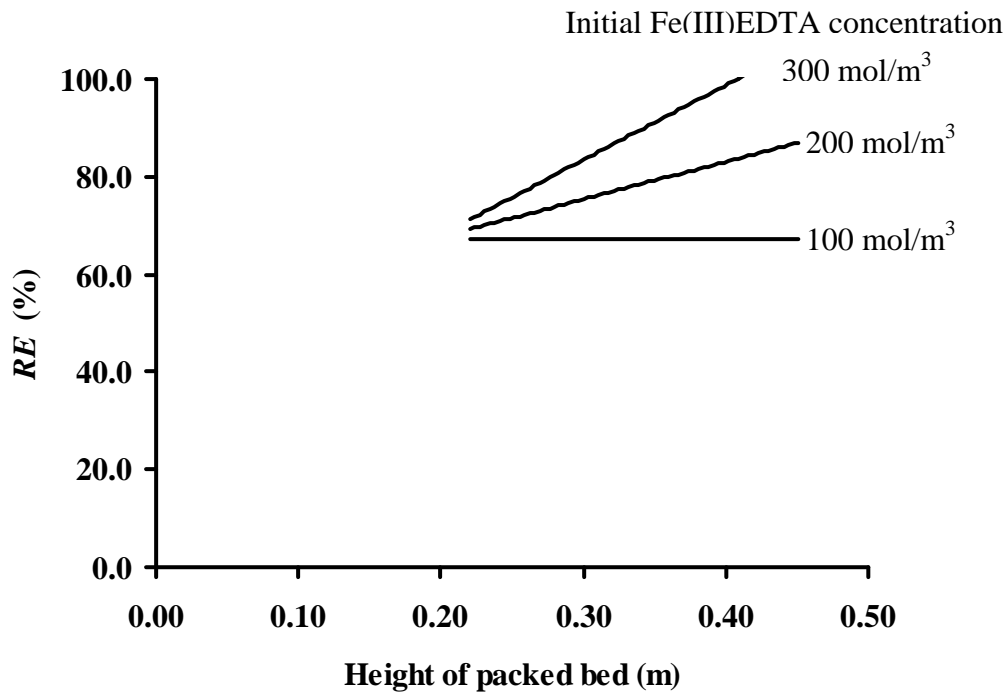


**Figure 3.12** Interaction between initial Fe(III)EDTA concentration ( $C_{Fe,0}$ ) and height of packed bed ( $h$ ) ( $L = 0.5 \text{ mL/s}$ ,  $G = 0.1 \text{ L/s}$ ,  $C_{H_2S(g),in} = 0.08 \text{ mol/m}^3$ )

In contrast, increasing the initial  $H_2S$  concentration leads to a reduction in removal efficiency. The interaction between the initial  $H_2S$  concentration and height of packed bed is shown in Figure 3.13. The  $H_2S$  absorption by Fe(III)EDTA is mainly controlled by the mass transfer in the liquid phase, therefore changes in the  $H_2S$  concentration will cause the amount of  $H_2S$  transferring across the gas-liquid interface to change. However, if the system has enough mass transfer area or the enough packed bed height the  $H_2S$  will be completed absorbed.

Interaction between scrubbing liquid flow rate and initial Fe(III)EDTA concentration is shown in Figure 3.14. It is obvious that raising the liquid flow rate cause the removal efficiency to be more sensitive to the packed bed height. An increase in liquid circulating rate provides a greater degree of liquid spreading on the packing surface (Setameteekul *et al.*, 2008). The increasing packed bed height increases the transfer area, thereby enhancing the performance of the system.

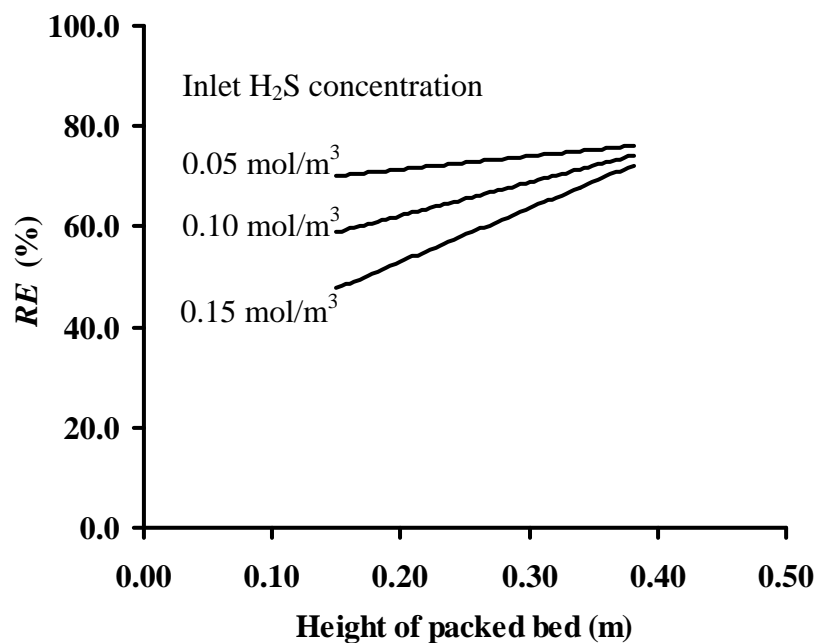


**Figure 3.13** Interaction between inlet  $H_2S$  concentration ( $C_{H_2S(g),in}$ ) and packing bed height ( $h$ ). ( $L = 0.5 \text{ mL/s}$ ,  $C_{Fe,0} = 160 \text{ mol/m}^3$ ,  $G = 0.1 \text{ L/s}$ )

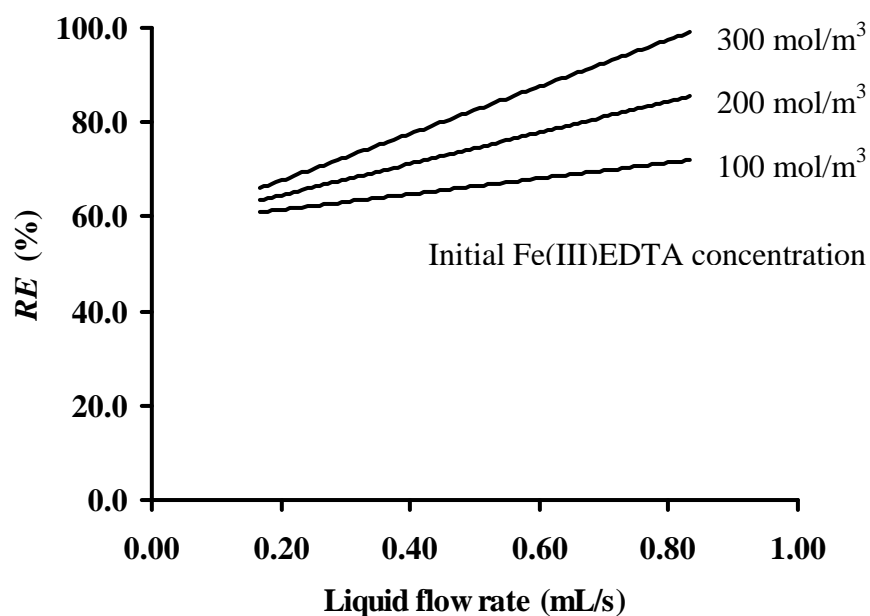


**Figure 3.14** Interaction between initial Fe(III)EDTA concentration ( $C_{Fe,0}$ ) and liquid flow rate ( $L$ ). ( $h = 0.30 \text{ m}$ ,  $G = 0.1 \text{ L/s}$ ,  $C_{H_2S(g),in} = 0.08 \text{ mol/m}^3$ )

### 3.5 Conclusion

The removal of  $H_2S$  in biogas or another gas streams from various industries is very important due to its toxic effect and in order to obtain the fuel without corrosive substance. Simultaneous absorption and reaction of  $H_2S$  from gaseous stream into an aqueous Fe(III)EDTA solution using packed bed column has been studied experimentally using RSM for experimental design. The Empirical model correlating the removal efficiency to the five variables, the scrubbing liquid flow rate, the gas flow rate, the inlet  $H_2S$  concentration, the initial Fe(III)EDTA concentration and the packed bed height was developed. The model obtained in these experiments provides a basis for further study with larger scale packed columns for removing  $H_2S$  in industrial gas streams.

## CHAPTER 4

### The degradation of Fe-EDTA in hydrogen sulfide removal

#### 4.1 Abstract

Available data on the degradation of Fe-EDTA liquid redox H<sub>2</sub>S removal processes are reviewed and the effect of H<sub>2</sub>S molar flow rate, the initial concentration of Fe(III)EDTA and the presence of sodium citrate in Fe-EDTA solution was investigated in this study. The semibatch with continuous flow of H<sub>2</sub>S containing biogas was used under a wide range of experimental conditions; pH=7.0, H<sub>2</sub>S molar flow rate,  $Q_{H_2S}$  ( $1.08 \times 10^{-3}$ - $3.40 \times 10^{-3}$  mol/h), the initial concentration of Fe(III)EDTA,  $C_{Fe,0}$  ( $2.17$ - $8.16$  mol/m<sup>3</sup>) and the concentration of sodium citrate,  $C_{CI}$  ( $0$ - $300$  mol/m<sup>3</sup>). The result showed that sodium citrate acted as stabilizer with a good ability to reduce the degradation rate. The degradation rate of Fe-EDTA was found to follow pseudo first order kinetics. Empirical correlations expressed the degradation rate constant as a function of significant H<sub>2</sub>S molar flow rate, the initial Fe(III)EDTA and sodium citrate concentration were successfully developed for the prediction of Fe-EDTA degradation rate. Moreover, the precipitated solid, called sulfur cake was recovered and its composition was investigated. The result revealed that the sulfur cake contained more than 98% sulfur element and almost balances with iron and no significant EDTA was degraded into the solid form.

#### 4.2 Introduction

The polyamino polycarboxylate chelated iron process is extremely effective and allows total conversions of hydrogen sulfide to be obtained. It is also a very flexible process and has in fact been widely diffused throughout the world. This process, however, has various drawbacks. Above all, when operating in an alkaline solution, there is the radical oxidation of the iron ligand with the degradation of the ligand itself and the precipitation of iron as sulfide. This has two strong consequences

on the process: the ligand, which is expensive, must be continuously reintegrated, furthermore the sulfur produced is impure of iron sulfide and this makes it absolutely unsuitable for commercialization. In practice, the lost of the chelating agents turn out to be the most significant factor affecting the economic feasibility of large scale operation.

A few of the prior art workers have acknowledged that chelated iron solutions are unstable and that undesirable precipitation of iron compounds may occur. Nichol and Sapiro (1965a and 1965b) recommended careful control of the regeneration of the catalyst solution to avoid over oxidation of the iron chelate. Thompson (1980) indicates that restricting the molar ratio of chelating agent to iron is an important consideration in avoiding breakdown of the chelate molecule. Lynn and Dubs (1981) suggests the addition of selected amine salt stabilizers to achieve chelate stability at low pH levels. The Diaz (1983a; 1983b and 1983c) and Blytas (1983) propose the addition of various sulfur containing and nitrogen containing compounds as stabilizers to reduce the rate of chelate degradation. Bedell (1990) disclosed that soluble chemical compounds having a high affinity for hydroxyl radicals are effective stabilizers for chelating agents used in the hydrogen sulfide removal process. The researcher exposed the aromatic compounds can further retard the degradation of the original metal chelate solution by reducing the amount of free hydroxyl radicals in the solution and by later complexing with metal ions released by degraded chelating agents before the aromatic compounds are degraded by additional hydroxyl radicals. Preferred compounds can be selected based upon solubilities, costs and relative effectiveness. These prior art studied have not provided an effective, environmentally acceptable, and inexpensive solution to the problem of chelate degradation. Moreover, there has been no adequate explanation of the mechanism of chelate instability in a hydrogen sulfide removal process. Until Chen *et al.* (1993 and 1995) observed that polyaminocarboxylic acid tend to rupture at the weakent locations, for example, ethylene moiety of EDTA which leads to dechelation and then degradation of Fe-EDTA. Cleavage is presumably ascribed to the presence of hydroxyl free radicals produced from the reoxidation of ferrous chelate product into active ferric chelate via a Fenton mechanism.



McManus and Kin (1993) studied the effectiveness of sodium thiosulfate as a stabilizing additive in an aqueous NTA-iron chelate solution when used in a cyclic hydrogen sulfide removal catalyst regeneration process. The result showed the NTA concentration changed from 10.09 g/L to 8.73 g/L (a decrease of 13.5%) in 92.5 hours, whereas in the control run the NTA was totally degraded shortly after 47 hours. The soluble Fe changed from 990 to 900 g/L (10%) in the presence of sodium thiosulfate whereas in the control run the soluble Fe concentration decreased about 30% within 92.5 hours.

Sunda and Huntsman (2003) investigated that temperature, pH, and light also effect on equilibrium dissociation constant for Fe-EDTA chelates, which indicates the strength of binding between Fe and EDTA. They found that increases in pH (7.7-9) increased equilibrium dissociation constants for Fe-EDTA chelates, apparently due to the formation of mixed EDTA-hydroxy chelates. Light also increased the dissociation constant due to photo reductive dissociation of ferric-EDTA chelates. A decrease in temperature from 20 and 10 °C had little effect on dissociation constants in the dark, indicating that rate constants for Fe-EDTA association and dissociation were about equally affected by temperature.

More recently, De Angelis *et al.* (2007) studied the oxidation of hydrogen sulfide to sulfur by mean of treatment with an aqueous acid solution containing trivalent iron and a hetero polyacid. The oxidation cycle of hydrogen sulfide to sulfur (10 hours), filtration of the sulfur and re-oxidation of the solution with air (4 hours) were repeated fours times, on the same solution. They found that no any decrease in the catalyst performance. However, the preparation of this oxidation solution is very complex.

To our knowledge, no kinetics study has been done on the degradation of Fe-EDTA in H<sub>2</sub>S removal system and no Fe-EDTA degradation rate equation has been presented. The prediction of the extent and rate of Fe-EDTA (or Fe(total)-EDTA) degradation is vital in the estimation of the exact Fe(III)EDTA make-up rate needed to maintain the H<sub>2</sub>S absorption capacity of the removal process. The goal of this research was to determine the potential for Fe-EDTA degradation as a function of degradation parameters such as the H<sub>2</sub>S molar flow rate, the initial Fe(III)EDTA

concentration, and the concentration of the new stabilizer which was investigated in this study based on the initial Fe-EDTA degradation rate.

### **4.3 Materials and Method**

#### **4.3.1 Chemical**

40% w/w Ferric chloride solution ( $\text{FeCl}_3$ ) and  $\text{EDTANa}_4 \cdot 4\text{H}_2\text{O}$  powder with commercial grade were purchased from L.B. Science LTD, Thailand. Sodium thiosulfate  $5 \cdot \text{H}_2\text{O}$  (99.5%, Ajax Finechem), Sodium citrate (99.0%, Ajax Finechem) were used. Biogas (1,300-1,600 ppm  $\text{H}_2\text{S}$  content) produced from Mongkol pig farming located at Phattalung province were used in this study.

A Fe(III)EDTA solution was prepared using the following recipe. A 187 g of EDTA·4 Na powder was dissolved into 900 mL of water wherein 100 mL of 40%  $\text{FeCl}_3$  solution was added. The Fe(III)EDTA solution was obtained with the concentration of 0.35 mol Fe/L. And the mole ratio of iron and EDTA in the solution was 1:1.2. Working solution for experiments was freshly prepared with deionized water. The calculated stabilizers amount was mixed with the 0.35 mol Fe/L Fe-EDTA solution to obtain the expected concentration. The solution was adjusted to pH 7.0 by adding 3 N HCl.

#### **4.3.2 Experimental procedure**

The oxidation reaction of  $\text{H}_2\text{S}$  by Fe(III)EDTA in the presence and absence of the stabilizers was performed in the 1000 mL semibatch reactor where the biogas was continuously fed into liquid Fe-EDTA solution as illustrated in Figure 4.1. From Figure 4.1 the gas phase, biogas and air were introduced separately as bubble into the 750 mL of predetermined concentration Fe(III)EDTA solution. Air flow rate used in all experiments were 1 L/min throughout the reaction in order to reoxidize ferrous into the active ferric form. The ferrous regeneration efficiency was more than 90% in all experiments. The soluble Fe(II) concentration with time are shown in Table A-3.8-A-3.10. The biogas volumetric flow rate was varied between 0.5-2.0

L/min. As Fe-EDTA degradation is a very slow process, each experiment requires a long experimentation time of 30 h. During the experiment, the gas and liquid sample were collected at every 3 h. To ensure actual representation of samples collected at each time interval, the gas introduction and sample removal dip tube was first rinsed to get rid of the old sample left in the tube from the last sample collection. The H<sub>2</sub>S concentrations in biogas were determined at the inlet and the outlet of reactor by iodometric method. The iodometric method procedure is described in Appendix B-1. Because of the ferric in the form of ion in solution, it can oxidized H<sub>2</sub>S to the element sulfur. Thus, the degradation of Fe-EDTA is the abatement of iron concentration in the solution. The concentration of soluble Fe in the solution was determined using Atomic absorption spectroscopy. The procedure of iron determination using atomic absorption spectroscopy is described in Appendix B-2.2. All experiments were performed at ambient temperature of  $30 \pm 2$  °C.

After 30 h of reaction time the solid product were filtered, washed, dried and analyzed with CHNS-analyzer to determine % weight of carbon, hydrogen, nitrogen and sulfur element.

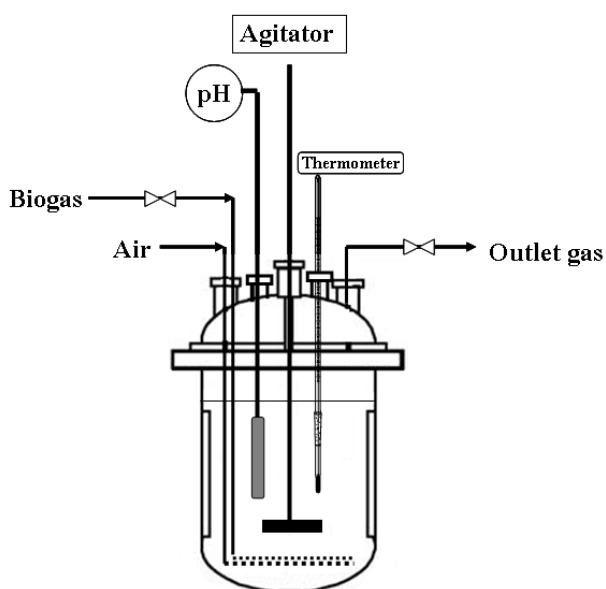


**Figure 4.1** The semi-batch system

## 4.4 Results and discussion

### 4.4.1 Degradation of Fe-EDTA kinetics studies

The rate equation was formulated based on the assumption that Fe(III)EDTA reacted only in the liquid phase with dissolved H<sub>2</sub>S, which allowed the degradation kinetics to be formulated as a homogeneous liquid phase system. Although, mass transfer could possibly control the degradation rate of H<sub>2</sub>S, but the mass transfer limitation is insignificant during the degradation time (e.g. 0–30 h of degradation time) if an appropriate stirring speed is used (Supap *et al.*, 2009). The interference from degradation products could also be neglected. These assumptions were used to formulate the kinetic model in this study.

Figure 4.2 and 4.3 represent soluble Fe concentration versus time relationship which indicates a first approach. Thus, the degradation of Fe-EDTA can be described by pseudo first order kinetics with respect to Fe concentration as expressed in Equation (4.1).

$$R_d = -\frac{dC_{Fe}}{dt} = k_d C_{Fe} \quad (4.1)$$

Separating and integrating Equation (4.1) we obtain Equation (4.2)

$$-\ln(C_{Fe,t} / C_{Fe,0}) = k_d t \quad (4.2)$$

where  $R_d$  represents the Fe-EDTA degradation rate,  $k_d$  represents the pseudo first order degradation rate constant,  $C_{Fe,0}$  and  $C_{Fe,t}$  represents the concentration of soluble Fe at an initial and at any reaction time, respectively. In this case, a plot of  $-\ln(C_{Fe,t} / C_{Fe,0})$  versus time in every experiment must lead to a straight line with slope of  $k_d$ .  $k_d$  may be a function of several variables as in Equation (4.3).

$$k_d = \text{fn} (Q_{H_2S}, C_{Fe,0}, C_{CI}, \dots) \quad (4.3)$$

where  $Q_{H_2S}$  represents H<sub>2</sub>S molar flow rate and  $C_{CI}$  represents the concentration of sodium citrate

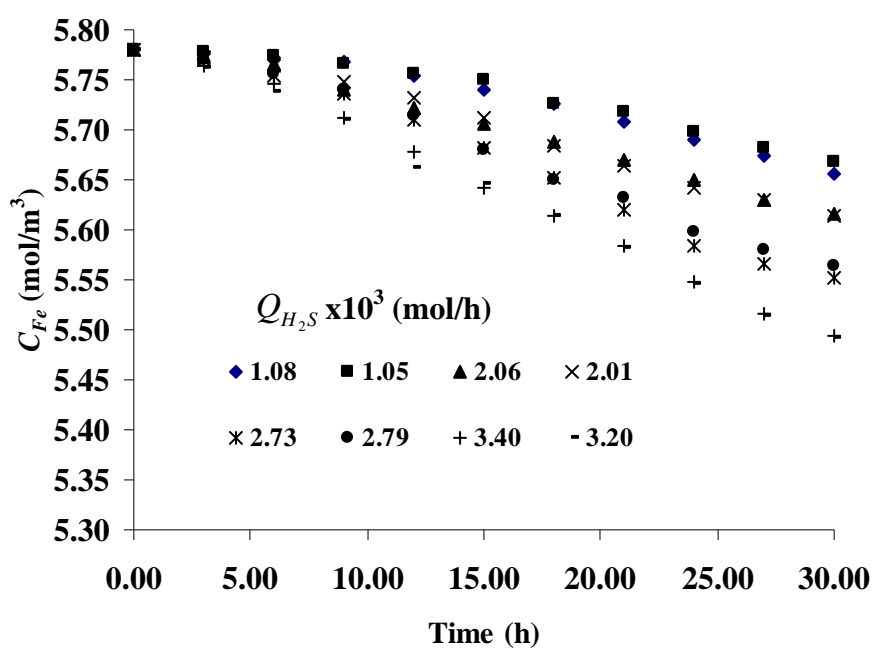


**Figure 4.2** Soluble Fe concentration ( $C_{Fe}$ )-time of various  $H_2S$  molar flow rate ( $Q_{H_2S}$ ) at initial Fe(III)EDTA concentration ( $C_{Fe,0}$ ) of  $5.78 \text{ mol/m}^3$

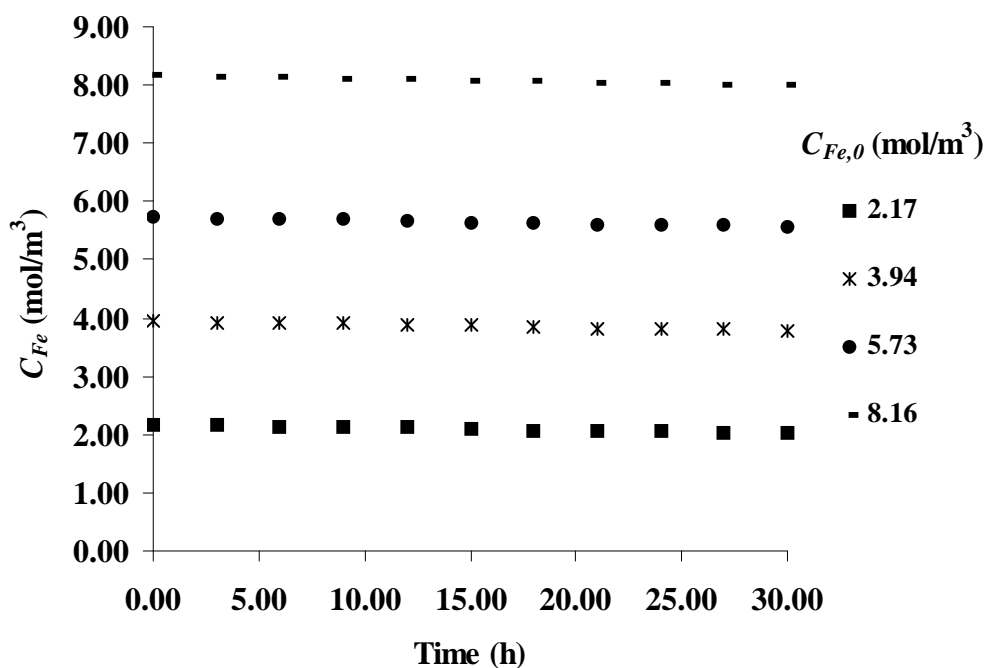


**Figure 4.3** Soluble Fe concentration ( $C_{Fe}$ )-time of various initial Fe(III)EDTA concentration ( $C_{Fe,0}$ ) at the  $H_2S$  molar flow rate ( $Q_{H_2S}$ ) of  $2.0 \times 10^{-3} \text{ mol/h}$

The effect of H<sub>2</sub>S molar flow rate was evaluated by using 5.78 mol/m<sup>3</sup> initial Fe(III)EDTA concentration, while the average H<sub>2</sub>S molar flow rate of 2.0 x10<sup>-3</sup> mol/h was used to study the effect of the initial Fe(III)EDTA concentration. The Fe-EDTA degradation rates ( $R_d$ ) of each experimental run are listed in Table 4.1. It can be observed that  $R_d$  increases rapidly with increasing  $Q_{H_2S}$ , but it only slightly decrease with increasing  $C_{Fe,0}$ . This can conclude that the effect of  $Q_{H_2S}$  on  $R_d$  is greater than the effect of  $C_{Fe,0}$ .

**Table 4.1** Fe-EDTA degradation rate ( $R_d$ ) at various H<sub>2</sub>S molar flow rate ( $Q_{H_2S}$ ) and initial Fe(III)EDTA concentration ( $C_{Fe,0}$ )

Run no.	$Q_{H_2S} \times 10^3$ (mol/h)	$C_{Fe,0}$ (mol/m <sup>3</sup> )	$R_d$ (mol m <sup>-3</sup> h <sup>-1</sup> )
1	1.08	5.78	0.00356
2	1.05	5.78	0.00323
3	2.06	5.78	0.00528
4	2.01	5.78	0.00535
5	2.73	5.78	0.00746
6	2.79	5.78	0.00707
7	3.40	5.78	0.00939
8	3.20	5.78	0.00950
9	1.79	2.17	0.00493
10	1.81	2.17	0.00508
11	1.94	3.94	0.00511
12	1.90	3.94	0.00515
13	2.16	5.73	0.00556
14	2.13	5.73	0.00539
15	2.37	8.16	0.00556
16	2.40	8.16	0.00514

This result is consistent with Chen *et al.* (1993) who observed that the iron chelate degradation occurs during the re-oxidation of the ferrous to ferric system

with air (molecular oxygen), They suggested that only free radicals have enough energy to degrade these chelating ligands which lead to dechelation (degradation) of iron chelate and also indicates that the hydroxyl radical may be formed under the reaction conditions.

The main degradation products identified by Chen *et al.* (1995) are iminodiacetic acid (IDA) and ethylenediaminediacetic acid (EDDA). All of the oxidation intermediates being formed by hydroxylation of one of the CH<sub>2</sub> groups, either on the ethylene bridge or side chain acetate groups. Following hydroxylation, the aldehyde formed by hydrolytic cleavage is rapidly converted to the corresponding carboxylate. It is worth noting that the pH in all the experiments decreased during the reaction going from 7.0 to 4.5. Data are shown in Table A-3.11 - A-3.13. A such pH value, Chen *et al.* (1993) reported that the Fe chelated degradation rate is slightly promoted under acidic condition.

All results can be described by the pseudo first order kinetics as evident by the plot of  $-\ln(C_{Fe,t}/C_{Fe,0})$  versus time as illustrated in Figure 4.4 and 4.5. It can be observed in these figures that the linear relationship between  $-\ln(C_{Fe,t}/C_{Fe,0})$  and time were highly with the coefficients of determination greater than 0.91. In experiments carried out in duplicate as can be seen in Figure 4.6 and 4.7, the pseudo first order rate constant,  $k_d$  respect to H<sub>2</sub>S molar flow rate ( $Q_{H_2S}$ ) and initial Fe(III)EDTA concentration ( $C_{Fe,0}$ ), respectively, varied by less than 10%. The observed degradation rate constant,  $k_d$  increase with increasing H<sub>2</sub>S molar flow rate while the increasing of the initial Fe(III)EDTA concentration decrease  $k_d$ .

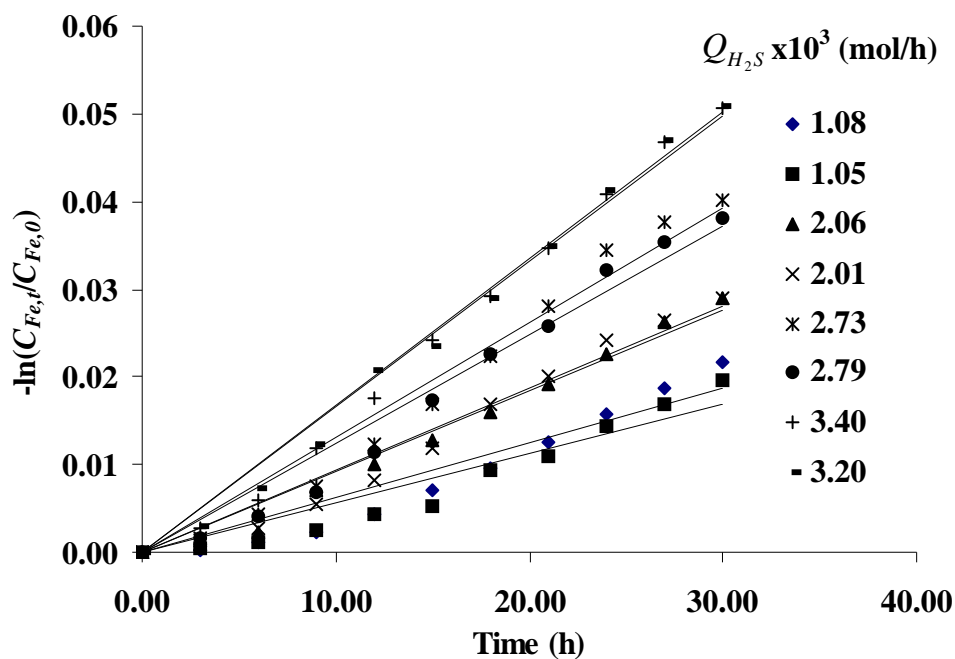


**Figure 4.4** Effect of H<sub>2</sub>S molar flow rate ( $Q_{H_2S}$ ) on the degradation of Fe(III)EDTA.

First order plots for Fe(III)EDTA degradation at the initial Fe(III)EDTA concentration of  $5.78 \text{ mol/m}^3$

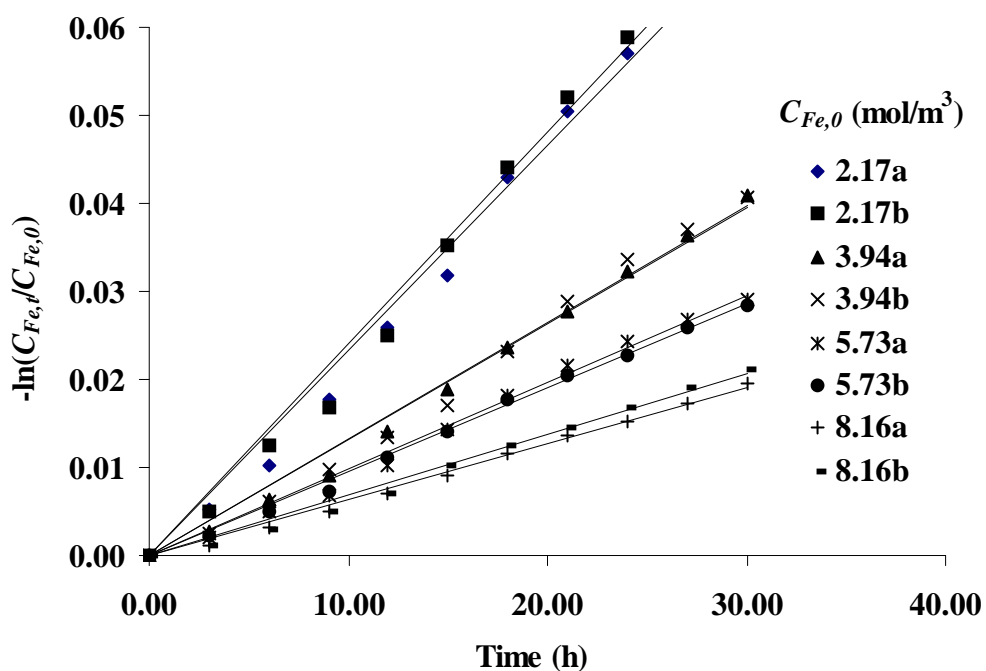


**Figure 4.5** Effect of initial Fe(III)EDTA concentration ( $C_{Fe,0}$ ) on the degradation of Fe(III)EDTA. First order plots for Fe(III)EDTA degradation at the H<sub>2</sub>S molar flow rate of  $2.0 \times 10^{-3} \text{ mol/h}$



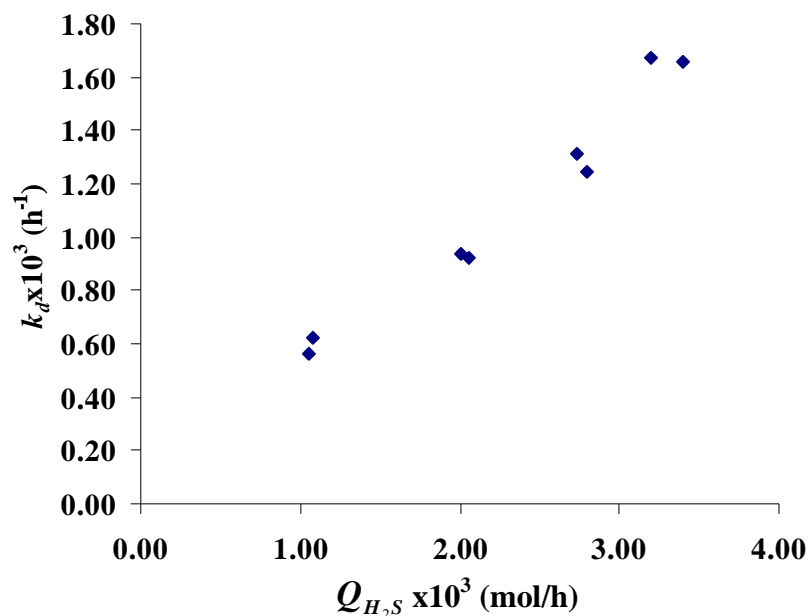


**Figure 4.6** Effect of  $H_2S$  molar flow rate ( $Q_{H_2S}$ ) on observed degradation rate constant ( $k_d$ ) at the initial Fe(III)EDTA concentration of  $5.78 \text{ mol/m}^3$

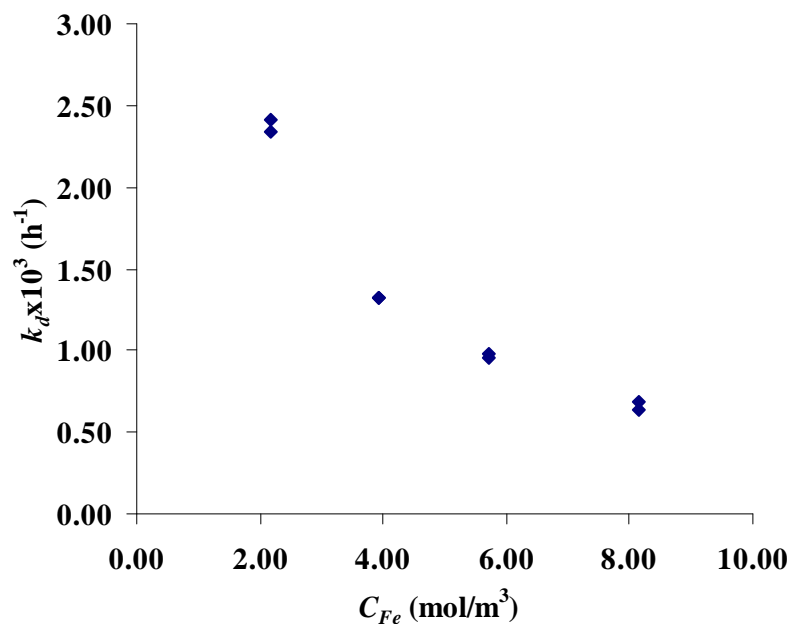


**Figure 4.7** Effect of initial Fe(III)EDTA concentration ( $C_{Fe,0}$ ) on observed degradation rate constant ( $k_d$ ) at the average  $H_2S$  molar flow rate of  $2.0 \times 10^{-3} \text{ mol/h}$

The relationship between  $k_d$  and  $Q_{H_2S}$  and  $C_{Fe,0}$  was formulated using linear regression method. Result is given in the following equation,

$$k_d(Q_{H_2S}, C_{Fe,0}) = 3.446 - 0.784C_{Fe,0} + 0.0452C_{Fe,0}^2 + 0.111 \times 10^{-3} Q_{H_2S}^2 \quad (4.4)$$

The empirical equation was evaluated based on the coefficient of determination value  $R^2$  and adjusted  $R^2$  of 0.982 and 0.978, respectively. This indicated that there was a good agreement between the experimental and predicted  $k_d$  value. A visual comparison of the model and experimental  $k_d$  is shown in Figure 4.8.

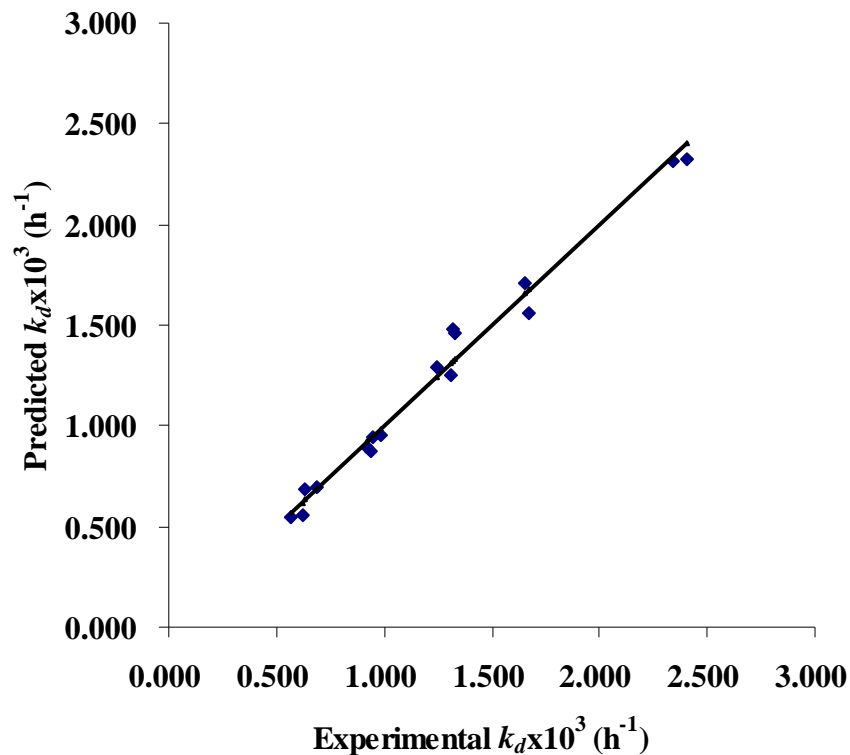


**Figure 4.8** Plot of experimental and predicted  $k_d$  (from Equation (4.4))

Now,  $k_d$  can be predicted from Equation (4.4) and Fe-EDTA degradation rate ( $R_d$ ) was then calculated by multiplying  $k_d$  and  $C_{Fe}$ . The comparison between the calculated and the measured  $R_d$  were made as given in Figure 4.9. It can be observed that they showed a good agreement in the proposed model of Equation (4.1).

Thus, Fe-EDTA degradation rate ( $R_d$ ) calculated using  $k_d$  from the empirical Equation (4.4) was sufficient precision under a wide range of the experimental condition.

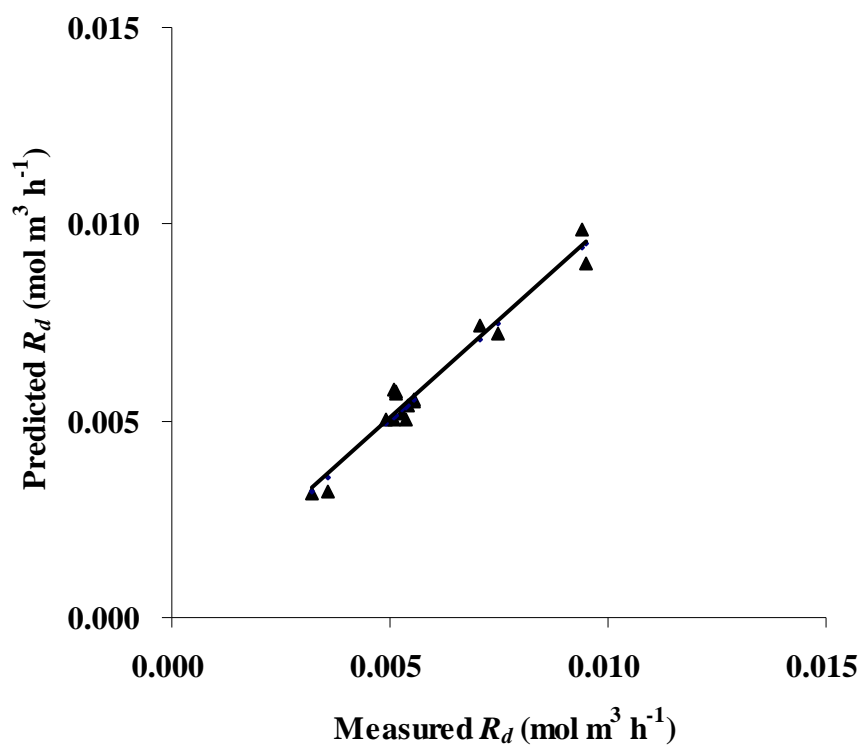


**Figure 4.9** Plot of *measured*  $R_d$  and predicted  $R_d$  calculated using  $k_d(Q_{H_2S}, C_{Fe,0})$  model

#### 4.4.2 Analysis of sulfur cake

The species presented in the precipitate or sulfur cake from  $H_2S$  oxidation were identified in this studied. Due to the main species that assume to be in the sulfur cake are C, H, N and O from EDTA degradation, S from  $H_2S$  oxidation and Fe from Fe-EDTA dechelation. The CHNS analyzer and UV-VIS spectrophotometer (samples were treat treated by phenanthroline method) was used to analyze the quantity of C, H, N and S element, and Fe, respectively. The analyzed sulfur cake result is shown in Table 4.2. The sum of amount of elements in sulfur cake showed a mass balance of about 100%. As expected, S (more than 98% by weight) was the main element in the sulfur cake with small amount Fe and very small amount of C, H

and N. The amount of Fe found in sulfur cake was almost consistent with Fe degraded from the solution. The data are shown in Table A-3.2. It can be noted that no significant EDTA degrades into the solid form. The remained EDTA and its ruptured products were still in the solution. However, the products cleavage from EDTA does not have high affinity enough to maintain Fe in the solution from.

**Table 4.2** The composition of sulfur cake for each sample

$Q_{H_2S} \times 10^3$ (mol/h)	$C_{Fe,0}$ (mol/m <sup>3</sup> )	Sulfur cake (g)	% Elements (wt)					
			N	C	H	S	Fe	Sum
1.08	5.78	0.805	0.19	0.96	0.12	98.36	0.40	100.03
2.73	5.78	2.251	0.11	0.83	0.10	99.10	0.35	100.49
3.20	5.78	2.675	0.12	0.68	0.08	99.01	0.56	100.45
1.81	2.17	1.535	<0.01	0.74	0.09	98.62	0.28	99.73
1.94	3.94	1.693	<0.01	0.72	0.08	98.97	0.24	100.01
2.13	5.73	1.922	<0.01	0.56	0.07	99.93	0.23	100.79
2.40	8.16	2.106	<0.01	0.59	0.07	99.23	0.32	100.21

#### 4.4.3 The effect of chemicals additive into Fe-EDTA solution

Fe(III)EDTA is capable use for the oxidation of H<sub>2</sub>S to element sulfur. The main difficult with the process is the degradation of Fe-EDTA catalyst. The loss of Fe-EDTA is caused by the degradation of EDTA. Chen *et al.* (1993) suggested that degradation is promoted by hydroxyl radicals. A number of additives that function as radical scavengers have been used to slow down radical induced oxidative degradation. There are many such additives that maybe used. A very effective and inexpensive free radical scavenger is thiosulfate ion (300 mol/m<sup>3</sup>), usually supplied as sodium thiosulfate.

In this study the common hydroxyl scavenger, sodium citrate was used. Citric acid and its salts have many applications in everyday life. Among others, it is used as an additive in food and in the production of cold drinks (Gautier *et al.*, 2006).

Many literatures reported that citrate has ability to reduce free radical formation (Szentmihályi *et al.*, 2003; Delvecchio *et al.*, 2005) and also is a ligand with high affinity complex with iron. The comparison of the capability to reduce Fe-EDTA degradation rate between using sodium citrate and sodium thiosulfate in this study is shown in Table 4.3. The result demonstrated the effectiveness of sodium citrate as a stabilizer was slightly higher than sodium thiosulfate. A suitable stabilizer is required to reduce the degradation rate and keep the iron in solution. Sodium citrate was chosen as a stabilizer in this degradation kinetics study based on the following reasons. Using thiosulfate, the sulfur compounds in the system is raised that it can be converted to H<sub>2</sub>S or other toxic compounds such as sulfite. This is not a problem of sodium citrate. The cost of citrate is lower than thiosulfate because sodium citrate can be produced from citric acid and sodium hydroxide which are cheap and commercial. Thus, sodium citrate is a suitable stabilizer for reducing the Fe-EDTA degradation rate.

**Table 4.3 Fe-EDTA degradation rate ( $R_d$ ) with and without additive**

$Q_{H_2S} \times 10^3$ (mol/h)	$C_{Fe,0}$ (mol/m <sup>3</sup> )	Additive	$R_d$
1.07	5.84	No additive	0.00536± 0.00001
2.04	5.85	Sodium citrate	0.00278±0.00012
2.41	5.70	Sodium thiosulfate	0.00322±0.00004

#### 4.4.4 The effect of sodium citrate concentration in Fe-EDTA degradation

According to the previous section, sodium citrate is the suitable additive which can be used as stabilizer based upon the solubility, cost and relative effectiveness. The experiments were set to determine the relationship of sodium citrate concentration ( $C_{CI}$ ) and the Fe-EDTA degradation rate ( $R_d$ ). The experimental runs were conducted using the sodium citrate concentration of 0-300 mol/m<sup>3</sup> with the H<sub>2</sub>S molar flow rate and the initial Fe(III)EDTA concentration of 1.84x10<sup>-3</sup> mol/h and 5.80 mol/m<sup>3</sup>, respectively.

Again, the degradation of Fe-EDTA followed by the first order degradation rate as supported by the relationship between  $-\ln(C_{Fe,t}/C_{Fe,0})$  and time which is shown in Figure 4.10 with the coefficients of determination value higher than 0.93.

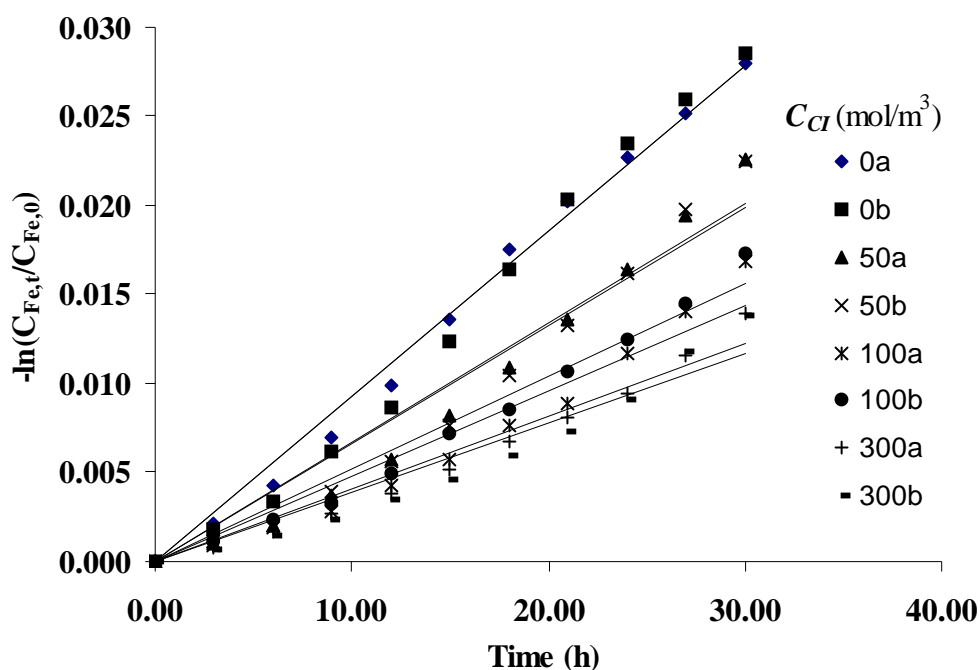


**Figure 4.10** Effect of sodium citrate concentration ( $C_{CI}$ ) on the degradation of Fe(III)EDTA. First order plots for Fe(III)EDTA degradation at the  $H_2S$  molar flow rate of  $1.84 \times 10^{-3}$  mol/h and initial Fe(III)EDTA concentration of  $5.80 \text{ mol/m}^3$

$k_d$  decreases with an increase in  $C_{CI}$  as illustrated in Figure 4.11. It is also observed that the reduction of  $R_d$  may constant as  $C_{CI}$  greater than that  $300 \text{ mol/m}^3$ . The relationship between  $k_d$  and  $C_{CI}$  up to  $300 \text{ mol/m}^3$  were fitted. The empirical model with  $R^2$  and adjusted  $R^2$  of 0.983 and 0.976, respectively, was obtained as given by Equation (4.5).

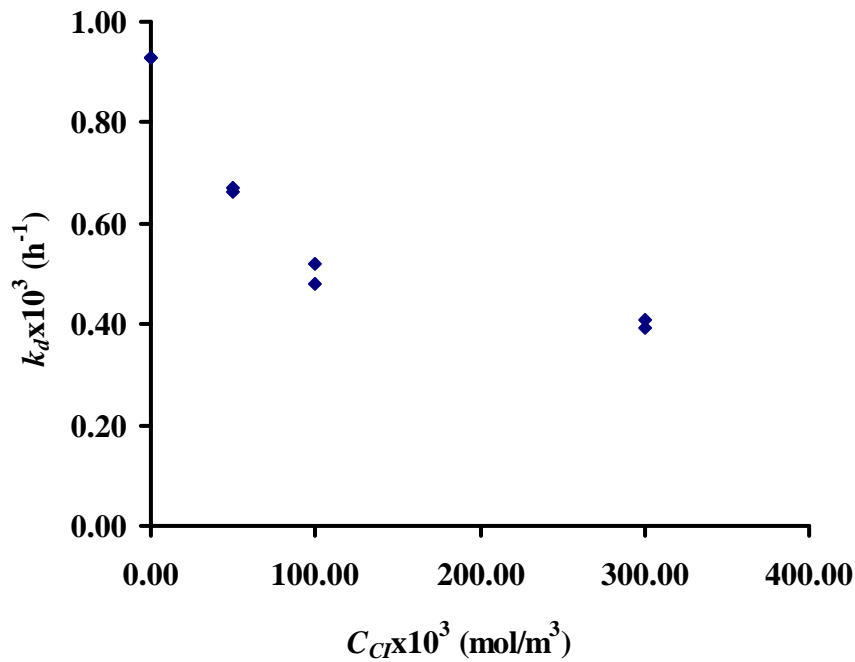


**Figure 4.11** Effect of sodium citrate concentration ( $C_{CI}$ ) on observed degradation rate constant ( $k_d$ ) at the average  $H_2S$  molar flow rate of  $1.84 \times 10^{-3}$  mol/h and initial Fe(III)EDTA concentration of  $5.80 \text{ mol/m}^3$

$$k_d(C_{CI}) = 0.921 - 0.00526C_{CI} + 1.176 \times 10^{-5} C_{CI}^2 \quad (4.5)$$

It can be noted from Equation and (4.5) that the  $k_d$  at the absence of sodium citrate was equal to  $0.921 \text{ h}^{-1}$ . This value represents the effect of  $Q_{H_2S}$  and  $C_{Fe,0}$  on the degradation of Fe-EDTA. Thus, the truly effect of  $C_{CI}$  are just the last two terms of Equation (4.5).

Moreover, the  $k_d$  evaluated from slope of Figure 4.4, 4.5 and 4.10 at corresponding  $Q_{H_2S}$ ,  $C_{Fe,0}$  and  $C_{CI}$  were together analyzed by linear regression method. The best fitted model with  $R^2$  and adjusted  $R^2$  of 0.986 and 0.982 is shown in Equation (4.6).

$$k_d(Q_{H_2S}, C_{Fe,0}, C_{CI}) = 3.429 - 0.773C_{Fe,0} + 0.0443C_{Fe,0}^2 + 0.110 \times 10^{-3} Q_{H_2S}^2 - 0.00698C_{CI} + 1.546 \times 10^{-5} C_{CI}^2 \quad (4.6)$$

It can be noticed that all terms in Equation (4.4) and (4.5) are presented in Equation (4.6) with quite same magnitude of coefficient except the intercept in Equation (4.5). This supported the assumption above, the intercept in Equation (4.4) is the effect from  $Q_{H_2S}$  and  $C_{Fe,0}$  only. Thus, it can say that the equation of  $k_d$  related to all parameters can be obtained by the summation of each (real)  $k_d$  equation.

The  $R_d$  calculated using the  $k_d$  ( $Q_{H_2S}, C_{Fe,0}, C_{Cl}$ ) in Equation (4.6) have a good agreement with the measured  $R_d$  as demonstrated in Figure 4.12.

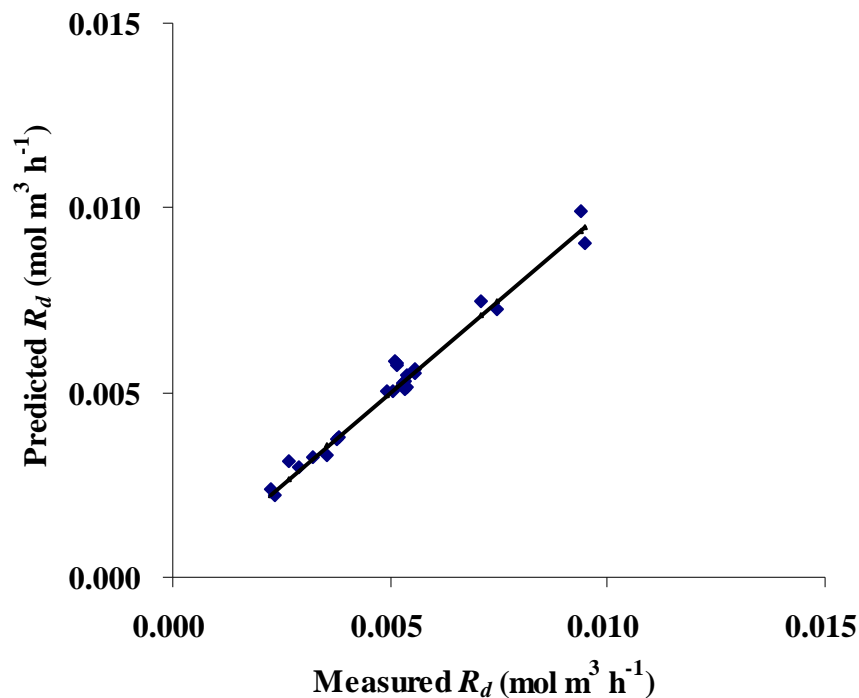


**Figure 4.12** Plot of measured  $R_d$  and predicted  $R_d$  calculated using  $k_d(Q_{H_2S}, C_{Fe,0}, C_{Cl})$  model

The concentration of Fe-EDTA at anytime in the reaction can be predicted by Equation (4.7) which is rewriting from Equation (4.2)

$$C_{Fe,t} = C_{Fe,0} e^{-k_d t} \quad (4.7)$$

where  $k_d$  can be calculated using Equation (4.6)



Equation (4.7) is very useful in the H<sub>2</sub>S removal by oxidation with Fe(III)EDTA. When all parameters,  $Q_{H_2S}$ ,  $C_{Fe,0}$  and  $C_{Cl}$  are known, it can be used to predict the concentration of Fe-EDTA at any interested time, so we can predict that how long the system still gave high efficiency and when the system needs to be made up with new Fe(III)EDTA solution.

#### 4.5 Conclusion

The degradation rate of Fe-EDTA followed pseudo first order. The effect of H<sub>2</sub>S molar flow rate, the initial Fe(III)EDTA and sodium citrate concentration were investigated and the empirical correlations expressed the degradation rate constant as a function of significant H<sub>2</sub>S molar flow rate, initial Fe(III)EDTA and sodium citrate concentration were successfully developed. The result demonstrated that the degradation rate of Fe-EDTA in H<sub>2</sub>S removal system could be predicted with sufficient precision via the developed correlation model. Sulfur cake was also recovered. It was found that the sulfur cake contained more than 98% sulfur element and almost balances with iron and no significant EDTA was degraded into the solid form.

The kinetics knowledge obtained from this work can be used to develop the H<sub>2</sub>S removal process from biogas or other gas stream, particularly the chemical quantity used in system. A kinetic evaluation also helps in the formulation of a degradation prevention strategy which is considered to be the overall goal of degradation studies.

## CHAPTER 5

### **Economic comparison of using various chemical scrubbing liquid to remove H<sub>2</sub>S from biogas in packed column**

A range of technologies are available to treat H<sub>2</sub>S in gas stream among which the chemical scrubbing in packed column is an established technique which is effective in low contact times. Fe(III)EDTA is an effective chemical scrubbing solution to remove H<sub>2</sub>S from biogas. Spent Fe-EDTA can be easily regenerated by oxygen. However, it can be degraded during the process as described in Chapter 4. The cost analysis in H<sub>2</sub>S removal system will indicate the economic feasibility in biogas cleaning before use as energy. This information can help the operator decide to use this technology or not.

Because of the scale of H<sub>2</sub>S removal system depends on the biogas production and utilization rate. And the estimate cost can be scaled up linearly base on H<sub>2</sub>S loading. Thus, we used the information of column size and operating condition from Chapter 3 and 4 in the economic analysis. The cost estimation for removing H<sub>2</sub>S by using chemical absorption was divided into 2 parts, the investment and operating cost. The investment cost includes packed column, packing material, sedimentation tank, regeneration tank, liquid circulation pump air compressor and chemical solution. The operating cost includes the electricity usage and the chemical make up needed. The cost estimation using common oxidant, KMnO<sub>4</sub> (potassium permanganate) and NaOCl (sodium hypochlorite) as chemical scrubbing liquid were also compared to Fe(III)EDTA. As shown in Table 5.1 the operating condition, gas flow rate, scrubbing liquid flow rate, inlet H<sub>2</sub>S concentration and initial scrubbing liquid concentration were specified. Using these condition, the initial Fe(III)EDTA concentration must be at least 135 mol/m<sup>3</sup> in order to keep 100 % H<sub>2</sub>S removal efficiency. However, the concentration of 160 mol/m<sup>3</sup> of Fe(III)EDTA and also KMnO<sub>4</sub> and NaOCl were used to ensure the high efficiency.

The Fe-EDTA degradation rate during H<sub>2</sub>S removal process was calculated using the knowledge obtained in Chapter 4 while the KMnO<sub>4</sub> and NaOCl

consumption rate were calculated from the stoichiometric. The mole of  $\text{KMnO}_4$  and  $\text{NaOCl}$  needed to remove one mole  $\text{H}_2\text{S}$  are 0.67 and 4, respectively as shown in Equation 5.1 and 5.2.

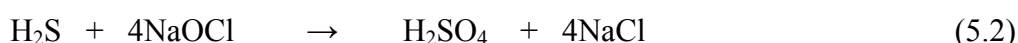


**Table 5.1** Economic comparison of using Fe(III)EDTA,  $\text{KMnO}_4$  and  $\text{NaOCl}$  as a chemical scrubbing liquid in  $\text{H}_2\text{S}$  removal from biogas

<b>Packed column characteristics</b>	
<b>Column</b>	
Material	Stainless steel
Diameter (cm)	5
Height (cm)	70
<b>Packing media</b>	
Type	Plastic raschig ring
Size (mm)	6
Bed Height (cm)	45
<b>Vessels (Sedimentation and air bubbling tanks)</b>	
Type	Polyethylene
Volume (L)	2.5
<b>Instruments</b>	
Liquid circulation pump (W)	20
Air compressor (W) (For Fe(III)EDTA system only)	186.5 (0.25 HP)
<b>Operating condition</b>	
gas flow rate (L/min)	2
inlet $\text{H}_2\text{S}$ concentration ( $\text{mg}/\text{m}^3$ )	1,300
$\text{H}_2\text{S}$ molar flow rate (mmol/h)	4.51
scrubbing liquid flow rate (mL/s)	0.833
initial scrubbing liquid concentration ( $\text{mol}/\text{m}^3$ )	160

**Table 5.1** Economic comparison of using Fe(III)EDTA, KMnO<sub>4</sub> and NaOCl as a chemical scrubbing liquid in H<sub>2</sub>S removal from biogas (continued)

<b>Operating condition (continued)</b>		
Air flow rate (L/min)		5
scrubbing liquid volume (L)		4
<b>Chemical scrubbing liquid disappear rate (mol/month)</b>		
Fe(III)EDTA		0.035
KMnO <sub>4</sub>		2.17
NaOCl		12.99
<b>Investment cost (Baht)</b>		
Packed column system		
Fe(III)EDTA		10,000 – 15,000
KMnO <sub>4</sub> and NaOCl		7,000 - 12,000
Chemical scrubbing solution (Excluding the preparation cost)		
Fe(III)EDTA (*Price: 95.63 Baht/mol)		60
KMnO <sub>4</sub> (*Price: 21.3 Baht/mol)		14
NaOCl (*Price: 7.99 Baht/mol)		5
<b>Operating cost (Baht/month)</b>		
Electricity (Using electricity rate of 2.5 unit/baht)		
Fe(III)EDTA		70
KMnO <sub>4</sub> and NaOCl		36
Chemical make up		
Fe(III)EDTA		3.06
KMnO <sub>4</sub>		46.32
NaOCl		103.79
<b>Total operating cost</b>		
	<b>Baht/kg H<sub>2</sub>S</b>	<b>Baht/m<sup>3</sup> biogas</b>
Fe(III)EDTA	639	0.81
KMnO <sub>4</sub>	748	0.95
NaOCl	1,721	1.62

\* The chemical prices from L.B. Science LTD, Thailand

The investment cost refer to the initial cost for the packed column system, which is paid only once during the operation. Because in Fe(III)EDTA system, air compressor is required to supply air for the regeneration, thus, the investment cost of this system was higher than  $\text{KMnO}_4$  and  $\text{NaOCl}$  system as shown in Table 5.1. In operation, electricity was the main cost for Fe(III)EDTA system, this contrast to in  $\text{NaOCl}$  system that chemical make up was the main cost, while for  $\text{KMnO}_4$  system the cost of electricity and chemical make up was not much different.

The operating cost per kg  $\text{H}_2\text{S}$  and  $\text{m}^3$  biogas loaded for Fe(III)EDTA system was slightly lower than  $\text{KMnO}_4$  system but it about 2 times lower than that of  $\text{NaOCl}$  system. It should be noted that the cost estimation in Table 5.1 did not include maintenance cost and labor cost. However, It can be said that Fe(III)EDTA was the most proper chemical scrubbing liquid for removing  $\text{H}_2\text{S}$  from biogas in long period operation.

## CHAPTER 6

### Summary and Future works

#### 5.1 Summary

A chemical oxidation using Fe(III)EDTA in a packed column is proposed for H<sub>2</sub>S removal from the biogas produced from wastewater of concentrated latex industry in this study. The experimental results show that combination of absorption and oxidation by iron-chelated solution catalyzed by Fe(III)EDTA can remove H<sub>2</sub>S from biogas with an efficiency up to 97% and the Fe(III)EDTA can be easily regenerated by bubbling air into the absorbing liquid. We conclude that chemical oxidation using an iron chelated solution, catalyzed by Fe(III)EDTA is an economically promising technique to remove H<sub>2</sub>S from biogas even at high H<sub>2</sub>S concentrations. Additionally, a mathematical model of the absorption and the reaction between H<sub>2</sub>S and Fe(III)EDTA in a packed column was proposed and verified against the experimental data. The results confirm the potential use of the model for the design of a packed column for H<sub>2</sub>S removal from biogas using absorption coupled with oxidation by Fe(III)EDTA.

The operating variables which are known to influence a packed column performance such as, the scrubbing liquid flow rate, the gas flow rate, the inlet H<sub>2</sub>S concentration, the initial Fe(III)EDTA concentration and the packed bed height has been studied in laboratory scale packed column. Empirical correlation expressed as a function of these process variables and their interaction was successfully developed for prediction of H<sub>2</sub>S removal efficiency in packed column system. The model obtained in these experiments provides a basis information in order to design the larger scale packed columns for removing H<sub>2</sub>S from gas streams.

Moreover, the kinetics degradation of Fe-EDTA has been studied under with and without stabilizer, sodium citrate. Applying the pseudo first order degradation rate assumption, the first order degradation rate constant as a function of H<sub>2</sub>S molar flow rate, the initial Fe-EDTA concentration and stabilizer concentration

were determined. The Fe-EDTA degradation rate predicted from the development model shows a good agreement with the experimental data. The degradation kinetics knowledge obtained from this work can be used to determine amount of Fe(III)EDTA that warrant the constant removal efficiency.

Finally, the cost of H<sub>2</sub>S removal from biogas using the packed column were analyzed. The investment cost for removing 1,300 mg/m<sup>3</sup> of H<sub>2</sub>S from biogas at 2 L/min was about 10,000 – 15,000 Baht while the operating cost was 0.81 Baht/m<sup>3</sup> biogas. The cost comparison of using Fe(III)EDTA with other oxidant, KMnO<sub>4</sub> and NaOCl was investigated and it revealed that the operating cost for Fe(III)EDTA system was slightly lower than KMnO<sub>4</sub> system but about two times lower than that of NaOCl.

## 5.2 Future works

1. Installation of the H<sub>2</sub>S removal using Fe(III)EDTA in packed column system to treat biogas before supplying to the engine should be done.
2. Fe-EDTA degradation products should be identified.
3. Other chemical additive or chelating agents should be studied for improving the effective and durance of Fe-EDTA solution.
4. pH control during H<sub>2</sub>S oxidation should be studied.
5. The effective and suitable sulfur cake separation unit should be studied.
6. The cost of H<sub>2</sub>S removal system with long period operation should be investigated.
7. H<sub>2</sub>S removal together with CO<sub>2</sub> removal should be studied.



## REFERENCES

- Abatzoglou, N. and Boivin, F. 2009. A review of biogas purification processes. *Biofuels Bioproduct and Biorefining*, 3: 42-71.
- Annadurai, G., Ling, L.Y. and Lee, J.F. 2008. Statistical optimization of medium components and growth conditions by response surface methodology to enhance phenol degradation by *pseudomonas putida*. *Journal of Hazardous Materials*, 151: 171-178.
- APHA, AWWA and WPCF. 1985. *Standard Methods for The Examination of Water and Waste*. 6<sup>th</sup> ed. Washington, DC, US.
- Arthur I. 1961. *VoGel. A text-book of quantitative inorganic analysis*. 3<sup>rd</sup> edition. The English Language Book Society, London.
- Bird, R.B., Stewart, W.E. and Lightfoot, E.N. 2002. *Transport Phenomena*, 2<sup>nd</sup> ed. New York: John Wiley&Sons, Inc.
- Blanco, M.C., Mcira, A., Baldomir, D., Rivas, J. and López-Quintela M.A. 1994. UV-VIS spectra of small iron particles. *IEEE Transactions on Magnetics*, 30(2): 739-741.
- Buonicore, t. and Davis, W. (Eds). 1992. *Air pollution Engineering Manual. Air and Waste Management*, New York: Van Norstrand Reinhold.
- Busca, G and Pistarino, C. 2003. Technologies for the abatement of sulphide compounds from gaseous streams: a comparative overview. *Journal of Loss Prevention in the Process Industries*, 16: 363-371.
- Chapman, S.J. 2005. *MATLAB Programming for Engineers*. 3<sup>th</sup> ed. Thomson, Canada.
- Chen, D., Martell, A.E. and McManus. 1995. Studies on the mechanism of chelate degradation in iron-based, liquid redox H<sub>2</sub>S removal processes *Canadian Journal of chemistry*. 73: 264-274.
- Chen, D., Motekaitis, R.J., Martell, A.E. and McManus, D. 1993 Oxidation of H<sub>2</sub>S to S by air with Fe(III)-NTA as a catalyst: catalyst degradation. *Canadian Journal of chemistry*. 71: 1542-1531.

- Chen, L., Huang, J. and Yang, C.L. 2001. Absorption of H<sub>2</sub>S in NaOCl caustic aqueous solution. *Environmental Progress*, 20(3): 175-181.
- Couvert, A., Charron, I., Laplanche, A., Renner, C., Patria, L. and Requieme, B. 2006. Treatment of odorous sulphur compounds by chemical scrubbing with hydrogen peroxide application to a laboratory plant. *Chemical Engineering Science*, 61: 7240-7248.
- Deberry, D.W. 1993. Rates and mechanisms of reaction of hydrogen sulfide with Iron chelates. Topical Report. Gas Research Institute. Apr.
- Delvecchio, F.C., Brixuela, R. M., Khan, S.R. Byer, K. Li, Z., Zhong, P. and Preminger, G.M. 2005. Citrate and vitamin E blunt the shock wave-induced free radical surge in an in vitro cell culture model. *Urological Research*, 33: 448-452.
- Demmink, J. F. and Beenackers, A. A. C. M. 1998. Gas desulfurization with Ferric chelates of EDTA and HEDTA: New Model for the Oxidative Absorption of Hydrogen Sulfide. *Industrial & Engineering Chemistry Research*, 37: 1444-1453.
- Demmink, J. F., Mehra, A.A. and Beenackers, A. C. M. 1998. Gas absorption in the presence of particles showing interfacial affinity: case of fine sulfur precipitates. *Chemical Engineering Science*, 53: 2885-2902.
- Demmink, J. F., Mehra, A.A. and Beenackers, A. C. M. 2002. Absorption of hydrogen sulfide into aqueous solutions of ferric nitrilotriacetic acid: local auto-catalytic effects. *Chemical Engineering Science*, 57: 1723-1734.
- Douglas C. M. 2001. Design and analysis of experiments. 5<sup>th</sup> ed. Arizona State University.
- Dawson, D. S. 1993. Biological Treatment of Gaseous Emissions. *Water Environment Research*, 65: 368-371.
- Edgar, T.F. and Himmelblau, D.M. 1988. Optimization of Chemical Process. McGraw-Hill Book Company.
- EPA Method 11, Determination of Hydrogen Sulfide Content of Fuel Gas Streams in Petroleum Refineries, CFR40, Part 60, Appendix A.
- Fogler, H.S. 1999. Elements of Chemical Reaction Engineering. 3<sup>th</sup> ed. Prentice-Hall, Inc., USA.

- Gao, L., Keener, T.C., Zhuang, L. and Siddiqui, K.F. 2002. A technical and economic comparison of biofiltration and wet chemical oxidation (scrubbing) for odor control at wastewater treatment plants. *Environmental Engineering and Policy*, 2: 203-212.
- Gautier, L.I., Bertet, P. Jeunet, A. Serratrice, G. And Louis Pierre, J. 2006. Iron citrate complexes and free radicals generation: Is citric acid an innocent additive in foods and drinks? *Bio Metals*, 20: 793-796
- Geankoplis, C.J. 1993. *Transport Processes and Unit Operations*, 3<sup>th</sup> ed. USA: A Simon&Schuster Company.
- Godini, H.R. and Mowla, D. 2008. Selectivity study of H<sub>2</sub>S and CO<sub>2</sub> absorption from gaseous mixtures by MEA in packed beds. *Chemical engineering research and design*, 86: 401–409.
- Hatta, S., *Technological Reports, Tôhoku University*, 10, 119 (1932); from Levenspiel, O. 1999. *Chemical Reaction Engineering*, 3<sup>th</sup> ed. John Willey and Sons, Inc., USA.
- Heguy, D.L. 2003. The state of Iron-Redox Sulfur Plant Technology new developments to a Long- Established Process Technology, published in hydrocarbon processing; Available online: <http://www.gtp-merichem.com/> (April 16, 2007).
- Horikawa, M.S., Rossi, F., Gimenes, M.L., Costa, C.M.M. and Silva, da M.G.C. 2004. Chemical absorption of H<sub>2</sub>S for biogas purification. *Brazilian Journal of Chemical Engineering*, 21: 415 – 422.
- Iliuta, I., Grandjean, B.P.A., Piche, S. and Larachi, F. 2003. Two fluid model for counter-current dumped packing containing Columns. *Chemical Engineering Science*, 58: 1373-1380.
- Iliuta, I. and Larachi, F. 2003. Concept of bifunctional redox iron-chelate process for H<sub>2</sub>S removal in pulp and paper atmospheric emissions. *Chemical Engineering Science*, 58: 5305-5314.
- Kolthoff, I.M., Sandell, E.B., Meehan, E.J. and Stanley Bruckenstein. 1963. *Quantitative Chemical Analysis*. 4<sup>th</sup> edition. The Macmillan Company Collier-Macmillan Limited, London.

- Kratzer, F.H. and Vohra, P. 1986. Chelate In Nutrition, CRC Press, Inc. Boca Raton, Florida, U.S.A.
- Levenspiel, O. 1999. Chemical Reaction Engineering, 3<sup>th</sup> ed. John Willey and Sons, Inc., USA.
- Martell, A.E., Motekaitis, R.J. Chen, D. Hancock, R.D. and McManus, D. 1996. Selection of new Fe(III)/Fe(II) chelating agents as catalysts for the oxidation of hydrogen sulfide to sulfur by air. Canadian Journal of Chemistry, 74: 1872-1879.
- McCabe, W.L., Smith, J.C. and Harriott, P. 2001. Unit Operations of Chemical Engineering. 3<sup>th</sup> ed. McGraw-Hill.
- McManus, D. and Martell, A.E. 1997. The evolution, chemistry and applications of chelated iron hydrogen sulfide removal and oxidation processes. Journal of Molecular Catalysis A: Chemical, 117: 289-297.
- Michael, A.M., Khepar, S.D. and Sondhi, S.K. 2008. Water well and pump. 2<sup>nd</sup> ed.
- Moosavi, G.R., Naddafi, K., Mesdaghinia, A, Vaezi, F. and Mahmoudi, M. 2005 H<sub>2</sub>S removal in an oxidative packed bed scrubber using different chemical oxidant. Journal of Applied Sciences, 5(4): 651-654.
- Onda, K., Takeuchi, H. and Okumoto, Y., 1968. Mass transfer coefficients between gas and liquid phases in packed columns. Journal of Chemical Engineering of Japan 1, 56.; from Iliuta, I. and Larachi, F. 2003. Concept of bifunctional redox iron-chelate process for H<sub>2</sub>S removal in pulp and paper atmospheric emissions. Chemical Engineering Science, 58: 5305-5314.
- OSHA (2002), Occupational Safety and Health Administration; Available online: [www.OSHA.gov](http://www.OSHA.gov) (16 April 2007).
- Oskouie, S.F.G., Tabandeh, F., Yakhchali, B. and Eftekhari, F. 2008. Response surface optimization of medium composition for alkaline protease production by *Bacillus clausii*. Biochemical Engineering Journal, 39: 37-42.
- Perry, R.H. and C.H. Chilton, Eds., Chemical Engineers' Handbook, 6<sup>th</sup> ed.; McGraw-Hill Book Company: New York, 1984.
- Piché, S., Grandjean, B.P.A. and Larachi, F. 2002. Reconciliation Procedure for Gas-Liquid Interfacial Area and Mass-Transfer Coefficient in Randomly Packed Towers. Industrial and Engineering Chemistry Research, 41: 4911-4920

- Piché, S., Levesque, S., Grandjean, B.P.A. and Larachi, F. 2003. Prediction of HETP for randomly packed towers operation: integration of aqueous and non-aqueous mass transfer characteristics into one consistent correlation. *Separation and Purification Technology*, 33: 145-162.
- Piché, S. and Larachi, F. 2006a. Dynamics of pH on the oxidation of HS<sup>-</sup> with iron(III) chelates in anoxic conditions. *Chemical Engineering Science*, 61: 7673-7683.
- Piché, S. and Larachi, F. 2006b. Kinetic effect of electrolytes on the oligomerization of hydrosulfide into polysulfides and colloidal sulfur with iron(III) *trans*-1,2-diaminocyclohexanetetraacetic acid in anoxic aqueous solutions. *Chemical Engineering Science*, 61: 7171-7176.
- Piché, S., Ribeiro, N., Bacaoui, A. and Larachi, F. 2005. Assessment of a redox alkaline/iron-chelate absorption process for the removal of dilute hydrogen sulfide in air emissions. *Chemical Engineering Science*, 6: 6452-6461.
- Rafson, I. and Harold, J. 1998. *Odour and VOC Control Handbook*, McGraw Hill, New York, U.S.A.
- Rerngnarong, A. 2007. *Treatment of Concentrated Latex Industrial Wastewater by UASB System. A Thesis Submitted in Partial Fulfillment of the Requirements for the Degree of Master of Engineering in Chemical Engineering*. Prince of Songkla University.
- Rouessac, F. and Rouessac, A. 2000. *Chemical analysis modern instrumentation methods and techniques*. John Wiley&Sons, England.
- Sayan, E and Edecan, M.E. 2008. An optimization study using response surface methods on the decolorization of Reactive Blue 19 from aqueous solution by ultrasound. *Ultrasonics Sonochemistry*, 15: 530-538.
- Setameteekul, A., Aroonwilas, A. and Veawab, A. 2008. Statistical factorial design analysis for parametric interaction and empirical correlations of CO<sub>2</sub> absorption performance in MEA and blended MEA/MDEA processes. *Separation and Purification Technology*, 64: 16-25.

- Sieres, J. and Seara, J.F. 2007. Experimental investigation of mass transfer performance with some random packings for ammonia rectification in ammonia–water absorption refrigeration systems. *International Journal of Thermal Sciences*, 46: 699-706.
- Spiegel, R. J. and Trocciola, J.C. 1997. Test Results for Fuel-Cell Operation on Landfill Gas, *Energy* 22(8): 777-786.
- Steppan, D.D., Werner, J. and Yeater, R.P. 1998. *Essential Regression and Experimental Design for Chemists and Engineers*.
- Sunda and Huntsman (2003). Effect of pH, light, and temperature on Fe–EDTA chelation and Fe hydrolysis in seawater *Marine Chemistry* 84: 35-47.
- Supap, T., Idem, R., Tontiwachwuthikul, P. and Saiwan, C. 2009. Kinetics of sulfur dioxide and oxygeninduced degradation of aqueous monoethanolamine solution during CO<sub>2</sub> absorption from power plant flue gas streams. *International journal of greenhouse gas control*, 3: 133-142.
- Szentmihályi, K. Blázovics, A. And Vinkler, P. 2003. Free radical properties of metal complexes. *Acta Biologica Szegediensis*, 47(1-4): 107-109.
- Tautkus, S., Steponeniene, L. and Kazlauskas, R. 2004. Determination of iron in natural and mineral waters by flame atomic absorption spectrometry. *Journal of Serbian Chemical Society*. 69(5) :393-402.
- Tee E Siang, Khor Swan Chao and Siti Mizura Shahid. 1989. Determination of iron in foods by the atomic absorption spectrophotometric and colorimetric methods. *Pertanika* 12(3): 313-322.
- Furia, T.E. 1972. *CRC Handbook of Food Additives*. 2<sup>nd</sup> ed. ; Available online: [http://www.coldcure.com/html/stability\\_constants.html](http://www.coldcure.com/html/stability_constants.html) (10 January 2009)
- Turpin, A., Couvert, A., Laplanche, A. and Paillier, A. 2008. Experimental study of mass transfer and H<sub>2</sub>S removal efficiency in a spray tower. *Chemical Engineering and Processing*, 47: 886–892.
- Wellinger, A., Linberg, A. (2000). *Biogas Upgrading and Utilization*. IEA Bioenergy Task 24: Energy from biological conversion of organic waste.
- Wozik, B.A.A.V and Westerterp, K.R. 2000. Measurement of interfacial areas with the chemical method for a system with alternating dispersed phases. *Chemical Engineering and Processing*, 39: 299-314.

- Wubs, H.J. and Beenackers, A.A.C.M. 1993. Kinetics of the oxidation of ferrous chelates of EDTA and HEDTA in aqueous solution. *Industrial and Engineering Chemistry Research*, 32: 2580.
- Wubs, H. J. and Beenackers, A.A.C.M. 1994. Kinetics of H<sub>2</sub>S absorption into aqueous ferric solution of EDTA and HEDTA. *American Institute of Chemical Engineering Journal*. 40: 433-444.
- Zicari, S.M. 2003. Removal of hydrogen sulfide from biogas using cow-manure compost. A Thesis Presented to the Faculty of the Graduate School of Cornell University in Partial Fulfillment of the Requirements for the Degree of Master of Science.
- Zarzycki, R and Chacuk, A. 1993. Absorption: Fundamentals and Applications. 1<sup>st</sup> ed. B.P.C.C. Wheatons Ltd, Great Britain.

### **Patents**

- Baker, R.A., Costello, R.C. and Engel, M.J. 1986. Removal of sulfur from aqueous suspension using filtration. United States Patent. US 4631068, issued December 23.
- Bedell, S.A. 1990. Stabilized chelating agents for removing hydrogen sulfide. United States Patent. US4891205, issued January 2.
- Blytas, G.C. 1983. Method of removing hydrogen sulfide from gases utilizing a stabilized metal chelate solution. . United States Patent. US4421733, issued December 20.
- Blytas, G.C. and Diaz, Z. 1982a. Method of removing hydrogen sulfide from gases. United States Patent. US 4348368, issued September 7.
- Blytas, G.C. and Diaz, Z. 1982b. Sulphur recovery process. European Patent. EP0066310, issued August 12.
- Blytas, G.C. and Diaz, Z. 1982c. Removal of H<sub>2</sub>S and COS. United States Patent. US 4409199, issued October 11.
- Chang, D. and Bedell, S.A.1987. Automatic pH control in a process for removal of hydrogen sulfide from a gas. United States Patent. US 4643886, issued February 17.

- De Algelis, A., Bellussi, G., Pollesel, P., Romano, U. and Perego, C. 2007. Process for the removal of hydrogen sulfide, by means of its oxidation in the presence of hetero polyacids. United States Patent. US 2007/0178033 A1, issued August 2.
- Diaz, Z. 1983a. Method of removing hydrogen sulfide from gases utilizing a stabilized iron chelate solution. United States Patent. US4382918, issued May 10.
- Diaz, Z. 1983b. H<sub>2</sub>S Removal. United States Patent. US4388293, issued June 14.
- Diaz, Z. 1983c. H<sub>2</sub>S Removal process. United States Patent. US4400368, issued August 23.
- Diaz, Z. 1984. Method of removing hydrogen sulfide from gases utilizing a stabilized chelate solution. United States Patent. US4461754, issued July 24.
- Hartmann, A. 1999. Process for the filtration of suspensions containing sulfur. United States Patent. US 5861099 , issued January 19.
- Kliem, E. Weber, G. and Kunz, A. 1989. Separation of a mixture of sulfur and alkaline solution and apparatus. United States Patent. US 4876079, issued October 24.
- Lampton, R. D. and Thomas M. H. 1986. Process for the removal of H<sub>2</sub>S from geothermal steam and the conversion to sulfur. United States Patent. US 4629608, issued December 16.
- Lynn, S. 1982. Method of oxidizing a polyvalent metal. United States Patent. US4330478, issued May 18.
- Lynn, S. and Dubs, B.J. 1981. Oxidative removal of hydrogen sulfide from gaseous streams. United States Patent. US 4278646, issued July 14.
- Mcmanus, D. and Kin, F. R. 1993. Hydrogen sulfide removal. European Patent. EP0257124, issued April 4.
- Meuly, W.C. 1965. Process for the removal of hydrogen sulfide from gaseous streams by catalytic oxidation of hydrogen sulfide to sulfur while inhibiting the formation of sulfur oxides. United States Patent. US patent 4009251, issued February 22.
- Nagl G.J., Reicher, M. and McManus, D. 2008. Oxidizer and oxidation process for a desulphurization process. United States Patent. US patent 7344682, issued March 18.



- Nichol, R. J. and Sapiro, R. H. 1965a. Purification of gases. European Patent. GB999799, issued July 28.
- Nichol, R. J. and Sapiro, R. H. 1965b. Purification of gases. European Patent. GB999800, issued July 28.
- Primack, H.S., Reedy, D.E. and Kin, F.R. 1984. Method of stabilizing chelated polyvalent metal solutions. United States Patent. US 4455287, issued June 19.
- Roberts, M. L., Johnson, C. E and Miller, R. C. 1971. Composition for the removal of hydrogen sulfide from gaseous streams. United States Patent. US 3622273, issued November 23.
- Roberts, M. L., Johnson, C. E and Miller, R. C. 1972. Composition for the removal of hydrogen sulfide from gaseous streams. United States Patent. US 3676356, issued July 11.
- Thompson, R.B. 1980. Catalytic removal of hydrogen sulfide from gases. United States Patent. US 4189462, issued February 19.
- Winkler, H.J. S. Process for the removal of H<sub>2</sub>S and CO<sub>2</sub> from gaseous streams. 1978. United States Patent. US 4091073, issued May 23.

## APPENDIX A

### Experimental Results

#### A-1 Removal of H<sub>2</sub>S in Biogas from Concentrated Latex Industry with Iron(III)chelate in Packed Column

**Table A-1.1** H<sub>2</sub>S removal efficiency (%) with time in the oxidation reaction with Fe(III)EDTA (**Run No. 1:**  $G = 5.61 \times 10^{-3} \text{ m}^3/\text{s}$ ,  $C_{\text{H}_2\text{S}}(\text{g})_{,\text{in}} = 0.57 \text{ mol}/\text{m}^3$ ,  $C_{\text{Fe(III)EDTA},\text{in}} = 59.1 \text{ mol}/\text{m}^3$ , Volume of Fe-EDTA = 0.350 m<sup>3</sup> and Air flow rate = 0.07 m<sup>3</sup>/min)

Time (min)	H <sub>2</sub> S concentration (mg/m <sup>3</sup> )		% H <sub>2</sub> S Removal
	Inlet	Outlet	
30	17,091	2,091	87.77
60	19,532	4,868	75.08
120	19,227	6,806	64.60
180	19,777	8,057	58.90
240	20,204	8,942	54.78
300	19,715	8,454	58.16
360	20,722	11,445	41.95

**Table A-1.2** H<sub>2</sub>S removal efficiency (%) with time in the oxidation reaction with Fe(III)EDTA (**Run No. 2:**  $G = 5.44 \times 10^{-3} \text{ m}^3/\text{s}$ ,  $C_{\text{H}_2\text{S}}(\text{g})_{\text{in}} = 0.71 \text{ mol/m}^3$ ,  $C_{\text{Fe(III)EDTA},\text{in}} = 268.6 \text{ mol/m}^3$ , Volume of Fe-EDTA = 0.350 m<sup>3</sup> and Air flow rate = 0.07 m<sup>3</sup>/min)

Time (min)	H <sub>2</sub> S concentration (mg/m <sup>3</sup> )		% H <sub>2</sub> S Removal
	Inlet	Outlet	
20	28,907	1,706	94.10
40	27,777	5,855	78.92
60	24,035	5,227	78.25
80	25,721	6,127	76.18
100	23,614	6,036	74.44
120	22,770	3,702	83.74
140	25,346	5,296	79.11
160	20,561	5,423	73.63
180	24,848	6,372	74.35
210	21,851	12,634	42.18
240	18,854	11,503	38.99
300	24,890	14,293	42.58

**Table A-1.3** H<sub>2</sub>S removal efficiency (%) with time in the oxidation reaction with Fe(III)EDTA (**Run No. 3:**  $G = 5.52 \times 10^{-3} \text{ m}^3/\text{s}$ ,  $C_{\text{H}_2\text{S}}(\text{g})_{,\text{in}} = 0.36 \text{ mol}/\text{m}^3$ ,  $C_{\text{Fe(III)EDTA},\text{in}} = 268.6 \text{ mol}/\text{m}^3$ , Volume of Fe-EDTA = 0.50 m<sup>3</sup> and Air flow rate = 0.30 m<sup>3</sup>/min)

Time (min)	H <sub>2</sub> S concentration (mg/m <sup>3</sup> )		% H <sub>2</sub> S Removal
	Inlet	Outlet	
20	16,294	573	96.48
40	9,999	801	91.99
60	10,935	47	99.57
80	11,898	50	99.58
100	11,081	45	99.59
120	11,454	240	97.91
140	10,739	180	98.32
160	12,404	579	95.33
180	11,636	504	95.67
200	12,689	639	94.97
220	12,171	998	91.80
240	12,716	14	99.89
260	12,290	53	99.57
280	12,151	56	99.54
300	12,434	462	96.29
320	13,573	693	94.90
340	13,279	212	98.40
360	13,547	338	97.50

**Table A-1.4** H<sub>2</sub>S removal efficiency (%) with time in the oxidation reaction with Fe(III)EDTA (**Run No. 4:**  $G = 5.16 \times 10^{-3} \text{ m}^3/\text{s}$ ,  $C_{\text{H}_2\text{S}}(\text{g})_{\text{in}} = 0.77 \text{ mol/m}^3$ ,  $C_{\text{Fe(III)EDTA},\text{in}} = 268.6 \text{ mol/m}^3$ , Volume of Fe-EDTA = 0.50 m<sup>3</sup> and Air flow rate = 0.30 m<sup>3</sup>/min)

Time (min)	H <sub>2</sub> S concentration (mg/m <sup>3</sup> )		% H <sub>2</sub> S Removal
	Inlet	Outlet	
20	25,611	300	98.83
40	28,264	1,580	94.41
60	28,530	175	99.39
80	28,683	1,361	95.26
100	26,644	406	98.48
120	23,176	107	99.54
140	31,141	523	98.32
160	27,426	215	99.22
180	22,886	188	99.18
200	26,309	1,036	96.06
220	27,966	855	96.94
240	24,414	1,329	94.55
260	25,332	1,664	93.43
280	25,586	645	97.48
300	25,376	559	97.80
320	24,285	1,099	95.47
340	23,073	645	97.20
360	26,967	513	98.10

**Table A-1.5** Change of Fe(III)EDTA concentration ( $\text{mol/m}^3$ ) as function of reaction time of Run No. 2

<b>Time (min)</b>	<b>Fe(III)EDTA concentration (<math>\text{mol/m}^3</math>)</b>
0	268.58
30	232.78
60	207.45
90	189.40
120	186.14
150	159.87
180	129.51
210	121.40
240	116.31
270	101.72
300	88.16

**Table A-1.6** Change of Fe(III)EDTA concentration ( $\text{mol/m}^3$ ) as function of reaction time of Run No. 4

<b>time (min)</b>	<b>Fe(III)EDTA concentration (<math>\text{mol/m}^3</math>)</b>
0	268.58
30	259.66
60	252.87
90	249.24
120	248.38
150	238.28
180	234.91
210	231.82
240	226.36
270	218.98
300	214.13
330	207.74
360	201.24

**Table A-1.7** Temperature profile of the scrubbing liquid of Run No. 1

<b>Time (min)</b>	<b>Temperature (°C)</b>	<b>Time (min)</b>	<b>Temperature (°C)</b>
0	30.0	195	40.0
15	30.0	210	40.5
30	32.0	225	41.0
45	32.0	240	41.5
60	34.0	255	42.0
75	35.0	270	42.0
90	36.0	285	42.5
105	37.0	300	42.5
120	37.5	315	43.0
135	38.5	330	43.0
150	39.0	345	43.5
165	39.5	360	44.0
180	40.0		

**Table A-1.8** Temperature profile of the scrubbing liquid of Run No. 2

<b>Time (min)</b>	<b>Temperature (°C)</b>	<b>Time (min)</b>	<b>Temperature (°C)</b>
0	32.0	130	41.0
10	32.0	140	41.5
20	33.0	150	42.0
30	34.0	160	42.0
40	35.0	170	42.5
50	36.0	180	43.0
60	36.5	190	43.0
70	37.0	200	43.5
80	37.0	210	43.0
90	38.0	230	43.0
100	39.0	240	43.5
110	39.5	300	43.5
120	40.5		

**Table A-1.9** Temperature profile of the scrubbing liquid of Run No. 3

<b>Time (min)</b>	<b>Temperature (°C)</b>	<b>Time (min)</b>	<b>Temperature (°C)</b>
0	29.0	195	37.0
15	29.5	210	38.0
30	30.0	225	39.0
45	31.0	240	39.0
60	31.0	255	40.0
75	31.5	270	40.0
90	34.0	285	41.0
105	34.0	300	41.0
120	34.0	315	41.0
135	35.5	330	41.0
150	36.0	345	42.0
165	37.0	360	42.0
180	37.0		

**Table A-1.10** Temperature profile of the scrubbing liquid of Run No. 4

<b>Time (min)</b>	<b>Temperature (°C)</b>	<b>Time (min)</b>	<b>Temperature (°C)</b>
0	31.0	195	40.0
15	31.0	210	41.0
30	33.0	225	42.0
45	34.0	240	42.0
60	35.0	255	42.5
75	35.5	270	43.0
90	36.0	285	43.0
105	37.0	300	44.0
120	37.5	315	44.0
135	38.0	330	45.0
150	39.0	345	45.0
165	40.0	360	45.0
180	40.0		



**A-2 Statistical Optimization of Packed Column Operating Conditions by Response Surface Methodology on Iron(III)chelate Absorption Process for the Removal of Hydrogen Sulfide**

**Table A-2.1** H<sub>2</sub>S removal efficiency (*RE*) at reaction time 10, 15, 20 and 25 min at various conditions

Run No.	<i>h</i> (m)	<i>L</i> (mL/s)	<i>C</i> <sub>Fe,0</sub> (mol/m <sup>3</sup> )	<i>G</i> (L/s)	<i>C</i> <sub>H<sub>2</sub>S</sub> (g) <sub>,in</sub> (mol/m <sup>3</sup> )	<i>RE</i> at time (min)					SD
						10	15	20	25	mean	
1	0.300	0.500	160	0.033	0.061	91.6	94.5	92.3	91.3	92.4	1.4
2	0.375	0.333	85	0.067	0.067	75.9	72.4	76.7	74.9	75.0	1.9
3	0.225	0.667	85	0.067	0.070	80.9	79.3	82.3	82.9	81.4	1.6
4	0.225	0.333	235	0.067	0.055	74.9	76.8	78.8	78.6	77.3	1.8
5	0.375	0.667	235	0.067	0.077	98.9	99.8	99.5	98.9	99.3	0.4
6	0.225	0.333	85	0.067	0.149	67.0	65.3	61.2	62.1	63.9	2.7
7	0.375	0.667	85	0.067	0.179	75.0	78.0	77.3	73.8	76.0	2.0
8	0.375	0.333	235	0.067	0.161	85.6	84.5	80.3	83.2	83.4	2.3
9	0.225	0.667	235	0.067	0.141	78.4	78.4	79.9	77.9	78.7	0.9
10	0.300	0.500	160	0.100	0.025	74.1	72.0	71.9	70.3	72.1	1.6
11	0.300	0.500	10	0.100	0.065	58.4	58.3	54.9	54.3	56.5	2.2
12	0.300	0.167	160	0.100	0.084	54.6	56.0	56.8	56.7	56.0	1.0
13	0.150	0.500	160	0.100	0.071	70.8	71.8	69.3	70.9	70.7	1.0
14	0.300	0.500	160	0.100	0.146	62.8	62.8	61.6	63.9	62.8	0.9
15	0.300	0.500	310	0.100	0.071	88.2	86.8	86.1	87.0	87.0	0.9
16	0.300	0.833	160	0.100	0.084	75.2	76.0	74.0	74.6	75.0	0.9
17	0.450	0.500	160	0.100	0.071	85.2	86.3	82.4	83.2	84.3	1.8
18	0.300	0.500	160	0.100	0.084	73.0	70.0	69.0	68.0	70.0	2.2
19	0.300	0.500	160	0.100	0.084	70.1	69.0	69.0	68.0	69.0	0.9
20	0.300	0.500	160	0.100	0.072	74.8	75.3	71.1	75.7	74.2	2.1
21	0.225	0.333	85	0.133	0.071	65.0	65.0	64.8	64.9	64.9	0.1
22	0.375	0.667	85	0.133	0.062	60.0	62.0	62.0	63.8	62.0	1.6
23	0.375	0.333	235	0.133	0.059	71.7	72.7	70.3	71.9	71.7	1.0
24	0.225	0.667	235	0.133	0.053	67.4	64.3	64.1	65.6	65.4	1.5

Run No.	$h$ (m)	$L$ (mL/s)	$C_{Fe,0}$ (mol/m <sup>3</sup> )	$G$ (L/s)	$C_{H_2S(g),in}$ (mol/m <sup>3</sup> )	$RE$ at time (min)					SD
						10	15	20	25	mean	
25	0.375	0.333	85	0.133	0.089	54.3	52.3	51.0	51.3	52.2	1.5
26	0.225	0.667	85	0.133	0.116	50.5	42.3	46.5	46.8	46.5	3.4
27	0.225	0.333	235	0.133	0.106	48.7	43.8	46.7	47.8	46.8	2.1
28	0.375	0.667	235	0.133	0.125	80.4	83.2	81.4	81.1	81.5	1.2
29	0.300	0.500	160	0.167	0.100	54.7	56.7	56.3	57.0	56.2	1.0
30	0.225	0.500	156	0.100	0.072	74.2	71.0	70.4	68.3	71.0	2.4
31	0.375	0.500	156	0.100	0.070	77.5	79.8	78.4	78.2	78.5	1.0
32	0.300	0.667	156	0.100	0.082	72.3	71.2	70.1	73.4	71.8	1.4
33	0.300	0.500	157	0.100	0.060	73.1	70.3	70.0	68.2	70.4	2.0
34	0.300	0.500	156	0.100	0.119	55.5	58.9	59.0	57.1	57.6	1.7
35	0.300	0.500	157	0.067	0.091	79.8	79.8	80.8	80.1	80.1	0.5
36	0.300	0.500	156	0.133	0.100	58.6	57.9	57.9	58.6	58.3	0.4
37	0.300	0.333	157	0.100	0.077	57.8	55.2	59.5	59.9	58.1	2.1
38	0.300	0.500	81	0.100	0.066	65.2	65.4	65.9	65.2	65.4	0.3
39	0.300	0.500	216	0.100	0.068	82.5	84.6	86.5	87.4	85.3	2.2

### A-3 The degradation of Fe(III)EDTA in hydrogen sulfide removal

**Table A-3.1** Experimental conditions for Fe-EDTA kinetics degradation study

Run no.	$C_{Fe,0}$ (mol/m <sup>3</sup> )	$Q_{H_2S}$ x10 <sup>3</sup> (mol/h)	$C_{Cl}$ (mol/m <sup>3</sup> )
1	5.78	1.08	0
2	5.78	1.05	0
3	5.78	2.06	0
4	5.78	2.01	0
5	5.78	2.73	0
6	5.78	2.79	0
7	5.78	3.40	0
8	5.78	3.20	0
9	2.17	1.79	0
10	2.17	1.81	0
11	3.94	1.94	0
12	3.94	1.90	0
13	5.73	2.16	0
14	5.73	2.13	0
15	8.16	2.37	0
16	8.16	2.40	0
17	5.84	2.03	0
18	5.84	2.10	0
19	5.77	2.19	50
20	5.77	2.16	50
21	5.75	2.41	100
22	5.75	2.37	100
23	5.80	2.43	300
24	5.80	2.49	300
25	5.80	2.43	100 <sup>a</sup>
26	5.80	2.38	100 <sup>a</sup>

<sup>a</sup> = the additive is sodium thiosulfate

**Table A-3.2** Soluble Fe(total) concentration (mol/m<sup>3</sup>)-time data of Run no.1-8

Time (h)	Run no.							
	1	2	3	4	5	6	7	8
0	5.78	5.78	5.78	5.78	5.78	5.78	5.78	5.78
3	5.78	5.78	5.77	5.77	5.77	5.77	5.76	5.76
6	5.77	5.77	5.77	5.76	5.75	5.76	5.75	5.74
9	5.77	5.77	5.74	5.75	5.74	5.74	5.71	5.71
12	5.75	5.76	5.72	5.73	5.71	5.71	5.68	5.66
15	5.74	5.75	5.71	5.71	5.68	5.68	5.64	5.65
18	5.73	5.73	5.69	5.68	5.65	5.65	5.61	5.61
21	5.71	5.72	5.67	5.66	5.62	5.63	5.58	5.58
24	5.69	5.70	5.65	5.64	5.58	5.60	5.55	5.55
27	5.67	5.68	5.63	5.63	5.57	5.58	5.52	5.51
30	5.66	5.67	5.62	5.61	5.55	5.56	5.49	5.49

**Table A-3.3** Soluble Fe(total) concentration (mol/m<sup>3</sup>)-time data of Run no.9-16

Time (h)	Run no.							
	9	10	11	12	13	14	15	16
0	2.17	2.17	3.94	3.94	5.73	5.73	8.16	8.16
3	2.16	2.16	3.93	3.93	5.72	5.72	8.15	8.15
6	2.15	2.14	3.91	3.92	5.70	5.70	8.13	8.14
9	2.13	2.13	3.90	3.90	5.69	5.69	8.12	8.12
12	2.11	2.12	3.88	3.89	5.67	5.67	8.10	8.10
15	2.10	2.10	3.87	3.87	5.65	5.65	8.09	8.08
18	2.08	2.08	3.85	3.85	5.63	5.63	8.07	8.06
21	2.06	2.06	3.83	3.83	5.61	5.61	8.05	8.04
24	2.05	2.05	3.82	3.81	5.59	5.60	8.04	8.02
27	2.03	2.03	3.80	3.80	5.58	5.58	8.02	8.01
30	2.02	2.02	3.78	3.78	5.57	5.57	8.00	7.99

**Table A-3.4** Soluble Fe(total) concentration ( $\text{mol/m}^3$ )-time data of Run no.17-26

Time (h)	Run no.									
	17	18	19	20	21	22	23	24	25	26
0	5.84	5.84	5.77	5.77	5.75	5.75	5.80	5.80	5.80	5.80
3	5.82	5.83	5.76	5.76	5.74	5.74	5.80	5.80	5.79	5.80
6	5.81	5.82	5.75	5.75	5.74	5.73	5.79	5.79	5.79	5.78
9	5.80	5.80	5.74	5.74	5.73	5.73	5.79	5.79	5.77	5.77
12	5.78	5.79	5.73	5.73	5.72	5.72	5.78	5.78	5.76	5.76
15	5.76	5.77	5.72	5.72	5.71	5.71	5.77	5.77	5.76	5.75
18	5.74	5.74	5.70	5.71	5.70	5.70	5.76	5.77	5.74	5.74
21	5.72	5.72	5.69	5.69	5.70	5.69	5.75	5.76	5.73	5.72
24	5.71	5.70	5.67	5.67	5.68	5.68	5.75	5.75	5.71	5.71
27	5.69	5.69	5.65	5.65	5.67	5.66	5.73	5.73	5.69	5.69
30	5.68	5.67	5.64	5.64	5.65	5.65	5.72	5.72	5.68	5.68

**Table A-3.5**  $-\ln(C_{Fe,t}/C_{Fe,0})$ -time data of Run no.1-8

Time (h)	Run no.							
	1	2	3	4	5	6	7	8
0	0.0000	0.0000	0.0000	0.0000	0.0000	0.0000	0.0000	0.0000
3	0.0003	0.0004	0.0010	0.0013	0.0016	0.0016	0.0028	0.0030
6	0.0012	0.0012	0.0024	0.0028	0.0044	0.0041	0.0059	0.0073
9	0.0022	0.0025	0.0070	0.0054	0.0075	0.0069	0.0119	0.0124
12	0.0044	0.0043	0.0101	0.0082	0.0124	0.0114	0.0176	0.0207
15	0.0070	0.0052	0.0128	0.0119	0.0170	0.0173	0.0242	0.0235
18	0.0095	0.0093	0.0159	0.0169	0.0225	0.0227	0.0292	0.0291
21	0.0125	0.0108	0.0192	0.0201	0.0281	0.0258	0.0346	0.0348
24	0.0157	0.0143	0.0227	0.0243	0.0345	0.0321	0.0409	0.0412
27	0.0187	0.0170	0.0262	0.0264	0.0376	0.0353	0.0467	0.0470
30	0.0217	0.0197	0.0289	0.0291	0.0402	0.0381	0.0506	0.0509

**Table A-3.6**  $-\ln(C_{Fe,t}/C_{Fe,0})$ -time data of Run no.9-16

Time (h)	Run no.							
	9	10	11	12	13	14	15	16
0	0.0000	0.0000	0.0000	0.0000	0.0000	0.0000	0.0000	0.0000
3	0.0052	0.0049	0.0027	0.0025	0.0021	0.0023	0.0012	0.0011
6	0.0102	0.0124	0.0064	0.0061	0.0050	0.0050	0.0033	0.0030
9	0.0178	0.0168	0.0091	0.0097	0.0068	0.0072	0.0050	0.0050
12	0.0259	0.0249	0.0141	0.0134	0.0102	0.0112	0.0071	0.0071
15	0.0317	0.0351	0.0188	0.0171	0.0144	0.0142	0.0091	0.0102
18	0.0429	0.0442	0.0235	0.0232	0.0182	0.0177	0.0115	0.0126
21	0.0506	0.0520	0.0278	0.0289	0.0217	0.0204	0.0136	0.0145
24	0.0570	0.0588	0.0322	0.0337	0.0243	0.0228	0.0151	0.0167
27	0.0645	0.0660	0.0364	0.0370	0.0269	0.0260	0.0172	0.0190
30	0.0709	0.0731	0.0408	0.0407	0.0292	0.0283	0.0196	0.0211

**Table A-3.7**  $-\ln(C_{Fe,t}/C_{Fe,0})$ -time data of Run no.17-24

Time (h)	Run no.							
	17	18	19	20	21	22	23	24
0	0.0000	0.0000	0.0000	0.0000	0.0000	0.0000	0.0000	0.0000
3	0.0021	0.0018	0.0010	0.0011	0.0009	0.0011	0.0008	0.0007
6	0.0043	0.0034	0.0020	0.0021	0.0019	0.0024	0.0017	0.0015
9	0.0070	0.0062	0.0037	0.0039	0.0028	0.0033	0.0027	0.0024
12	0.0099	0.0086	0.0057	0.0056	0.0042	0.0050	0.0038	0.0035
15	0.0137	0.0124	0.0082	0.0077	0.0057	0.0072	0.0052	0.0046
18	0.0175	0.0165	0.0109	0.0105	0.0076	0.0085	0.0068	0.0060
21	0.0202	0.0204	0.0136	0.0133	0.0089	0.0107	0.0081	0.0073
24	0.0227	0.0235	0.0164	0.0162	0.0117	0.0124	0.0095	0.0091
27	0.0252	0.0260	0.0194	0.0198	0.0141	0.0145	0.0116	0.0118
30	0.0280	0.0285	0.0226	0.0225	0.0168	0.0173	0.0140	0.0138

**Table A-3.8** Soluble Fe(II) concentration (mol/m<sup>3</sup>) -time data of Run no.1-8

Time (h)	Run no.							
	1	2	3	4	5	6	7	8
0	0.00	0.00	0.00	0.00	0.00	0.00	0.00	0.00
3	0.18	0.19	0.28	0.22	0.28	0.24	0.46	0.42
6	0.11	0.17	0.20	0.29	0.37	0.38	0.49	0.55
9	0.22	0.26	0.34	0.37	0.46	0.48	0.55	0.43
12	0.15	0.34	0.36	0.25	0.43	0.26	0.53	0.46
15	0.22	0.19	0.33	0.46	0.54	0.36	0.54	0.53
18	0.18	0.28	0.52	0.33	0.37	0.51	0.36	0.45
21	0.29	0.35	0.21	0.37	0.39	0.46	0.54	0.58
24	0.26	0.24	0.34	0.46	0.35	0.49	0.49	0.62
27	0.54	0.43	0.43	0.30	0.50	0.36	0.46	0.44
30	0.44	0.43	0.52	0.44	0.48	0.43	0.37	0.58

**Table A-3.9** Soluble Fe(II) concentration (mol/m<sup>3</sup>) -time data of Run no.9-16

Time (h)	Run no.							
	9	10	11	12	13	14	15	16
0	0.00	0.00	0.00	0.00	0.00	0.00	0.00	0.00
3	0.22	0.18	0.23	0.23	0.20	0.22	0.22	0.15
6	0.26	0.20	0.28	0.24	0.17	0.23	0.24	0.38
9	0.32	0.18	0.43	0.35	0.21	0.31	0.19	0.31
12	0.35	0.27	0.36	0.46	0.25	0.35	0.37	0.27
15	0.27	0.43	0.31	0.57	0.29	0.37	0.39	0.24
18	0.40	0.33	0.28	0.44	0.33	0.46	0.27	0.19
21	0.24	0.31	0.37	0.34	0.37	0.48	0.39	0.33
24	0.19	0.23	0.26	0.28	0.29	0.33	0.30	0.35
27	0.39	0.24	0.26	0.34	0.32	0.32	0.26	0.38
30	0.29	0.21	0.33	0.36	0.34	0.32	0.30	0.35

**Table A-3.10** Soluble Fe(II) concentration (mol/m<sup>3</sup>) -time data of Run no.17-24

Time (h)	Run no.							
	17	18	19	20	21	22	23	24
0	0.00	0.00	0.00	0.00	0.00	0.00	0.00	0.00
3	0.25	0.24	0.24	0.21	0.24	0.22	0.19	0.22
6	0.37	0.27	0.26	0.34	0.24	0.24	0.27	0.26
9	0.38	0.19	0.26	0.30	0.28	0.28	0.29	0.28
12	0.44	0.36	0.29	0.25	0.28	0.28	0.33	0.29
15	0.38	0.39	0.29	0.36	0.31	0.33	0.35	0.43
18	0.40	0.40	0.30	0.37	0.43	0.36	0.43	0.36
21	0.40	0.47	0.35	0.37	0.37	0.52	0.45	0.44
24	0.39	0.40	0.47	0.38	0.44	0.47	0.39	0.46
27	0.40	0.38	0.52	0.44	0.35	0.44	0.40	0.49
30	0.47	0.43	0.27	0.45	0.37	0.04	0.42	0.50

**Table A-3.11** pH-time data of Run no. 1-8

Time (h)	Run no.							
	1	2	3	4	5	6	7	8
0	7.00	7.00	7.00	7.00	7.00	7.00	7.00	7.00
3	6.75	6.75	6.75	6.75	6.75	6.75	6.50	6.50
6	6.75	6.75	6.75	6.75	6.75	6.75	6.00	6.00
9	6.50	6.50	6.50	6.50	6.50	6.50	6.00	6.00
12	6.50	6.50	6.50	6.50	6.50	6.50	5.50	5.50
15	6.50	6.50	6.50	6.50	6.50	6.50	5.50	5.50
18	6.00	6.00	6.00	6.00	6.00	6.00	5.00	5.00
21	6.00	6.00	6.00	6.00	5.50	5.50	5.00	5.00
24	5.50	5.50	5.50	5.50	5.50	5.50	4.50	4.50
27	5.50	5.50	5.50	5.50	5.00	5.00	4.50	4.50
30	5.00	5.00	5.00	5.00	5.00	5.00	4.50	4.50



**Table A-3.12** pH-time data of Run no. 9-16

Time (h)	Run no.							
	9	10	11	12	13	14	15	16
0	7.00	7.00	7.00	7.00	7.00	7.00	7.00	7.00
3	6.75	6.75	6.75	6.75	6.75	6.75	6.75	6.75
6	6.75	6.75	6.75	6.75	6.75	6.75	6.75	6.75
9	6.50	6.50	6.50	6.50	6.50	6.50	6.50	6.50
12	6.50	6.50	6.50	6.50	6.50	6.50	6.50	6.50
15	6.50	6.50	6.50	6.50	6.50	6.50	6.00	6.00
18	6.00	6.00	6.00	6.00	6.00	6.00	6.00	6.00
21	6.00	6.00	6.00	6.00	5.50	5.50	5.50	5.50
24	5.50	5.50	5.50	5.50	5.50	5.50	5.50	5.50
27	5.50	5.50	5.50	5.50	5.00	5.00	5.50	5.50
30	5.00	5.00	5.00	5.00	5.00	5.00	5.50	5.50

**Table A-3.13** pH-time data of Run no. 17-24

Time (h)	Run no.							
	17	18	19	20	21	22	23	24
0	7.00	7.00	7.00	7.00	7.00	7.00	7.00	7.00
3	6.75	6.75	6.75	6.75	6.75	6.75	6.75	6.75
6	6.75	6.75	6.75	6.75	6.75	6.75	6.75	6.75
9	6.50	6.50	6.50	6.50	6.50	6.50	6.75	6.75
12	6.50	6.50	6.50	6.50	6.50	6.50	6.50	6.50
15	6.50	6.50	6.50	6.50	6.50	6.50	6.50	6.50
18	6.00	6.00	6.00	6.00	6.50	6.50	6.50	6.50
21	5.50	5.50	5.50	5.50	6.00	6.00	6.00	6.00
24	5.50	5.50	5.50	5.50	6.00	6.00	6.00	6.00
27	5.00	5.00	5.00	5.00	5.50	5.50	6.00	6.00
30	5.00	5.00	5.00	5.00	5.50	5.50	5.50	5.50

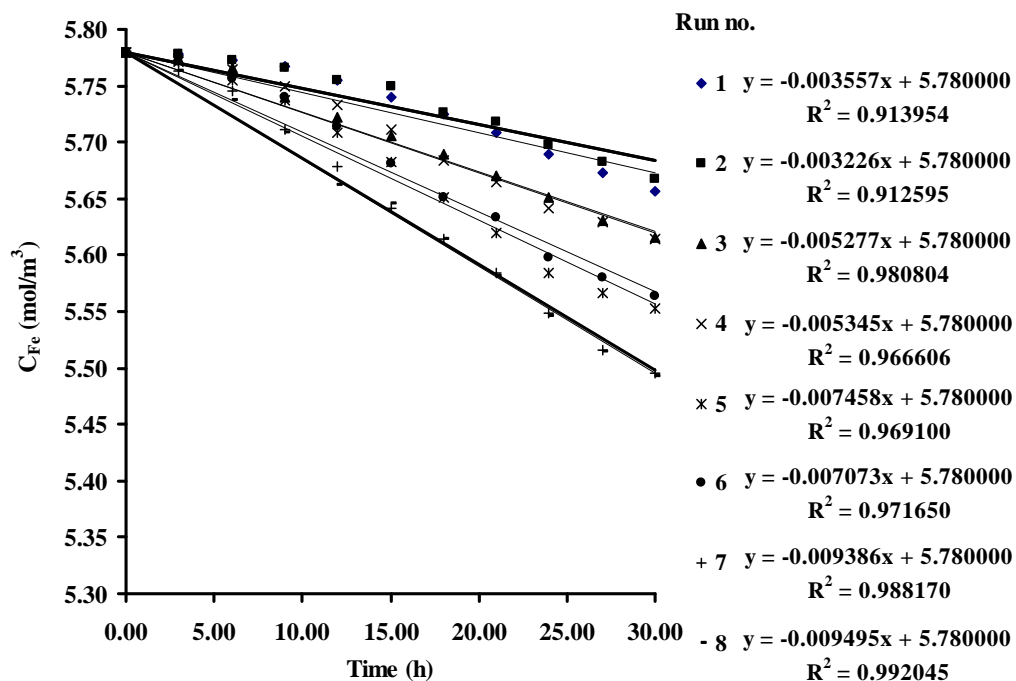


**Figure A-3.1** Soluble Fe concentration-time of Run no.1-8: linear equations with  $R^2$  values

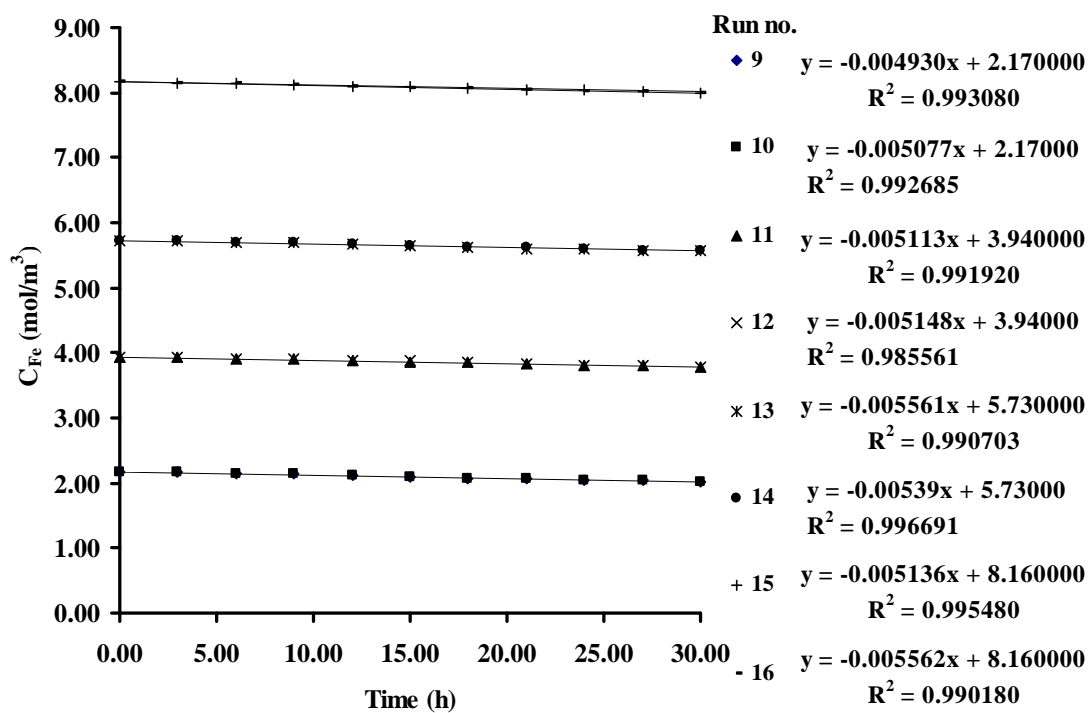


**Figure A-3.2** Soluble Fe concentration-time of Run no.9-16: linear equations with  $R^2$  values

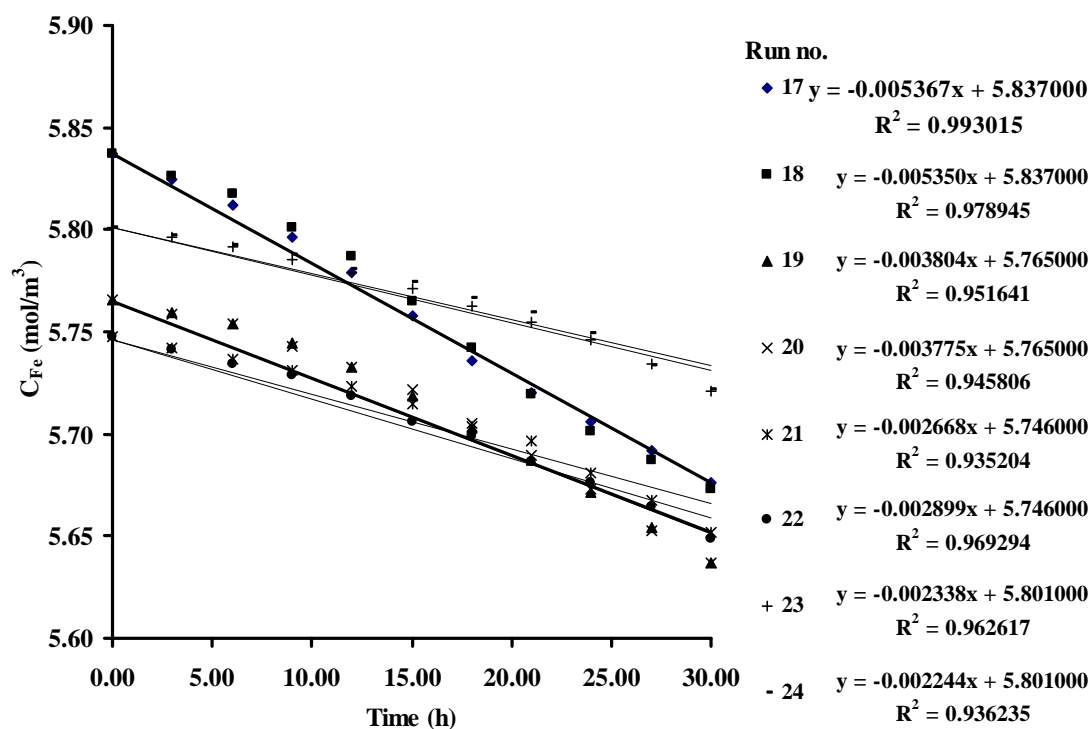


Figure A-3.3 Soluble Fe concentration-time of Run no.17-24: linear equations with  $R^2$  values

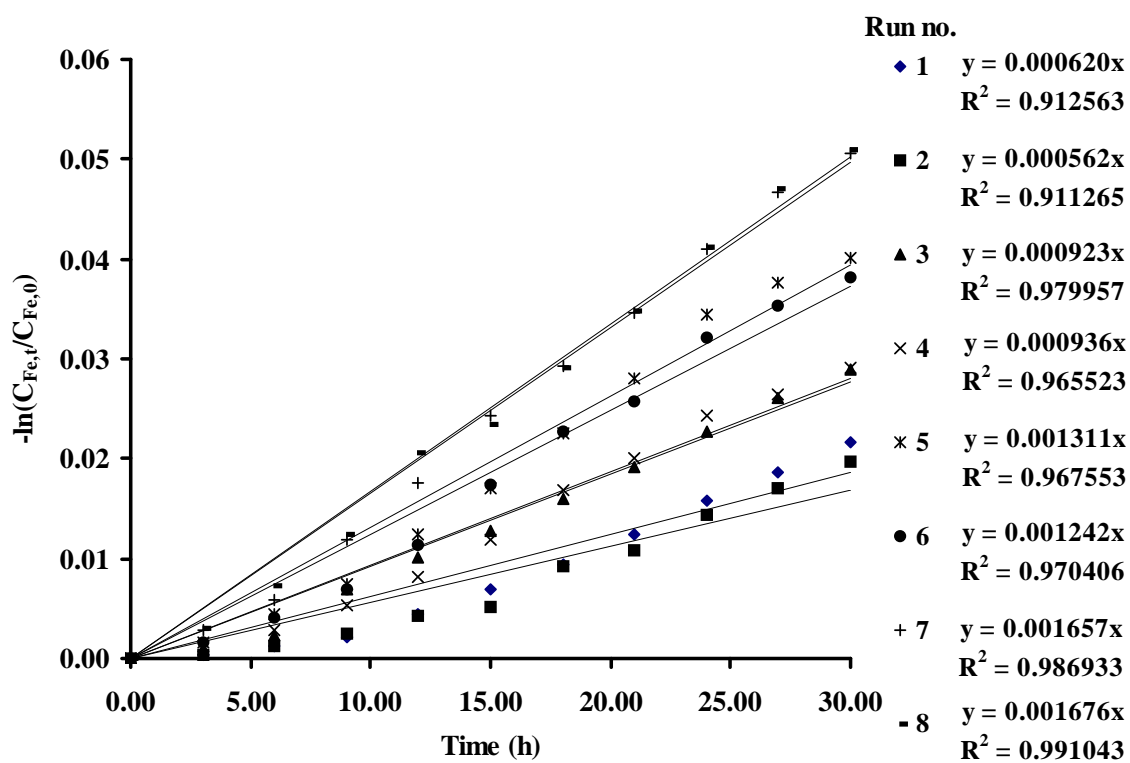


Figure A-3.4  $-\ln(C_{Fe,t}/C_{Fe,0})$ -time of Run no.1-8: linear equations with  $R^2$  values

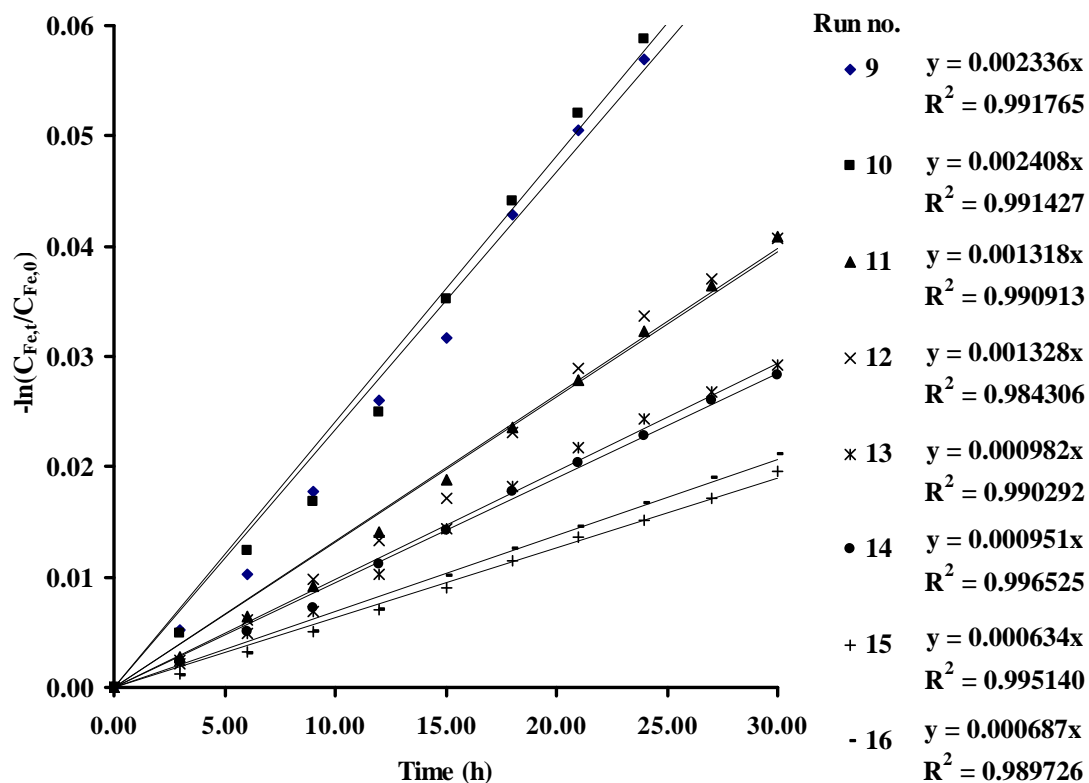


Figure A-3.5  $-\ln(C_{Fe,t}/C_{Fe,0})$ -time of Run no.9-16: linear equations with  $R^2$  values

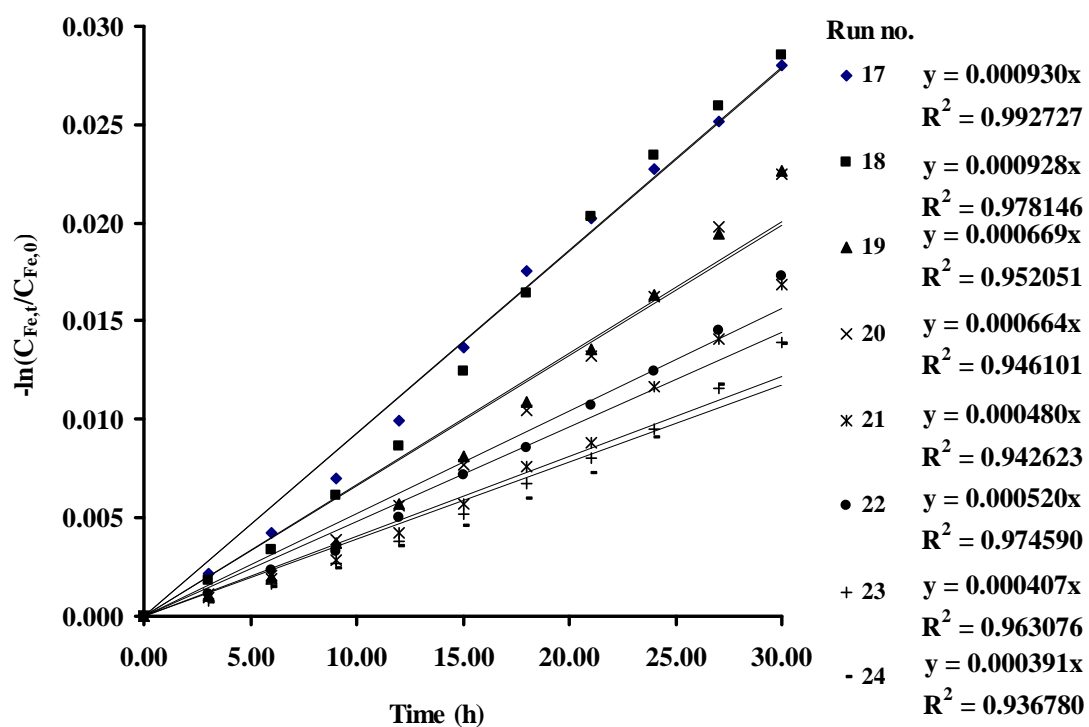


Figure A-3.6  $-\ln(C_{Fe,t}/C_{Fe,0})$ -time of Run no.17-24: linear equations with  $R^2$  values

**Table A-3.14**  $k_d$  values of each experimental run.

Run no.	$k_d \times 10^3 \text{ (h}^{-1}\text{)}$			
	Experimental	Predicted form Eq. (4.4)	Predicted form Eq. (4.5)	Predicted form Eq. (4.6)
1	0.62	0.55	-	0.57
2	0.56	0.55	-	0.56
3	0.92	0.90	-	0.91
4	0.94	0.87	-	0.88
5	1.31	1.25	-	1.26
6	1.24	1.29	-	1.30
7	1.66	1.71	-	1.71
8	1.68	1.56	-	1.57
9	2.34	2.31	-	2.31
10	2.41	2.32	-	2.32
11	1.32	1.48	-	1.49
12	1.33	1.46	-	1.47
13	0.98	0.95	-	0.97
14	0.95	0.94	-	0.95
15	0.63	0.68	-	0.69
16	0.69	0.70	-	0.70
17	0.93	-	0.92	0.88
18	0.93	-	0.92	0.91
19	0.67	-	0.69	0.66
20	0.66	-	0.69	0.65
21	0.48	-	0.51	0.54
22	0.57	-	0.51	0.52
23	0.41	-	0.40	0.38
24	0.39	-	0.40	0.42

**Table A-3.15**  $R_d$  values of each experimental run.

Run no.	$R_d$			
	Experimental	Predicted using $k_d$ in Eq. (4.4)	Predicted using $k_d$ in Eq. (4.5)	Predicted using $k_d$ in Eq. (4.6)
1	0.00356	0.00320	-	0.00329
2	0.00323	0.00316	-	0.00325
3	0.00528	0.00517	-	0.00524
4	0.00535	0.00504	-	0.00511
5	0.00746	0.00722	-	0.00728
6	0.00707	0.00745	-	0.00750
7	0.00939	0.00986	-	0.00989
8	0.00950	0.00901	-	0.00905
9	0.00493	0.00502	-	0.00501
10	0.00508	0.00504	-	0.00504
11	0.00511	0.00582	-	0.00585
12	0.00515	0.00575	-	0.00579
13	0.00556	0.00547	-	0.00554
14	0.00539	0.00538	-	0.00545
15	0.00556	0.00557	-	0.00562
16	0.00514	0.00569	-	0.00575
17	0.00537	-	0.00538	0.00512
18	0.00535	-	0.00538	0.00531
19	0.00380	-	0.00397	0.00381
20	0.00378	-	0.00397	0.00374
21	0.00267	-	0.00295	0.00312
22	0.00290	-	0.00295	0.00300
23	0.00234	-	0.00233	0.00221
24	0.00224	-	0.00233	0.00241

**Table A-3.16** Analysis of variance (ANOVA) for the regression model Equation (4.4)

$$k_d = 3.446 - 0.784C_{Fe} + 0.0452C_{Fe}^2 + 0.111Q_{H_2S}^2 \quad (4.4)$$

ANOVA						
<i>Source</i>	<i>SS</i>	<i>SS%</i>	<i>MS</i>	<i>F</i>	<i>F Signif</i>	<i>df</i>
<b>Regression</b>	4.719	98	1.573	221.50	9.06635E-11	3
<b>Residual</b>	0.08521	2	0.00710			12
<b>Total</b>	4.804	100				15

R = 0.991, R<sup>2</sup> = 0.982, R<sup>2</sup> adjusted = 0.978, R<sup>2</sup> for Prediction = 0.969, Standard Error = 0.084, Coefficient of Variation = 6.889

**Table A-3.17** The least square fit and model coefficients (significant of regression coefficients) for the regression model Equation (4.4)

<b>Model terms</b>	<b>Coefficients</b>	<b>P value</b>	<b>Std Error</b>	<b>-95%</b>	<b>95%</b>	<b>t Stat</b>	<b>VIF</b>
Intercept	3.446	2.76E-11	0.150	3.119	3.773	22.97	
$C_{Fe}$	-0.784	2.20E-08	0.0608	-0.916	-0.651	-12.87	21.78
$C_{Fe}^2$	0.04520	5.27E-06	0.0058	0.032	0.057	7.738	21.33
$Q_{H_2S}^2$	0.111	8.35E-09	0.0079	0.094	0.129	14.03	1.116

**Table A-3.18** Analysis of variance (ANOVA) for the regression model Equation (4.5)

$$k_d(C_{Cl}) = 0.921 - 0.00526C_{Cl} + 1.176 \times 10^{-5} C_{Cl}^2 \quad (4.5)$$

ANOVA						
<i>Source</i>	<i>SS</i>	<i>SS%</i>	<i>MS</i>	<i>F</i>	<i>F Signif</i>	<i>df</i>
<b>Regression</b>	0.309	98	0.155	143.34	3.84747E-05	2
<b>Residual</b>	0.00539	2	0.00108			5
<b>Total</b>	0.315	100				7

R = 0.991, R<sup>2</sup> = 0.983, R<sup>2</sup> adjusted = 0.976, R<sup>2</sup> for Prediction = 0.958, Standard Error = 0.033, Coefficient of Variation = 5.215

**Table A-3.19** The least square fit and model coefficients (significant of regression coefficients) for the regression model Equation (4.5)

Model terms	Coefficients	P value	Std Error	-95%	95%	t Stat	VIF
Intercept	0.921	1.43E-07	0.021	0.864	0.977	42.04	
$C_{Cl}$	-0.00526	9.12E-05	0.0004	-0.0064	-0.00408	-11.39	20.54
$C_{Cl}^2$	1.175E-05	0.0004	1.408E-06	8.13E-06	1.53E-05	8.346	20.54

**Table A-3.20** Analysis of variance (ANOVA) for the regression model Equation (4.6)

$$k_d(Q_{H_2S}, C_{Fe}, C_{Cl}) = 3.429 - 0.773C_{Fe} + 0.0443C_{Fe}^2 + 0.110Q_{H_2S}^2 - 0.00698C_{Cl} + 1.546 \times 10^{-5} C_{Cl}^2 \quad (4.6)$$

ANOVA						
Source	SS	SS%	MS	F	F Signif	df
Regression	6.900	99	1.380	256.49	4.514E-16	5
Residual	0.096	1	0.00538			18
Total	6.997	100				23

R = 0.993, R<sup>2</sup> = 0.986, R<sup>2</sup> adjusted = 0.982, R<sup>2</sup> for Prediction = 0.975, Standard Error = 0.073, Coefficient of Variation = 7.153

**Table A-3.21** The least square fit and model coefficients (significant of regression coefficients) for the regression model Equation (4.5)

Model terms	Coefficients	P value	Std Error	-95%	95%	t Stat	VIF
Intercept	3.429	6.63E-16	0.129	3.158	3.699	26.61	
$C_{Fe}$	-0.773	1.25E-11	0.0514	-0.881	-0.665	-15.02	20.95
$C_{Cl}$	-0.0069	2.10E-08	0.00073	-0.00853	-0.00543	-9.454	17.34
$C_{Cl}^2$	1.546E-05	7.67E-06	2.49E-06	1.021E-05	2.07E-05	6.189	17.01
$C_{Fe}^2$	0.0442	5.05E-08	0.00497	0.03384	0.05470	8.917	20.44
$Q_{H_2S}^2$	0.110	3.50E-12	0.00679	0.09583	0.124	16.21	1.116



**Table A-3.22** The comparison of Fe found in sulfur cake and degraded from solution after 30 h of reaction

$Q_{H_2S} \times 10^3$ (mol/h)	$C_{Fe,0}$ (mol/m <sup>3</sup> )	Sulfur cake (g)	Fe (mg)	
			In sulfur cake	Degraded from solution
1.08	5.78	0.805	3.22	5.33
2.73	5.78	2.251	7.88	9.68
3.20	5.78	2.675	10.38	12.17
1.81	2.17	1.535	4.30	6.26
1.94	3.94	1.693	4.06	6.56
2.13	5.73	1.922	4.42	6.69
2.40	8.16	2.106	6.74	7.32

## **APPENDIX B**

### **Analytical Methods**

#### **B-1 Determination of Hydrogen Sulfide Content in Biogas**

(refer by **State of California Air Resources Board** ([arbis.arb.ca.gov](http://arbis.arb.ca.gov)))

##### **B-1.1 Principle and applicability**

Hydrogen sulfide ( $\text{H}_2\text{S}$ ) is collected from a source in a series of midget impingers and absorbed in pH 3.0 Cadmium sulfate solution to form Cadmium sulfide ( $\text{CdS}$ ). The latter compound is then measured iodometrically. An impinger containing hydrogen peroxide ( $\text{H}_2\text{O}_2$ ) is included to remove  $\text{SO}_2$  as an interfering species.

This method is applicable for the determination of the  $\text{H}_2\text{S}$  content of in gas stream and Biogas from anaerobic wastewater treatment process.

##### **B-1.2 Interference**

Any compound that reduces iodine ( $\text{I}_2$ ) or oxidizes iodide ion will interfere in this procedure, provided it is collected in the Cadmium sulfate impingers. Sulfur dioxide in concentrations of up to  $2,600 \text{ mg/m}^3$  is eliminated by the  $\text{H}_2\text{O}_2$  solution. Thiols precipitate with  $\text{H}_2\text{S}$ . In the absence of  $\text{H}_2\text{S}$ , only co-traces of thiols are collected. When methane- and ethane-thiols at a total level of  $300 \text{ mg/m}^3$  are present in addition to  $\text{H}_2\text{S}$ , the results vary from 2 percent low at an  $\text{H}_2\text{S}$  concentration of  $400 \text{ mg/m}^3$  to 14 percent high at an  $\text{H}_2\text{S}$  concentration of  $100 \text{ mg/m}^3$ . Carbon oxysulfide at a concentration of 20 percent does not interfere. Certain carbonyl containing compounds react with iodine and produce recurring end points. However, acetaldehyde and acetone at concentrations of 1 and 3 percent, respectively, do not interfere.

### B-1.3 Apparatus

**B-1.3.3.1 Impingers.** Five midjet impingers, each with 25-mL capacity. The internal diameter of the impinger tip is 1 mm.

**B-1.3.3.2 Flow Meter.** Rotameter, to measure flow rates in the range from 0.5 to 2 L/min.

#### **B1.3.3.3 Gas sampling pump, SKC, Model 224-PCXR8**

### B-1.4 Reagents

Unless otherwise indicated, it is intended that all reagents conform to the specifications established by the Committee on Analytical Reagents of the American Chemical Society, where such specifications are available. Otherwise, use best available grade.

#### **B-1.4.1 Sampling**

**B-1.4.1.1 Cadmium sulfate, absorbing Solution.** Dissolve 41 g (0.05 mol) of  $\text{CdSO}_4$  and 15 mL of 0.1 M sulfuric acid in a 1-L volumetric flask that contains approximately 3/4 L of water. Dilute to volume with deionized, distilled water. Mix thoroughly. The pH should be  $3 \pm 0.1$ .

#### **B-1.4.2 Sample Recovery**

**B-1.4.2.1 Hydrochloric Acid (HCl) Solution, 3 M.** Add 240 mL of concentrated HCl (specific gravity 1.19) to 500 mL of water in a 1 L volumetric flask. Dilute to 1 L with water. Mix thoroughly.

**B-1.4.2.2 Iodine Solution, 0.1 N.** Dissolve 24 g of potassium iodide (KI) in 30 mL of water. Add 12.7 g of resublimed iodine ( $\text{I}_2$ ) to the KI solution. Shake the mixture until the  $\text{I}_2$  is completely dissolved. If possible, let the solution stand overnight in the dark. Slowly dilute the solution to 1 L with water, with swirling. Filter the solution if it is cloudy. Store solution in a brown glass reagent bottle.

**B-1.4.2.3 Standard  $\text{I}_2$  Solution, 0.01 N.** Pipette 100.0 mL of the 0.1 N iodine solution into a 1 L volumetric flask, and dilute to volume with water.

Standardize daily. This solution must be protected from light. Reagent bottles and flasks must be kept tightly stoppered.

**B-1.4.2.4 Standard Sodium Thiosulfate Solution, 0.1 N.**

Dissolve 24.8 g of or 15.8 g of anhydrous sodium thiosulfate ( $\text{Na}_2\text{S}_2\text{O}_3$ ) in 1 L of water, and add 0.01 g of anhydrous sodium carbonate ( $\text{Na}_2\text{CO}_3$ ) and 0.4 mL of chloroform ( $\text{CHCl}_3$ ) to stabilize. Mix thoroughly by shaking or by aerating with nitrogen for approximately 15 minutes, and store in a glass stoppered, reagent bottle.

**B-1.4.2.5 Standard Sodium Thiosulfate Solution, 0.01 N.**

Pipette 50.0 mL of the standard 0.1 N  $\text{Na}_2\text{S}_2\text{O}_3$  solution into a volumetric flask, and dilute to 500 mL with water.

**B-1.4.2.6 Starch Indicator Solution.** Suspend 10 g of soluble starch in 100 mL of water, and add 15 g of potassium hydroxide (KOH) pellets. Stir until dissolved, dilute with 900 mL of water, and let stand for 1 hour. Neutralize the alkali with concentrated HCl, using an indicator paper similar to Alkacid test ribbon, then add 2 mL of glacial acetic acid as a preservative.

**Note:** Test starch indicator solution for decomposition by titrating with 0.01 N  $\text{I}_2$  solution, 4 mL of starch solution in 200 mL of water that contains 1 g of KI. If more than 4 drops of the 0.01 N  $\text{I}_2$  solution are required to obtain the blue color, a fresh solution must be prepared.)

## **B-1.5 Procedure**

### **B-1.5.1 Sampling**

Connect sample line with pump and impinger containing  $\text{CdSO}_4$  and, then set rate of 1 L/min, open the pump and sample for 1 min. For sample recovery, cap the open ends, and remove the impinger train to a clean area that is away from sources of heat. The area should be well lighted, but not exposed to direct sunlight.

### **B-1.5.2 Sample Recovery**

**B-1.5.2.1** Pipette exactly 50 mL of 0.01 N  $\text{I}_2$  solution into a 125-mL Erlenmeyer flask. Add 10 mL of 3 M HCl to the solution. Quantitatively rinse all the  $\text{I}_2$  from the impingers, connectors, and the beaker into the iodine flask using water. Stopper the flask and shake briefly.

**B-1.5.2.2** Allow the flask to stand about 30 minutes in the dark for absorption of the  $\text{H}_2\text{S}$  into the  $\text{I}_2$ , then complete the titration analysis as in Section 6.3.

**B-1.5.2.3** Prepare a blank by adding 25 mL  $\text{CdSO}_4$  absorbing solution to flask. Pipette exactly 50 mL of 0.01 N  $\text{I}_2$  solution into a 125-mL Erlenmeyer flask. Add 10 mL of 3 M HCl. Follow the same impinger extracting and quantitative analysis procedures carried out in sample analysis. Stopper the flask, shake briefly, let stand 30 minutes in the dark, and titrate with the samples.

Note: The blank must be handled by exactly the same procedure as that used for the samples.

### **B-1.5.3 Analysis**

Note: Titration analyses should be conducted at the sample-cleanup area in order to prevent loss of  $\text{I}_2$  from the sample. Titration should never be made in direct sunlight.

**B-1.5.3.1** Using 0.01 N  $\text{Na}_2\text{S}_2\text{O}_3$  solution (or 0.01 N  $\text{C}_6\text{H}_5\text{AsO}$ , if applicable), rapidly titrate each sample in an iodine flask using gentle mixing, until solution is light yellow. Add 4 mL of starch indicator solution, and continue titrating slowly until the blue color just disappears. Record  $V_{\text{TT}}$ , the volume of  $\text{Na}_2\text{S}_2\text{O}_3$  solution used in mL.

**B-1.5.3.2** Titrate the blanks in the same manner as the samples. Run blanks each day until replicate values agree within 0.05 mL. Average the replicate titration values which agree within 0.05 mL.

## **B-1.6 CALIBRATION AND STANDARDS**

### **B-1.6.1 Standardizations**

**B-1.6.1.1** Standardize the 0.01 N  $\text{I}_2$  solution daily as follows: Pipette 25 mL of the  $\text{I}_2$  solution into a 125-mL Erlenmeyer flask. Add 2 mL of 3 M HCl. Titrate rapidly with standard 0.01 N  $\text{Na}_2\text{S}_2\text{O}_3$  solution or with 0.01 N  $\text{C}_6\text{H}_5\text{AsO}$  until the solution is light yellow, using gentle mixing. Add four drops of starch indicator solution, and continue titrating slowly until the blue color just disappears. Record  $V_{\text{T}}$ , the volume of  $\text{Na}_2\text{S}_2\text{O}_3$  solution used, or  $V_{\text{AS}}$ , the volume of  $\text{C}_6\text{H}_5\text{AsO}$

solution used, in mL. Repeat until replicate values agree within 0.05 mL. Average the replicate titration values which agree within 0.05 mL, and calculate the exact normality of the I<sub>2</sub> solution using Equation A-3. Repeat the standardization daily.

**B-1.6.1.2** Standardize the 0.1 N Na<sub>2</sub>S<sub>2</sub>O<sub>3</sub> solution as follows: Oven-dry potassium dichromate (K<sub>2</sub>Cr<sub>2</sub>O<sub>7</sub>) at 180 to 200° C (360 to 390° F). Weigh to the nearest milligram, 2 g of the dichromate. Transfer the dichromate to a 500-mL volumetric flask, dissolve in water and dilute to exactly 500 mL. In a 500 mL iodine flask, dissolve approximately 3 g of KI in 45 mL of water, then add 10 mL of 3 M HCl solution. Pipette 50 mL of the dichromate solution into this mixture. Gently swirl the solution once, and allow it to stand in the dark for 5 minutes. Dilute the solution with 100 to 200 mL of water, washing down the sides of the flask with part of the water. Titrate with 0.1 N Na<sub>2</sub>S<sub>2</sub>O<sub>3</sub> until the solution is light yellow. Add 4 mL of starch indicator and continue titrating slowly to a green end point. Record V<sub>S</sub>, the volume of Na<sub>2</sub>S<sub>2</sub>O<sub>3</sub> solution used, in mL. Repeat until replicate analyses agree within 0.05 mL. Calculate the normality using Equation A-1. Repeat the standardization each week, or after each test series, whichever time is shorter.

## B-1.7 CALCULATIONS

Carry out calculations retaining at least one extra decimal figure beyond that of the acquired data. Round off results only after the final calculation.

### B-1.7.1 Normality of the Standard (0.1 N) Thiosulfate Solution

$$N_s = \frac{2.039 W}{V_s} \quad (\text{B-1})$$

Where:

W = Weight of K<sub>2</sub>Cr<sub>2</sub>O<sub>7</sub> used, g.

V<sub>S</sub> = Volume of Na<sub>2</sub>S<sub>2</sub>O<sub>3</sub> solution used, mL.

N<sub>S</sub> = Normality of standard Na<sub>2</sub>S<sub>2</sub>O<sub>3</sub> solution, g-eq/L.

2.039 = Conversion factor = (6 eq I<sub>2</sub>/mole K<sub>2</sub>Cr<sub>2</sub>O<sub>7</sub>)(1,000 mL/L) divided by [(294.2 g K<sub>2</sub>Cr<sub>2</sub>O<sub>7</sub>/mole)(10 aliquot factor)]

### B-1.7.2 Normality of Standard Iodine Solution

$$N_I = \frac{N_T V_T}{V_I} \quad (\text{B-2})$$

Where:

N<sub>I</sub> = Normality of standard I<sub>2</sub> solution, g-eq/LmL.

V<sub>I</sub> = Volume of standard I<sub>2</sub> solution used, mL.

N<sub>T</sub> = Normality of standard (0.01 N) Na<sub>2</sub>S<sub>2</sub>O<sub>3</sub> solution; assumed to be 0.1 N<sub>S</sub>, g-eq/L.

V<sub>T</sub> = Volume of Na<sub>2</sub>S<sub>2</sub>O<sub>3</sub> solution used, mL.

**B-1.7.3 Concentration of H<sub>2</sub>S.** Calculate the concentration of H<sub>2</sub>S in the gas stream at standard conditions using the following equation:

$$C_{\text{H}_2\text{S}} = 17.04 \times 10^3 \frac{(V_{IT} N_I - V_{TT} N_T)_{\text{sample}} - (V_{IT} N_I - V_{TT} N_T)_{\text{blank}}}{V_{m(\text{std})}} \quad (\text{B-3})$$

Where:

C<sub>H<sub>2</sub>S</sub> = Concentration of H<sub>2</sub>S at standard conditions, mg/dscm.

17.04 x 10<sup>3</sup> = Conversion factor = (34.07 g/mole H<sub>2</sub>S)(1,000 L/m<sup>3</sup>)(1,000 mg/g) divided by [(1,000 mL/L)(2H<sub>2</sub>S eq/mole)]

V<sub>IT</sub> = Volume of standard I<sub>2</sub> solution, 50 mL.

N<sub>I</sub> = Normality of standard I<sub>2</sub> solution, g-eq/L.

V<sub>TT</sub> = Volume of standard (0.01 N) Na<sub>2</sub>S<sub>2</sub>O<sub>3</sub> solution, mL.

N<sub>T</sub> = Normality of standard Na<sub>2</sub>S<sub>2</sub>O<sub>3</sub> solution, g-eq/L.

V<sub>m(std)</sub> = Standard dry gas volume, L.

Note: If C<sub>6</sub>H<sub>5</sub>AsO is used instead of Na<sub>2</sub>S<sub>2</sub>O<sub>3</sub>, replace N<sub>T</sub> and V<sub>TT</sub> in Equation 11-5 with N<sub>A</sub> and V<sub>AT</sub>, respectively.

### **B-1.8 STABILITY**

The absorbing solution is stable for at least 1 month. Sample recovery and analysis should begin within 1 hour of sampling to minimize oxidation of the acidified CdS.

### **BIBLIOGRAPHY**

1. EPA Method 11, Determination of Hydrogen Sulfide Content of Fuel Gas Streams in Petroleum Refineries, CFR40, Part 60, Appendix A
2. ARB Method 6, Determination of Sulfur Dioxide Emissions from Stationary Sources

### **B-2 Determination of iron concentration**

For the determination of iron different spectrochemical methods are used. However, flame atomic absorption spectrometry (FAAS) is one of the most extensively used techniques for determining various elements with significant precision and accuracy. However, when the concentration of Fe(II) or Fe(III) required, the colorimetric method is a better choice. In the colorimetric method, several steps are required in preparing solutions for reading in a spectrophotometer. All glassware, chemicals, and water used should be iron free to prevent contamination to the test solutions. Fortunately, the red color complex formed is stable for a number of hours. The procedure is also relatively much cheaper, requiring only a low-cost spectrophotometer operating in the visible range. In the hands of a careful worker, the method can perform satisfactorily. The FAAS method, on the other hand, requires the purchase of a high cost spectrophotometer which is also rather expensive to operate and maintain. It is however, a relatively simpler procedure.

Both of two methods mentioned above were used to determine iron concentration in the experiments. Phenanthroline method (colorimetric method) was used in Chapter 2 and 3,4 while FAAS method was used in Chapter 4 because a lot of samples needed to be analyzed. The procedures were described as the following.



## **B-2.1 Iron determination by Phenanthroline method (APHA, 1985).**

### **B-2.1.1 General discussion**

1. Principle: Iron is brought into solution, reduced to the ferrous state by boiling with acid and hydroxylamine, and treated with 1,10-phenanthroline at pH 3.2 to 3.3. Three molecules of phenanthroline chelate each atom of ferrous iron to form an orange-red complex. The colored solution obeys Beer's law; its intensity is independent of pH from 3 to 9. At pH between 2.9 and 3.5 insures rapid color development in the presence of an excess of phenanthroline. Color standards are stable for at least 6 months.

2. Interference: Among the interfering substances are strong oxidizing agents, cyanide, nitrite, and phosphates (polyphosphates more so than orthophosphate), chromium, zinc in concentrations exceeding 10 times that of iron, cobalt and copper in excess of 5 mg/L, and nickel in excess of 2 mg/L. Bismuth, cadmium, mercury, molybdate, and silver precipitate phenanthroline. The initial boiling with acid converts polyphosphates to orthophosphate and remove cyanide and nitrite that otherwise would interfere. Adding excess hydroxylamine eliminates errors caused by excessive concentrations of interfering metal ions, use a larger excess of phenanthroline to replace that complexed by the interfering metals. Where excessive concentration of interfering metal ions are present, the extraction method may be used. If noticeable amounts of color or organic matter are present, it may be necessary to evaporate the sample, gently ash the residue, and redissolve in acid. The ashing may be carried out in silica, porcelain, or platinum crucibles that have been boiled for several hours in 1 + 1 HCl. The presence of excessive amounts of organic matter may necessitate digestion before use of the extraction procedure.

3. Minimum detectable concentration: Dissolve or total concentrations of iron as low as 10 µg/L can be determined with a spectrophotometer using cells with a 5 cm or longer light path. Carry a blank through the entire procedure to allow for correction.

### B-2.1.2 Apparatus

1. Colorimetric equipment: HP 8453 UV-VIS Spectrophotometer.
2. Acid-washed glassware: Wash all glassware with conc hydrochloric acid (HCl) and rinse with distilled water before use to remove deposits of iron oxide.

### B-2.13 Reagents

Use reagents low in iron. Use iron free distilled water in preparing standard and reagents solution. Store reagents in glass stoppered bottles. The HCl and ammonium acetate solution were stable indefinitely if tightly stoppered. The hydroxylamine, phenanthroline, and stock iron solutions are stable for several months. The standard iron solutions are not stable; prepare daily as needed by diluting the stock solution. Visual standards in nessler tubes are stable for several months if seal and protected from light.

1. Hydrochloric acid, HCl, containing less than 0.00005% iron.
2. Hydroxylamine solution: Dissolve 10 g  $\text{NH}_2\text{OH}\cdot\text{HCl}$  in 100 mL water.
3. Ammonium acetate buffer solution: Dissolve 250 g  $\text{NH}_4\text{C}_2\text{H}_3\text{O}_2$  in 150 mL water. Add 700 mL conc (glacial) acetic acid. Because even a good grade of  $\text{NH}_4\text{C}_2\text{H}_3\text{O}_2$  contains a significant amount of iron, prepare new reference standards with each buffer preparation.
4. Sodium acetate solution: Dissolve 200 g  $\text{NaC}_2\text{H}_3\text{O}_2\cdot 3\text{H}_2\text{O}$  in 800 mL water.
5. Phenanthroline solution: Dissolve 100 mg 1,10-phenanthroline monohydrate,  $\text{C}_{12}\text{H}_8\text{N}_2\cdot\text{H}_2\text{O}$  in 100 mL water by stirring and heating to 80 °C. Do not boil. Discard the solution if it darkens. Heating is unnecessary if 2 drops conc HCl are added to the water. (One milliliter of this reagent is sufficient for no more than 100 µg Fe)
6. Stock iron solution: Slowly add 20 mL conc  $\text{H}_2\text{SO}_4$  to 50 mL water and dissolve 1.404 g ferrous ammonium sulfate ( $\text{Fe}(\text{NH}_4)_2(\text{SO}_4)_2\cdot 6\text{H}_2\text{O}$ ). Add 0.1 N

potassium permanganate ( $\text{KMnO}_4$ ) dropwise until a faint pink color persists. Dilute to 1000 mL with water and mix; 1.00 mL = 200  $\mu\text{g}$  Fe

7. Standard iron solution: Prepare daily for use.

7.1 Pipet 50.00 mL stock solution into a 1000 mL volumetric flask and dilute to mark with water; 1.00 mL = 10.00  $\mu\text{g}$  Fe.

7.2 Pipet 5.00 mL stock solution into a 1000 mL volumetric flask and dilute to mark with water; 1.00 mL = 1.00  $\mu\text{g}$  Fe.

#### **B-2.1.4 Procedure**

1. Total iron: Mix sample thoroughly and measure 50.0 mL into a 125 mL Erlenmeyer flask. If this sample volume contains more than 200  $\mu\text{g}$  iron use a smaller accurately measured portion and dilute to 50.0 mL. Add 2 mL conc HCl and 1 mL  $\text{NH}_2\text{OH}\cdot\text{HCl}$  solution. Add a few glass beads and heat to boiling. To insure dissolution of all the iron, continue boiling until volume is reduced to 15 to 20 mL. (If the sample is ashed, take up residue in 2 mL conc HCl and 5 mL water.) Cool to room temperature and transfer to a 50 or 100 mL volumetric flask or nessler tube. Add 10 mL  $\text{NH}_4\text{C}_2\text{H}_3\text{O}_2$  buffer solution and 4 mL phenanthroline solution, and dilute to mark with water. Mix thoroughly and allow at least 10 to 15 min for maximum color development.

2. Ferrous iron. Determine ferrous iron at sampling site because of the possibility of change in the ferrous-ferric ratio with time in acid solution. To determine ferrous iron only, acidify a separate sample with 2 mL conc HCl/100 mL sample at time of collection. Fill bottle directly from sampling source and stopper. Immediately withdraw a 50 mL portion of acidified sample and 20 mL phenanthroline solution and 10 mL  $\text{NH}_4\text{C}_2\text{H}_3\text{O}_2$  solution with vigorous stirring. Dilute to 100 mL and measure color intensity within 5 to 10 min. Do not expose to sunlight. (Color development is rapid in the presence of excess phenanthroline. The phenanthroline volume given is suitable for less than 50  $\mu\text{g}$  total iron; if larger amounts are present, use a correspondingly larger volume of phenanthroline or a more concentrated reagent. Excess phenanthroline is required because of the kinetics of the complexing

process.). Calculate ferric iron by subtracting ferrous from total iron. The standard curve.

3. Color measurement. Prepare a series of standard accuracy (0.600 – 4.000 mg/L) or unknown samples. Set the wavelength at 510 nm. Read standard (or unknown samples) against distilled water set at zero absorbance. Each calibration point and samples was repeated three times to ensure reproducibility. Absorbance at 510 nm of all samples obtained from this technique were determined by extracted from the calibration curve. The calibration curve was plotted as shown in Figure B-2.1.

**Table B-2.1** Results for performing calibration curve in phenanthroline method

<b>Fe concentration</b>		<b>Absorbance</b>		
<b>mg/L</b>	<b>mmol/m<sup>3</sup></b>	<b>STD1</b>	<b>STD2</b>	<b>average</b>
0.60	10.74	0.117	0.117	0.117
1.00	17.91	0.190	0.198	0.194
1.70	30.44	0.334	0.333	0.334
2.00	35.81	0.401	0.397	0.399
2.60	46.55	0.511	0.511	0.511
3.40	60.88	0.650	0.654	0.652
4.00	71.62	0.777	0.780	0.779

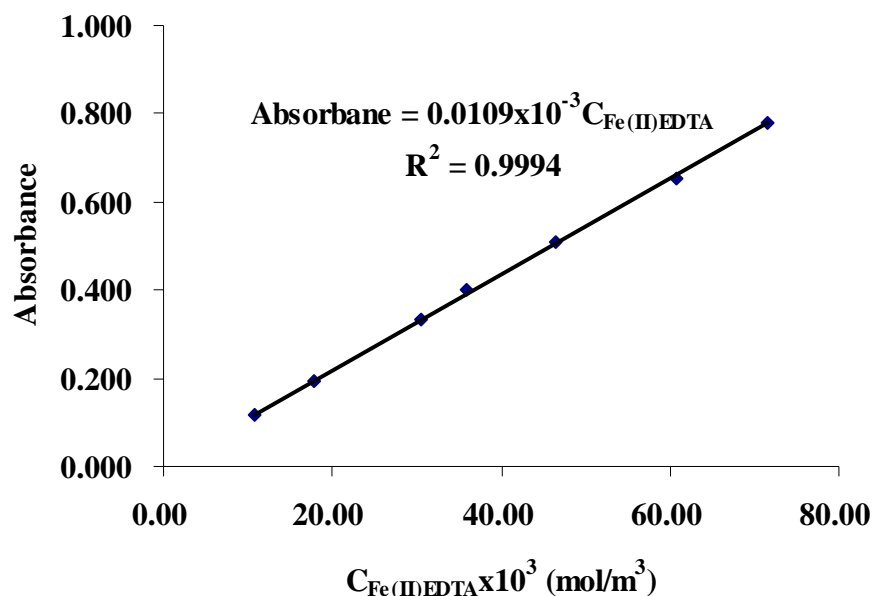


**Figure B-2.1** Calibration curve for Fe determination by phenanthroline method at 510 nm

## B-2.2 Iron determination by atomic absorption spectrometry

### B-2.2.1 Principle common to the method

The principle behind this method of elemental analysis depends on measurements made on an analysis that is transformed into free atom. For this technique, the sample is heated in the instrument to a temperature of between 2000 and 3000 degrees to break chemical bonds, liberate the elements present and transform them into a gaseous atomic state. Thus, the total concentration of the element is measured without distinguishing the chemical structure present in the cold sample. The thermal device used to elevate the temperature consists of a burner fed with a gaseous combustible or, alternatively, in atomic absorption, by a small electric oven that contains a graphite rod resistor heated by the Joule effect. In atomic absorption spectroscopy, the optical absorption of atom in their ground state is measured when the sample is irradiated with the appropriate source. Measurement of

the transmitted radiation is carried out at a wavelength specific for absorption of each element analyzed (Rouessac and Rouessac, 2000).

### **B-2.2.2 Interferences**

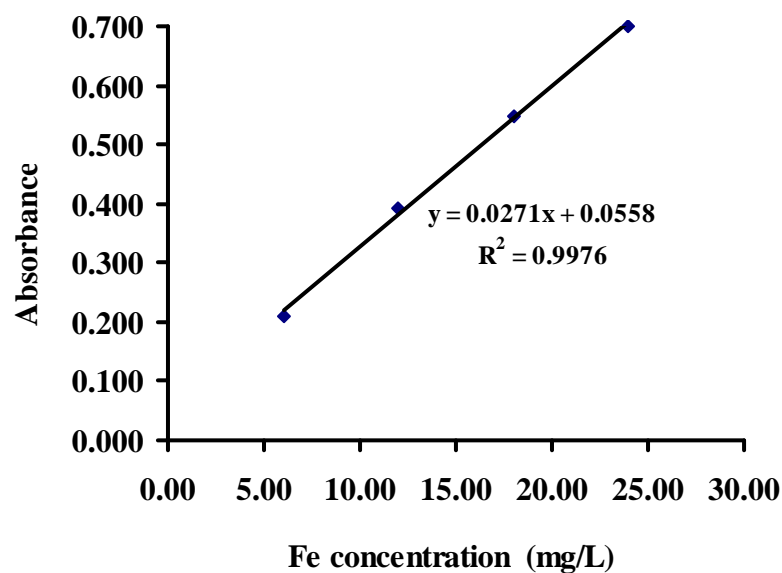
When iron is determined in the presence of cobalt, copper and nickel, a reduction in sensitivity is observed. These interferences are strongly dependent on flame conditions, and can be controlled by using a very lean (hot) flame. Silicon depresses the iron signal, and can be overcome by the addition of 0.2% calcium chloride. Many interferences can be reduced or eliminated in a nitrous oxide-acetylene flame, but sensitivity will be reduced.

### **B-2.2.3 Procedure**

Perkin Elmer Model AAnalyst 100 flame atomic absorption spectrometer equipped with hollow cathode lamps was used for the analyses. The instrumental parameters were adjusted according to the manufacturer's recommendations. An Fe hollow cathode lamp operating at 248.3 nm was used as the radiation source with slit width of 0.70 nm. The flame composition was: air-acetylene, the acetylene flow is about 4 L/min. 1 mg/mL Ferric chloride solution for atomic absorption spectrophotometry from Farmitalia Carlo Erba was used as standard. The iron standard solution was diluted by 2% HNO<sub>3</sub> to the range of 6-24 mg/L to working standard solution of iron (This is the same method for preparing the samples). Each standard solution was run in triplicate. A calibration curve for determination of iron by AAS was established by plot the standard concentrations versus their average absorption. The calibration curve for iron determination was shown in Figure B-2.2.

**Table B-2.2** Results for Fe calibration curve using atomic absorption spectrometry

Fe STD concentration (mg/L)	Absorbance		
	STD1	STD2	Average
6.00	0.208	0.209	0.209
12.00	0.389	0.398	0.394
18.00	0.541	0.553	0.547
24.00	0.698	0.700	0.699

**Figure B-2.2** Calibration curve for iron determination by using atomic absorption spectrometry

Not only Fe species contain in the sample solution but also the other. In order to know whether the matrix would interfere with the measurement of dissolved Fe by FAAS technique, the slope of standard calibration curve was compared to a standard addition one. The results show no interference from the matrix of sample before and after reaction for Fe determination.

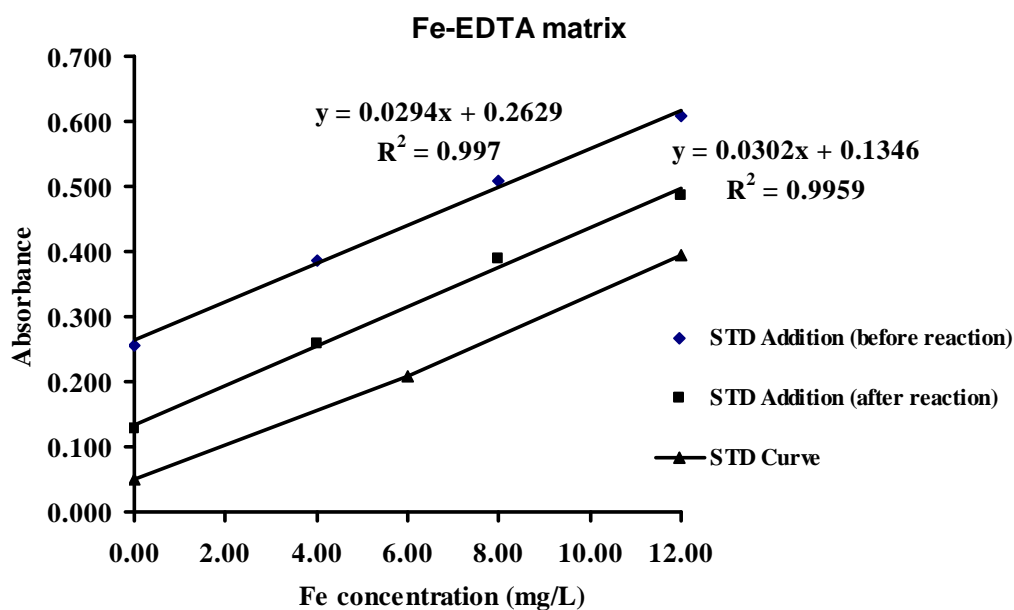


**Figure B-2.3** Comparison Fe standard calibration curve and standard addition curve method of Fe-EDTA sample before and after reaction

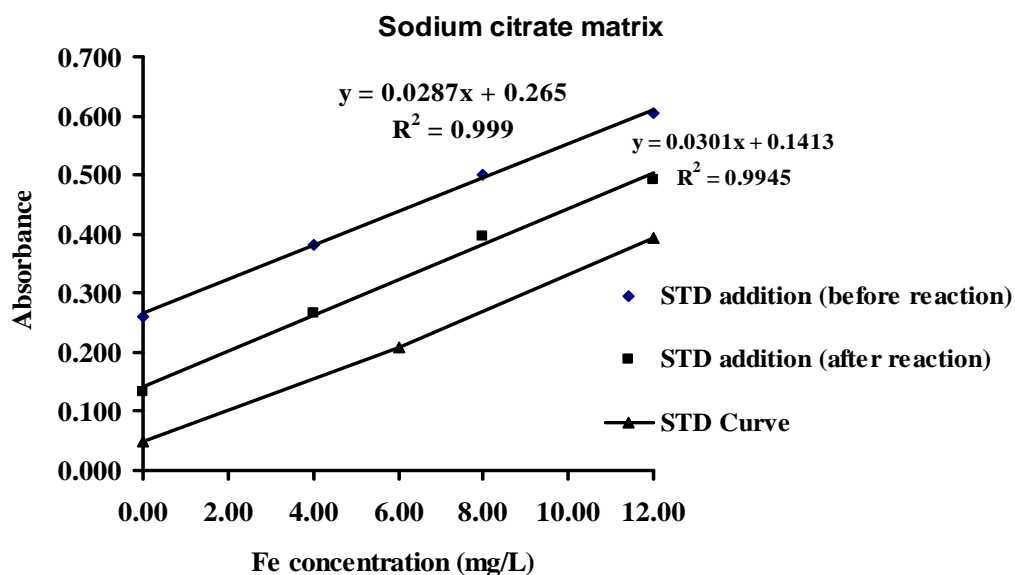


**Figure B-2.4** Comparison Fe standard calibration curve and standard addition curve method of Fe-EDTA+sodium citrate sample before and after reaction



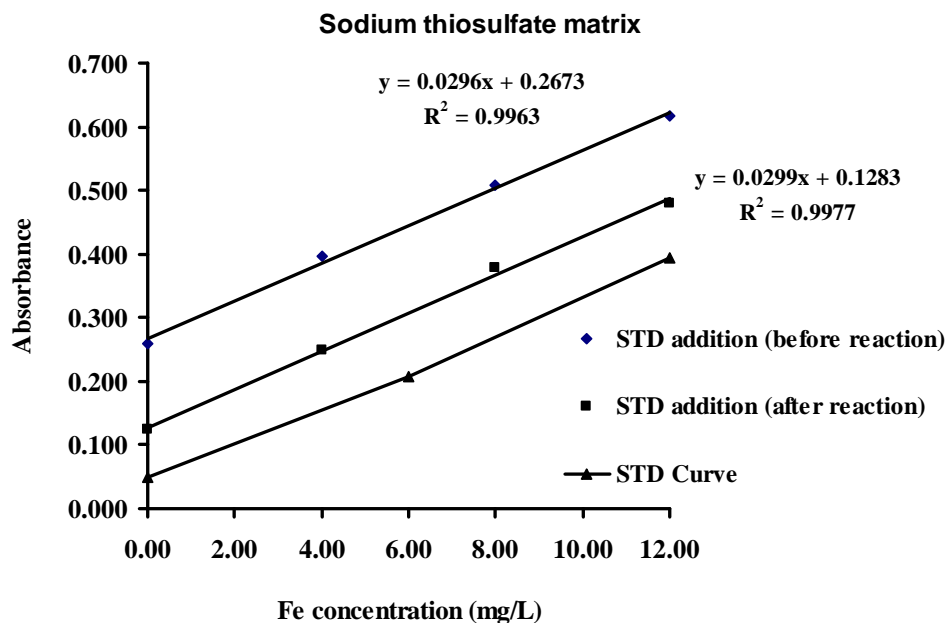


**Figure B-2.5** Comparison Fe standard calibration curve and standard addition curve method of Fe-EDTA+sodium thiosulfate sample before and after reaction

Moreover, in comparison there was generally good agreement in the results obtained by phenanthroline method and FAAS method as can be seen from Table B-2.3.

**Table B-2.3** Iron concentration in samples as determined by phenanthroline method and atomic absorption spectrophotometric method

Sample	Fe concentration (mg/L)	
	Phenanthroline method	AAS
A	5.30±0.05	5.42±0.03
B	10.30±0.05	10.56±0.11
C	15.71±0.05	15.54±0.11
D	20.11±0.11	20.08±0.03
E	25.88±0.02	25.78±0.06

These results are consistent with the determination of iron in natural and mineral waters by using both two methods (Tautkus *et al.*, 2004), and also support the result of comparative study of this two method to Determine iron in foods (Siang *et al.*, 1989)

### **B-3 Determination of CH<sub>4</sub> and CO<sub>2</sub> in biogas by Gas chromatography**

(From Scientific Equipment Center, Prince of Songkla University)

**Instrument:** HP 6890N Gas Chromatograph with Thermal Conductivity Detector

**Test Condition:**

**Inlet temperature:** 100 °C

**Oven temperature:** 40 °C, hold for 3 min,  
Ramp to 120 °C at 3°C/min, hold 120 for 3 min

**Detector temperature:** 200 °C

**Column:** ShinCarbon ST 100/120 micropacked column, length 2 m., 1.0 mm I.D

### **B-4 Determination of carbon, hydrogen, nitrogen and sulfur elements in the sulfur cake** (From Scientific Equipment Center, Prince of Songkla University)

**Instrument:** CE Instrument Flash 1112 Series EA CHNS-O Analyzer

**Technique:** Dynamic Flash Combustion

**Test Condition:**

**Furnace temperature:** 900 °C

**Oven temperature:** 65 °C

**Oxygen flow:** 250 mL/min

**Carrier flow:** 130 mL/min

**Reference flow:** 100 mL/min

## APPENDIX C

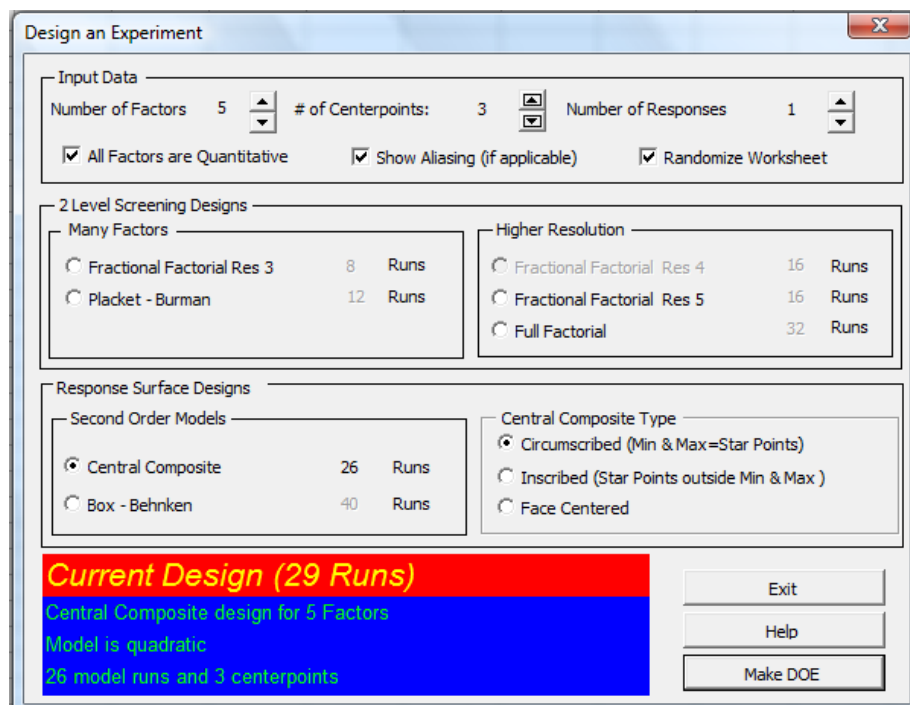
### Essential Experimental Design and Essential Regression

#### C-1 Creating a simple experimental design and analyzing it with Essential Experimental Design (EED) software

The procedure to design the experimental set for the study of the effect of process variables such as scrubbing liquid flow rate ( $L$ ), initial Fe(III)EDTA concentration ( $[Fe]$ ), gas flow rate ( $G$ ), inlet  $H_2S$  concentration ( $[H_2S]_{in}$ ), and height of packed bed ( $H$ ) on  $H_2S$  removal efficiency ( $RE$ ) by using central composite design in Essential Experimental Design (EED) software was described as following,

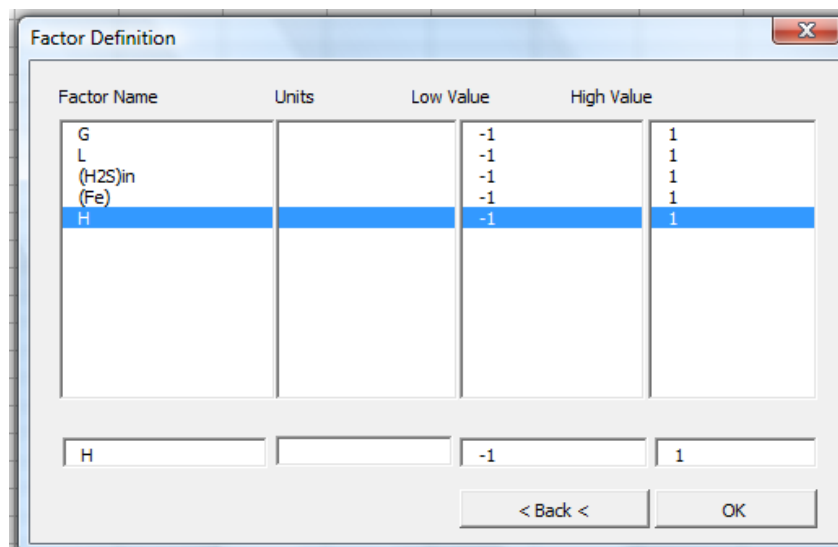
C-1.1 In Excel, assume EED is loaded and the **DOE** menu is visible. First, select the **Design An Experiment** option in the **DOE** menu. This brings up the Design an Experiment Dialog.

C-1.2 Create a circumscribed **central composite design** (CCD) with 5 factors and 3 center points to assess curvature and experimental error. The dialog look like this the below window:



C-1.3 In the colored section at the bottom, the dialog shows that our design 29 runs or experiments (including the center points), and that the underlying model has quadratic terms.

C-1.4 Press the “Make DOE” button. EED creates the “Aliasing” worksheets giving information how certain effects are aliased with others, and the Factor Definition Dialog will be displayed:



C-1.5 Here, you can set the lows and highs for the design factors. For our purposes, simply EED will create the “Experiments” worksheet and the following confirmation message will appear. Simply press “OK” to continue

C-1.6 Finally, in the “Experiments” worksheet, the table of designed experiments and the underlying model are created.

## C-2 Performing a Regression Analysis using the experimental results

After all experiment was done, the experimental data were analyzed using multiple regression menu from Essential Experimental Design (EED) software. The procedure was described as following,

C-2.1 Load experimental result table to the worksheet. The regressor variables  $H$ ,  $L$ ,  $[Fe]$ ,  $G$ ,  $[H_2S]_{in}$  and the response,  $RE$ , are arranged in columns, the observations are arranged in rows.

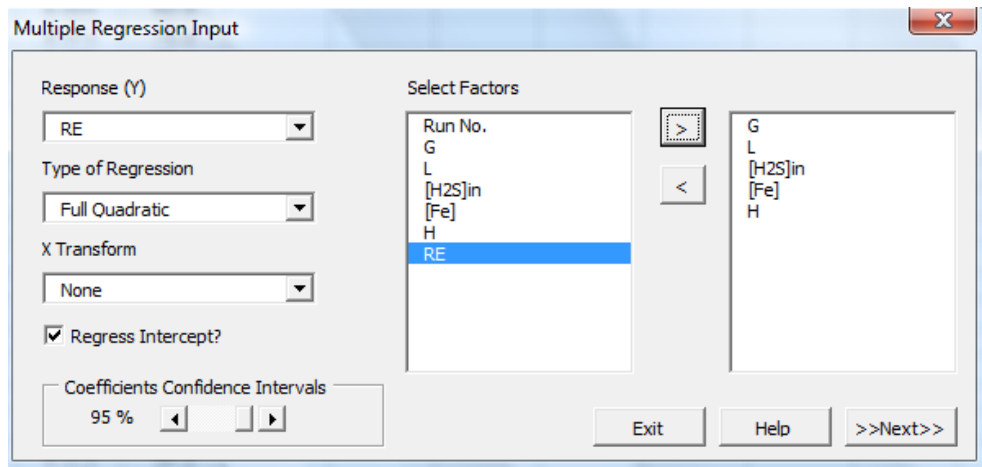
C-2.2 In the **Regress** menu, select **Multiple Regression**. This will activate the **Multiple Regression Input Dialog**.

C-2.3 Select the “*RE*” variable as the response

C-2.4 To select factors or input variables, add *H*, *L*, *[Fe]*, *G* and *[H<sub>2</sub>S]<sub>in</sub>* from the list in the left window to the right window by using the “>” button between the windows.

C-2.5 Go to the “Type of Regression” drop-down box and select “Full Quadratic” from the list.

C-2.6 Do not change the remaining options. The dialog box should now look like this



C-2.7 Click “>>Next>>”. This opens the “Multiple Regression” Main Dialog.

C-2.8 In the upper left quadrant of the “Multiple Regression” Main Dialog you’ll find the “Select Term” window with a list of all possible terms in the model based on the “Full quadratic” model selected in the previous dialog: linear, squared, and interaction terms. Note that Essential Regression creates this list automatically.

C-2.9 Select “>>” button. The terms currently in the model from the “Select Term” window are listed in the “Current Model” Window. This creates a linear model with all terms. To perform the regression, click the “Regress” button to the right of the “Current Model” window. This executes the regression analysis and the dialog should now look like this:

**Multiple Regression**

Input: Select Term (20 Total) | Current Model (20 Terms)

AutoRegress: AutoFit | Fit All

Output: Summary | ANOVA - 39 Total Data Points

Term	Coefficient	Std Error	t Statistic	Significance	VIF
Constant	194.21	38.28	5.074	7.920e-05	81.58900
G	-513.79	237.68	-2.162	0.04436	108.4838
L	-13.36	54.81	-0.244	0.810	136.5230
(H2S)in	-140.48	257.64	-0.545	0.592	86.31424
(Fe)	-308.23	109.33	-2.819	0.01136	104.7803
H	-443.36	119.71	-3.703	0.00163	36.16829
G*G	1633.7	777.80	2.100	0.05005	39.94134
G*L	-29.51	231.27	-0.128	0.900	48.56474
G*(H2S)in	-2463.6	1396.8	-1.764	0.09474	

Summary:

R2	0.935
R2 adjusted	0.864
Standard Error	4.472
PRESS	3226.9
R2 Prediction	0.421
DurbinWatson d	1.351
Autocorrelation	0.197
Collinearity	3.104e-23
CV	6.346
Precision Index	106.75

ANOVA:

Source	SS	SS%	MS	F	F Signif	df
Regression	5210.307	94	260.5153	13.02370	5.592e-07	20
Residual	360.0570	6	20.00317			18
LOF Error	359.5570	6 (100)	21.15041	42.30082	0.120386	17
Pure Error	0.500000	0 (0)	0.500000			1
Total	5570.364	100				38

Regression Equation:

$$RE = b_0 + b_1G + b_2L + b_3(H2S)in + b_4(Fe) + b_5H + b_6G*G + b_7G*L + b_8G*(H2S)in + b_9G*(Fe) + b_{10}G*H + b_{11}L*L + b_{12}L*(H2S)in + b_{13}L*(Fe) + b_{14}L*H + b_{15}(H2S)in*(H2S)in + b_{16}(H2S)in*(Fe) + b_{17}(H2S)in*H + b_{18}(Fe)*(Fe) + b_{19}(Fe)*H + b_{20}H*H$$

C-2.10 The “Multiple Regression” Main Dialog displays most of the results needed to evaluate a regression model instantly. In the “Output” area, the “Summary”, “ANOVA”, and regression coefficients or “Term” window show the parameters needed to assess the quality of the selected model. For example, you can see that the coefficient of determination  $R^2$  for the linear model is .935, the adjusted  $R^2$  is .864, and the so-called  $R^2$  for prediction, estimating the prediction accuracy of the model, is .421. In the ANOVA table, the F-value is low (13.02), and the F-significance is rather high (5.59e-07), indicating non significant regression model.

C-2.11 Apparently, our model contains “unnecessary” terms. How can we find out fast what is the “best” model among the possible combinations of linear, quadratic, and interaction terms? In Essential Regression, we have the possibility to perform **forward and backward stepwise regression** based on a threshold significance which can be adjusted by the user.

Multiple Regression

Input  
Select Term (20 Total)

Current Model (7 Terms)

Regress

AutoRegress  
AutoFit Fit All

All Transforms  
>Forward> >>

Crit Signif .05

<<Back Elimination<<

Crit Signif .05

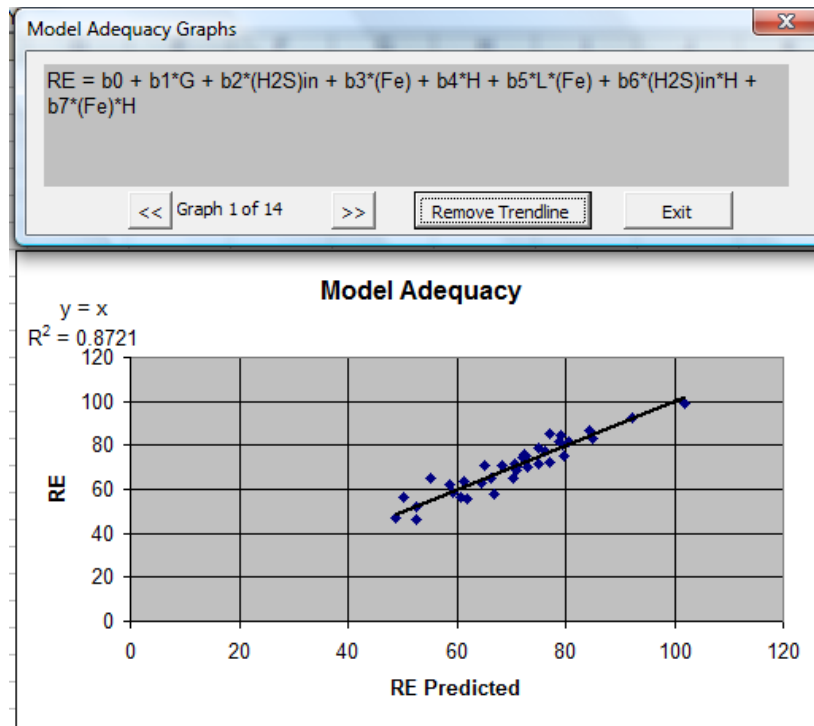
Output  
Summary Previous ANOVA - 39 Total Data Points

	Previous	Source	SS	SS%	MS	F	F Signif	df	
R2	0.872	Regression	4857.808	87	693.9726	30.19155	3.874e-12	7	<Back <
R2 adjusted	0.843	Residual	712.5553	13	22.98566			31	Help
Standard Error	4.794	LOF Error	712.0553	13 (100)	23.73518	47.47036	0.114429	30	Print
PRESS	1149.8	Pure Error	0.500000	0 (0)	0.500000			1	Exit
R2 Prediction	0.794	Total	5570.364	100				38	
DurbinWatson d	1.751	RE = b0 + b1*G + b2*(H2S)in + b3*(Fe) + b4*H + b5*L*(Fe) + b6*(H2S)in*H + b7*(Fe)*H							
Autocorrelation	0.07612								
Collinearity	0.000309								
CV	6.802								
Precision Index	165.63								

Term	Coefficient	Std Error	t Statistic	Significance	VIF
Constant	134.98	16.04	8.413	1.675e-09	
G	-285.12	28.50	-10.00	3.176e-11	1.020963
(H2S)in	-344.32	119.56	-2.880	0.00715	25.58369
(Fe)	-231.24	67.74	-3.413	0.00181	28.83939
H	-132.69	50.28	-2.639	0.01290	16.08828
L*(Fe)	165.98	33.15	5.006	2.109e-05	2.729301
(H2S)in*H	801.02	375.37	2.134	0.04087	33.87580
(Fe)*H	762.84	214.25	3.560	0.00122	34.44818

C-2.12 The selected model contains the terms  $G$ ,  $[H_2S]$ ,  $[Fe]$ ,  $H$ ,  $L[Fe]$ ,  $[H_2S]_{in}$ ,  $H$ ,  $[Fe]H$  and the constant term or intercept. Note that this model does not generally have higher  $R^2$  terms than the full quadratic model (the  $R^2$  for prediction is higher), but the F-value is higher (30.19) (or, meaning the same, the “F-Significance” value is lower), indicating a more significant model. All the model terms are highly significant, indicated by the very low “Significance” values in the coefficients window.

C-2.13 The “Multiple Regression” dialog allows to perform model adequacy checking. The “outlier” button produces a list showing outliers, leverage, and influential cases in our database. The “Graph” button opens another dialog which shows a variety of scatter plots useful for residual analysis. For example, click the “Graph” button and then “Add Trend line” in the graph dialog. It should look like this:



C-2.14 This graph shows a plot of the y-values predicted by the model (“*RE* predicted”) vs. the observed “*RE*” values and the corresponding linear trend line.

There a variety of plots is available which can be selected with the arrow buttons.

C-2.15 Create a permanent Excel output worksheet by press the “Make XLS” button in the main dialog.

C-2.16 After exiting the main dialog, the output sheet (“data\_1”) should be the active window. Note the buttons on the left hand side in the first column. By pressing these buttons, you can perform a series of useful actions as described below,

- Reregress the model (goes back to the Main Dialog),
- Delete the output sheet if needed,
- Predict new responses based on new data points,
- See scatter plots similar to the ones described above for residual analysis (“Graph”),
- Evaluate a data table including residual analysis for each data point,
- Go to a regression coefficients table like the one in the main dialog,
- “optimize”, i.e., find a set of inputs which gives a specific output,



- Check the confidence ranges for the regression in a scatter plot,
- View the outlier table,
- Print selected output ranges from the sheet,
- Look at the correlation matrix (R matrix).

Summary

R	0.934
R <sup>2</sup>	0.872
R <sup>2</sup> adjusted	0.843
Standard Error	4.794
# Points	39
PRESS	1149.76
R <sup>2</sup> for Prediction	0.794
Durbin-Watson d	1.751
First Order Autocorrelation	0.076
Collinearity	0.000
Coefficient of Variation	6.802
Precision Index	165.635

ANOVA

Source	SS	SS%	MS	F	F Signif	df
Regression	4857.8	87	693.97	30.19	3.8739E-12	7
Residual	712.56	13	22.99			31
LOF Error	712.06	13 (100)	23.74	47.4704	0.114	30
Pure Error	0.500	0 (0)	0.500			1
Total	5570.4	100				38

Regression Equation

$$RE = b0 + b1*G + b2*(H2S) + b3*(Fe) + b4*H + b5*L*(Fe) + b6*(H2S)*H + b7*(Fe)*H$$

	P value	Std Error	-95%	95%	t Stat	VIF	
b0	134.98	1.67455E-09	16.04	102.25	167.70	8.413	
b1	-285.12	3.17555E-11	28.50	-343.25	-227.00	-10.00	1.021
b2	344.32	0.00715	119.56	588.16	100.49	2.880	25.58

## VITAE

**Name** Miss Rattana Saelee  
**Student ID** 4813003

### Educational Attainment

Degree	Name of Institution	Year of Graduation
Bachelor of Science (Industrial Chemistry)	Prince of Songkla University	2005

### Scholarship Awards during Enrolment

Prince of Songkla University Graduate Studies Grant, Academic Year 2005-2009

### List of Publication and Proceedings

#### Publication

Rattana Saelee, Juntima Chungsiriporn, Janya Intamane and Charun Bunyakan.  
2009. Removal of H<sub>2</sub>S in Biogas from Concentrated Latex Industry with Iron(III)chelate in Packed Column. Songklanakarin Journal of Science and Technology, 31(2): 195-203.

#### Proceedings

Saelee, R., Bunyakan, C. and Chungsiriporn, J. 2008. The Removal of H<sub>2</sub>S in Biogas from Concentrated Latex Industry with Iron(III)chelate in Packed Column. Technology and Innovation for Sustainable Development Conference (TISD2008), Faculty of Engineering, Khon Kaen University, Thailand 28-29 January 2008.

Rattana Saelee, Charun Bunyakan and Juntima Chungsiriporn. 2008. Hydrogen Sulfide Removal from Gas Stream using Absorption and Oxidation by Iron(III)chelates in Packed Column. The 18<sup>th</sup> Thailand Chemical Engineering and Applied Chemistry conference (TICChE 18), Faculty of Engineering, Mahidol University, Thailand 20-21 October 2008.